UNIVERSITY OF BELGRADE
FACULTY OF CIVIL ENGINEERING

Marko D. Orešković

MIX DESIGN METHODOLOGY OF HOT MIX ASPHALT WITH HIGH CONTENT OF RECLAIMED ASPHALT PAVEMENT

Doctoral Dissertation

Belgrade, 2020

UNIVERZITET U BEOGRADU
GRAĐEVINSKI FAKULTET

Marko D. Orešković

METODOLOGIJA PROJEKTOVANJA VRUĆIH ASFALTNIH MEŠAVINA SA VISOKIM SADRŽAJEM STRUGANOG ASFALTA

doktorska disertacija

Beograd, 2020

Advisor: Dr Goran Mladenović, Associate Professor
               University of Belgrade, Faculty of Civil Engineering, Serbia

Committee: Dr Goran Mladenović, Associate Professor
               University of Belgrade, Faculty of Civil Engineering, Serbia

               Dr Sara Bressi, Assistant Professor
               University of Pisa, Italy

               Dr Nicolas Bueche, Professor
               Bern University of Applied Sciences, Switzerland

               Dr Igor Jokanović, Assistant Professor
               University of Novi Sad, Faculty of Civil Engineering Subotica, Serbia

Defence date:

Acknowledgements

First, I would like to extend heartfelt appreciation to my research advisor, Professor Dr Goran Mladenović, for his patience, motivation, profound knowledge and the invaluable guidance that he provided throughout the research. His useful advices helped to improve the quality of the dissertation.

I am sincerely thankful to Professor Dr Sara Bressi, who was always willing to help solve the most difficult issues related to the statistical analysis of the experimental data and development of the predictive models. The depth of her knowledge regarding the field of asphalt recycling made a significant contribution to the dissertation.

I would also like to express my sincerest gratitude to two other committee members, Professor Nicolas Bueche and Professor Igor Jokanović, who greatly enriched this thesis with their comments.

The experimental part of the study would have been impossible to perform without my colleagues from the laboratory, Milovan Mihailović and Momčilo Jakšić, who invested their time and effort to help me to prepare and test specimens.

I would also like to thank Professor Dr Marko Radišić, who helped me to carry out the Fourier transformation, and Professor Dr Nikola Tošić who gave me useful advices during thesis preparation. I owe a special thanks to Professor Dr Jasna Plavšić who provided me with significant assistance in the field of statistical analysis.

I am extremely grateful to the company "Energoprojekt niskogradnja" d.o.o., which provided component materials (bitumen, filler, and virgin aggregate fractions), companies "ITERCHIMICA" and "KRATON", who provided rejuvenators, and Dr Laurent Porot, who carried out rheological tests on binder blends with different rejuvenators.

I would like to acknowledge the asphalt technologists of the RILEM Technical Committee 264-RAP for the fruitful discussions and feedback that have significantly enriched the dissertation.

This study is supported by the Ministry of Education Science and Technological Development of the Republic of Serbia through the research project TR 36017 — "Utilization of By-Products and Recycled Waste Materials in Concrete Composites in the Scope of Sustainable Construction Development in Serbia: Investigation and Environmental Assessment of Possible Applications" and the bilateral project between the University of Belgrade, Faculty of Civil Engineering and the University of Pisa, Italy, titled "Hot Mix Asphalt with High Reclaimed Asphalt Content (HARAC)", and these supports are gratefully acknowledged.

Last, but definitely not least, I am greatly indebted to my family members. Their true love, care, and tolerance supported me in the most difficult moments during the preparation of the dissertation. Without them, the preparation of this dissertation would be much more difficult.

I would like to dedicate this dissertation especially to my late father, to whom I promised this dissertation before he passed away.

Abstract

The construction of new roads requires large amounts of virgin aggregate, filler, and virgin bitumen (VB). As these materials are available in limited quantities, seeking alternative solutions to decrease/replace their usage is inevitable. At the same time, the reconstruction of existing roads results in an increased amount of stockpiled materials and the need for new materials. These issues can be overcome if reclaimed asphalt pavement (RAP)—which is, in principle, a 100%-recyclable material—is partially or completely used in the production of new asphalt mixtures. Because of the presence of aged binder within the RAP (RAPb), the total amount of virgin bitumen that should be added in an asphalt mixture could be decreased; hence, the highest potential of using RAP is within hot mix asphalt (HMA) and warm mix asphalt (WMA).

However, the extensive use of RAP is precluded by many limitations, from the lack of guidelines/policies and road agency specifications, to technological issues, and, most commonly, barriers related to RAP as a componental material. An understanding of the blending phenomena between the RAPb and recycling agent (RA), rejuvenators or lubricants, is a priority when high RAP contents are used. Equally important is determining the optimal preheating temperature because, besides the effect on RAP performance, it is a critical aspect affecting energy consumption. Overall, it remains unclear how to include these issues in a mix design procedure. Although a large number of studies have been performed on these topics, many issues remain unresolved, including, but not limited to questions such as "What quantity of RAPb is activated during the manufacturing of asphalt mixtures?", "How do RA and preheating temperature improve blending?", "How is RAPb blended with RA?", "What is the optimal preheating temperature of RAP?", and "How should blending be included in a mix design procedure?"

Three parameters (Degree of binder Activity, Degree of Binder Availability, and Degree of Blending) are clearly defined in this study, due to the lack of consensus on basic blending parameters in the current specifications and studies. These parameters also present the basis for further studies. A summarized review of testing methods used for their determination in previous studies, together with recommendations for further research, is also provided.

Since determining the optimal preheating temperature is an initial step in the HMA manufacturing process, and considering that there are no standardized methods for its determination, a methodology, applicable to any RAP, was developed in this study. Two types of recycled asphalt mixtures (RAM), made of only RAP and RAP+RA, were prepared using Marshall and gyratory compactors after preheating at different temperatures (from 70°C to 190°C). Air void content, stiffness, indirect tensile strength (ITS), and the cracking susceptibility parameter (CT_{index}) of each mixture were determined. A multi-objective optimization step was further applied to determine the optimal preheating temperature of RAP, integrating the uncertainties in determining the different properties through a Monte Carlo simulation. Testing results showed that the optimal preheating temperature of RAP in this study is approximately 130°C, regardless of the compaction method, whereas adding RA decreased it by 14.5°C and 7.2°C when gyratory and Marshall compactors were used, respectively.

In the main phase of the study, a mix design methodology of HMA with 50% RAP was developed. For this purpose, seven asphalt mixtures with 50% RAP and different VB and RA contents were prepared according to Doehlert's experimental design. Air void content, stiffness and ITS at 25°C were measured on Marshall specimens of each mixture, whereas CT_{index} was calculated. Predictive response models were then developed for each parameter using a response surface methodology and their accuracy was assessed by using various statistical methods. Criteria were established for each parameter and two additional

mixtures were prepared to validate the developed models and to determine the optimal VB and RA contents in the base course mix with 50% RAP. Testing results showed that 1.62% VB and 0.11% RA (relative to the total mass of the asphalt mixture) are optimal contents, and these amounts were later used for the preparation of RAM with 50% RAP.

Finally, to investigate if the mixture was properly designed, it was decided to compare its properties with the control asphalt mixture (made with 3.6% VB and virgin aggregate) and the asphalt mixture with 15% RAP, that is widely used in the practice. The newly designed mixture showed better rutting resistance, fatigue and freeze-thaw resistance, similar performance considering cracking resistance, and slightly increased water sensitivity than the control mixture, whereas stiffness varied depending on the testing temperature: it had higher stiffness than the control mixture in the domain of high testing temperatures (above 20°C), and lower stiffness than the control mixture in the domain of low testing temperatures (below 20°C).

Key words: *pavements, Hot Mix Asphalt (HMA), asphalt recycling, Reclaimed Asphalt Pavement (RAP), asphalt recycling agent/additive, mix design methodology, asphalt mixture performance*

Scientific field: *Civil Engineering*

Scientific subfield: *Construction and Maintenance of Roads and Airports*

Sažetak

Za izgradnju novih puteva koriste se velike količine novog kamenog materijala, filera i novog bitumena. S obzirom da su količine ovih materijala ograničene, dolazi do potrebe za primenom alternativnih materijala, koji će smanjiti njihovu upotrebu ili ih potpuno zameniti. Istovremeno sa tim, usled rekonstrukcije postojećih puteva dolazi do nagomilavanja iskorišćenih materijala, kao i do povećane potrebe za novim materijalima. Ovi problemi mogu biti prevaziđeni ukoliko se koristi strugani asfalt (RAP), materijal koji teorijski može u potpunosti da se ponovo upotrebi (reciklira). Usled prisustva ostarelog bitumena u struganom asfaltu, smanjuje se potreba za novim bitumenom u novoj asfaltnoj mešavini. Zbog toga je najveći potencijal upotrebe struganog asfalta u asfaltnim mešavinama proizvedenim po toplom (*WMA*) i vrućem postupku (*HMA*).

Međutim, postoje mnoga ograničenja u upotrebi struganog asfalta, posebno u većim količinama, počevši od nedostatka smernica/pravilnika i specifikacija putnih uprava, preko tehnoloških poteškoća, do ograničenja koja se najčešće odnose na strugani asfalt kao sastavni materijal asfaltne mešavine. Razumevanje fenomena umešavanja između bitumena iz struganog asfalta i aditiva/agensa za reciklažu asfalta, osveživača ili lubrikanta, je od ključne važnosti kada se koriste velike količine struganog asfalta. Jednako važno je i određivanje optimalne temperature zagrevanja struganog asfalta prilikom proizvodnje asfaltnih mešavina, koja, pored negativnog uticaja na njegove karakteristike, značajno utiče i na potrošnju energije potrebne za zagrevanje. Međutim, još uvek nije jasno kako uključiti sve ove uticajne faktore u proceduru projektovanja asfaltnih mešavina sa visokim sadržajem struganog asfalta. Iako je sproveden veliki broj istraživanja sa tim ciljem, još uvek postoji mnogo nejasnoća i pitanja poput „Koliko bitumena iz struganog asfalta se aktivira prilkom proizvodnje asfaltnih mešavina?", „Šta je optimalna temperatura zagrevanja struganog asfalta?", „Kako temperatura zagrevanja i aditiv za recikliranje unapređuju stepen umešavanja između aditiva i bitumena iz struganog asfalta?" i „Kako uključiti stepen umešavanja u metodologiju projektovanja asfaltnih mešavina sa visokim sadržajem struganog asfalta?".

Usled nedostatka konsenzusa o osnovnim terminima u aktuelnim specifikacijama i studijama, u okviru ove disertacije su uspostavljeni termini za sledeće parametre: stepen aktiviranja bitumena iz struganog asfalta, stepen dostupnosti bitumena iz struganog asfalta i stepen umešavanja između bitumena iz struganog asfalta i aditiva za recikliranje asfalta. U okviru disertacije je dat i zbirni prikaz metoda za određivanje vrednosti ovih parametara korišćenih u prethodnim istraživanjima, zajedno sa preporukama za buduća istraživanja.

S obzirom da je određivanje optimalne temperature zagrevanje struganog asfalta početni korak u postupku proizvodnje asfaltnih mešavina po toplom postupku i da trenutno ne postoje standardizovane metode za njeno određivanje, u okviru ove disertacije je razvijena metodologija koja može biti primenjena na bilo kom struganom asfaltu. Dve asfaltne mešavine, jedna sačinjena samo od struganog asfalta, a druga od struganog asfalta i aditiva za recikliranje, su pripremljene upotrebom Maršalovog i žiroskopskog nabijača nakon zagrevanja na različitim temperaturama (od 70°C do 190°C). Nakon toga su određeni sadržaj šupljina, krutost, čvrstoća pri indirektnom zatezanju (ITS) na 25°C i pokazatelj otpornosti na pojavu pukotina, CT_{index}, svih uzoraka asfaltnih mešavina. Višekriterijumska optimizacija je zatim upotrebljena kako bi se izračunala optimalna temperatura zagrevanja struganog asfalta, i to uključujući nepravilnosti nastale prilikom ispitivanja primenom Monte Karlo simulacije. Rezultati ispitivanja su pokazali da optimalna temperatura zagrevanja struganog asfalta korišćenog u ovoj disertaciji iznosi oko 130°C, bez obzira na način pripreme uzoraka, dok dodatak aditiva za recikliranje snižava temperaturu zagrevanja za 14.5°C u slučaju pripreme uzoraka u žiroskopskom nabijaču i za 7.2°C kada su uzorci pripremljeni u Maršalovom nabijaču.

U glavnom delu ovog istraživanja je razvijena metodologija za projektovanje asfaltne mešavine po vrućem postupku sa 50% struganog asfalta. Kako bi se to postiglo, ukupno je pripremljeno sedam asfaltnih mešavina sa 50% struganog asfalta i različitim sadržajima novog bitumena i aditiva za recikliranje asfalta, a sve u skladu sa Dolertovim (Doehlert) planom eksperimenta. Uzorci su pripremljeni primenom Maršalovog nabijača i određene su njihove karakteristike: sadržaj šupljina, krutost i čvrstoća pri indirektnom zatezanju na 25°C, dok je vrednost parametra CT_{index} izračunata. Nakon analize rezultata, razvijeni su modeli koji opisuju promenu parametara u zavisnosti od sadržaja bitumena i aditiva za recikliranje primenom metodologije površine odziva. Kako bi se odredila tačnost modela koji su razvijeni za svaki parametar, primenjene su različite statističke metode. Nakon toga su uspostavljeni kriterijumi za pojedinačne parametre i u skladu sa time su pripremljene još dve asfaltne mešavine kako bi se potvrdila tačnost razvijenih modela i odredio optimalni sadržaj novog bitumena i aditiva za recikliranje u asfaltnoj mešavini za izradu nosećeg sloja sa 50% struganog asfalta. Rezultati ispitivanja su pokazali da je optimalno upotrebiti 1.62% novog bitumena i 0.11% aditiva za recikliranje, u odnosu na ukupnu masu asfaltne mešavine, pa su u nastavku eksperimenta te količine korišćene za pripremu asfaltne mešavine sa 50% struganog asfalta.

Na kraju istraživanja su određene karakteristike projektovane mešavine i upoređene sa istim karakteristikama kontrolne asfaltne mešavine (napravljene od 3.6% novog bitumena i novog kamenog materijala) i asfaltne mešavine sa 15% struganog asfalta, koja se često koristi u praksi, kako bi se utvrdilo da li je asfaltna mešavina ispravno projektovana. Novoprojektovana asfaltna mešavina je pokazala bolju otpornost u pogledu otpornosti na dejstvo kolotraga, zamor i smrzavanje i odmrzavanje, slično ponašanje u pogledu otpornosti na pukotine, i nešto veću osetljivost na otpornost na dejstvo vode u poređenju sa kontrolnom mešavinom. Krutost mešavine je zavisila od temperature ispitivanja: u opsegu visokih temperatura ispitivanje (preko 20°C), krutost je bila veća, a u domenu niskih temperatura ispitivanja (ispod 20°C) niža u poređenju sa kontrolnom mešavinom.

Na osnovu sprovedenih ispitivanja može se zaključiti da laboratorijski napravljena asfaltna mešavina po vrućem postupku sa 50% struganog asfalta, u skladu sa metodologijom razvijenom u okviru disertacije, ima slične karakteristike kao kontrolna mešavina i mešavina sa 15% struganog asfalta. Međutim, pouzdanost razvijene metodologije treba proveriti i na asfaltnim mešavinama sa različitim sadržajima struganog asfalta i različitim sastavnim materijalima.

Ključne reči: *kolovozne konstrukcije, asfaltna mešavina po vrućem postupku (HMA), recikliranje asfalta, strugani asfalt (RAP), agens/aditiv za recikliranje asfalta, projektovanje asfaltnih mešavina, karakteristike asfaltnih mešavina*

Naučna oblast: *Građevinartvo*

Uža naučna oblast: *Građenje i održavanje puteva i aerodroma*

List of Abbreviations

Abbreviation	Meaning
2D	Two Dimensions
3D	Three Dimensions
AASHTO	American Association of State Highway and Transportation Officials
AC	Asphalt Concrete
AFM	Atomic Force Microscopy
AI	Ageing Index
ANOVA	ANalysis Of VAriance
ASTM	American Society for Testing and Materials
BBR	Bending Beam Rheometer
BR	Black Rock
BR	RAP Blending Ratio
CCD	Central Composite Designs
CM	Control Mixture
COV	Coefficient of Variation
CT	Computed Tomography
DEM	Discrete Element Method
df	Degree of Freedom
DoA	Degree of Binder Activity
DoAv	Degree of Binder Availability
DoB	Degree of Blending
DSR	Dynamic Shear Rheometer
EDXS	Energy Dispersive X-Ray Spectroscopy
EDX	Energy Dispersive X-Ray Spectroscopy
EDS	Energy Dispersive X-Ray Spectroscopy
ER	Energy Ratio
ESEM	Environmental Scanning Electron Microscopy
FEM	Finite Element Method
FTIR	Fourier-Transform Infrared Spectroscopy
GPC	Gel Permeation Chromatography

HMA	Hot Mix Asphalt
IDEAL-CT	**In**direct **Te**nsile **A**sphalt **C**racking **T**est
IT-CY	Indirect Tensile test on Cylindrical-shaped specimens
ITS	Indirect Tensile Strength
ITSM	Indirect Tensile Stiffness Modulus
ITSR	Indirect Tensile Strength Ratio
JMF	Job Mix Formula
LA	Los Angeles
LoF	Lack of Fit
LMSP	Large Molecular Size Percentage
LTAb	Long-Term Activated binder
LVDT	Linear Variable Differential Transducer
MC	Monte Carlo
MGV	Mean Grey Value
micro-CT	Micro Computed Tomography
MS	Mean Squares
MSCR	Multiple Stress Creep Recovery
PAV	Pressure Ageing Vessel
PE	Pure Error
PG	Performance Grade
PmB	Polymer Modified Bitumen
PRD	Proportional Rut Depth
QC/QA	Quality Control/Quality Assessment
RA	Recycling Agent
RAC	Recycling Agent Content
RAPb	Reclaimed Asphalt Pavement binder
RAM	Recycled Asphalt Mixture
RAP	Reclaimed Asphalt Pavement
RAP15	RAM with 15% RAP
RAP50	RAM with 50% RAP
RAP100	RAM with 100% RAP
RAS	Reclaimed Asphalt Shingles
RD	Rut Depth
RILEM	*Réunion Internationale des Laboratoires et Experts des Matériaux, systèmes de construction et ouvrages*—The International Union of Laboratories and Experts in Construction Materials, Systems and Structures
RSM	Response Surface Methodology

RTFOT	Rolling Thin Film Oven Test
RV	Rotational Viscometer
RVB	Replaced Virgin Binder
SE	Send Equivalent
SEC	Size Exclusion Chromatography
SEM	Scanning Electron Microscopy
SS	Sum of Squares
SS_R	Sum of Squares due to Regression
SS_T	Total Sum of Squared Deviations from the Mean
SSD	Saturated Surface Dry
STAb	Short-Term Activated Binder
SUPERPAVE	SUperior PERforming asphalt PAVEments
T	Temperature
TC	Technical Committee
TG	Task Group
TSR	Tensile Strength Ratio
UV	Ultraviolet Light
VB	Virgin Bitumen
VBC	Virgin Bitumen Content
WA	Water Absorption
WL	White Light
WMA	Warm Mix Asphalt
WTS	Wheel-Tracking Slope
XCT	X-Ray Computed Tomography
XEDS	Energy Dispersive X-Ray Spectroscopy
ΔEA	Activation Energy

List of Symbols

Symbol	Meaning	Unit
%R	Recovery component of a binder during MSCR test	%
$y_{i,j}, y_j$	Observations	%, kPa, MPa, -
$\overline{y_i}$	The mean response at each X_i level	%, kPa, MPa, -
$\widehat{y_i}$	The corresponding fitted value	%, kPa, MPa, -
$\widehat{y_j}, \widehat{y_l}$	Regression estimates	%, kPa, MPa, -
$\overline{y_j}, \overline{y_l}$	"Local" average of observations	%, kPa, MPa, -
$\widehat{E}(F)$	Estimated value of output variable	%, kPa, MPa, -
$\beta_0, \beta_1, .. \beta_{11}, .. \beta_n$	Regression coefficients	-
$\hat{\sigma}(F)$	Estimated standard deviation of output variable F	%, kPa, MPa, -
$|E^*|$	The measured dynamic modulus of asphalt mixture	MPa
$|G^*|$	Complex shear modulus	Pa
$A(RAP_{agg})_{blend\ binder}$	Binder property "A" of blending binder coating the RAP aggregate	-
$A(virgin_{agg})_{blend\ binder}$	Binder property "A" of blending binder coating the virgin aggregate	-
A_0	Fitting parameter of fatigue line	-
A_1	Slope of the fatigue line	-
$A_{RAP\ virgin\ binder\ 0\ blend}$	Binder property "A" of the RAP and virgin binder that coats the RAP aggregate assuming 0% blending	-
$A_{virgin\ binder}$	Binder property "A" of virgin binder	
B_{BR}	Virgin binder ratio	%
BR	RAP blending ratio	%
C=O	The area of the carbonyl	-
$CoarseLMS$	The LMS% of the coarse aggregate	%
D	The diameter of the specimen	mm

D	The diameter of the testing specimen	mm
d_{10000}	Rut depth after 10.000 load cycles	mm
d_{5000}	Rut depth after 5.000 load cycles	mm
D_n	The maximum absolute difference between the theoretical and step function	-
$D_{n,0.05}$	Critical region (Kolmogorov-Smirnov statistic test)	-
E_n^*	Complex modulus in the n-th cycle	MPa
FineLMS	The LMS% of the fine aggregate	%
F_j	Fitness performance	-
F_k	Results of simulations	-
G_f	Fracture energy	
H	The height of the specimen	mm
ITS	Indirect tensile strength at 25ºC	kPa
ITS_{DRY}	Indirect tensile strength of dry (unconditioned) set of specimens	kPa
$ITSM_{AC-50\% RAP}$	The stiffness modulus of AC samples with 50% RAP	MPa
$ITSM_{control}$	The stiffness of the control mixture	MPa
ITSR	Indirect tensile strength ratio of ITS_{WET} and ITS_{DRY}	%
ITS_{RAP}	ITS test result of the only RAP preheated at a specific temperature "X"	kPa
ITS_{WET}	Indirect tensile strength of wet set of specimens	kPa
$J_{nr0.1}$	Non-recoverable creep compliance at 0.1 kPa shear stress	kPa^{-1}
$J_{nr3.2}$	Non-recoverable creep compliance at 3.2 kPa shear stress	kPa^{-1}
l	Displacement	mm
log(max)	Limiting maximum stiffness modulus	MPa
log(min)	Limiting minimum stiffness modulus	MPa
m_{75}	The slope at the point of the post-peak 75% of maximum load	kN
$maxITS_{RAP}$	A maximum ITS test result of the RAP	kPa
n	Number of observations	-
n	Number of loading cycles	-
$N_{i,j,k}$	Fatigue function	-
n_s	Number of simulations	-
P	The peak load	kN
P	Applied load (CT_{index})	kN
PGH_{base}	The high PG temperature of virgin binder	°C
PGH_{blend}	The high PG temperature of binder blend	°C
PGH_{RAP}	The high PG temperature of RAPb	°C

PGH_{RAS}	The high PG temperature of RAS	°C
PRD_{AIR}	Proportional rut depth	%
R'_c	Specific property parameters for a coarse-mixture binder	-
R^2	Coefficient of determination	-
RAP_{BR}	RAP binder ratio	%
RAS_{BR}	RAS binder ratio	%
RD_{AIR}	Rut depth	mm
R_E	The energy ratio	-
R_{new}^2	R square of the "new" regression	-
R_p	Specific binder property parameters for the proportion binder	-
R_v	Specific binder property parameters for the virgin binder	-
RVB	The replaced virgin binder	%
R_σ, R_ε	Energy ratio in stress and strain-controlled modes	-
$S(t)$	Creep stiffness	
SE	Send equivalent	%
S_{td}	Average indirect tensile strength of the unconditioned (dry) subset	kPa
$S_{tm,n}$	Average indirect tensile strength of the freeze-thaw conditioned subset after *n* cycles (3 and 6)	kPa
T	Test temperature	°K
t	The thickness of the testing specimen	mm
Tr	Reference temperature	°K
W_0, W_n	Dissipated energy in the first and n-th loading cycle	-
WA_{24}	Water absorption	%
$W_{absorbedRAPb}$	The amount of absorbed RAPb	g
$W_{activatedRAPb}$	The amount of activated RAPb	g
$W_{activeRAPb}$	The amount of active RAPb	g
$W_{availableRAPb}$	The amount of available RAPb	g
$W_{blackrockRAPb}$	The amount of "black rock" RAPb	g
w_i	Weights assigned to each parameter	-
$W_{inactive}$	The amount of inactive RAPb	g
$W_{liquidRAPb}$	The portion of the liquid RAPb	g
W_{LTAb}	The amount of long term activated RAPb	g
$W_{RAPb,total}$	Total amount of RAPb	g
$W_{residRA}$	The amount of a residual recycling agent	g
$W_{softerRAPb}$	The amount of softer RAPb	g
W_{STAb}	The amount of short term activated RAPb	g

WTS_{AIR}	Mean wheel-tracking slope	mm/10^3 cycles
y_{ij}	Value of the i-parameter at each preheating temperature	%, kPa, MPa, -
Y_{RAP}	A property of only RAP specimens (ITS and stiffness)	kPa, MPa
$Y_{reference}$	The same property of reference RAP specimens	kPa, MPa
α	Phase angle	°
α	Level of significance	%
β, γ	Fitting parameters	-
ΔEA	Activation energy	kJ/mol
ΔT	Decrease in RAP preheating temperature	°C
$\varepsilon_0, \varepsilon_n$	Strain levels in the first and n-th load cycles	%
ε_6	Strain at 10^6 load cycles	μm/m
ε_i	Initial strain amplitude measured at the 100th load cycle	μm/m
η^*	Rotational viscosity	Pa.s
ϱ_{rd}	Particle density of an oven-dried basis	Mg/m^3
σ_0, σ_n	Stress levels in the first and nth loading cycle	N
φ_0, φ_n	Phase angles in the first and nth loading cycle	°
ω_R	Reduced frequency	Hz

Table of Content

List of Figures

List of Tables

Chapter 1. Introduction

1.1 Research Topic

As road pavement engineering is making use of a life-cycle-based design approach, the implementation of end-of-life strategies for Reclaimed Asphalt Pavement (RAP), such as road pavement asphalt mixtures with high RAP content (≥50%), is of paramount interest for road authorities and contractors (*AllBack2Pave*, 2014; *COREPASOL*, 2014; *DIRECT-MAT*, 2011; *EARN*, 2014; *Re-Road*, 2012; *SUP&R ITN*, 2017). This growing popularity comes from the need to dismantle high quantities of stockpiled material and decrease/replace the use of finite resources, such as bituminous binder and virgin aggregates. Furthermore, the successful implementation of these technologies is economical and environmentally sustainable, and this reason is enough for the asphalt and road pavement industries to encourage the use of Recycled Asphalt Mixtures (RAM), designed to minimise the amount of virgin materials — with recycling as default practices. Many limitations are still preventing the shift to RAM: a lack of information about the long-term performance and durability, lack of guidelines/policies and road agency specifications for the production and quality control, technical issues related to the complexity of the formulation itself and to the capabilities of the asphalt plants (RAP may not be directly heated as a virgin aggregate because if it is exposed to high temperatures, binder from RAP will smoke and can be severely damaged (R. C. West, 2015); so, for mixtures with high RAP content, the use of parallel flow drum is required).

However, the most common barriers are related to RAP as a component material. Copeland (2011) reported that the homogeneity, quality control, dust, and moisture content of RAP, as well as the aged binder grade and blending between the aged binder and recycling agent, rejuvenator, or lubricant, are concerns cited most often with regards to the quality of RAMs. The latter two parameters are strongly correlated to the performance of RAM because increased amounts of aged binder within RAMs significantly change their properties and performance during the exploitation period: rutting resistance (Anderson & Daniel, 2013; Boriack et al., 2014; Colbert & You, 2012; Silva et al., 2012a), indirect tensile strength (Shu et al., 2008; Vukosavljevic, 2006), and stiffness increase (Boriack et al., 2014; Mogawer et al., 2012; Shu et al., 2008; Valdés et al., 2011; Vukosavljevic, 2006), whereas cracking resistance (both thermal and fatigue) decreases (Anderson & Daniel, 2013; Mogawer et al., 2012; M Sabouri et al., 2015). These reasons are at the base of the differences in regulations and approaches used for RAM production in different EU countries and beyond. In fact, the amount of RAP in surface courses is mostly limited to 10–30% (Hungary, Belgium, Denmark) or even prohibited (Spain, Czech Republic), whereas in other countries (Germany, Austria, Norway), RAP can be used up to 100% in new RAM, regardless of the course type (Mollenhauer et al., 2010; Partl et al., 2013).

To be considered as sustainable solutions, whether they are obtained with a hot or warm process, the RAMs with a low content of virgin materials should meet at least the same requirements valid for traditional mixtures (composed of all virgin materials or those with low recycled content). However, RAP is a complex material, which is different, especially in terms of variability, from the traditional components used in asphalt mixtures. RAP represents a family of materials that are still being studied and characterized to provide recommendations for their classification (Tebaldi et al., 2018), as well as for the improved design and better performance prediction of the resulting RAMs. Some of the aspects that play a fundamental role in this process are (Bressi et al., 2015; Copeland, 2011; Di Mino et al., 2015; Hossain, Musty, & Sabahfer, 2012; Howard, Cooley, & Doyle, 2009; Lo Presti et al., 2015; Newcomb, Ray Brown, & Epps, 2007; Orešković, Bressi, Di Mino, & Lo Presti, 2017; Partl et al., 2013):

- variability of RAP properties due to the often-unknown nature and heterogeneity of RAP
- lack of specifications for the characterization and classification of RAP
- lack of methods for accurately measuring the properties of the aged binder
- uncertainties when polymers are presented in RAP
- uncertainties in adapting existing mix design procedures
- lack of fundamental understanding of some of the mechanisms involved during RAP mixing with the other components, such as recycling agents
- lack of a widely accepted nomenclature to describe key quantities linked with the blending phenomena

With this in mind, and with a particular focus on the last two points, it was necessary to provide a theoretical explanation and nomenclature of the key mechanisms linked to the blending phenomena, together with a pragmatic framework to identify and possibly quantify three properties related to the binder blending. The first property is the minimum amount of aged binder available from a selected RAP, here defined as the Degree of binder Activity (DoA), which is introduced to improve the classification of RAP materials. The second, the Degree of Blending (DoB) between the aged asphalt binder coming from the RAP and the virgin binder (VB) and/or recycling agent (RA), should serve to define the mix design procedures for RAM. And the last property, Degree of binder Availability (DoAv), represents the binder available for blending, formed not only of the binder activated during the manufacturing process and the residual amount of a RA but also of the binder activated under the influence of the RA.

In addition to these issues, which may affect RAM performance, RAM manufacturing process also plays an important role. Beside the mixing and conditioning time, as well as the mixing temperature of RAP, a preheating temperature of RAP presents an equally important parameter within the production procedure of RAM (Liu et al., 2019; Ma et al., 2016; Madrigal et al., 2017; Silva et al., 2012a; B. Yu et al., 2017). On one hand, a higher than optimal preheating temperature will additionally age the already aged RAPb (Daniel & Lachance, 2005), making a RAM mixture stiffer (Madrigal et al., 2017) and more resistant to rutting (Liu et al., 2019) but also more sensitive to low-temperature cracking (Liu et al., 2019; Madrigal et al., 2017) and moisture damage (Liu et al., 2019; Madrigal et al., 2017). Alternatively, the insufficiently high preheating temperature of RAP will be unable to activate the RAPb, which will then behave like a "black rock" (Daniel & Lachance, 2005), leading to inferior rutting resistance, moisture sensitivity, and low temperature cracking (Ma et al., 2016). The importance of optimal temperature was highlighted by Ma et al., (2016) who concluded that after reaching optimal temperature, there are no more positive effects of RAP heating on RAM performance.

Therefore, it is important to determine the optimal preheating temperature of any RAP used in a new RAM before performing a mix design procedure. Existing guidelines usually recommend the preheating temperature of RAP based on practical experience, regardless the extent of stiffness of the RAPb, although it should be taken into the account. This issue was carefully investigated by West et al. (2013), who showed that optimal preheating time and temperature strongly depend on the RAP type and properties.

For a satisfactory design, RAP testing should be coupled with an appropriate mix design method. Some of the previous mix design methods, developed for mixtures with new materials, may not be appropriate for RAM. For example, Hveem and Bailey methods are based on the specific surface area of the aggregate, but due to the high heterogeneity of RAP, irregular shape of RAP grains and the presence of RAP clusters, these methods can exhibit inappropriate results if RAP is used (Bressi, Dumont, et al., 2016; Stimilli et al., 2015). Furthermore, the Marshall method, which considers volumetric properties, stability, and flow, may also cause problems when designing RAM. For instance, the RAM the virgin mixture may have the same volumetric properties as the virgin mixture, but worse mixture performance (Kaseer et al., 2020).

These problems, which appear during the manufacturing process, are significantly more evident when high amounts of RAP are used (>30%). Due to this fact, when designing RAMs with more than 25% RAP, blending charts, which typically assume full blending between RAPb and RA, should be used (*AASTHO M323-12: Standard Specification for Superpave Volumetric Mix Design*, 2012). Nonetheless, full blending does not usually occur in reality. Therefore, Shirodkar et al. (2013) and Jiménez del Barco Carrión et al. (2015) recommended the inclusion of the real degree of blending in the mix design process. Although there have been many procedures in previous studies that aimed to assess, estimate, or simply describe DoA/DoAv/DoB, there are still no fully developed and standardized testing procedures on how to determine these amounts and include them in the mix design procedure.

In addition to these issues with RAP and fairly unknown blending phenomena, the use of polymer-modified bitumen and the application of alternative materials (asphalt shingles, recycled concrete aggregate, fly ash, etc.) have made this system even more complex and led to the pavement industry's need to develop new mix design method(s) adaptable to these materials. A promising attempt to improve the mix design method of RAM includes the balance mix design approach, which was developed based on the assumption that asphalt mixtures should be designed to achieve not only a certain volumetric composition (air void content), as is the case with the Superpave mix design procedure (*AASHTO Guide for Design of Pavement*, 1993), but also satisfactory rutting and cracking performance (Im et al., 2016; Martins Zaumanis et al., 2018). This approach has shown high potential to be used for the design of RAMs (Zhou et al., 2011) because it ensures the identification of the impact of different virgin bitumen content (VBC), recycling agent content (RAC), or polymer on mixture performance (Van den Bergh et al., 2017). However, the preparation of testing specimens for mix design purposes may require additional time for cutting and sawing, making this procedure more complicated when compared to traditional methods.

Overall, it can be concluded that there is an evident need to establish a simple, easy-to-perform procedure that will allow contractors to determine the optimal preheating temperature of RAP to save resources without compromising RAM properties and develop an affordable and reliable mix design method as a capable tool to predict mixture performance depending on the different components. The research in this dissertation is based on four research hypotheses:

- The optimal preheating temperature of RAP can be decreased if a recycling agent is used.
- The degree of binder activity depends on the preheating temperature.
- Small amounts of RAP (up to 15%) do not significantly affect the characteristics of the hot asphalt mixtures, and such mixtures have similar properties to the control mixture.
- RAM with 50% RAP can have similar properties to the control mixture if the appropriate mix design procedure of HMA is performed.

1.2 Research Objectives

The main objective of the dissertation is to develop a mix design methodology of hot mix asphalt with a high content of RAP, which would have properties as close as possible to the control mixture, composed of virgin materials.

To realize the main objective, the following objectives are defined:

- The collection and analysis of the previous research in the field of RAP application in HMA, with a special emphasis on the blending phenomena between aged binder coming from the RAP and virgin bitumen.
- Due to lack of consensus on the theoretical mechanisms linked with the blending phenomena in previous studies, it is necessary to provide a theoretical explanation and nomenclature of key mechanisms linked with the blending phenomena (DoA,

- DoAv and DoB), together with a pragmatic framework to identify and possibly quantify them.

- The selection of the most efficient RA, among the three available RAs of different origin used in the dissertation, considering the basic and rheological properties of binder blends after prolonged ageing time.

- The development of a methodology for determination of the optimal preheating temperature of RAP, depending on the compaction type and presence of RA.

- The development of a mix design methodology of HMA with a high content of RAP (50%), i.e. determination of the optimal RA and VB contents.

- The realization of an experimental plan to verify if the developed RAM is properly designed by comparing its physical-mechanical properties with the properties of the control mixture and mixture with 15% RAP.

1.3 Research Methodology

For this study, a quantitative research method is applied. Initially, a literature review was performed, with a tendency to use research reports and papers from scientific journals and conferences of a more recent date. Experimental data are collected by performing laboratory tests, mostly based on standardized testing methods. During the development of a procedure for determining the optimal preheating temperature of RAP, correlation and probabilistic optimization method are used. When considering the development of mix design procedure of HMA with high RAP content, response surface methodology is used to develop predictive response models of four parameters (air void content, stiffness, indirect tensile strength, and CT_{index}), and regression analysis is applied to these models to assess their accuracy. Finally, descriptive statistics is used to compare properties among three asphalt mixtures (control, and those with 15% and 50% RAP, respectively).

1.4 Dissertation's Structure

This doctoral dissertation consists of seven main chapters.

In the *first chapter*, the research topic, the scope of the research, and the research questions and objectives of the dissertation are described. The importance of using high RAP content in new HMA and the complexity of the mix design procedure of HMA with high RAP content are explained.

The second chapter is divided into two parts. In the first part, an overview is provided of the literature review on the factors affecting the blending phenomena between RAP and RA. Then, the anticipated theoretical explanation and practical framework to assess the DoA, DoAv and DoB are followed by the conclusions and recommendations for the further studies. The second part of the chapter provides state-of-the-art testing methods used in previous research studies to help both the scientific and practitioner community to find the appropriate method(s) for the evaluation of the mentioned parameters. The used testing methods are explained in detail, and their advantages and disadvantages are given together with recommendations for assessment of blending parameters. Finally, the methods that have only been used in the evaluation of parameters considered are summarized.

The research methodology of the study, i.e. short descriptions and simplified flow-charts of performed tests, is described in *the third chapter*. There is also given a short explanation of all laboratory tests performed within the dissertation.

The fourth chapter shows the measured properties of the componental materials used in the study (virgin bitumen, virgin aggregate, RAs, and RAP), then explains the methods for the preparation of testing specimens, depending on the purpose of the test, and finally describes the testing methods in detail.

The fifth chapter consists of two parts. In the first part, a methodology for determining the optimal preheating temperature of RAP, with and without RA, is developed. Four specimens of RAP and RA

were compacted in Marshall and gyratory compactors after preheating at different temperatures (70°C, 100°C, 140°C, and 170°C), whereas only RAP specimens were compacted at one more temperature (190°C). The volumetric properties of each specimen were determined before measuring their stiffness and indirect tensile strength (ITS), as well as before the calculation of CT_{index} parameters, which represents the cracking susceptibility of the asphalt mixture.

Obtained results were then included in a probabilistic optimization method (the Monte Carlo technique) to determine the optimal heating temperature of RAP considering the compaction type and RA presence. The testing results, in terms of ITS and stiffness, were also used in the assessment of DoA regarding different preheating temperatures. This was achieved by comparing these properties with the same properties of mixture where full binder activation is forced (binder and aggregate were initially extracted; binder was later recovered and then re-blended with the extracted aggregate).

In the second part of this chapter, a mix design methodology of hot mix asphalt with high RAP content (50%) was developed. Seven mixtures, with different contents of RA and VB, were prepared according to Doehlert's experimental design. Four specimens of each mixture were compacted in a Marshall compactor, and volumetric properties, stiffness, ITS and CT_{index} were determined. Testing results were then applied to the response surface methodology (RSM) to develop appropriate models. The reliability of developed models was analysed by applying different statistical methods, which ere then verified by preparing two additional asphalt mixtures that satisfied certain criteria for each parameter considered. Based on the developed models, the optimal RA and VB contents in the asphalt mixture with 50% RAP were determined.

In *the sixth chapter,* three mixtures are investigated: control (composed of all virgin materials), with 15% RAP, and with 50% RAP, designed according to the fifth chapter. The following properties of each mixture are determined and later compared: stiffness, water sensitivity, freeze-thaw, cracking (CT_{index}), fatigue resistance, and resistance to permanent deformation (rutting resistance).

The seventh chapter summarizes the general conclusions of the study and gives several recommendations for further studies.

This page intentionally left blank

Chapter 2. About the Blending Between Reclaimed Asphalt Binder and Recycling Agent: A Literature Review

2.1 On the Degree of Binder Activity of Reclaimed Asphalt and Degree of Blending with Recycling Agents[1]

2.1.1 State of the Art: Degree of Blending and Related Factors

When a RAP is incorporated within the manufacturing of hot or warm asphalt mixtures, a portion of the aged bitumen surrounding the RAP aggregate acts as a binder in the new formulation and is eventually combined with a recycling agent — defined here as the family of additives/admixtures added within the RAM's manufacturing process. This family of additives/admixtures has two different purposes:

1. To restore the properties of the RAPb (i.e. neat bitumen, naphthenic oils, etc.) to a desirable level — they are known as "rejuvenators".
2. To facilitate the mixing production process by allowing lower manufacturing temperatures and, hence, higher RAP content (i.e. warm mix technologies) — they are known as "lubricants".

An explanation regarding the quantity of RAP binder (RAPb) used in the final binder blend of RAM has not yet been clearly established in previous studies. This quantity is sometimes identified as the asphalt binder replacement, recycled binder ratio, effective RAPb, RAPb contribution, RAPb activity, RAP working binder, RAPb availability (Kaseer et al., 2019), replaced virgin binder (Davide Lo Presti et al., 2016) or the amount of re-activated binder (Stimilli et al., 2015). In mix design practices, this quantity is a percentage of RAPb respecting the total mass of binder blend in RAM. However, its accurate estimation still raises concerns due to its ultimate effect on mix performance. Although the current practices allow asphalt technologists to assess the binder content of RAP, it remains unclear how much of this available binder will actually contribute to the properties of the asphalt mixtures incorporating RAP.

Therefore, asphalt technologists typically consider two opposite scenarios: "full availability" and "black rock" (Kaseer et al., 2019). Full availability (white aggregate in Figure 2.1) assumes that 100% of the RAPb content can be used in the new mix design as a part of the new binder blend. "Black rock" states that 0% of the RAPb will be available for blending and that the RAP actually behaves as "black aggregate" (black aggregate in Figure 2.1). However, it is widely believed that in the mixture, the RAPb does not act only like a "black rock" and that full availability would be unlikely to occur. A more realistic hypothesis lies between these two extremes and is usually described as the "partial availability" concept (grey aggregate in Figure 2.1). Although this concept is well-recognized, the mix design of asphalt mixtures incorporating RAP typically considers the RAPb to be fully available (*AASTHO M323-12*, 2012).

When discussing the blending phenomena, it is vital to distinguish between the amount of available RAPb and its blending efficiency with a recycling agent. The first is linked to the degree of aged binder

---

activity and to what will be defined here as "Degree of binder Activity (DoA)", and the second is what will be referred to here as "Degree of Blending (DoB)". These phenomena should be carefully considered since they may affect the mix design process differently: (i) Degree of Activity/Availability allows the use of a lower quantity of virgin binder when this is used as a recycling agent; (ii) DoB allows estimating the contribution that RAPb and recycling agent have in the conventional/rheological properties of the final binder in the new RAM formulation. The DoA refers to the amount of RAPb that can be considered in mix design practices, as mentioned above, whereas the DoB indicates how well, in terms of binder and/or mixture properties, RAPb and recycling agents are blending.

These concepts seem to be widely recognized by the scientific community. However, the results of a literature review (Table 2.1) highlighted that practitioners have not yet achieved a consensus on the terms related to the blending phenomena, and authors use the following concepts and terms interchangeably: blending efficiency (Bowers, Huang et al., 2014; Bowers, Moore et al., 2014; Ding, Huang, & Shu, 2016; Xu et al., 2018), blending status (S. Zhao et al., 2016), blending ratio (Delfosse et al., 2016), rate of intermixing (Oliver, 2001), binder transfer (Zhang et al., 2015), mobilization rate (Bressi et al., 2015; Ding et al., 2018; Vassaux et al., 2018; S. Zhao et al., 2015), meso-blending (Gundla & Underwood, 2015) and the most used terminology by far degree of blending (Abd et al., 2018; Al-Qadi et al., 2009; Booshehrian et al., 2013; Castorena et al., 2016; Cavalli et al., 2017; Coffey, Dubois, Mehta, & Purdy, 2013; Gaitan et al., 2013; Kriz et al., 2014; Liphardt et al., 2015; Mogawer et al., 2013, 2012; Navaro et al., 2012; Norton et al., 2014; Rinaldini et al., 2014; Shirodkar et al., 2011, 2013; Stephens et al., 2001).
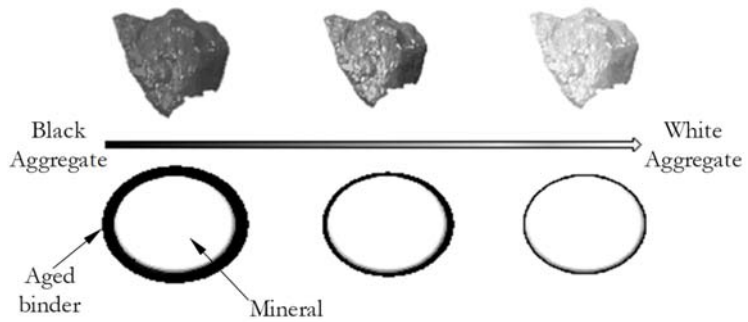
Figure 2.1 *Null-Partial-Full availability concept*

These definitions create confusion and overlapping, which ultimately result in communication issues amongst practitioners, but they also highlight the lack of a consensus on the theoretical mechanisms linked with the blending phenomena. This is also because the phenomenon occurring when a selected RAP is heated and blended with a recycling agent is extremely complex, and several factors influence the outcome. To clarify this key aspect, a literature review has also been undertaken to identify the factors that influence RAPb blending phenomena. Table 2.2 and Table 2.3 show the summary of the literature review for each parameter and explanation of the role played within the blending phenomenon. Some of the factors identified are linked to the design and manufacturing of the asphalt mixture containing RAP (Table 2.2), whereas others are strictly related to the RAP properties (Table 2.3).

Table 2.1 *Definitions of terms related to the blending phenomena as found in the literature*

Reference	Definition
(Shirodkar et al., 2011)	The degree of blending presents the amount of RAPb that will be available for blending with the virgin binder.
(Coffey, Dubois, Mehta, Nolan, & Purdy, 2013; Coffey, Dubois, Mehta, & Purdy, 2013; Shirodkar et al., 2013)	The degree of blending is the percentage of RAPb that is effectively mobilized within the mix.
(Norton et al., 2014)	The amount of residual binder that is active in a mix is known as the degree of blending.
(Stimilli et al., 2015)	Re-activated binder represents a partially melted aged binder that coats the RAP fraction and interacts with the virgin binder contributing to the overall performance of the resulting RAM.

Reference	Definition
(Gundla & Underwood, 2015)	Meso-blending refers to the blending of asphalt at scales above the micro- or molecular levels. It is less concerned with the homogenization of the molecular constituents and more so with the formation of a third binding material that may be considered homogeneous at the scale wherein rheological properties manifest (millimetres and smaller). It is at this scale that the asphalt binder imparts its rheological characteristics to the mixture.
(Ashtiani et al., 2018)	Binder contribution describes the quantity of asphalt binder from RAP that participates as an effective binder in a mixture design.
(Vassaux et al., 2018)	The remobilization represents the ability for the virgin binder to make mobile again and disperse the RAPb layer.
(Gottumukkala et al., 2018)	Blending ratio is defined as the ratio of the weight of RAPb blended with virgin binder to the total weight of RAPb.
(Ding et al., 2018)	The mobilization rate is the percentage of RAPb that can be mobilized during mixing, peeled off RAP aggregate, and made available for blending with recycling agents.
(Vassaux et al., 2019)	"Blend" presents the ability of two components to create a homogenous product where the chemical composition is identical everywhere at the scale observation of the study.

Table 2.2 *Influencing factors on the DoB: Design and manufacturing of asphalt mixture containing RAP*

Parameter	Explanation of the influence (or lack of effect) on DoB and the reference
Mixing temperature	If the mixing temperature is high enough, the RAPb should become softer, or even fluid, making it easily blendable (Bowers, Moore, et al., 2014; Campher, 2012; Cavalli et al., 2017; Ding, Huang, Shu, Zhang, & Woods, 2016; He, Alavi, Harvey, & Jones, 2016; Kaseer, Arámbula-Mercado, & Martin, 2019; Kriz et al., 2014; Lo Presti et al., 2015; Nahar et al., 2013; Navaro et al., 2012; Oliver, 2001; Rad, Sefidmazgi, & Bahia, 2014; Stephens et al., 2001; Zhang et al., 2015; Zhao et al., 2015).
	Only one research study showed that mixing temperature seems not to influence the DoB (Gaitan et al., 2013).
Conditioning time	If the conditioning time is prolonged enough, the blending process may result in an increased blending of the virgin and the RAP binder (He et al., 2016; Kaseer et al., 2019; Rad et al., 2014).
Mixing time	If the mixing time is prolonged, it may be possible that RAP particles begin to interact with each other, increasing the amount of the available RAPb (Bowers, Moore, et al., 2014; Nahar et al., 2013; Navaro et al., 2012; Oliver, 2001; Rad et al., 2014; Zhang et al., 2015; S. Zhao et al., 2016; Gaitan et al., 2013).
	Only one research study showed that this is not the case (Stephens et al., 2001).
RAP content in RAM	If the RAP content is too high, more energy would be required to activate the RAPb (Booshehrian et al., 2013; Gottumukkala et al., 2018; Huang, Pauli, Grimes, & Turner, 2014; Kriz et al., 2014; McDaniel, Soleymani, Anderson, Turner, & Peterson, 2000; Oliver, 2001;

Parameter	Explanation of the influence (or lack of effect) on DoB and the reference
	Shirodkar et al., 2011; Stimilli et al., 2015; Zhang et al., 2015; Zhao et al., 2015).
	However, one study showed that small RAP content does not influence the amount of active binder (B. Huang et al., 2005a).
Virgin aggregate shape	When virgin aggregate grains have high angularity, it should be easier to release the aged binder from RAP particles compared to more rounded aggregate (S. Zhao et al., 2015).
Binder additives and admixtures	Recycling agents, anti-stripping agents, or other additives may be mixed with the RAP or added to the virgin binder to soften or activate the RAPb (Bowers, Moore, et al., 2014; Gaitan et al., 2013; Kaseer et al., 2019; Liphardt et al., 2015; Mogawer et al., 2013)
Virgin binder properties	If the virgin binder has low viscosity, it will easily cover RAP particles and improve DoB (Booshehrian et al., 2013; Gottumukkala et al., 2018; Hofko et al., 2016; Nahar et al., 2013; Norton et al., 2014; Rad et al., 2014; Shirodkar et al., 2013, 2011).
	This does not seem to be the case for the research study conducted by Huang et al. (2014).
Filler particles	High quantities of filler particles will absorb a recycling agent before it covers RAP and starts to soften the available RAPb (Al-Qadi et al., 2009; Stimilli et al., 2015).
Aggregate absorption	Aggregate with high porosity will absorb a recycling agent, decreasing the active amount of recycling agent that is considered during the mix design phase (Al-Qadi et al., 2009).
Mixture reheating	Successive heating of asphalt mixtures containing RAP can increase the diffusion process, improving the DoB (Booshehrian et al., 2013).
Surface texture of virgin aggregate	Recycling agent can fulfil convex parts of the grains before blending with the RAPb, decreasing the designed amount of a recycling agent (Cavalli et al., 2016, 2017).
Virgin aggregate (type, source, fraction size)	No influence (Orešković et al., 2017; Stephens et al., 2001)

Table 2.3 *Influencing factors on the DoB: RAP characteristics*

Parameter	Explanation of the influence (or lack of effect) on DoB, and the reference
RAP conditioning time/temperature	Conditioning the RAP for a prolonged time at high operative temperatures seems to be beneficial for softening and activating the RAP binder (He et al., 2016; Rad et al., 2014).
	One research study showed that this is not the case (Gaitan et al., 2013).
RAP binder properties	With the increase of the RAPb stiffness, it will be more difficult to increase the DoB (Booshehrian et al., 2013; Hofko et al., 2016; Kaseer et al., 2019; Nahar et al., 2013; Norton et al., 2014; Rad et al., 2014; Shirodkar et al., 2013, 2011).
	This does not seem to be the case for one research study (S.-C. Huang et al., 2014).

Parameter	Explanation of the influence (or lack of effect) on DoB, and the reference
RAPb film thickness	If the RAPb film is thicker, there will be more binder, which may be activated and blended during the mixing phase, increasing the DoB (Cavalli et al., 2016, 2017; Kriz et al., 2014; Liphardt et al., 2015; Stimilli et al., 2015).
RAP fraction size	Due to the increase of the specific surface area with a reduction in the size of the RAP particles, the amount of RAPb will be higher, which means that more binder will become available for blending (Castorena et al., 2016; Ding, Huang, & Shu, 2016; Stephens et al., 2001; Stimilli et al., 2015).
	However, this does not seem the case for Shirodkar et al. (2011)
RAP Variability	High RAP variability can contribute to an unequal distribution of both RAPb and aggregate causing various DoB within a RAM (Cavalli et al., 2016; Norton et al., 2014).
RAP moisture content	The mixing time is limited during the asphalt mixture production phase, and heating the RAP will first cause the release of water (due to its high moisture content), not the softening of the RAPb (Campher, 2012; Zhang et al., 2015).
Surface texture and the micro geometrical inhomogeneity of RAP aggregate	If the RAP aggregate is geometrically inhomogeneous, the RAPb will be trapped in the convex parts of grains and possibly will not be released during the mixing phase (Cavalli et al., 2016, 2017).

2.1.1.1 The Need for the Degree of Binder Activity

From a careful analysis of the findings reported in Table 2.1-1.3, it is possible to highlight that the blending phenomena is certainly influenced by the selected pre-processing conditions of the RAP: mixing temperature and time, RAP content, RAP type, and applied recycling agent. In all the studies found in literature, the blending phenomena have always been studied in a scenario where the RAP is blended with a recycling agent (hereinafter referred to as "RAP + recycling agent scenario"). This is certainly the most common scenario possible in practice, if not the only so far. However, the "only-RAP scenario" deserves to be considered, especially in the classification of a RAP. Furthermore, Table 2.3 shows that the amount of RAPb made available/active may vary, regardless of the addition of recycling agents. Hence, for the sake of improving RAP characterization and classification, and to perform a more informed design procedure for RAM, the concepts of RAPb availability and DoB must also be linked to an intrinsic property of the RAP only, and the term Degree of binder Activity (DoA), here defined as "*the minimum amount of active RAP binder that a designer can consider for a selected RAP and a selected asphalt mixture manufacturing process*", must be introduced. This is necessary since DoA is an intrinsic property of RAP, unrelated to the presence of recycling agents, and it changes by varying RAP type and processing conditions (i.e. time, temperature).

Degree of binder Activity (DoA): the minimum amount of active RAP binder that a designer can consider for a selected RAP and a selected asphalt mixture manufacturing process.

2.1.2 Theoretical Framework of the Blending Phenomena

A theoretical framework of the blending phenomena will be first explored in this section. The framework identifies quantities whose preliminary determination is fundamental for mix design purposes. Key

mechanisms, relative definitions, and, when possible, formulations of DoA, DoAv and DoB are provided to perform further research towards their validation and the definitions of methodologies to assess the identified key quantities.

2.1.2.1 Key Mechanisms for Aged Binder Activity and Blending

A main assumption of the theoretical framework is that the presence of a recycling agent significantly affects the blending phenomena. So, the framework is here discussed within two scenarios: "Only-RAP" and "RAP + recycling agent".

"Only-RAP scenario": The aged binder is present in two different phases in the RAP: available and unavailable (Figure 2.2). If only RAP is considered in the system, the available RAPb is equal to the active binder and represents the minimum amount of aged binder, that at certain processing conditions (mixing temperature — T, and time — t) can be considered available/active in the formulation of RAM. It consists of two components, and together, they represent the active/available binder (Equation 1.1):

$$W_{activeRAPb}(RAP\ type, t, T) = W_{liquidRAPb} + W_{softerRAPb}\ [g] \hspace{2cm} \textit{Equation 1.1}$$

where $W_{liquidRAPb}$ is equal to the portion of the liquid RAPb that moves from one RAP particle to other RAP particles or virgin aggregates [g], and $W_{softerRAPb}$ is equal to the layer of aged binder that remains stuck for RAP particles while becoming softer and acting as a glue [g].

Alternatively, the amount of aged binder that cannot be considered available in a new formulation is defined as the unavailable/inactive binder (Figure 2.2). This quantity is made of two components:

- "Black rock" RAP binder — the amount of aged binder that has become so stiff and brittle that is considered as part of the RAP aggregate, showing no change in physical-chemical behaviour and properties of itself at certain processing conditions.

- Absorbed RAP binder — the amount of aged binder that is absorbed by RAP aggregate and is not considered effective as a binder film.
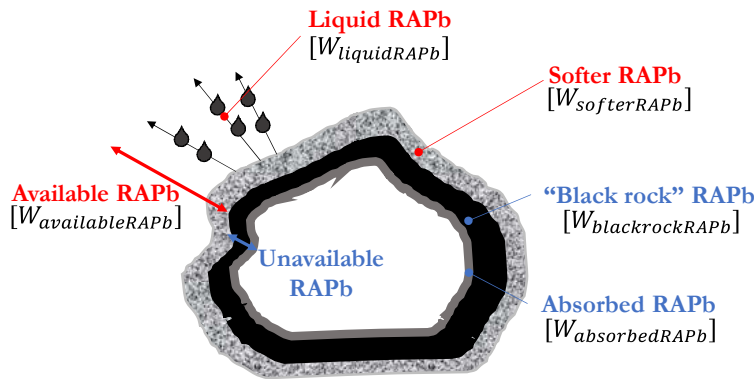
Figure 2.2 *Example of the RAPb components*

Hence, within the system with only-RAP, the total ($W_{RAPb,total}$) and available amounts of RAPb ($W_{availableRAPb}$) for a new formulation are given by Equations 1.2 and 1.3:

$$W_{RAPb,total} = W_{activeRAPb} + W_{inactiveRAPb} = W_{liquidRAPb} + W_{softerRAPb} + W_{blackrockRAPb} + W_{absorbedRAPb}\ [g]\ \textit{Equation 1.2}$$

$$W_{availableRAPb}("only\ RAP - scenario") = W_{activeRAPb}(RAP\ type, t, T)\ [g] \hspace{1.5cm} \textit{Equation 1.3}$$

where $W_{liquidRAPb}$ is the amount of liquid RAPb [g], $W_{softerRAPb}$ is the amount of softer RAPb [g], $W_{blackrockRAPb}$ is the amount of "black rock" RAPb [g], and $W_{absorbedRAPb}$ is the amount of absorbed RAPb [g].

"RAP + recycling agent" scenario:

When any recycling agent is added to the mixture, the available and unavailable binder amounts may change due to further activities that are proportional to the efficiency of the combination of the processing conditions and the recycling agent, as follows:

- Short-term activated binder (STAb): short-term activity happens when the recycling agent comes into contact with the RAPb at fixed processing conditions, resulting in a decrease of the "black rock" and possibly absorbed binder.

- Long-term activated binder (LTAb): long-term activity is due to an eventual diffusion of the recycling agent into the RAPb over time, and it might result in an even bigger decrease of the unavailable RAPb.

The activation of a certain amount of "black rock" RAPb and absorbed RAPb due to the effect of the recycling agent, time, and temperature forms the activated binder, which is here defined as:

$$W_{activatedRAPb}(\text{Rec. ag. type, RAP type, t, T}) = W_{STAb} + W_{LTAb}\ [g] \hspace{2cm} \textit{Equation 1.4}$$

Figure 2.3 clearly shows the difference between the 'active' RAP binder ("Only-RAP" scenario) and the 'activated' binder ("RAP + recycling agent" scenario).
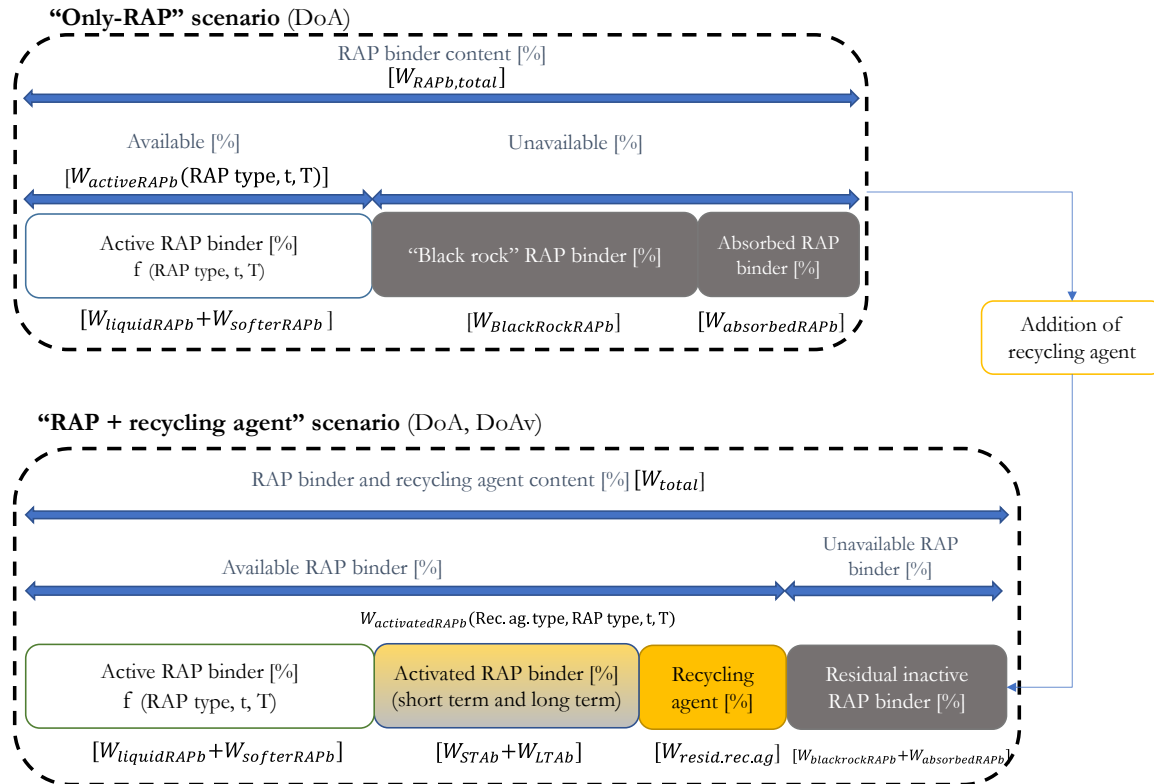
Figure 2.3 *Schematic representation of the theoretical framework of the blending phenomena*

Consequently, in the presence of a recycling agent, the key mechanisms of the "only-RAP" scenario will change. If the recycling agent is effective in activating a portion of the inactive aged binder, the available binder phase will increase due to the short-term and long-term activations (activated binder) as shown in Figure 2.3. Hence, the inactive RAPb can be defined as the amount of aged binder that can only be partially activated by the combined effect of time, temperature, and a recycling agent. Also, the total amount of binder within this scenario (*W_total*), as shown in Equation 1.5, will increase exactly by the amount of recycling agent that will contribute forming the activated binder and will possibly stay in the blend as a residual component. Equation 1.6 presents the formulation of the available amount of binder, considering the intrinsic characteristics of the RAP and the recycling agent effect.

$$W_{total} = W_{liquidRAPb} + W_{softerRAPb} + W_{STAb} + W_{LTAb} + W_{blackrock} + W_{absorbed} + W_{resid.rec.ag} \, [g] \qquad \textit{Equation 1.5}$$

$$W_{availableRAPb}(RAP + rec.ag.) = W_{activeRAPb}(RAP \, type, t, T) + W_{activatedRAPb}(Rec.ag.type, RAP \, type, t, T) \, [g] \quad \textit{Equation 1.6}$$

where W_{STAb} is the amount of short term activated RAPb [g], W_{LTAb} is the amount of long term activated RAPb [g], $W_{blackrockRAPb}$ is the amount of "black rock" RAPb [g], $W_{absorbedRAPb}$ is the amount of absorbed RAPb [g], and $W_{resid.rec.ag.}$ is the amount of a residual recycling agent [g].

2.1.2.2 Degree of Binder Activity (DoA)

Based on the presented framework, the "Degree of Binder Activity" (DoA) can be defined as the ratio between the minimum amount of aged binder that can be considered active for the formulation of the new recycled asphalt mixes (active binder) and the total aged asphalt binder. Hence, DoA is considered here to be an intrinsic property of each RAP material, and it will vary by changing the RAP type and processing conditions (i.e. mixing temperature and time), regardless of the addition of recycling agents before and/or during the RAM manufacturing. The activity is intended to characterize the minimum amount of aged binder that can be considered available in new RAM; hence, it does not need replacing by a recycling agent. The DoA can be expressed as follows:

$$DoA = \frac{W_{activeRAPb}(RA \, type, t, T)}{W_{RAPb,total}} \cdot 100 \, [\% \, mass] \qquad \textit{Equation 1.7}$$

where $W_{activeRAPb}$ is the amount of active RAPb with no influence of a recycling agent ($W_{liquidRAPb}$, and $W_{softerRAPb}$ binders) [g], and $W_{RAPb,total}$ is the total amount of binder in RAP [g] obtained by bitumen extraction according to standards (ASTM D2172/D2172M-17e1, EN 12697-1:2012).

The definition of the DoA is deemed necessary to improve the classification of the RAP materials family, concerning its use in RAM. On this basis, the Task Group "DoA" of the RILEM Technical Committee 264 RAP is currently undertaking an inter-laboratory exercise to provide asphalt technologists with a procedure to assess it (Davide Lo Presti et al., 2017; Tebaldi & Dave, 2015).

2.1.2.3 Degree of binder Availability (DoAv)

Within the only-RAP scenario, the available binder is equal to the active binder; hence, there is no need to determine any other quantity. However, if a recycling agent is added, the amount of binder made available for mix design purposes will change. The extent of change depends on the properties of both the aged binder and the recycling agent, as well as on a series of factors described in Table 2.2 and Table 2.3. Hence, the available binder is believed to be formed by the active binder complemented by the activated binder and the residual amount of recycling agent (Figure 2.3). Therefore, the degree of binder availability (DoAv) will probably be higher than the DoA, and it can be estimated from the following equation:

$$DoAv = \frac{W_{availableRAPb}(RAP + rec.ag.)}{W_{RAPb,total}} \cdot 100 \, [\% \, mass] \qquad \textit{Equation 1.8}$$

Degree of binder Availability (DoAv): The binder available for blending formed not only of the binder activated during the manufacturing process and the residual amount of a recycling agent, but also of the binder activated under the influence of the recycling agent

Assuming the correct DoA/DoAv for a selected RAP is crucial to obtain RAM that complies with specific design standards. In fact, mix design methodologies typically aim to estimate the optimum binder content of a given asphalt mixture; hence, the risk is to use too much or too little asphalt binder for RAM. This will lead to the lower performance of RAMs with high RAP content than traditional ones (Coffey, Dubois, Mehta, Nolan et al., 2013), and, in turn, it will affect the pavement design and durability (Norton et al., 2014, Kaseer et al., 2019) and also increase marine ecotoxicity, fossil depletion, and human toxicity (Bressi et al., 2019). It needs to be underlined that activated RAPb is defined as the sum of a component immediately available during asphalt manufacturing (STAb) and as a component that will be activated

through diffusion (LTAb). Asphalt technologists might need to consider these differences within the design of asphalt mixture incorporating RAP since these components might be available at different stages, whereas ageing might play a significant role in this picture.

2.1.2.4 Towards a Formulation for the Degree of Blending

The presence of a recycling agent will not change the active binder but will most likely change the available binder of a selected RAP. The extent of this effect will, in turn, significantly affect the conventional/rheological properties of the final binder and/or asphalt mixture. Hence, this study aims to clearly separate definitions and proposes a new definition of the Degree of Blending (DoB):

> **Degree of Blending (DoB): an indicator describing to what extent the RAP binder contributes to the final properties of the asphalt mixture's binder blend composed of aged binder and recycling agent.**

This definition permits us to focus on the degree to which the blending efficiency of the available binder, rather than the amount of binder, impacts the properties of the final blend. Although this is fundamental to adapt mix design procedure, formulating the DoB hinders several issues, such as the uncertainty in selecting a property of the binder/mixture (physical, mechanical, rheological) and the hypothesis of full-partial-null blending.

Table 2.4 reports the most recent formulations of DoB from the literature. From a careful analysis, it can be seen that approaches are quite different. Most of them were focused on the binder level by measuring rheological, mechanical, and chemical properties. Analyses of binder require binder extraction, which may give inaccurate results due to the negative impact of the solvent used for binder extraction. Furthermore, some of them force blending between a recycling agent and RAPb, which may also cause inaccurate results.

Due to this complexity, the identification of a formula to describe the DoB is not included in this study. However, conventional/rheological/chemical properties of the RAP binders, as well as the link with DoA/DoAv, should be considered in a possible formulation of the DoB. Further studies should not be restricted to binders only, and they should include testing the RAP, mastics/mortars, and mixtures.

Table 2.4 *Proposed formulas for determination of the DoB from investigated literature*

Reference	Formula
(Shirodkar et al., 2011)	$Blending\ ratio = \frac{\left\|A(virgin_{agg})_{blend\ binder} - A(RAP_{agg})_{blend\ binder}\right\|}{\left\|A_{virgin\ binder} - A_{RAP\ virgin\ binder\ 0\ blend}\right\|}$ *Equation 1.9*

where A(virgin$_{agg}$)$_{blend\ binder}$ is equal to the binder property "A" of blended binder coating the virgin aggregate, A(RAP$_{agg}$)$_{blend\ binder}$ is equal to the binder property "A" of binder blend coating the RAP aggregate, A$_{virgin\ binder}$ is equal to the binder property "A" of the virgin binder; and A$_{RAP\ virgin\ binder\ 0\ blend}$ is equal to the binder property "A" of the RAP and virgin binder that coats the RAP aggregate, assuming 0% blending.

$Degree\ of\ partial\ blending\ (\%) = 100|1 - Blending\ ratio|$ *Equation 1.10*

Reference	Formula	
(Bowers, Moore, et al., 2014)	$Blending\ ratio = \frac{Coarse\ LMS\%}{Fine\ LMS\%}$	*Equation 1.11*
	where *Coarse LMS%* is the LMS% of the coarse aggregate, and *Fine LMS%* is the LMS% of fine aggregate. LMS% is defined by the area beneath the chromatogram obtained by using Gel Permeation Chromatography (GPC). When dividing the chromatogram into 13 slices, the first 5 are considered the LMS and can be expressed as follows:	
	$LMS\% = \frac{Area\ of\ first\frac{5}{13}of\ chromatogram}{Total\ Area\ beneath\ chromatogram}x100$	*Equation 1.12*
(Kaseer et al., 2018)	$PGH_{blend} = (RAP_{BR} \times PGH_{RAP}) + (RAS_{BR} \times PGH_{RAS}) + (B_{BR} \times PGH_{Base})$ *Equation 1.13*	
	where *PGH$_{blend}$* is equal to the high PG temperature of binder blend, *RAP$_{BR}$* is equal to the RAP binder ratio, *PGH$_{RAP}$* is equal to the high PG temperature of RAP binder, *RAS$_{BR}$* is equal to the Reclaimed Asphalt Shingle (RAS) ratio (if used), *PGH$_{RAS}$* is equal to the high PG temperature of RAS (if used), *B$_{BR}$* is equal to the virgin binder ratio, and *PGH$_{Base}$* is equal to the high PG temperature of virgin binder.	
(Yu, Shen, Zhang, Zhang, & Jia, 2017; Shuai Yu, Shen, Zhou, & Li, 2018)	$BR = \frac{\ln(R'_c)-\ln(R_v)}{\ln(R_p)-\ln(R_v)}x100\%$	*Equation 1.14*
	where *BR* is the RAP blending ratio, R'_C is the specific property parameter for a coarse-mixture binder, R_v is the specific binder property parameter for the virgin binder, and R_p is the specific binder property parameter for the proportion binder.	
(Abed et al., 2018)	$DoB\% = \frac{ITSM_{AC-50\%RAP}}{ITSM_{control}} \times 100\%$	*Equation 1.15*
	where *DoB%* is equal to the percentage of the degree of blending between RAP and soft binders, ITSM$_{AC-50\%RAP}$ is equal to the stiffness modulus of AC samples with 50% of RAP, and ITSM$_{control}$ is equal to the stiffness of the control mixture.	
(Ding et al., 2018; S. Zhao et al., 2015)	$\alpha_M = \frac{P_{(b,virgin)} \times RAP\ binder\ (\%)_{blend}}{P_{(b,RAP)} \times (1-RAP\ binder\ (\%)_{blend})}$	*Equation 1.16*
	where α$_M$ is the RAPb mobilization rate, *P$_{(b,virgin)}$* is the percentage of virgin bitumen per total mixture, *P$_{(b,RAP)}$* is the percentage of RAPb by total mixture, and *RAP binder (%)$_{blend}$* is the RAPb content in the blend.	

2.1.2.5 Introducing DoB in Mix Design Procedures

In the era of performance-based design, considering the properties of the final blend is a target is of paramount importance. In fact, AASHTO specification (*AASTHO M323-12*, 2012) prescribes that if less than 15% RAP is used, there should be no change in the virgin binder grade. Furthermore, if RAP content is between 15% and 25%, one grade softer virgin binder should be used, while if more than 25% RAP is added to the mixture, blending charts should be used (Soleymani et al., 1999). Figure 2.4 is an example of a blending chart, which helps in determining the amount of RAP that should satisfy certain binder properties, in this case, high PG temperature, defined as T$_{critical}$. Linking the DoB to the final binder blend properties, therefore, seems to be fundamental, but it is not yet established which properties should be considered.

Another important remark towards the formulation of DoB is that this quantity should be lined with the previously defined DoA/DoAv. In fact, the final properties (mechanical, chemical, physical) of a binder blend may be correctly predicted by using blending charts, but only if they are linked with the real amount of active/available binder from the RAP and, eventually, a recycling agent. Additionally, it was concluded that the blending charts proposed by AASHTO M 323-12 assume that the properties of a binder blend change linearly as the percentage of RAP increases, although it is uncertain whether this will be the case due to the uncertainty in the amount of

Figure 2.4 *Blending chart and predicted law based on high PG temperature (adapted from McDaniel et al. (2000))*

binder "supplied" by the RAP. In support of this, a previous study has shown that linear blending charts have limitations when high percentages of RAP are used (>25%) (Shirodkar et al., 2013).

Al-Qadi, Elseifi, & Carpenter (2007), Hajj et al. (2012), and Stephens et al. (2001) concluded similarly that blending charts, which are based on the assumption of full blending, might be invalid if virgin binder and RAPb do not interact completely.

Since the full blending scenario means that the whole amount of RAPb is blended with the recycling agent, the use of some blending charts may wrongly predict the properties of the final binder blend if they do not consider real DoB. To overcome this issue, Jiménez del Barco Carrión, Lo Presti, & Airey (2015) suggested modifying the mix design methodologies by adapting the calculation of the replaced virgin binder (RVB) considering the uncertainty of the DoB:

$$RVB(\%) = 100 \cdot \frac{RAP\ content\ in\ the\ mixture \cdot DoB \cdot RAP\ binder\ content(1+REJ\ ratio)}{binder\ content\ in\ the\ mixture} \qquad Equation\ 1.17$$

where *RAP content in the mixture* is the total RAP percentage to add in the mixture by weight, *RAP binder content* is the RAPb content, *REJ ratio* is the ratio between rejuvenator and RAPb, *binder content in the mixture* is the designed final binder content in the mixture, and *DoB* is the assumed degree of blending between RAP and virgin binder (60% and 100%) (Lo Presti et al., 2016).

According to these studies, results allow mix designers to verify whether the quality of the selected recycling agents is suitable to obtain a final binder blend achieving the desired properties, while considering the effect of the DoB. Based on this evidence, and keeping in mind that current practices consider mostly the "full blending" approach, it is important to re-define the full-partial-null blending concept, including the link between DoA, DoAv, and DoB (Figure 2.5):

a) DoA = DoAv = 0%   b) 0%<DoA<DoAv<100%   c) 0%<DoA<DoAv<100%
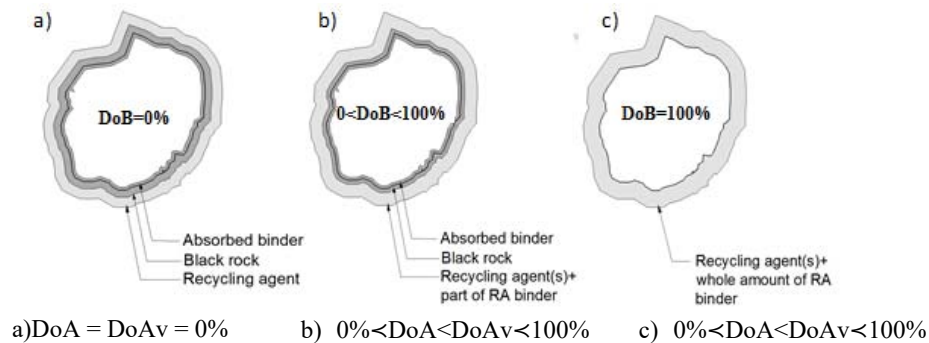
Figure 2.5 *Full-partial-null blending concepts including DoA, DoAv and DoB*

- DoB = 0% or *null blending* is possible only when the RAPb is not active (DoA = DoAv = 0%); so, there is no aged binder available to modify the physical/mechanical properties of final binder blend/mixture (Figure 2.5a).

- 0%≺DoB≺100%, or *partial blending*, presents the case when only a certain amount of RAPb is activated within asphalt mixture (0%≺DoA≺ DoAv≺100%); hence, it only partially contributes to the change in properties of the final binder blend/mixture (Figure 2.5b).
- DoB = 100%, or *full blending*, is an ideal scenario where the amount of RAPb engaged blends perfectly with the recycling agents; hence, the final binder blend/mixture properties are proportional to the amount of RAPb content over the total binder amount in the mixture. It is vital to underline that a full blending scenario could also happen without a full availability scenario (0%≺DoA≺ DoAv≺100%), as it is displayed in Figure 2.5c.

2.2 Quantitative Assessment of the Parameters Linked to the Blending Between Reclaimed Asphalt Binder and Recycling Agent[2]

2.2.1 Investigation Methods for Evaluation/Assessment of DoA, DoAv and DoB

Even in an era in which 100% RAP is used in RAM, some important questions remain to be answered: How much binder is actually activated from RAP within the new asphalt concrete manufacturing process, and how does it blend with the recycling agent? One possible reason why these questions are still un-answered is that assessing the DoA and DoAv of RA and/or the DoB of the blend constitutes a multi-variable problem, with several factors influencing the outcome. However, these parameters are so crucial that identifying suitable methodologies for assessing them would be of key significance in controlling the contribution of aged binder in the RAM and selecting the optimal amount of a recycling agent. This section presents the results of a critical literature review specifically examining methodologies used so far for determining DoA, DoAv and DoB. The most relevant studies that quantify or simply describe these parameters are shown in this section.

Figure 2.6 *Methodologies used for the determination of DoA, DoAv and DoB*

The investigation methods for the determination of blending parameters (DoA, DoAv, and DoB) from previous studies are grouped in four macro-areas related to their approach (mechanical, chemical, visualization and mechanistic), as displayed in Figure 2.6. A mechanical approach includes mechanical blending, binder testing, asphalt mixture testing, and nanoindentation technique. A chemical approach covers spectroscopy and chromatography techniques; visualization approach covers microscopy and computed tomography (CT), and finally, a mechanistic approach includes numerical simulation techniques and modelling techniques.

2.2.1.1 Mechanical Approach

Testing methods where any mechanical act is applied on a testing sample/specimen during a test (i.e. mixing between RAP, aggregate and/or recycling agent; asphalt mixture testing, etc.), belong to mechanical approach for determining blending parameters. This approach includes mechanical blending, binder testing, asphalt mixture testing and nanoindentation techniques. This approach has the highest potential to be used in the assessment of all blending parameters.

2.2.1.1.1 Mechanical Blending
Mechanical blending methods may be used for determining both DoA and DoAv. Within these methods, different fractions of RAP and virgin aggregate are blended, with or without the addition of recycling agents, for a certain period of time under certain conditions.

The coating study (Figure 2.7) presents the procedure: the RAP fine particles are blended with virgin coarse aggregate particles, or without the addition of a recycling agent and then separated using a "threshold" sieve. This coating study aims to estimate the DoA, i.e. the quantity of RAPb mobilized from RAP particles to virgin aggregate particles by only using the mechanical action of mixing under different processing conditions, various RAP content, and fraction size.

Coarse virgin aggregate   Fine RAP   Coarse virgin aggregate coated with RAPb   Fine RAP
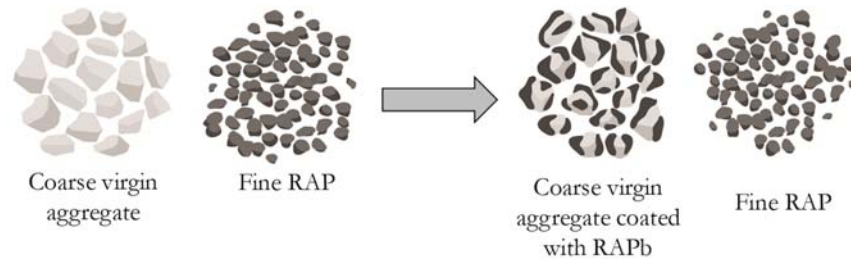
Figure 2.7 *Coating study*

A similar procedure, but with the addition of a recycling agent, is called a blending study (Figure 2.8). It is typically the initial stage of further binder blend analysis used to determine DoAv (B. Huang et al., 2005b; Shirodkar et al., 2011), but it can also be independently used to determine it (Kaseer et al., 2019; Orešković et al., 2017). The blending study may also be performed with the use of an artificial aggregate (i.e. round-shaped gravel, glass, or steel beads) instead of a part of virgin aggregate to analyze DoAv (S. Zhao et al., 2015), although this kind of aggregate does not realistically simulate the situation in the asphalt plant.

Coarse virgin aggregate   Fine RAP   Coarse virgin aggregate coated with RAPb and recycling agent   Fine RAP coated with RAPb and recycling agent

Recycling agent
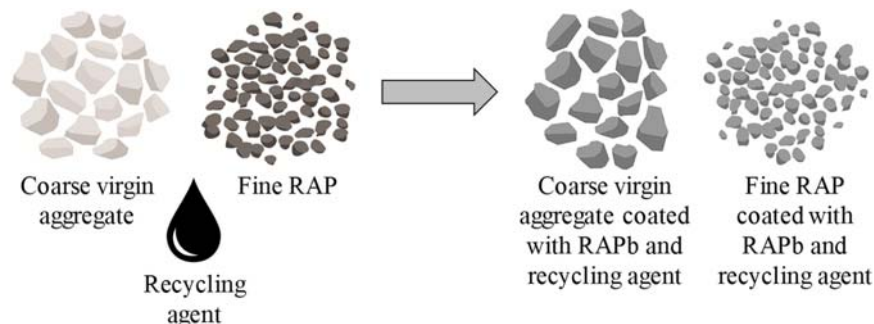
Figure 2.8 *Blending study*

Both procedures were developed by Huang et al. (2005b) and later explained by Shirodkar et al. (2011). The "threshold" sieve size, RAP content, mixing and storage time, and mixing and storage temperatures are variables that may change considerably. These variables have not been defined by a standard procedure; so, they typically depend on the researcher's choice.

Huang et al. (2005b) conducted the coating study using 10%–30% RAP at the mixing temperature of 190°C and the mixing time of 3 min. The DoA was around 11%, regardless of the RAP content. Shirodkar et al. (2011) used 25% and 35% RAP, under different conditions (mixing temperature: 177°C; mixing time: 10 min; storage time: 2 h and 30 min at mixing temperature) and obtained a DoA of 24% and 15%, for 25% and 35% RAP, respectively. Rinaldini et al. (2014) conducted a coating study by blending 50% previously preheated fine RAP particles with 50% of coarse virgin aggregate also preheated at 185°C, obtaining very low DoA values. Gottumukkala et al. (2018) used 20% and 35% RAP within the coating study at the mixing temperature of 160°C and obtained DoA of 12.4% and 10.4%, respectively.

Kaseer et al. (2019) performed a modified blending study, without any further testing, to evaluate DoAv where a virgin mix, consisting of three distinct fractions (coarse, intermediate, and fine), was mixed with virgin bitumen (VB). After blending, the binder content of each fraction was determined. Additional RAP mix was made in the same way but using RAP of intermediate size instead of virgin aggregate. The binder content of each fraction was also determined. The idea behind this concept is that if there is no difference between the binder content of intermediate fractions of both mixtures, DoAv is 100%. Four types of RAMs were later made to verify this approach: soft RAP (without ageing), stiff RAP (5 days ageing at 110°C), very stiff RAP (10 days ageing at 110°C) and extremely stiff RAP (10 days ageing at 110°C plus 3 days at 150°C). Results showed that DoAv was 91.9%, 85.0%, 66.4%, and 39.1% for these mixtures, respectively. In the same study, a couple of different RAP materials were analysed together with the addition of a recycling agent and different conditioning times (2 and 4 h) and mixing temperatures (140°C and 150°C). It was concluded that extending the conditioning time did not significantly increase DoAv that was going from 50% to 95%, and that the addition of recycling agents increased DoAv at the lower mixing temperatures.

To obtain bitumen from RAP, RAM, or materials from blending studies required for testing, it is first necessary to extract and then to recover it. The extraction procedure is usually a single stage, typically used for determining the binder content of an asphalt mixture or binder blend properties, whereas a staged (multistep, multiple) extraction procedure is a widely-used procedure for analysing the different binder layers around the RAP/aggregate particles. During the staged extraction procedure, particles coated with the binder are first soaked into a solvent for the time required to obtain the solution of the binder and solvent. After the first soak, the process is repeated with clean solvent for as many times as necessary, depending on the number of layers that the researchers want to characterize (Figure 2.9).
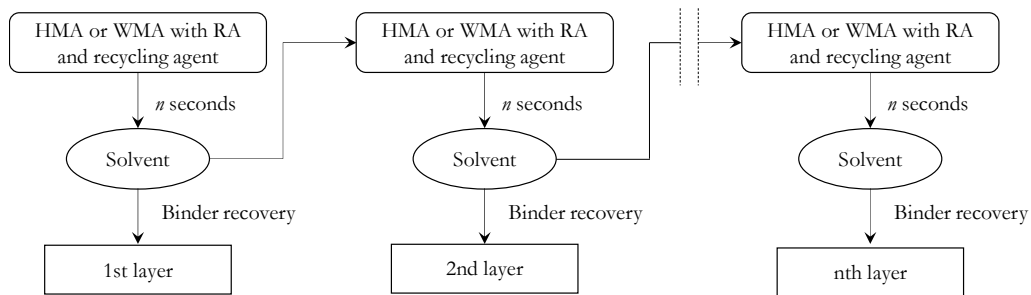
Figure 2.9 *Scheme of the staged extraction procedure*

During the extraction, standard or staged, both RAPb and VB, are soaked in a solvent, forcing their blending on that way. This can distort the determination of DoAv and DoB but may also affect the binder properties due to the influence of the solvent used (Xu et al., 2018). Although this method may provide vital information for estimating DoAv and DoB (Nahar et al., 2013), it needs further investigation to overcome the technical issues mentioned.

After the extraction procedure, the Abson recovery method, rotary evaporator, fractionating column or leaching system can be used to recover the asphalt binder from the solution before subjecting it to any testing.

2.2.1.1.2 Binder Testing

Rheological and physical properties of bituminous binder can provide significant contributions in the determination of DoAv and DoB, frequently in combination with other testing methods. The most commonly used equipment for performing rheological tests are (I) the Rotational Viscometer (RV) for binders at high service temperatures; (II) the Dynamic Shear Rheometer (DSR) at a whole range of temperatures, and (III) the Bending Beam Rheometer (BBR) at low operating temperatures. Output data are expressed in terms of the dynamic shear modulus ($|G^*|$), phase angle (δ), creep stiffness (S(t)), and/or rotational viscosity (η^*).

Gottumukkala et al. (2018) carried out a blending study on mixtures with 20% and 35% fine RAP particles (<4.75 mm) blended with coarse virgin aggregate (>9.5 mm) at 160°C and different virgin binder types. DoAv was evaluated on the binders recovered from both parts after determining the $G^*/\sin\alpha$ and penetration and softening point values, ranging from 16% to 87%, concluding that it depends on the VB type and RAP content. Yu et al. (2017) performed a blending study with fine RAP (<4.75 mm), coarse virgin aggregate (>9.5 mm) and VB. For this study, three mixtures were prepared, with 20%, 40% and 60% RAP, respectively. Rheological parameters (for rutting performance: $G^*/\sin\alpha$, $J_{nr0.1}$, and $J_{nr3.2}$, and for fatigue performance: $G^*\sin\delta$) were measured to assess DoAv, which was found to be, on average, 30%, 83%, and 72% for mixtures with 20%, 40%, and 60% RAP, respectively.

Stephens et al. (2001) used steel ball bearings to break RAMs with 15% and 25% RAP into fine and coarse particles to investigate DoB. Tests were performed on binders recovered from both fractions using DSR and BBR. DoB was not quantified, but it was concluded that the RAP aggregate source does not influence DoB, whereas the RAP quantity significantly influences it.

Shirodkar et al. (2011) performed a blending study on mixtures with 25% and 35% RAP where fine RAP (<2.36 mm) and coarse virgin aggregate (>4.75 mm) were blended with VB previously preheated to mixing temperature. The quantity of VB used in the blending study was determined as the difference between the appropriate designed binder content from the job mix formula and the estimated DoA obtained during after coating study from the same research. After blending, binders were recovered from both parts, and their properties ($|G^*|$ and δ) were determined. At the same time, the specific surface area of fine RAP aggregate was calculated, using Bailey's method, to determine the proportion of VB and RAPb that would coat the fine RAP aggregates under zero-blending conditions. Those amounts were then blended and exposed to short-term ageing before determining their properties ($|G^*|$ and δ). DoAv was estimated by comparing rheological properties of the recovered and blended binders: 70% for the mixture with 25% RAP, and 96% for the mixture with 35% RAP.

Gaitan et al. (2013) carried out the same procedure, comparing HMA and WMA with 25% RAP but using different testing conditions (mixing and conditioning time and mixing temperatures). It was concluded that the DoAv of WMA is higher than that of HMA (82–85% compared to 59%) due to the presence of a recycling agent. Also, it was observed that mixing time increases DoAv, whereas conditioning time and mixing temperature did not affect it.

Bressi et al. (2015) carried out a blending study where 50% and 90% RAP (0/4 mm and 0/16 mm, respectively) was preheated for 1 h at 135°C, whereas the coarse virgin aggregate (4/22 mm and 16/22 mm, respectively) was preheated for 3 h at 180°C. After preheating, these fractions were blended with VB and left in the oven at 180°C for 30 min. Binder was recovered from the coarse part that retained on the threshold sieve, and it was assumed that the RAPb of the coarse part was blended with VB if the $|G^*|$ value of the blend was higher than the $|G^*|$ value of VB. Results showed only a small amount of the RAPb was mobilized during the blending process.

Rinaldini et al. (2014) performed a blending study using 50% fine RAP particles (2.4/4 mm) in combination with coarse aggregate (8/11 mm) and 5% VB. Also, two more mixtures were prepared: one containing a coarse virgin aggregate fraction and VB, and a second one containing only the fine RAP.

Rheological tests were performed on binder blends recovered from the fine RAP and coarse virgin aggregate, as well as on binders recovered from the other two mixtures. DoAv was not quantified within this research, but the dynamic modulus master curves showed that a certain amount of RAPb was additionally activated under the influence of the VB.

Liphardt et al. (2015) went a step further from the assessment of DoAv and DoB based on the $|G^*|$ value and used the Multiple Stress Creep Recovery (MSCR) test. Binder tests were performed on the binders recovered after a staged extraction procedure from an asphalt mixture containing only RAP and VB. Although the DoB and DoAv were not quantified, it was concluded that there was no full blending. Also, MSCR showed high potential in the assessment of DoAv and DoB, especially if one of the binders is polymer-modified.

2.2.1.1.3 Asphalt Mixture Testing
Performances of asphalt mixtures may be predicted by carrying out the mixture performance tests, such as the wheel tracking test, the SUPERPAVE shear test, the indirect tension test, fatigue tests, etc. The comparison of various mixtures' performances, using the same test conditions, has been used in several studies to isolate the influence of RAP on RAM's performance (Al-Qadi et al., 2009; McDaniel et al., 2000; Mogawer et al., 2012). Since this approach may be useful in determining the influence of a certain parameter (e.g. RAP content, recycling agent type and content, etc.) on mixture performance, it has the highest potential to be used in estimating DoB.

Stephens et al. (2001) used an unconfined compression test and indirect tension test to determine the influence of RAP heating time, binder type, and aggregate source on the DoB of RAMs with 10–25% RAP. It was concluded that more complete blending occurs in RAM if the RAP reaches a temperature high enough to soften the aged binder and make it available for blending with the recycling agent.

Stimilli et al. (2015) developed an analytical method combining the performance-based equivalence principle and a specific surface area of aggregates from the mixture, assuming that amount of activated RAPb was proportional to the re-activated binder film thickness. The performance-based equivalence principle was based on the assumption that the "working" binder content in a virgin asphalt mixture and RAM are the same if the mechanical performances of both mixtures are comparable. Four RAMs were prepared for this research: one reference mixture, with 25% unfractionated RAP (0/16 mm), three mixtures with 40% fractionated RAP (one with coarse RAP fraction (8/16 mm), one with fine RAP fraction (0/8 mm), and one with combined coarse and fine fractions. Results showed that the reference mixture and mixtures with fine and combined fractions had approximately the same DoAv (70%), whereas the mixture with coarse RAP fraction had a lower DoAv value — around 50%. Furthermore, it was concluded that the proposed methodology overestimates the real amount of re-activated binder in the mixture with a high amount of fine RAP particles because a certain amount of RAP particles often tend to agglomerate together, in that way possessing a lower surface area than the one calculated from the original RAP aggregates obtained after binder extraction. The significant difference between real and calculated surface area may be a consequence of the applied surface area factors (Duriez, Hveem, Bailey's), which consider grains as a sphere or as a cube, whereas the RAP clusters introduce irregularities in the calculation of a specific surface area. Research results of this study were later confirmed by Bressi et al. (2016), with recommendations to adjust these factors, considering the real shape of the clusters.

Abd et al. (2018) used specially prepared cylindrical specimens of a gap-graded hot rolled asphalt mixture containing 40% RAP for testing in modified DSR equipment to estimate DoB. Although it was not quantified, the results showed that there was no complete blending between RAPb and VB, except in the case when a lubricant was used at higher mixing temperatures.

Abed et al. (2018) prepared RAMs with 50% RAP and 160/220 binder grade as rejuvenators, varying the RAP preheating temperature (95–135°C) and mixing time (1–5 min) to assess their influence on DoB, measuring the indirect tensile stiffness modulus (ITSM). Results showed that, depending on the processing conditions, DoB varied from partial to almost full blending: at low mixing time (1 min) and temperature (95°C), DoB was around 36%, whereas, at sufficiently high mixing temperature (135°C) and long mixing time (5 min), DoB was 96%.

2.2.1.1.4 Nanoindentation Technique

Nanoindentation is a technique that can be used for assessing the mechanical properties of a material at nano/micro-scale. The indentation process consists of three phases: loading, holding, and the unloading of a diamond tip on the material surface with a typical device configuration displayed in Figure 2.10. Based on a measured tip displacement, material properties (elastic modulus, stiffness, hardness, etc.) can be determined. It cannot be easily used for assessment of any of blending parameters, but it can help in measuring binder film thickness, which is frequently correlated with DoB.

Mohajeri et al. (2014) performed a nanoindentation test on a stone-binder-stone interface to determine DoAv and investigate the blending zone between the soft and hard binder. Figure 2.11 shows the three zones recognized: two stone zones, and one binder zone consisting of a soft and hard binder. The interface between two binders was not clearly identified, and it was impossible to measure DoAv, although the binder film thickness between stones could be precisely measured.
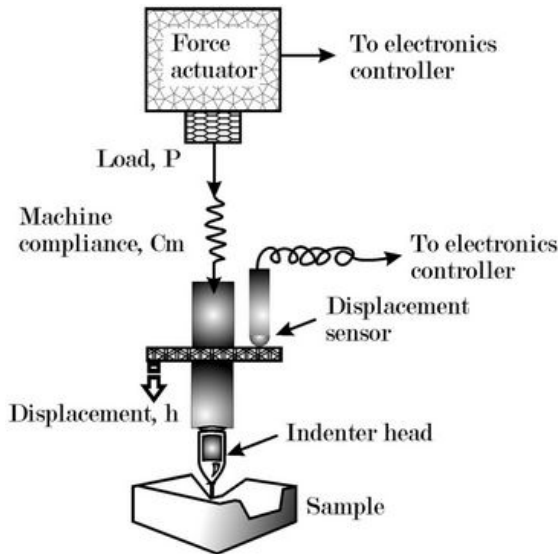
Figure 2.10 *A typical nanoindenter setup (Tiwari, 2012)*
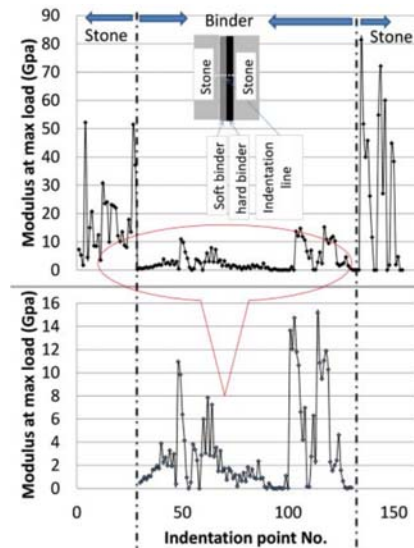
Figure 2.11 *Nanoindentation test results from a stone-binder-stone interface, adapted from Mohajeri et al. (2014)*

Abd et al. (2018) used a nanoindentation technique to determine DoB, concluding that the effect of the aggregate type on DoB can be neglected because the measured mechanical properties of RAP aggregate were almost the same as properties of the virgin aggregate. This confirmed the results of the binder testing in the same study — that there was no complete blending between RAPb and VB, except when a lubricant was used.

2.2.1.2 Chemical Approach

The chemical approach is based on the use of chemical techniques to analyse the composition of a binder. Binder for testing may be recovered from RAM, RAP, or mixtures obtained from a blending study, but it may also be analysed, without extraction, directly from a mixture. Having in mind that the chemical properties of bitumen change over the time under the influence of external factors (oxidation, water, etc.), and that recycling agents may help in the recovering of chemical properties. This approach becomes inevitable in the assessment of blending parameters. It includes two techniques: chromatography and spectroscopy.

2.2.1.2.1. Chromatography

Gel Permeation Chromatography (GPC) is a type of Size Exclusion Chromatography (SEC) used to separate molecules of a solution into various sizes. Typically, the relative molecular weight of polymer samples and the distribution of molecular weights are determined within this technique. Using this technique may also help to distinguish between RAPb from VB due to the higher amount of large molecules present in aged binders when compared with VB. This is frequently achieved using the large molecular size (LMS) percentage parameter.

The LMS parameter presents the area of the first five slices over all the other 13 slices beneath the chromatogram derived from the GPC (Figure 2.12). Within previous research, LMSP has been correlated with the binder absolute viscosity and dynamic shear modulus, showing its potential for use in DoAv/DoB investigations (S. Zhao et al., 2014).
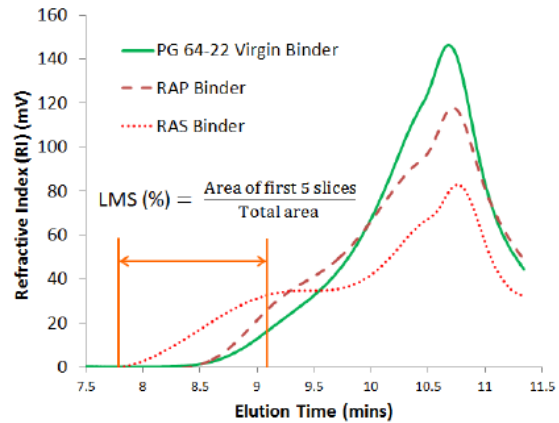
Figure 2.12 *GPC chromatograms and Calculation method, adapted from Zhao et al. (2015)*

Zhao et al. (2015) used round-shaped gravel as a tracking material to isolate the binder blended during the mixing phase of RAMs with different RAP content (10% to 80%). Results showed that DoB decreases with increasing RAP content, going from almost 100% for 10% RAP to approximately 24% for 80% RAP.

The same group of authors applied GPC on the binders recovered from coarse virgin aggregate and fine RAP aggregate obtained after the blending study (S. Zhao et al., 2016). DoAv was not quantified, but it was proven that the binder blend coating the virgin aggregate was more uniform than the binder blend surrounding RAP aggregate due to the un-mobilized binder still attached to the RAP.

Bowers et al. (2014) were investigating the influence of mixing temperature and time and WMA additives on DoAv by testing binders recovered from laboratory-prepared mixtures with 65% RAP after a blending study. Results showed that mixing time of 5 min should ensure 100% of DoAv, although it is not a realistic timeframe for mixing at a plant. Also, it was mentioned that increased mixing temperature increases DoAv, from 59% at 130°C to 76% at 180°C, and that lubricants may have a positive impact on it. Furthermore, the authors concluded that "black rock" phenomenon does not exist.

2.2.1.2.2 Spectroscopy

Fourier Transform Infrared Spectroscopy (FTIR) is a measurement technique that can be used to obtain an infrared absorption or emission spectrum of a solid, liquid, or gas. The FTIR spectrometer simultaneously collects high-spectral-resolution data over a wide spectral range and determines functional groups within a medium.
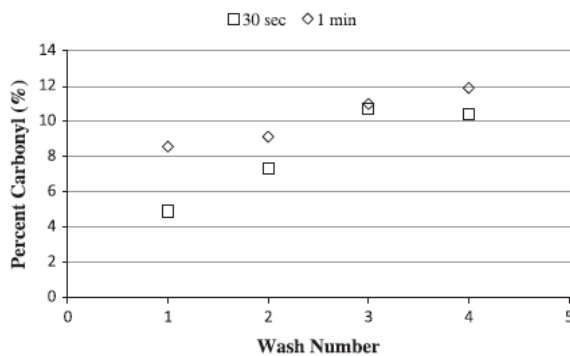
Figure 2.13 *FTIR evaluation of carbonyl increase in blend with artificial RAP, adapted from Bowers et al. (2014)*

Bowers, Huang, et al. (2014) tried to estimate DoAv by preparing an artificially aged binder by ageing a VB through a Rolling Thin Film Oven Test (RTFOT), followed by double Pressure Ageing Vessel (PAV) ageing. Further, 9.5 mm gravel had been mixed with VB and artificially aged binder for 2 min at 180°C, and a staged extraction procedure was then applied (immersion time was 30 s or 1 min). FTIR was further used on extracted binder blends to compare the ratio of the carbonyls (C=O) and the saturated C-C vibration. The objective of this method is to evaluate the degree of binder oxidation because an increase in the carbonyl indicates the oxidation (ageing) of the asphalt

binder. Within the study, it was discovered that the carbonyl content is higher as the binder layer is closer to the aggregate, leading to the conclusion that the binder blending was not completely uniform (Figure 2.13). Also, the higher percentage of carbonyl for the inner layer is a consequence of the aged binder presence. These results confirmed the findings from the same study obtained by using GPC.

A similar procedure, called the "leaching blending test", was performed by Delfosse et al. (2016). The test is also based on a staged extraction procedure, where the Carboxyl index[3] was determined through an infrared spectrum analysis of the leachates. Test results showed that HMAs containing 20% and 35% RAP, with PMB and straight-run asphalt binder, respectively, had high levels of DoB.

Ding et al. (2016) investigated three plant-produced RAMs with 50% RAP (one WMA and two HMA, one with a rejuvenator and one without) to characterize DoB. The FTIR procedure was applied on the binders recovered from different sizes of aggregate particles (passing No. 4 sieve (4.76 mm), passing ¾ in. sieve (19 mm) and retained on No. 4 sieve (4.76 mm), and retained on ¾ in. sieve. (19 mm)). This study could not exactly assess the DoB of each mixture, but it was possible to compare them using the so-called Ageing Index (AI). AI was defined as the ratio between the area of the carbonyl (C=O) band and the area of the saturated C-C stretch band. Testing results showed that WMA had the highest DoB and that a rejuvenator slightly improved the DoB of HMA.

Sreeram et al. (2018) used FTIR to assess both the DoAv and DoB of RAMs with 15%–50% RAP. Borosilicate glass beads of different diameters were used to isolate the binder from RAP and RAMs for further testing. Results showed that the DoAv was dependent on the mixing temperature and RAP content: it was around 5%, 15%, and 20% at a mixing temperature of 135°C and around 10%, 20%, and 40% at a mixing temperature of 165°C in mixtures with 15%, 30%, and 50% RAP, respectively. The measured DoB was more prone to the influence of temperature than to RAP content. It was varying from 50% to 60% for the samples prepared at 165°C, and from 30% to 40% for the samples prepared at 135°C.

Energy-dispersive X-ray spectroscopy (EDXS, EDX, EDS or XEDS) is the technique that allows obtaining information concerning the chemical composition of a sample (Sharma, 2012). Since the EDS (Castorena et al., 2016; Jiang et al., 2018) and EDX (Cavalli et al., 2017) equipment have been used as additional equipment to electron microscopes (visualization approach), their application within the field of blending parameters assessment is analysed in the next section.

2.2.1.3 Visualization Approach

Visualization methods at different scales have been used to investigate the uniformity of asphalt mixtures or to observe a certain place within a mixture rather than to quantify DoA, DoAv or DoB. These methods do not usually measure the physical, mechanical, or chemical properties of a material, but they may be used as auxiliary methods, mostly for describing DoB. However, some of the methods and equipment used to investigate DoB are microscopy techniques (optical, electron, fluorescence, and atomic force microscopy) and computed tomography (nano and micro-level). Figure 2.14 illustrates an overview of the different scales that have been used in some of the previous studies.
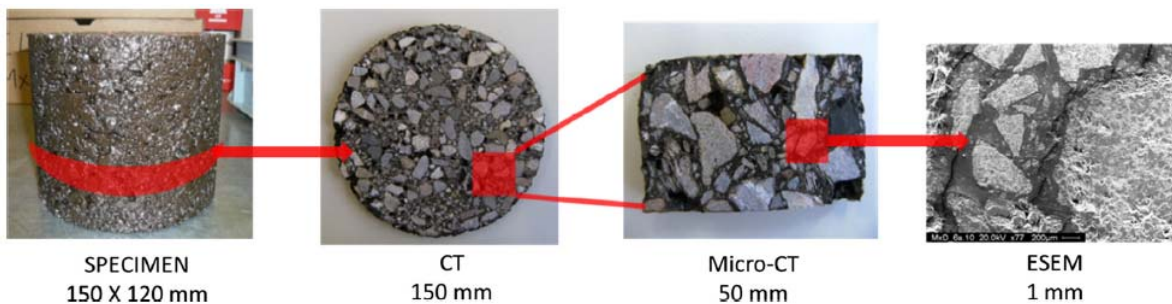
Figure 2.14 *Overview of the different investigation scales, adapted from Rinaldini et al. (2014)*

---

[3] A ratio between the area under 2 reference peaks (Methyl and Ethyl function wavenumber 1460 cm^{-1} and 1376 cm^{-1}), and they are under the studying peak -CO.

2.2.1.3.1 Microscopy

Scanning Electron Microcopy (SEM) can reveal information about the texture, chemical composition and crystalline structure of a sample, with magnification from 20 to 30000 times. In the field of pavement research, it has been used to determine the binder film thickness between aggregate particles Scanning Electron Microscopy (SEM) can reveal information about the texture, chemical composition, and crystalline structure of a sample, with magnification from 20 to 30000 times. In the field of pavement research, it has been used to determine the binder film thickness between aggregate particles (Al-Qadi et al., 2009; Bressi, Dumont et al., 2016) and to investigate if the VB and RAPb could be homogenously identified (Al-Qadi et al., 2009). This method is not typically suitable for quantifying DoB because it provides results based on singular spots, but it

Figure 2.15 *The crack formation between small RAP aggregates and large virgin aggregate, adapted from Rinaldini et al. (2014)*

may help in the observation of the binder blend homogeneity, and it may be used as an additional method to verify DoB.

In one research study (Navaro et al., 2012), an attempt was made to evaluate the DoB process through the homogeneity of the binder blend under different mixing temperatures and times. The image analysis protocol was conducted on images taken under white light (WL) and ultraviolet light (UVL). The main conclusion was that the homogeneity of RAM depends on the mixing temperature more than on the mixing time without precise determination of the DoB level.

A combination of the rheological tests, computed tomography, and electron microscopy was found to be promising for investigating DoB within asphalt mixtures (Rinaldini et al., 2014). This research shows that blending of the VB and the RAPb is commonly heterogeneous and that this technique cannot clearly quantify DoB, confirming the findings of Mohajeri et al. (Mohajeri et al., 2014), but it allows for the detection of micro-cracks in the intra-binder surface (Figure 2.15).

Energy-dispersive X-ray spectroscopy was used to analyse DoB in the RAM with large clumps of adhered RAP particles and in RAM with fractionated RAP (Castorena et al., 2016). Titanium dioxide was used as a tracer to understand the occurrence of blending between RAPb and VB. It was discovered that the mixture containing pre-processed RAP allowed lowering the formation of RAP clusters and, consequently, higher DoB. The same conclusions have been reported by Bressi et al. (2015).

Furthermore, Jiang et al. (2018) have been the first who quantified the DoB in RAMs using SEM and EDS. They proposed the element mass ratio of titanium over sulphur as a quantitative indicator of DoB in compacted RAM. DoB was assessed to be around 100% in RAM with 15% RAP, regardless of the ageing conditions. Additionally, it was concluded that DoB decreases with increasing RAP content and increases with ageing: in RAM with 30% RAP, DoB ranged from 78% under normal conditions to 90% after long-term ageing, whereas in RAM with 50% RAP, it ranged from 43% to 78%. In the same study, it was also concluded that the use of RAs significantly improves DoB, leading to the almost complete blending between RAPb and RA.

Fluorescence microscopy is a technique that uses the emission of fluorescence to study properties of organic or inorganic substances. It was employed to estimate the DoB of two plant-produced HMA, with and without a recycling agent, and one WMA with foaming technology, all containing 50% RAP (Ding et al., 2018). The binder recovered from the RAP was further blended with a VB at various contents and tested with fluorescence microscopy to develop blending charts using a newly developed mean grey value (MGV[4]) parameter, which was implemented in the Equation 1.16. The DoB was measured on aggregates obtained after blending study, whereas the overall The DoB of the asphalt mixture was estimated by

---

[4] MGV presents the average fluorescence strength of a fluorescence image derived from image post-processing.

combining MGV and the specific surface area of the RAM's aggregates. HMA mixtures with and without rejuvenator had a DoB of around 85%, whereas the WMA mixture had a DoB of around 92%, probably due to the positive impact of foaming technology on the RAPb activation.

Atomic Force Microscopy (AFM) is a scanning probe technique that reveals the surface topography and heterogeneity of materials with high spatial resolution. It can be used to characterize RAPb, VB, and their blending zone. Nahar et al. (2013) observed the presence of the blending zone at the interface of the two binders of different grades by using AFM images. It was stated that the DoB was 100% at the interface of RAP and VB, but only in a transition area. Furthermore, the extent of the blending zone will likely depend on parameters such as temperature, binder type, and contact time (Figure 2.16).

Xu et al. (2018) used AFM on the binder obtained after staged extraction of RAM with 50% RAP. Results confirmed previous studies' (Bowers, Huang, et al., 2014; B. Huang et al., 2005b) conclusions that non-homogeneous blending occurs between RAPb and VB and that higher DoB was found in outside layers than in the inner. Also, it was discovered that temperature and storage time have a crucial impact on the DoB in RAMs.
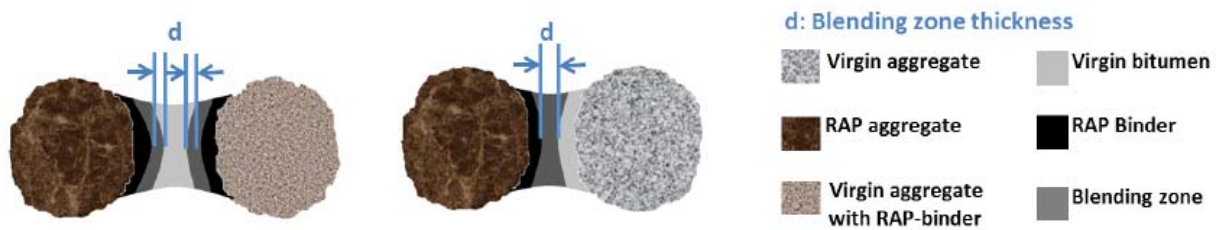
Figure 2.16 *Possibilities for the formation of a blended zone between the RAP and virgin aggregate, adapted from Nahar et al. (2013)*

2.2.1.3.2 Computed Tomography

Computed tomography (CT) uses many X-ray measurements, taken from various angles, to produce cross-sectional images of a scanned object or area without cutting the sample. There are several variations of CTs. The Environmental Scanning Electron Microscopy (ESEM) has been typically used for microscale characterization, and X-ray Computed Tomography (XCT) has been used for macro scale characterization. XCT inspects interior and exterior material structures, whereas microcomputed tomography (micro-CT) enables the achievement of higher spatial resolution than XCT. These techniques have not helped to quantify the DoB in previous studies, but they have been successfully used to describe it.

Rinaldini et al. (2014) concluded that XCT allows observation of the virgin and RAP materials grouped in homogenous, but distinct, clusters. XCT results confirmed the ESEM micrographs, obtained in the same study, that concluded that DoB is locally dependent. Mohajeri et al. (2014) did not succeed to differentiate binders in the RAM using nano-tomography scanning images but succeeded to determine the film thickness.
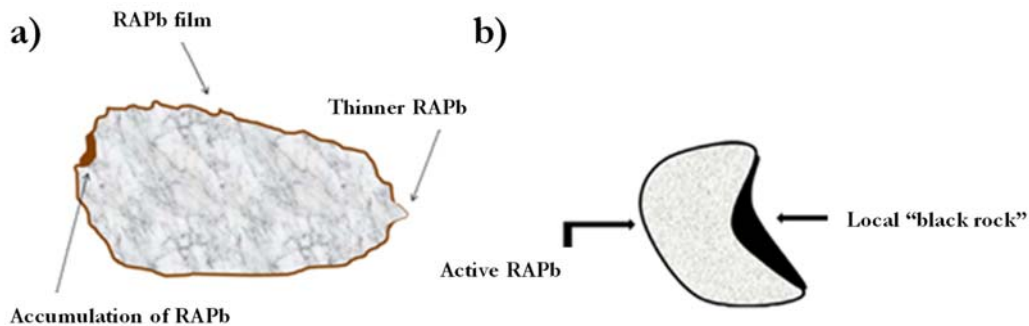
Figure 2.17 *Influence of local curvature on (a) the RAPb thickness and (b) the RAPb reactivation, adapted from Cavalli et al. (2017)*

Cavalli et al. (2016) used ESEM and XCT to investigate RAMs with 50% RAP, concluding that RAPb thickness tends to decrease by increasing the mixing temperature, which is in agreement with the assumption that the decrease of RAPb thickness is a consequence of the increased DoB level. It was also observed that increased local curvature of the aggregates may influence the RAPb film thickness (Figure 2.17a) and the RAPb reactivation (Figure 2.17b). The results of this study, regarding mixing temperature and micro geometrical inhomogeneity, were confirmed in the following research study (Cavalli et al., 2017).

2.2.1.4 Mechanistic Approach

The mechanistic approach does not include any laboratory tests. Within this approach, research results obtained from other approaches are combined to estimate the DoA, DoAv, or DoB. This approach covers modelling and numerical simulation techniques. For example, an experimental procedure of the coating study may be simulated using the Finite Element Method (FEM) to predict DoA.

2.2.1.4.1 Modelling Techniques
This approach uses different procedures to evaluate DoB by comparing the measured dynamic modulus of asphalt mixtures ($|E*|$) with predicted one (Bonaquist approach (Bonaquist, 2005)).

This technique usually consists of the following steps: first, the dynamic modulus of asphalt mixture $|E*|$ is measured; afterwards, the binder is recovered from the same mixture and $|G*|$ is measured in DSR; the data are then further applied to the Hirsch or similar model, together with volumetric properties of the mixture, to estimate the mixture's $|E*|$ value, which is later compared with the measured $|E*|$ value, where a high correlation of the data indicates a high DoB.

Mogawer et al. (2012) investigated HMA's with 20–40% RAP, whereas Mogawer et al. (2013) used mixtures with 40% RAP. In both cases, the Bonaquist approach was applied, showing that DoB may be affected by the production parameter (discharge temperature) and improved if recycling agents are used. Booshehrian et al. (2013) explained how to carry out this procedure, step-by-step, and tested mixtures with 20–40% RAP. Results showed that both the reheating process and discharge temperature affect the DoB, which was described as a good thing. Delfosse et al. (2016) tried to estimate the DoB of the HMA mixtures with 20% and 35% RAP and WMA with 20%, 40%, 50%, and 70% RAP. The differences between measured and estimated values of $|E*|$ were –4.5% and –3% for HMA mixtures, respectively, and –8.5%, 15%, –2.5% and –45% for WMA mixtures, respectively, suggesting that the estimation model should be improved, especially when the DoA is poor.

The same conclusion was obtained by Al-Qadi et al. (2009), leading to the conclusion that the Hirsch model may not be appropriate to back-calculate $|E*|$ from HMA with RAP and that DoB could not be accurately determined using this method. Ashtiani et al. (2018) reached a similar conclusion, but with an estimation that DoB, which varied between 40% and 60% in RAM with 15% RAP.

The first attempt at using a micromechanical model to examine DoB was carried out by Gundla & Underwood (2015). Temperature and frequency sweep tests were conducted on mastics containing 10–100% RAP that passed through a sieve opening of 0.075 mm. DoB was herein quantified as the amount of non-absorbed RAPb combined into a meso-homogeneous mass with the recycling agent. DoB was estimated by the comparison of $|G*|$ value, predicted by using micromechanical modelling and measured $|G*|$. Predicted $|G*|$ values were obtained by combining rheological results and the film shell assumption. Results show that DoB decreases with increasing RAP content: 100%, 66%, 55%, and 31% for the RAP content of 10%, 30%, 50%, and 100%, respectively.

2.2.1.4.2 Numerical Simulation Techniques
Discrete element method (DEM) presents a numerical technique for modelling of material performance under different conditions by using a large number of independent particles.

Zhang et al. (2015) conducted a coating study using different RAP contents (10%–50%), virgin aggregate temperatures (160–190°C) and RAP moisture contents (0–5%) to investigate their impact on DoA. Further, the particles movement and the applied forces (contact and the force of gravity) were simulated using the three-dimensional DEM (Figure 2.18). Simulations results confirmed the laboratory results: DoA was dependent on RAP content, mixing temperature, and time and moisture content. With an increase of RAP content and RAP moisture content, DoA decreases, whereas it increases as the virgin aggregate temperature increases. Regarding DoA, DEM results showed higher values (0.41%, 1.07% and 0.30% RAPb) when compared with laboratory results (0.16%, 0.21%, and 0.16% of RAPb) in mixtures with 10%, 30%, and 50% RAP, respectively, probably due to the limitations of the method (single-sized RAP particles were used during modelling). It was also concluded that the mixtures with higher RAP content,

Figure 2.18 *Comparison of mixing performance between laboratory test results (left) and simulation results (right), adapted from Zhang et al. (2015)*

higher moisture, and lower virgin aggregate temperature need a longer mixing time or higher virgin aggregate temperature to increase DoA. Overall, DEM has shown the potential for evaluating the qualitative effects of the RAP content and virgin aggregate temperature on DoA.

2.2.2 Summary of DoA, DoAv, and DoB determination approaches — Critical Discussion

Despite the research efforts dedicated to investigating the performance of aged binder in RAMs, there are no common and standardized procedures for quantifying the blending parameters. Due to this fact, a summary of the different methods used for these purposes is prepared, as presented in Table 2.5. The table shows the review of research studies that contributed to quantifying these parameters, whereas research studies where these phenomena were only described are not shown. Testing methods, levels of testing (index t), preparation (index p), or both (index p,t), RAP content, and whether recycling agents (excluding neat asphalt binder) were used or not, are shown as well. Furthermore, Table 2.5 shows the terms that were originally used in the cited papers and the terms according to the newly proposed definitions from the theoretical framework proposed by Lo Presti et al. (D. Lo Presti et al., 2019). Finally, the estimated values of the parameters are also given.

From Table 2.5, it can be seen that DoA was most often quantified by using mechanical blending methods, while DoAv was quantified mostly by using both mechanical blending and binder testing methods. DoB has not been frequently quantified in previous studies, but asphalt mixture testing and microscopy testing methods are probably the most promising.

Table 2.6 was tailored for summarizing the main advantages and disadvantages of the procedures described in this section. The same table also recommends which techniques and methods can be used for determining the individual values of each parameter.

Table 2.5 *Overview of the methodologies for the assessment of DoA, DoAv and DoB*

Reference	Original term	DoA	DoAv	DoB	Estimated value [%]	Mechanical blending	Binder testing	Asphalt mixture testing	Nanoindentation	Chromatography	Spectroscopy	Microscopy	Computed tomography	Modelling techniques	Numerical simulation techniques	Binder (blend)	RAP and aggregate	RAP, aggregate and recycling agent	Mastics	Asphalt mixture	Addition of RA (except neat ...)	RAP content [%]
						Mechanical approach				**Chemical approach**		**Visualization approach**		**Mechanistic approach**		**Level**						
(Kaseer et al., 2019)	RAPb availability factor		✔		50-95	✔												✔$_{p,t}$				30
(Zhang et al., 2015)	Binder transfer	✔			4-24										✔			✔$_{p,t}$				10-50
(Ding et al., 2018)	Mobilization rate		✔		84-92							✔						✔$_t$		✔$_p$	✔	50
(Zhao et al., 2015)	RAPb mobilization rate		✔		24-100					✔						✔$_t$				✔$_p$		10-80
(Stimilli et al., 2015)	Reactivated RAPb		✔		49-74			✔					✔					✔$_{p,t}$				25-40

Reference	Original term	DoA	DoAv	DoB	Estimated value [%]	Mechanical blending	Binder testing	Asphalt mixture testing	Nanoindentation	Chromatography	Spectroscopy	Microscopy	Computed tomography	Modelling techniques	Numerical simulation techniques	Binder (blend)	RAP and aggregate	RAP, aggregate and recycling agent	Mastics	Asphalt mixture	Addition of RA (except neat)	RAP content [%]
(Gaitan et al., 2013)	Degree of blending		✔		59-85	✔										✔t	✔p				✔	25
(Gundla & Underwood, 2015)	Blending			✔	31-100	✔												✔p,t				10-100
(B. Huang et al., 2005b)	RAPb loss	✔			11	✔											✔p,t					10-30
	Blended binder		✔		40		✔									✔t	✔p					
(Shirodkar et al., 2011)	RAPb transfer	✔			15-24	✔											✔p,t					25-35
	Degree of partial blending		✔		70-96	✔	✔									✔t	✔p					
(Gottumukkala et al., 2018)	Transferred binder	✔			10-12	✔											✔p,t					20-35
	Blending ratio		✔		16-87	✔	✔									✔t	✔p					

Reference	Original term	DoA	DoAv	DoB	Estimated value [%]	Mechanical blending	Binder testing	Asphalt mixture testing	Nanoindentation	Chromatography	Spectroscopy	Microscopy	Computed tomography	Modelling techniques	Numerical simulation techniques	Binder (blend)	RAP and aggregate	RAP, aggregate and recycling agent	Mastics	Asphalt mixture	Addition of RA (except neat)	RAP content [%]
(S. Yu et al., 2017)	Blending ratio	✔			21-83	✔	✔									✔t		✔p			✔	20-60
(Abed et al., 2018)	Degree of blending		✔		37-95			✔												✔p,t	✔	50
(Bowers, Moore, et al., 2014)	Blending ratio	✔			50-76					✔						✔t		✔p			✔	65
(Sreeram et al., 2018)	RAPb mobilization	✔			5-40	✔					✔					✔t		✔p				15-50
(Sreeram et al., 2018)	Blending efficiency		✔		30-60		✔				✔					✔t				✔p	✔	15-50
(Jiang et al., 2018)	Blending ratio		✔		43-100							✔								✔p,t	✔	15-50

Table 2.6 *Advantages and disadvantages of testing method summarized by recommended approaches*

Approach	Testing method/technique	Advantages	Disadvantages
Mechanical approach	Mechanical blending	• Testing equipment is present in almost every pavement laboratory. • Tests are usually easy to perform and do not require a lot of time and resources. • Results are easy and quick to analyze. • Due to simplicity, it is easy to repeat tests under different conditions (mixing time, temperature, RA content, etc.).	• It does not simulate realistic situation from an asphalt plant, as well as the use of an artificial aggregate (steel balls, round-shaped gravel, etc.). • Cannot be performed on RAM obtained from an asphalt plant. • Influence of a recycling agent on DoA/DoAv cannot be easily determined without further tests, which typically require bitumen extraction.
	Recommendation:	• DoA: ✓ • DoAv: ✓ • DoB: ✗	
	Binder testing	• Testing equipment is present in almost every pavement laboratory. • Tests are usually easy to perform and do not require a lot of time and resources. • High potential in analysing of bitumen levels surrounding RAP particles, which may help in determining DoAv.	• Preparation of testing samples is time-consuming if staged extraction procedure is applied. • There is no standardized procedure for staged extraction. • Bitumen should be recovered from the solvent, whereas it may negatively impact the chemical properties of bitumen. • Forced blending between the RAPb and VB during the extraction procedure might not always reflect what is happening during the mixing phase within a mixture.
	Recommendation:	DoA: ✗ DoAv: ✓ DoB: ✓	
	Asphalt mixture testing	• Testing equipment is present in almost every pavement laboratory. • Tests are usually daily routine in laboratories and do not require many resources to perform. • Highest potential in determining DoB because testing samples may be obtained by coring from the field or by compacting RAM obtained from a plant.	• There is not yet a proposed property of RAM that will assess DoB. • If asphalt samples are obtained from a plant, it is difficult to vary processing conditions (mixing temperature, mixing time, etc.).
	Recommendation:	DoA: ✗ DoAv: ✗ DoB: ✓	

Approach	Testing method/technique	Advantages	Disadvantages
	Nanoindentation	• The bitumen film thickness, frequently correlated with DoB, can be precisely measured.	• Testing equipment is not routinely available in pavement laboratories. • Not directly linked with any other parameter. • Testing results are not simple to analyse. • Civil engineers have a lack of experience in this field of research.
	Recommendation:	DoA: ✖ DoAv: ✖	DoB: ✓
Chemical approach	Chromatography Spectroscopy	• Testing time is relatively short (up to 30 min) and does not require a huge amount of material. • Chemical characteristics of RAPb can be determined and help to evaluate the DoAv or DoB. • The presence of recycling agent, polymer or solvent in binder blend can be detected. • The impact of a recycling agent on the chemical properties of bitumen can be determined.	• A key mixture's parameters are usually related to microstructure; so, these types of tests are not yet typical for the pavement industry. • The analysis of testing results may be complicated and time-consuming. • Tests are typically performed on binders obtained after the extraction procedure, causing the same problem as with mechanical methods – forced blending and the negative influence of solvent. • The parameters used to evaluate DoAv and DoB are not yet widely established.
	Recommendation:	DoA: ✖ DoAv: ✓	DoB: ✓
Visualization approach	Microscopy	• Non-destructive methods. • There is a possibility to combine a couple of methods (e.g. with EDS) to determine DoB. • The use of tracer materials allows the determination of the distribution of RAPb throughout RAMs, thus verifying the existence of the blending phenomenon and overall, at least describing DoB. • The interface between RAPb and VB can be observed and cracks detected.	• The use of tracers is not reasonable during the production of RAM at an asphalt plant. • Equipment is expensive and not widespread in pavement laboratories. • Handling is complex, and the analysis of testing results is time-consuming. • Requires additional knowledge from image analysis.
	Recommendation:	DoA: ✖ DoAv: ✖	DoB: ✓

Approach	Testing method/technique	Advantages	Disadvantages
	Computed tomography	• The analysis of samples is possible without their destruction. • The existence of the blending phenomenon and at least describing DoB are possible.	• Equipment is expensive, not widespread in pavement laboratories. • Handling is complex, and the analysis of testing results is time-consuming.
	Recommendation:	DoA: ✘ DoAv: ✘	DoB: ✔
Mechanistic approach	Modelling techniques	• The testing methods required for the determination of $|G^*|$ and $|E^*|$ are usually carried out routinely in laboratories, on laboratory prepared or field cored specimens. • Back-calculation can be conducted very quickly. • Obtained results strongly depend on the properties of material's components and testing conditions, which may be simulated using modelling techniques. • These techniques may able to quantify DoB, although it has been typically used for the description of DoB.	• They are typically a combination of different testing methods; so, it may be time-consuming. • A wider knowledge of researchers/technicians for testing and interpretation of the results is required. • Due to the inhomogeneity of the RAP, most of these methods are not reliable enough. For example, Bailey's method should be adjusted when RAP is used due to the presence of irregular grains. Furthermore, due to the different behaviour of RAPb, the Hirsch model might not provide an appropriate estimation of the mixture dynamic modulus.
	Recommendation:	DoA: ✘ DoAv: ✘	DoB: ✔
	Numerical simulation techniques	• High potential to be used in assessment of blending parameters. • Processing conditions can be easily changed in simulations.	• There are many parameters which should be considered during simulation (contact forces between particles, behavior of binder blend, etc.). • Laboratory tests may be required in order to obtain input parameters. • High variability of RAP may cause problems with models.
	Recommendation:	DoA: ✔ DoAv: ✔	DoB: ✔

2.3 Conclusions and Recommendations

Blending RAPb with a recycling agent is still a partially known phenomenon. The results of this section indicate that although key concepts are clear, in the scientific community, the blending phenomena is not yet totally clear. The lack of clear definitions of mechanisms and quantities creates confusion and overlapping, ultimately playing against the paramount shift towards RAMs. The study proposes a critical literature review of the factors influencing the blending phenomena, Degree of Blending (DoB) and Degree of Availability (DoAv), and, consequently, introduces the definition of the Degree of Binder Activity (DoA) as an intrinsic property of the RAP. Definitions and formulations of DoA and DoAv are reported, whereas the DoB was recognised to be still too complex to provide a specific formulation.

Hence, a review of recent formulations of DoB and its relation with DoA and DoAv is provided. As a result of this process, the asphalt technologist should now have a comprehensive theoretical explanation of the blending phenomena, a practical framework, and a nomenclature that, if validated, could improve mix design procedures for RAM, as well as the classification of RAP.

Common guidelines and protocols for determining so-called blending parameters (DoA, DoAv, and DoB) would contribute to support performance-based design practices and eliminate problems with the use of too much or too little of a recycling agent in RAMs, thus allowing a confident increase of reclaimed asphalt content. However, there is still a challenge to develop methodologies that will help in determining these parameters.

Within this process, it is first necessary to work on characterizing RAP, and second, to work on adapting methodology of mix design procedure that would allow for this new family of material to be considered as any other material in asphalt mixture production. This section aimed to review and identify the best methodologies for measuring these parameters, which may be vital for the improvement of the current practices.

General conclusions regarding methodologies for determining the DoA, DoAv and DoB are as follows:

- There are no overall accepted procedures for determining any of these parameters; thus, new standard test method(s) should be developed, or one of the existing methods should be adopted to make them measurable for mix design purposes.

- Measured values of these parameters varied substantially in previous studies due to various RAP sources, different testing and processing conditions, and various methodologies used.

- Some of the previous research studies, which quantified these parameters, should be repeated with other materials to validate these methods.

- Correlation between testing methods should be established since it is not always possible to conduct all the methods proposed.

During the development of new methodologies, it is essential to consider influencing parameters, such as mixing time, temperature, and the presence of recycling agents because they are not unequivocally defined; so, the correlations between them should be established. Furthermore, since most of the research studies conducted so far have been conducted at a laboratory level, future works should consider linking the laboratory mix design with field trials.

Chapter 3. Research Methodology

The research conducted within this study consists of four parts:

1) Characterization of the componential materials
2) Determination of the optimal preheating temperature of RAP
3) Development of the mix design methodology of HMA with high RAP content
4) Performances of asphalt mixtures

3.1   Characterization of the Componential Materials

In this study, the following componential materials were used:

- filler

- virgin aggregate

- virgin bitumen (VB)

- recycling agents (RA)

- reclaimed asphalt pavement (RAP)

All componential materials were sampled from a single source to avoid the introduction of additional variables within tests. In the first part of the study, componential materials were primarily characterized using standardized testing procedures. The experimental plan for this part of the research is given in Figure 3.1.

In this study, limestone filler, "Rujevac" — Ljig, was used, and its basic properties were evaluated:

- particle size distribution

- particle density

- Rigden voids

- assessment of fines (methylene-blue test)

Limestone aggregate from the quarry, "Podbukovi", consisted of the four fractions (0/4 mm, 4/8 mm, 8/16 mm, and 16/22 mm) and was used as a virgin aggregate in the study. Next, the properties of each fraction were determined as follows:

- 0/4 mm: sand equivalent, particle density, water absorption, and particle size distribution

- 4/8 mm: particle density, water absorption, and particle size distribution

- 8/16 mm: particle density, particle size distribution, and resistance to fragmentation

- 16/22 mm: particle density and particle size distribution
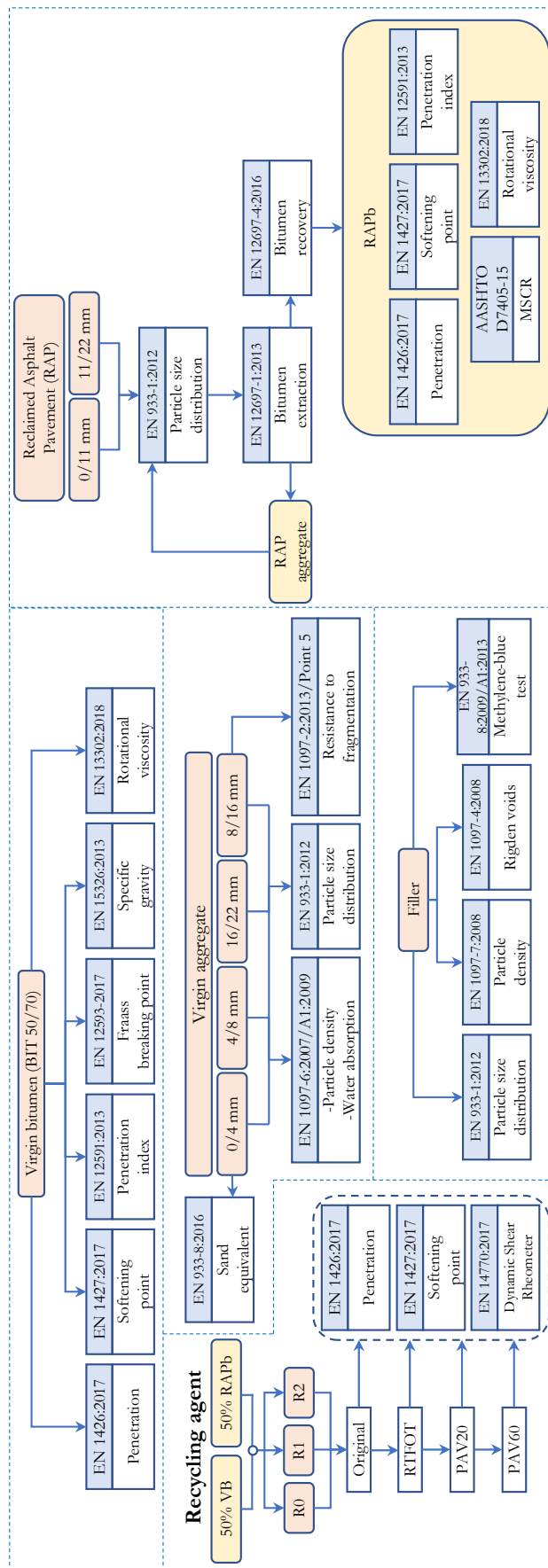
Figure 3.1 *Experimental plan of the componental materials testing*

Plain paving bitumen (type 50/70) from the Pančevo Oil Refinery was used as the virgin bitumen in this study. The following basic properties of the virgin bitumen were evaluated:

- penetration
- softening point
- penetration index
- Fraass breaking point
- specific gravity
- rotational viscosity

The RAP was collected from a stockpile near Belgrade. After collection, it was sieved into two fractions (0/11 mm and 11/22 mm), and the grading curves of both fractions were determined before their extraction (black curve). After their extraction, the bitumen content of each fraction was determined, as well as its grading curves (white curves). The RAPb was then characterized by determining the following properties:

- penetration
- softening point
- penetration index
- rotational viscosity
- $J_{nr,3.2}$ and %R values (after MSCR test)

Three types of recycling agents were initially selected to be used in this study. Two of them were industrial products, whereas the third is of an alternative origin (waste cooking oil). Their properties were not determined in this study, but their durability in binder blends with 50% RAPb is assessed. The penetration, softening point, complex shear modulus, and phase angle of each blend were measured in its original state, after short-term ageing, long-term ageing (20 h in PAV), and prolonged ageing (60 h in PAV). Finally, a recycling agent contained in a binder blend, which has shown the best properties after prolonged ageing time, was selected for use in the rest of the study.

3.2 Optimal Preheating Temperature of RAP

A methodology for the determination of the optimal preheating temperature of RAP, with and without RA, is proposed in the second part of the research (Section 5.2). Additionally, the degree of binder activation of RAP is also estimated. The experimental plan of the section is given in Figure 3.2.

For this part of the investigation, three types of RAMs were prepared:

- An only-RAP mixture composed of 100% RAP, previously preheated at temperatures between 70 and 190°C.
- A RAP+RA mixture composed of 100% RAP and RA (10% respecting the RAPb content), previously preheated at temperatures between 70 and 170°C.
- A reference RAP composed of extracted RAP aggregate and bitumen in the same ratio as in previous mixtures, in that way simulating full binder activation.

All RAMs in this part, as well as in the rest of the study, had grading curves as close as possible to the control mixture. Asphalt concrete used for base course layers, with a nominal grain size of 22 mm and neat virgin bitumen (AC22 BASE 50/70), was selected as control mixture in this study because base course layers have the highest potential for using high RAP content.

Four specimens of each mixture were compacted in Marshall and gyratory compactors with 2x50 blows and 30 gyrations, respectively, after preheating at different temperatures. The following properties of these specimens were further evaluated:

- air void content

- stiffness

- ITS

- cracking tolerance index (CT_{index})

The obtained testing results were initially used to estimate the DoA by comparing the properties of the only-RAP mixture with the properties of the reference RAP mixture.

In the last stage of this part, the probabilistic optimization method was applied to calculate the optimal preheating temperature of RAP, depending on the RA presence, integrating the uncertainties in determining the different properties through Monte Carlo (MC) simulation.
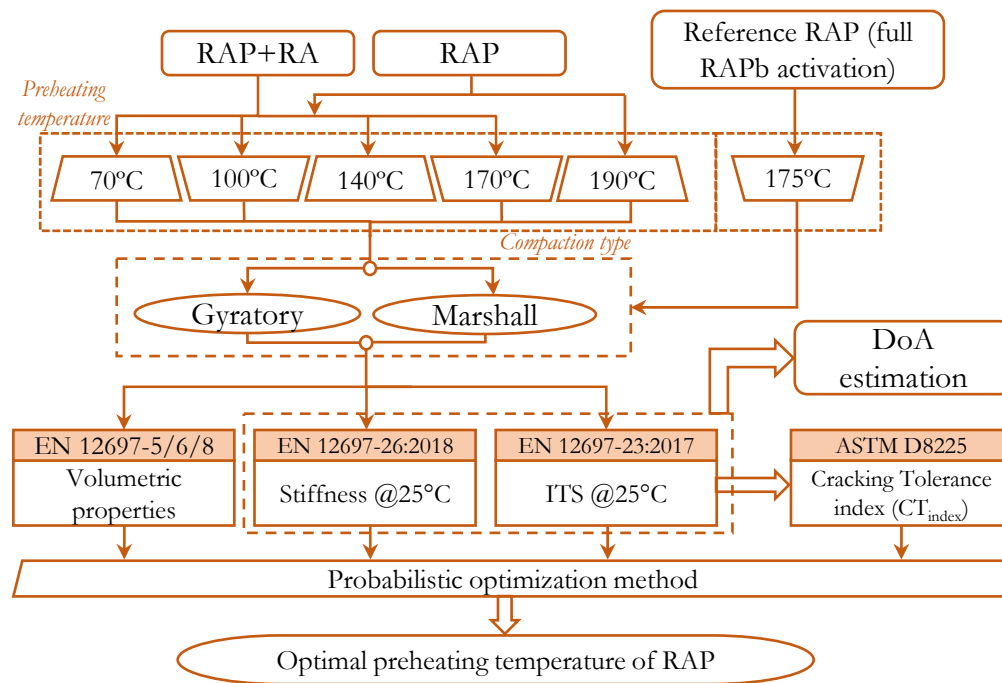
Figure 3.2 *Determination of the optimal preheating temperature of RAP – experimental plan*

3.3 Mix Design Methodology of Hot Mix Asphalt with High RAP Content

Mix design methodology of RAM with 50% RAP, which aims to determine optimal contents of VB and RA, is developed in the third part of the research (Section 5.2). The experimental plan of the mix design development is displayed in Figure 3.3.

Seven asphalt mixtures with 50% RAP, preheated at a temperature determined in the previous part, and different amounts of VB and RA were prepared according to Doehlert experimental design. Four specimens of each mixture were compacted using a Marshall compactor, and the same properties were evaluated as in the previous section.

Testing results were further used to validate multiple variable models using Response Surface Methodology. Different steps of statistics of the regression (Analysis of Variance, Goodness of Fit, and Lack of Fit) were computed on the developed models, together with preparation of two additional mixtures, to validate the developed models. Finally, the optimal contents of the RA and VB of the asphalt mixture with 50% RAP were determined.
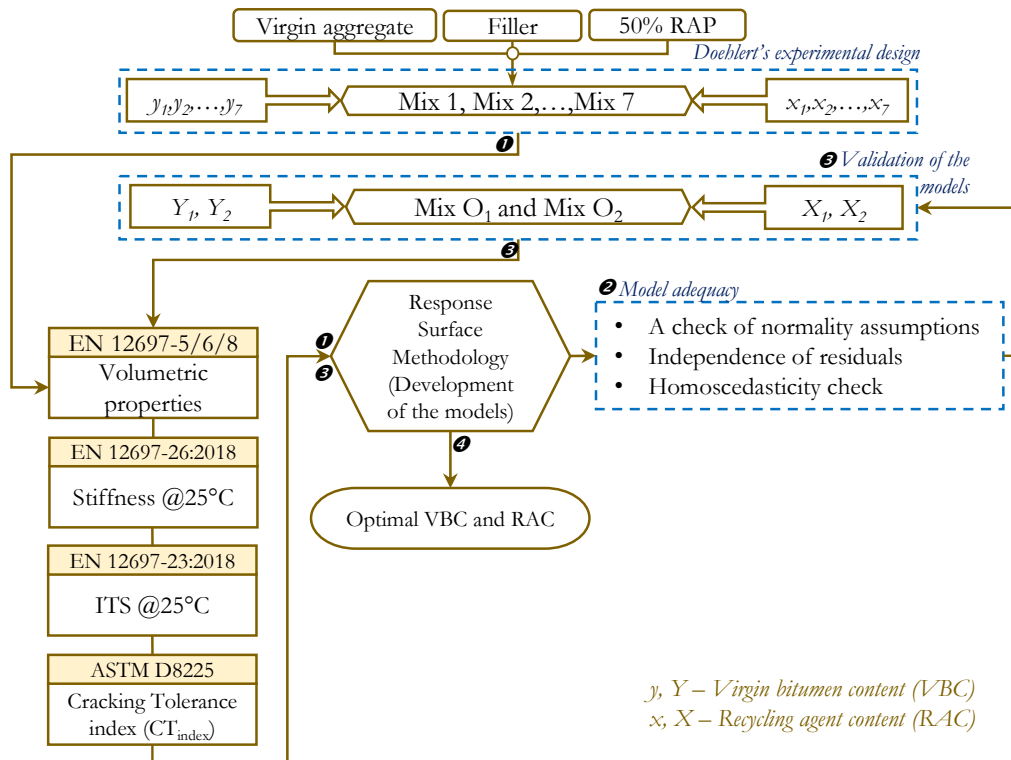
Figure 3.3 *Experimental plan of the mix design methodology development*

3.4 Performance of Asphalt Mixtures

To assess if the developed RAM with 50% RAP is properly designed, its performances were evaluated and compared with the same performances of the control mixture and the RAM with 15% RAP according to the experimental plan displayed in Figure 3.4. The following performances of each mixture were evaluated:

- volumetric properties
- water sensitivity
- freeze-thaw resistance
- resistance to permanent deformation (rutting resistance)
- fatigue resistance
- cracking tolerance index (CTindex)

The water sensitivity of the asphalt mixtures was determined according to EN 12697-12:2018, Method A.

In this study, freeze-thaw resistance was assessed by using the repeated Lottman test (AASHTO T283), which measures the effect of moisture and freezing on the ITS of the asphalt mixture and has a more aggressive impact on asphalt specimens compared to the European standard for water sensitivity (EN 12697-12).

The stiffness of the asphalt mixtures was measured according to EN 12697-26, Annex C, by applying the indirect tensile test on cylindrical specimens (IT-CY).
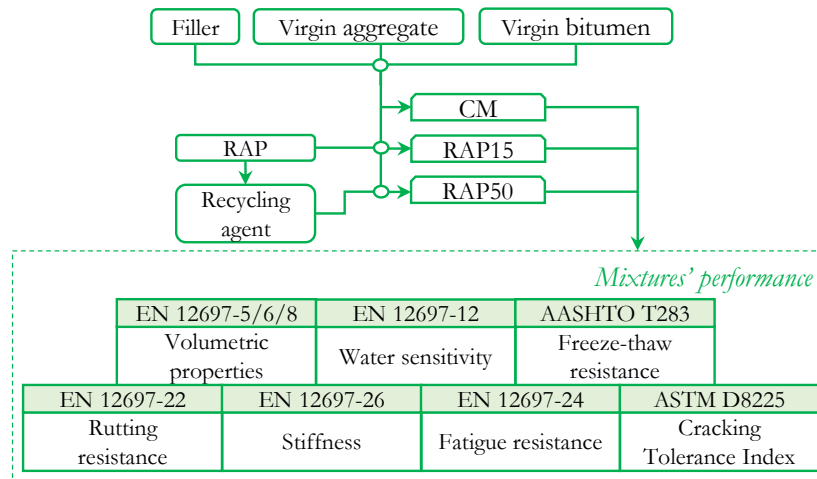
Figure 3.4 *Determining the properties of asphalt mixtures – experimental plan*

Chapter 4. Materials, Specimen Preparation and Testing Methods

4.1 Materials

4.1.1 Filler

Limestone filler was used for the production of asphalt mixtures. The particle size distribution and physical properties of the filler are given in Table 4.1 and Table 4.2.

Table 4.1 *Particle size distribution of the filler*

Sieve size [mm]	Standard	Percentage passing [%]
0.063		83.9
0.09	EN 933-1:2013	89.3
0.25		99.3
0.71		100

Table 4.2 *Physical properties of the filler*

Property	Unit	Standard	Testing results
Particle density	Mg/m^3	EN 1097-7:2008	2.705
Void content of dry compacted filler (Rigden voids)	%	EN 1097-4:2008	31.3
Methylene-blue value	g/kg	EN 933-9:2009+A1:2013	0.45

4.1.2 Virgin Aggregate

The virgin aggregate (of limestone origin) used in this study was extracted from the Podbukovi quarry near Valjevo (Figure 4.1), and it consists of four fractions: 0/4 mm, 4/8 mm, 8/16 mm and 16/22 mm.

Figure 4.1 *Podbukovi quarry* [5]

The particle size distribution and physical and mechanical properties of all fractions were determined for this study, and the results are shown in Table 4.3, whereas the grading curves are displayed in Figure 4.2.
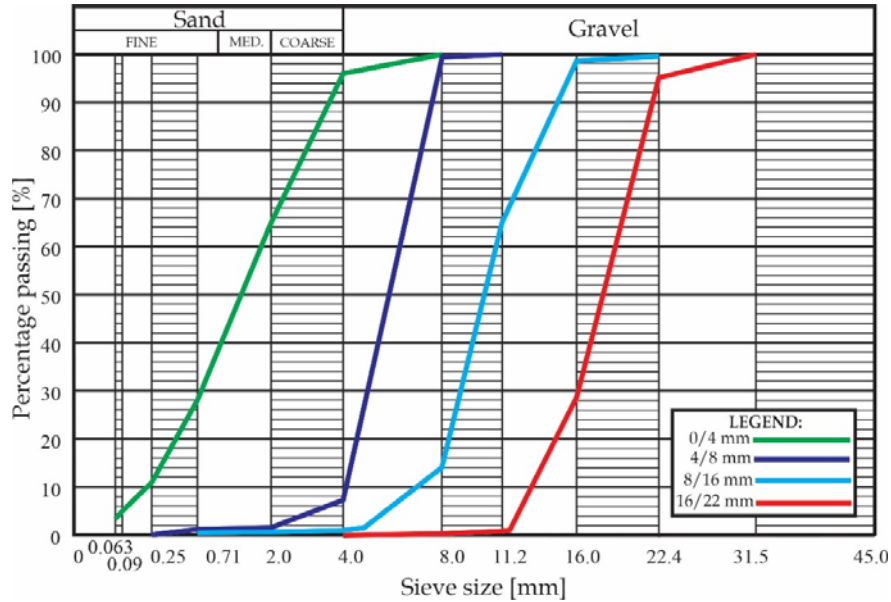
Figure 4.2 *Grading curves of virgin aggregate fractions*

Table 4.3 *Properties of the virgin aggregate fractions*

Property		Unit	Standard	Fraction [mm]			
				0/4	4/8	8/16	16/22
				Percentage passing [%]			
	Sieve size						
	0.063			3.1	0.1	0.0	0.1
	0.09			4.7	0.2	0.2	0.4
	0.25			10.4	0.9	0.6	0.7
	0.71			28.1	1.0	0.6	0.8
Particle size distribution	2.0			64.6	1.5	0.6	0.8
	4.0	mm	EN 933-1:2013*	95.8	7.2	0.6	0.8
	8.0			100	99.2	16.0	0.8
	11.2				100	65.7	1.1
	16.0					98.5	28.9
	22.4					100	95.1
	31.5						100
Oven-dry particle density (ϱ_{rd})		Mg/m^3	EN 1097-6:2007/A1:2009	2.720	2.718	2.710	2.710
Water absorption (WA$_{24}$)		%		0.3	0.5	-	-
Resistance to fragmentation (LA coefficient)		%	EN 1097-2:2013/Point 5	-	-	23.8	-
Sand equivalent (SE)		%	EN 933-8:2016	68.8	-	-	-

Standard proposes wet sieving, but in this case dry sieving was performed.

4.1.3 Virgin Bitumen

Plain paving bitumen (penetration grade 50/70), from the Pančevo Oil Refinery, was used as the virgin bitumen in this study. The basic properties of the virgin bitumen are shown in Table 4.4, including rotational viscosity, which was measured, according to EN 13302:2018, at elevated temperatures (from

135°C to 175°C, with increments of 10°C) and a single frequency of 0.59 Hz. The rotational viscometer and testing results are displayed in Figure 4.3 and Figure 4.4, respectively.

Table 4.4 *Properties of the virgin bitumen*

Properties	Unit	Standard	Testing results
Penetration	0.1 mm	EN 1426:2017	60.0
Softening point	°C	EN 1427:2017	48.0
Penetration index	-	EN 12591:2013, Annex A	-1.293
Fraass breaking point	°C	EN 12593:2017	-13
Specific gravity	Mg/m^3	EN 15326:2013	1.023
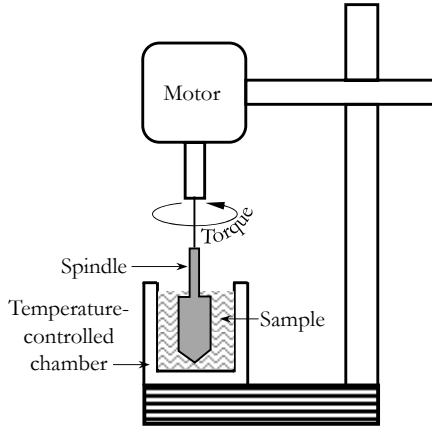
Figure 4.3 *Rotational viscometer*
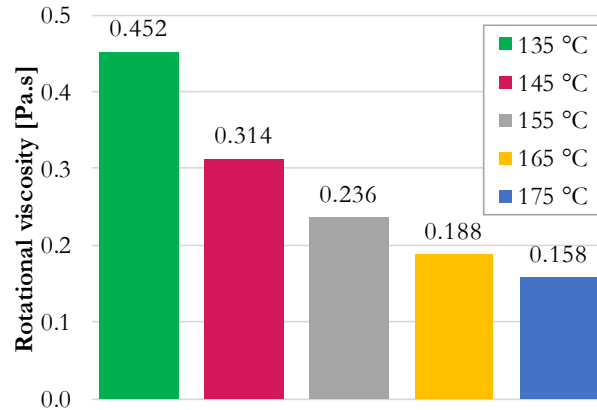
Figure 4.4 *Rotational viscosity of the virgin bitumen at elevated temperatures*

4.1.4 Reclaimed Asphalt Pavement

Reclaimed asphalt pavement was obtained primarily by the milling of the existing surface and binder courses of the E-75 motorway through Belgrade. It was collected at the asphalt plant in Bubanj Potok near Belgrade. Because of high variability of the RAP in landfills (Figure 4.5, lower row), where it was stockpiled without separation, it had been sampled at several locations and then separated into two fractions, 0/11 mm and 11/22 mm, to achieve higher quality control and reduce the variability in the RAP composition, as recommended by Don Brock & Richmond (2006). The following properties of both fractions were determined:

- bitumen content
- particle size distribution of the RA before extraction (Black curve)
- particle size distribution of the RA after extraction (White curve)
- RAP bitumen properties

The particle size distribution of each RAP fraction before the extraction procedure ("black curve") was determined according to EN 933-1:2013 (Appendix I and Figure 4.6 — Red and black curves). The aged bitumen was then extracted from both fractions according to EN 12697-1:2013, and the bitumen content of each fraction was determined (5.75% and 4.59% of bitumen in 0/11 mm and 11/22 mm fractions, respectively). The grading curve of the RAP aggregate after the bitumen extraction ("white curve") was determined according to EN 933-1:2013 (Appendix I and Figure 4.6 — Blue and green curves). Four repetitions were done of each test, and the average values and standard deviations are given in Appendix I. Figure 4.6 displays the average black-and-white grading curves of each fraction, including the minimum and maximum passing percentages obtained, from which it can be seen that both fractions have little variability.

Figure 4.5 RAP landfill near Belgrade (Bubanj Potok)
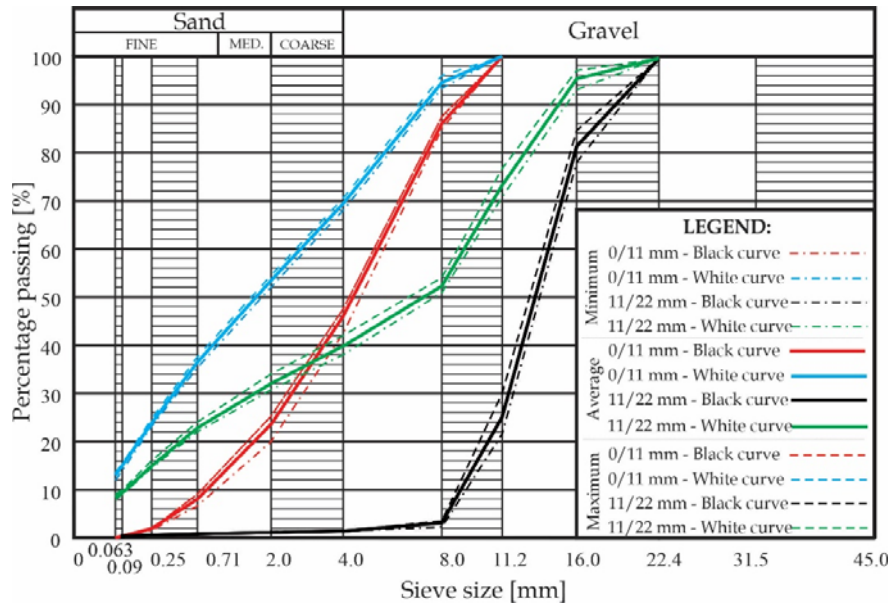
Figure 4.6 The black and white grading curves of RAP fractions

After extraction, the bitumen was recovered from the solution of solvent (trichloroethylene) and RAPb according to EN 12697-4:2016. The basic properties of the RAP binder (penetration and softening point) were determined, and the penetration index was calculated (Table 4.5).

Table 4.5 RAPb properties

Properties	Unit	Standard	Testing results
Penetration	0.1 mm	EN 1426:2017	22.2
Softening point	°C	EN 1427:2017	73.2
Penetration index	-	EN 12591:2013, Annex A	1.47

Furthermore, rotational viscosity was measured according to EN 13302:2018, at elevated temperatures (from 135 °C to 175 °C, with increments of 10 °C) and at single frequency of 0.59 Hz. Testing results are displayed in Figure 4.7.
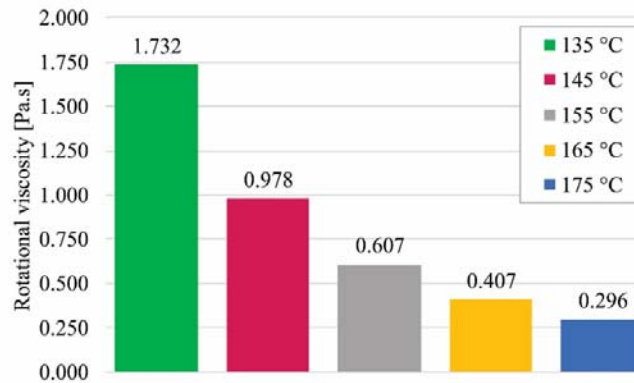
Figure 4.7 *Rotational viscosity of RAPb at elevated temperatures*

Because of a lack of data on the origin of RAPb, a Multiple Stress Creep Recovery (MSCR) test was performed, according to AASHTO D7405-15, to estimate the RAPb type. Tests were carried out at 64°C on the extracted RAPb and two additional bitumens (PMB 45/80-65 and BIT 50/70), both aged for 20h in a pressure ageing vessel (PAV). Testing results (Figure 4.8) showed that the RAPb (red line) and PMB 45/80-65 (green line) have the same sawtooth-shaped creep-recovery curve, contrary to that of the BIT 50/70 (blue line), which has a stair shape. Additionally, the recovery component (%R) and non-recoverable part of the cycles tested at a stress level of 3.2 kPa were calculated according to AASHTO D7405-15 (Table 4.6). Considering the requirements of AASHTO R 92, it can be concluded that tested RAPb has a %R value slightly below the limit for modified bitumen (55%) for the appropriate $J_{nr,3.2}$ value. Hence, considering the age of the bitumen (more than 25 years old) and the sawtooth shape of the creep-recovery curve, it can be concluded that the RAPb was probably slightly modified.
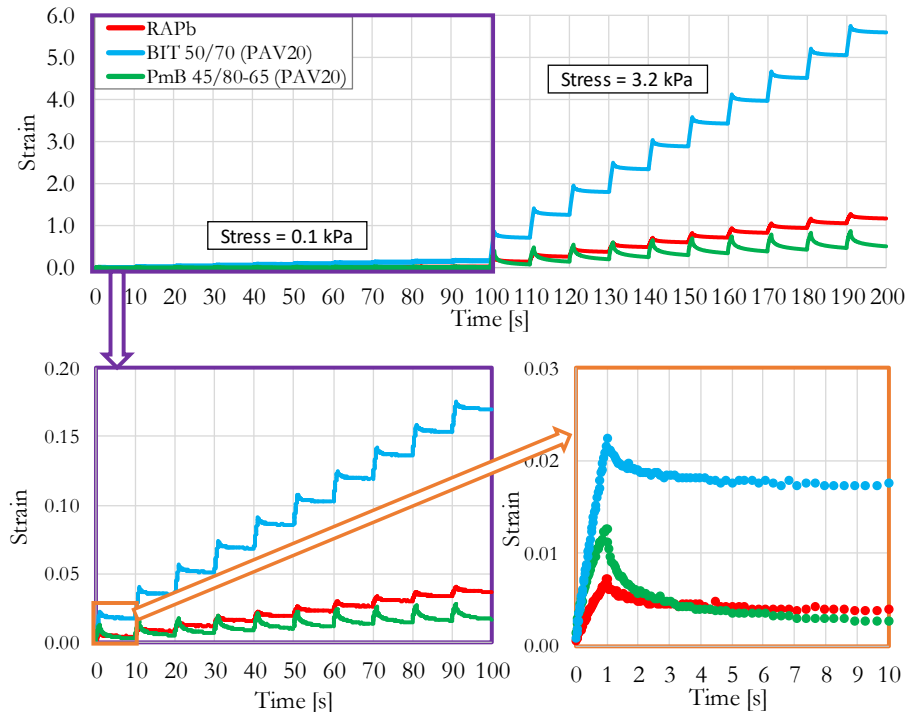
Figure 4.8 *MSCR testing results*

***Table 4.6** $J_{nr,3.2}$ and %R values of investigated binders*

Bitumen	$J_{nr,3.2}$ [kPa^{-1}]	%R	Minimum %R for measured $J_{nr,3.2}$ values according to AASHTO R 92	
			$J_{nr,3.2}$ [kPa^{-1}]	%R
RAPb	0.03	51.4	≤0.10	≥55%
PmB 45/80-65 (PAV20)	0.004	96.7		
BIT 50/70 (PAV20)	0.16	23.0	≤0.25	≥50%

4.1.5 Recycling Agents

When high RAP content is used in RAM, it is desirable to use a rejuvenator to restore the properties of RAPb. Since soft binders are not usually used in Serbia, and rejuvenating additives are more frequently used in the practice, additives were used in this study. As the VB and rejuvenating additives used in this study belong to the group of rejuvenators, the term "recycling agent" is used in the dissertation to avoid possible confusion.

Three types of recycling agents, denoted as R0, R1, and R2, were initially selected. R0 and R1 are factory products declared as rejuvenators, whereas R2 is a waste cooking oil (Figure 4.9).

To determine the most effective recycling agent, an additional amount of bitumen was recovered from the RAP collected from the top of the same stockpile, which was more exposed to ultraviolet radiation and oxidation, resulting in lower penetration and higher softening points than the abovementioned RAPb (Table 4.7). RAPb was blended with 50% VB and treated with a certain amount of each recycling agent to obtain the same penetration value as virgin bitumen (60x0.1 mm). After the binder blends were prepared, the RTFOT was conditioned for a short time, and the PAV, for long (20-hour) and prolonged (60-hour) ageing times, as extreme cases.

All binder blends were tested in their original state and after each ageing level. Penetration was measured at 25°C, as the measure of consistency at ambient temperature, and the softening point temperature, as the measure of consistency at high service temperature (Figure 4.10). Rheological properties, which are more fundamental, were measured using a Dynamic Shear Rheometer (DSR) according to EN 14770:2012. The tests were run at temperatures ranging from -30°C to +120°C at a single frequency of 10 rad/s and on a section of 10 mm and gap of 2.5 mm (Figure 4.11). This protocol enables the provision of a rheological profile of the material at a wide range of service temperatures without requiring shifting model (Porot, 2019).

***Table 4.7** Properties of RAPb used for selection of recycling agent*

Properties	Unit	Standard	Testing results
Penetration	0.1 mm	EN 1426:2017	11.6
Softening point	°C	EN 1427:2017	92.9
Penetration index	-	EN 12591:2013, Annex A	2.745

***Table 4.8** Penetration and softening point of binder blends at different ageing levels*

Ageing level	Binder (blend)											
	RAPb		Virgin		50RAPb		R0		R1		R2	
	Pen. [dmm]	Soft. p. [°C]	Pen. [dmm]	Soft. p. [°C]	Pen. [dmm]	Soft. p. [°C]	Pen. [dmm]	Soft. p. [°C]	Pen. [dmm]	Soft. p. [°C]	Pen. [dmm]	Soft. p. [°C]
Original	11.6	92.9	54.9	50.1	26.9	68.7	58.3	54.6	57.3	55.9	59.4	55.5
RTFOT	-	-	34.5	61.4	16.8	80.1	32.8	71.2	27.7	74.0	34.7	69.8
PAV20	-	-	22.1	67.4	10.1	91.4	21.8	81.7	11.0	94.9	23.2	82.3
PAV60	-	-	13.2	79.2	4.5	100.8	8.8	97.5	4.7	107.9	14.6	93.0

Figure 4.9 *Recycling agents*
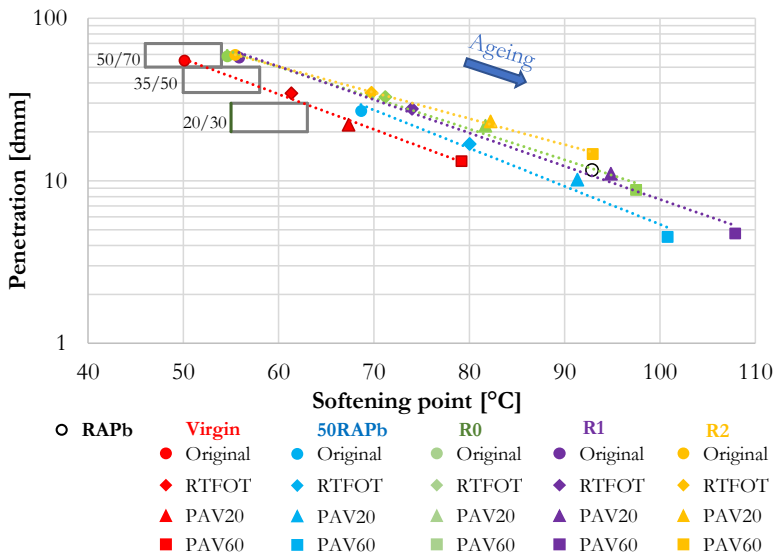
Figure 4.10 *Penetration vs softening point of binder blends at different ageing levels*
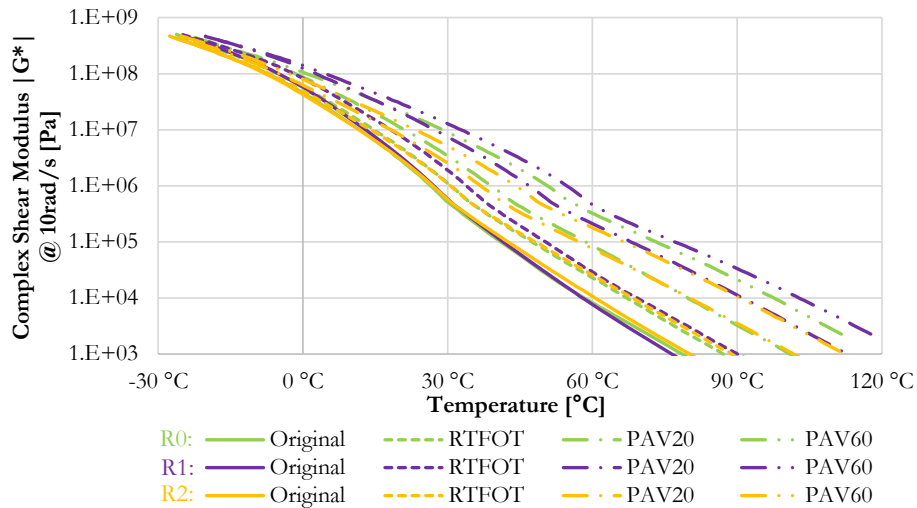
Figure 4.11 *Complex shear modulus evaluation of binder blends at different ageing levels*

From Figure 4.10 and Figure 4.11, it can be seen that all binder blends have similar properties in their original state and after short-term ageing. However, after exposing them to long-term ageing (20 hours in PAV), the blend with recycling agent R1 had a penetration and softening point and rheological properties significantly less favourable than virgin bitumen, which eliminated it from further use in this study. These properties of binder blend with agent R1 were similar to the properties of the other two blends but after prolonged ageing. The binder blend with R2 showed the best properties after 60 h of ageing, but because R0 is an industrial product (better production control), it was decided to use the recycling agent R0 in the remaining part of the study. A by-product of the paper industry, R0 is a yellow, thermally stable, bio-based additive derived from crude tall oil with a flash point higher than 280°C and viscosity of around 100 mm^2/s at 20°C.

4.1.6 Mix Design of Asphalt Mixtures

4.1.6.1 Control Mixture

The AC22 BASE BIT50/70 was selected for investigation in this study due to its highest potential for using RAP. The control mixture, composed of all virgin materials, was designed according to job mix formula (JMF) prepared by the IMS[6] Institute. The composition of the aggregate mixture was determined respecting the Technical specifications[7] for AC 22 BASE gradation. Five groups of specimens, with different bitumen content (from 3.0% to 4.6%), were prepared according to the Marshall method to determine the optimal bitumen content, which was 3.8% (Appendix II). The designed mixture composition, denoted as initial, is shown in Table 4.10, whereas the grading curve of the aggregate is displayed in Figure 4.12 with a red line.

It was decided to determine the resistance to permanent deformation of the designed control mixture to check if it satisfies the criterion from the Technical specifications (Proportional Rut Depth (PRD) <7% (Technical requirements for the construction of roads, 2012). The testing procedure was performed according to EN 12697-22, Procedure B: Small device (See Section 4.3.7), showing that the initial control mixture did not satisfy Technical specifications (PRD=7.5%, Appendix II). Hence, both the grading curve of the mineral aggregate and bitumen content were slightly corrected, and the test was repeated. The composition of the corrected control mixture is given in Table 4.10, and the grading curve of the aggregate is given in Figure 4.12 with a green line.

The repeated rutting resistance test showed that the corrected JMF satisfies requirements — the PRD was 5.5%; so, the corrected control mixture was adopted for further tests within this study.

Table 4.9 *Technical specifications for the AC 22 BASE grading curve and particle size distribution of the initial and corrected control mixtures*

Sieve size [mm]	0.09	0.25	0.71	2.0	4.0	8.0	11.2	16.0	22.4	31.5
Min	5	8	13	24	34	50	61	75	97	100.0
Max	11	17	27	40	53	70	81	94	100	100.0
Optimal	8.0	12.5	20.0	32.0	43.5	60.0	71.0	84.5	98.5	100.0
Initial	8.2	10.8	15.7	27.5	38.4	60.1	70.2	85.4	99.5	100.0
Corrected	9.0	12.3	18.5	31.5	44.5	60.6	71.7	84.7	99.0	100.0

Table 4.10 *The composition of the control mixture*

Component		Initial control mixture [%]		Corrected control mixture [%]	
		Mineral composition	Mixture composition	Mineral composition	Mixture composition
Filler from Rujevac, Ljig		4.0	3.9	4.0	3.9
Virgin aggregates from Podbukovi, Valjevo	0/4 mm	35.0	33.7	41.0	39.5
	4/8 mm	18.0	17.3	12.0	11.6
	8/16 mm	23.0	22.1	22.0	21.2
	16/22 mm	20.0	19.2	21.0	20.2
Bitumen BIT 50/70, NIS		-	3.8	-	3.6
	Total:	100.0	100.0	100.0	100.0

---

[6] Testing report No. A-111/16
[7] SRPS U.E9.021:1986
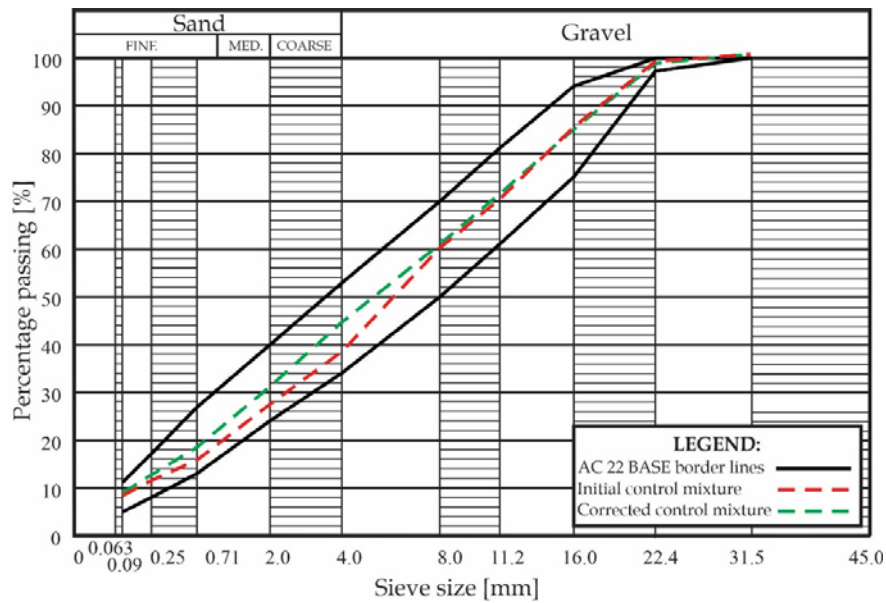
Figure 4.12 *Grading curves of the control mixture before and after correction*

4.1.6.2 RAM Mixtures

Three types of recycled asphalt mixtures with different RAP content were prepared, all having as similar grading curves to the control mixture (AC22 BASE 50/70) as possible: with 15% RAP (RAP15), 50% RAP (RAP50), and 100% RAP (RAP100). The RAP15 mixture was prepared without a recycling agent and any correction of bitumen content, assuming full blending between the RAPb and virgin bitumen (*AASTHO M323-12*, 2012). The RAP50 mixture always had the same amount of RAP, whereas the recycling agent, VB, and virgin aggregate contents had varied depending on the testing's aim (Section 5.2). Additionally, two RAP100 mixtures were prepared (with 10% RA, respecting the total mass of RAPb, and without it) to determine the optimal preheating temperature of RAP (Section 5.1). When designing each RAM, a grading curve as similar as possible to the control mixture's (Figure 4.13) was the objective. The white curves of RAP fractions (Appendix I) were considered for the mix design purposes; so, the composition of each RAM is given in Table 4.11.
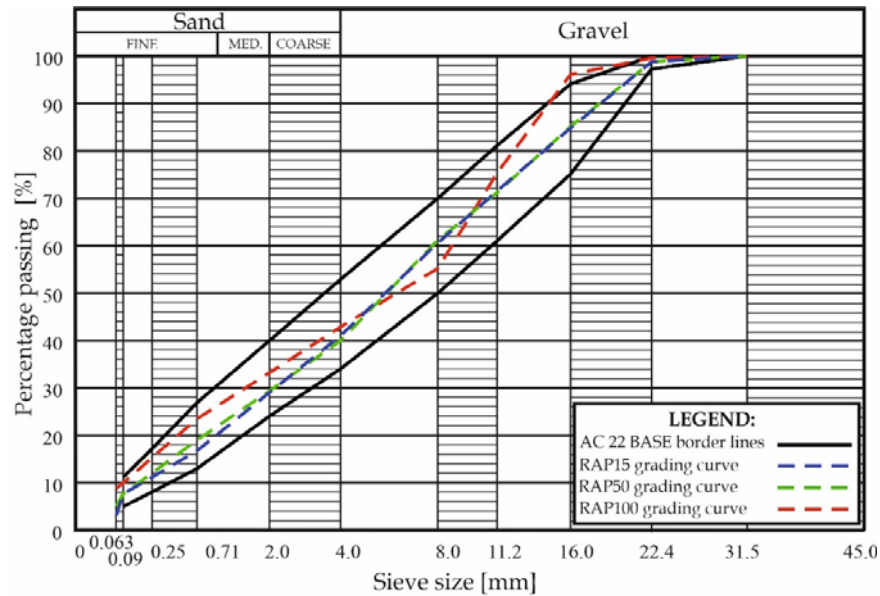
Figure 4.13 *The grading curves of RAMs*

***Table 4.11** Componential materials of RAMs*

Component [%]		Mixture		
		RAP15	RAP50	RAP100
Virgin materials	Filler	1.7	0.5	-
	0/4 mm	31.4	16.6	-
	4/8 mm	14.9	13.9	-
	8/16 mm	15.2	1.4	-
	16/22 mm	19.3	16.0	-
Bitumen	RAPb*	0.7	2.3	4.6
	Virgin	2.9	*Various (Section 5.2 and Chapter 6.)*	-
Recycling agent		-		*10% of total RAPb content*
RAP	0/11 mm	2	4	8
	11/22 mm	13	46	92
	Total	15	50	100

*Amount of bitumen coming from RAP

4.2 Specimen Preparation

In this study, fourteen sets of asphalt mixtures were prepared:

1) Two RAP100 mixtures, with and without a recycling agent, to determine the optimal preheating temperature of RAP and estimate its DoA (Section 5.1)

2) Nine RAP50 mixtures with different contents of VB and rejuvenator for mix design purposes (Section 5.2)

3) Three mixtures (CM, RAP15 and RAP50), designed according to the proposed mix design method, whose properties were compared among themselves (Chapter 6.)

Virgin aggregate fractions were preheated at 170−200°C, depending on the required mixing and compaction temperature (as determined in Section 5.2), for four hours before mixing. The RAP was not preheated for the preparation of RAP15 mixture, whereas it was preheated for four hours, at temperatures from 70°C to 190°C, to determine the optimal preheating temperature of the RAP. Finally, the RAP was preheated at optimal preheating temperature, determined in Section 5.1, for four hours when preparing RAP50 specimens. If RA was used, it was mixed with RAP by hand for one minute before preheating. The virgin aggregate and RAP were later mixed for five minutes in the laboratory mixer (Figure 4.14) and, after adding virgin bitumen, previously preheated at 150°C, were mixed for three more minutes. Finally, filler, also preheated at 170-200°C, was added to the mixture and blended in for five more minutes to improve the coating of the aggregate and RAP particles with VB and RA.

Depending on the testing requirements, specimens were compacted in a Marshall (Figure 4.15), gyratory (Figure 4.16), or slab compactor (Figure 4.17). Additionally, for the fatigue resistance test, four specimens were cored from every slab, as shown in Figure 4.18. It should be also mentioned that all asphalt mixtures were exposed to a short-term ageing procedure (four hours at 135°C) before slab compaction. The type of compaction, appropriate standard, and compaction energy applied during the specimen's preparation, as well as the usage of prepared specimens, are displayed in Table 4.12.

Table 4.12 *Compaction procedure types*

Compaction type	Number of blows/rotations	The use of specimens for:	Section
Marshall compactor (*Φ*100 mm) (EN 12697-30)	50 blows per side	Determination of the optimal preheating temperature of RAP	5.1
		Mix design procedure of HMA with high RAP content	5.2
		Stiffness	4.3.4 (6.1)
	35 blows per side	Water sensitivity	4.3.2
	35 blows per side	Freeze-thaw resistance	(6.4)
		Control mixture	4.3.3
			4.3.3
	55 blows per side	RAP15	
			4.3.3
	33 blows per side	RAP50	
Gyratory compactor (*Φ*100 mm) (EN 12697-31)	30 rotations	Determination of the optimal preheating temperature of RAP	5.1
Slab compactor (26x32x7 cm) (EN 12697-33)	-	Resistance to permanent deformation	4.3.7 (6.5)
		Fatigue resistance (after coring)	4.3.6 (6.6)

Figure 4.14 *Laboratory mixer*

Figure 4.15 *Marshall compactor*

Figure 4.16 *Gyratory compactor*

Figure 4.17 *Slab compactor*

Figure 4.18 *Preparation of testing specimens for fatigue resistance determination*

4.3 Testing Methods

4.3.1 Volumetric Properties

Before the start of testing, the following volumetric properties of every mixture/specimen were determined:

- Maximum density (EN 12697-5:2019, Procedure A: Volumetric procedure)

- Bulk density of saturated surface dry specimen (EN 12697-6:2013, Procedure B: Bulk density — Saturated surface dry (SSD))

- Void characteristics (EN 12697-8:2019)

4.3.2 Water Sensitivity

For this test, six cylindrical specimens of every mixture were prepared in Marshall compactor with 2x35 blows. The testing specimens were divided into two groups, dry and wet (three specimens each), with similar average thickness and bulk density. The dry set of specimens was kept at room temperature until the start of the test (20±5 °C), whereas the wet subset was placed in a desiccator, filled with water, and exposed to an absolute (residual) pressure of 6.7±0.3 kPa. After 10±1 minutes of vacuum exposure, specimens have been kept under the vacuum for another 30±5 minutes and left submerged in water for an additional 30±5 minutes. Specimens were further removed from water, and their dimensions were measured to check if their volume has increased by more than 2%. The wet subset of specimens was then placed in a water bath at a temperature of 40±1 °C for a period of 68-72 h.

Figure 4.19 *The testing head configuration*

The dry subset was conditioned in a thermostatically controlled air chamber, whereas the wet subset, after conditioning, was placed directly in a water bath. Both subsets were conditioned at the test temperature of 25°C for at least two hours before testing. The indirect tensile strength (ITS) of each specimen was determined according to EN 12697-23:2018 (a diametrical load was applied at a constant speed of deformation of 50±2 mm/min after the specimen's placement in the testing head (Figure 4.19)). During the test, the load and displacement have been recorded.

The ITS of each testing specimen was calculated according to the following equation:

$$ITS = \frac{2P}{\pi DH} \cdot 1000 \ [kPa] \qquad\qquad\qquad Equation\ 2.1$$

where *P* is the peak load [N], *D is* the diameter of the specimen [mm], and *H is* the height of the specimen [mm].

4.3.3 Freeze-Thaw Resistance

For this test, nine Marshall specimens of every mixture were prepared, all with air voids between 6.0 and 8.0%, which is achieved by the application of a different number of blows during compaction, depending on the mixture type (Table 4.12).

Figure 4.20 *Procedure of specimens' preparation for freeze-thaw resistance test*

After compaction, testing specimens were exposed to the conditioning procedure, as illustrated in Figure 4.20. They were divided into three subsets with similar average thickness and bulk density; unconditioned (dry) subset and subsets were further exposed to three and six freeze-thaw cycles. Before conditioning, all subsets, except dry, are partially saturated to a range of 60-80% in a vacuum exicator and then wrapped in a leak-proof plastic bag containing approximately 3 ml of distilled water. Specimens

were then sealed and placed into a cooling chamber at -18±2°C for at least 15 hours. After their removal from the chamber and release from the bags, they have been initially immersed in a water bath at 60±1°C for 24 hours and later, in another water bath at 25±1°C for at least one hour. This procedure was repeated three and six times, much more than the standard's requirement of only one cycle (*AASHTO T283*). After conditioning, the ITS of each specimen was determined according to Equation 2.1.

4.3.4 Stiffness

For this test, four Marshall specimens of every mixture were compacted in a Marshall compactor with 2x50 blows. After determining the volumetric properties, specimens were kept on a flat surface in a thermostatically controlled air chamber at a testing temperature (5°C, 10°C, 20°C, 30°C or 40°C) for at least four hours before testing.

During the test, a load was applied along the vertical diameter of the specimen, whereas a responsive horizontal diametral deformation was measured with a linear variable differential transformer (LVDT), as displayed in Figure 4.21. Load pulse had a haversine waveform (the same as displayed in Figure 4.23, but with three different loading times and pulse repetition period), and it was initially applied ten times to adjust the load magnitude required to achieve a target peak transient deformation of 0.005%. Additionally, five loading pulses with adjusted loads were applied, and the variations of load and horizontal deformation were measured and recorded. This procedure was reapplied for different loading times (125, 200 and 300 ms). Specimens were then rotated for 90±10° about the horizontal axis, and the procedure was repeated. If the average value of stiffness modulus from the second measurement differed more than 10%, or less than -20% of the stiffness modulus from the first measurement, obtained testing results have been rejected.
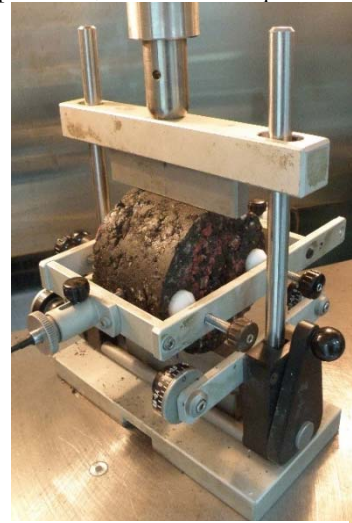
Figure 4.21 *The equipment for determination of stiffness*

Obtained data were further used for the construction of master curves (Section 6.1), which are used for the description of the asphalt mixture's performance across a wide range of frequencies and temperatures. However, since the procedure for the construction of master curves uses frequencies expressed in Hz, it was necessary to convert the loading signal from ms to Hz. That has been done using Fourier transformation, developed by colleague Dr Marko Radišić (Appendix III), obtaining frequencies of 2.0 Hz, 2.51 Hz, and 3.98 Hz for the loading times of 125 ms, 200 ms, and 300 ms, respectively.

4.3.5 Cracking Resistance (IDEAL-CT)

The **in**direct **t**ensile **a**sphalt **c**racking **t**est (IDEAL-CT) was used to determine the cracking susceptibility of asphalt mixtures (ASTM D8225, 2019). The test has been developed as a simple, practical, and efficient test that does not require cutting or drilling the testing specimens, purchasing new laboratory equipment, training laboratory personnel more, or, finally, testing for a prolonged period (Zhou et al., 2017). The IDEAL-CT is comparable to other laboratory cracking tests, such as the Texas Overlay Test and Illinois Flexibility Index Test (Zhou et al., 2019), and positively affects field performance in terms of fatigue, reflective, and thermal cracking (Zhou et al., 2017).

The test is very sensitive to key asphalt mixture components (bitumen type, RAP and RAS content, ageing of bitumen) and volumetric properties (bitumen content, air void content). It can be performed at different testing conditions (loading rate, testing temperature, dimensions of the specimen, etc.); so, it can be used for mix design and QC/QA (quality control and quality assurance), like any other cracking test.
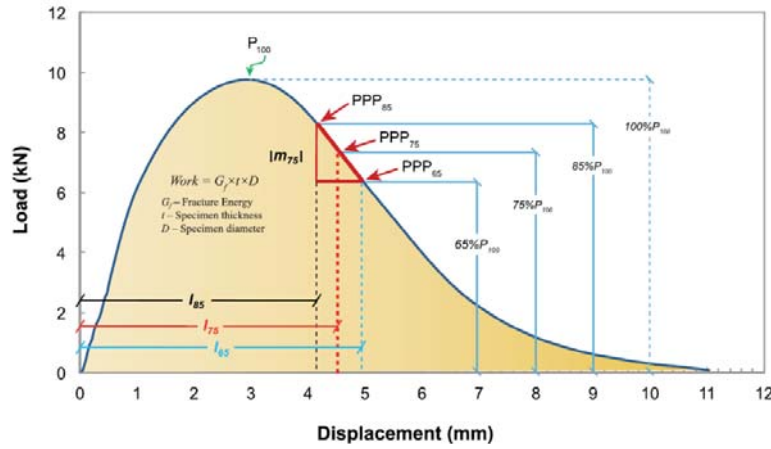
Figure 4.22 *Illustration of the PPP75 point and its slope |m75|,*
adapted from (Zhou et al., 2017)

IDEAL-CT is not a new test; it only analyses the data measured during an ITS test (displacement and load) in a different way than the traditional ITS test, which considers the peak load achieved during the test (P100 on Figure 4.22). A performance-related cracking parameter of IDEAL-CT, CT_{index}, is calculated according to the following equation:

$$CT_{index} = \frac{t}{62} \times \frac{G_f}{\frac{P}{l}} \times \left(\frac{l}{D}\right)$$

<div align="right">*Equation 2.2*</div>

where t is the thickness of the testing specimen [mm], G_f is fracture energy calculated as the work of fracture divided by the area of cracking fac, P/l is the modulus parameter, i.e. the slope $|m_{75}|$ at the point of the post-peak 75% of maximum load (PPP$_{75}$ on Figure 4.22), l/D is the strain tolerance parameter, where D is the diameter of specimen [mm], and l (or l_{75} on Figure 4.22) is the displacement of a specimen that can be tolerated when the load reaches PPP$_{75}$.

The larger the CT_{index}, the slower the cracking growth rate, i.e. the better the cracking resistance of asphalt mixtures.

Despite its numerous advantages, the procedure has a limitation. Arámbula-Mercado et al. (2019) discovered that an increase of 4% in the air void content could increase the CT_{index} up to 1.6 times; so, a recommendation proposed by Zhou et al., 2017, which states that comparison among different mixtures is possible only if they have similar air void content, was followed in this study.

4.3.6 Fatigue Resistance

The fatigue resistance of asphalt mixtures was assessed using an indirect tensile test on cylindrical-shaped specimens, according to EN 12697-24, Annex E (IT-CY), except for several deviations given in Table 4.13.

Testing specimens, with a diameter of 100±3 mm, were cored from the laboratory-prepared slabs, as explained in Section 4.2 and displayed in Figure 4.18. After the determination of their volumetric properties, deformation strips were glued on specimens on the opposite sides of the horizontal diametral plane. Specimens were then placed in a thermostatically controlled air chamber, at a testing temperature of 10°C, for at least four hours before testing. Once a specimen was mounted in the loading frame (Figure 4.24), a (ha)versine load with a frequency of 2 Hz was applied repeatedly (Figure 4.23). Tests were performed in a stress-controlled mode, at different stress levels, from 5500 N to 12000 N, with an

assumed Poisson's ratio of 0.35. The resulting horizontal deformation at the centre of specimen has been measured during the test, with two LVDTs mounted. The load was applied as many times as necessary until the established failure criteria are reached, as described in Section 6.6.

The maximum initial strain at the centre of the specimen and the number of loading cycles leading to the failure were recorded and used for the estimation of fatigue laws for each asphalt mixture (Section 6.6).
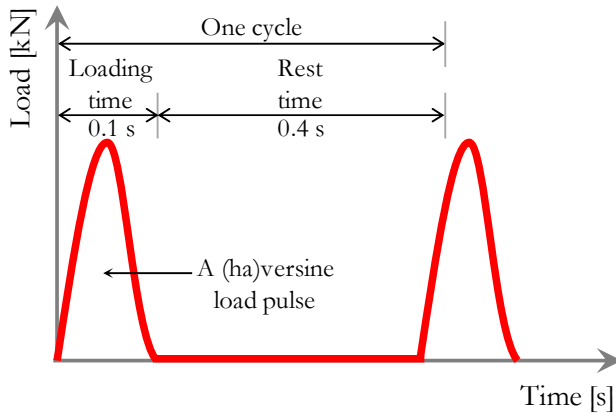
Figure 4.23 *A loading cycle*

Figure 4.24 *Specimen in the loading frame*

Table 4.13 *Testing conditions in the study, when different than standard's requirements*

Requirements	EN 12697-24:2018	Study
Specimen dimension	A diameter of (150±3) mm for a maximum aggregate size of more than 16 mm up to 32 mm.	A diameter of 100 mm.
Number of stress levels	Three.	Between 5 and 10.
Numbers of specimens	At least five at each stress level, 15-18 per mixture.	At least 10 per mixture.
The load and horizontal deformation monitoring	The first 200 load cycles should be measured continuously to enable the calculation of the initial stiffness modulus.	When a large number of loading cycles was applied, it was impossible to measure stiffness modulus in the first 200 cycles, due to software limitations.

4.3.7 Resistance to Permanent Deformation

Rutting resistance was determined according to EN 12697-22, Procedure B: Small device (in the air). Two specimens of every mixture were prepared in a segment compactor, as explained in Section 4.2.

Figure 4.25 *Wheel tracking device*

Testing specimens were mounted in a wheel tracking device (Figure 4.25) and kept at a testing temperature of 60±1°C for at least six hours before the test. A load of 700 N was applied for 10.000 cycles (20,000 wheel passes) over the contact surface of 1900 mm^2, giving a load frequency of approximately 0.88 Hz.

The vertical displacement of the wheel was read continuously during the test, and obtained results were further used for assessment of the resistance to permanent deformation (Section 6.5).

Chapter 5. Mix Design Methodology of RAM

5.1 Optimal Preheating Temperature of RAP

The standardized procedures for determination of optimal preheating temperature of RAP have not been established yet. Many attempts have been performed, mostly on the asphalt mixture level, requiring an extensive work in laboratory. Preheating temperatures of RAP have been varying a lot in previous studies, going from low (without heating) to very high (up to 170 ºC), as it is displayed in Figure 5.1. From the same figure it can be seen that RAP has typically been preheated to a certain temperature without clear explanation of selected temperature (red part of the Figure 5.1) The standardised procedures for the determination of the optimal preheating temperature of RAP have not yet been established. Many attempts have been performed, mostly on the asphalt mixture level, requiring extensive laboratory work. The preheating temperatures of RAP have greatly varied in previous studies, from low (without heating) to very high (up to 170ºC), as displayed in Figure 5.1. From the same figure, it can be seen that the RAP has typically been preheated to a certain temperature without a clear explanation of the selected temperature (red part of Figure 5.1) (Bailey & Zoorob, 2012; Boriack et al., 2014; Büchler et al., 2018; Colbert & You, 2012; Doh et al., 2008; Mamun & Al-Abdul Wahhab, 2018; Miguel Baptista et al., 2013; Molenaar et al., 2011; Mohammedreza Sabouri et al., 2015; Sivilevičius et al., 2017; Taherkhani & Noorian, 2018; Martins Zaumanis et al., 2018), whereas laboratory tests were performed only in several studies to determine the optimal preheating temperature (green part of Figure 5.1) (Liu et al., 2019; Ma et al., 2016; Madrigal et al., 2017; Silva et al., 2012a; R. West et al., 2013; B. Yu et al., 2017).

RAP, like any other componental material of the RAM, should be classified considering a specific property, such as, for example, virgin bitumen, which is classified through its penetration. Tebaldi et al. (2018), for instance, proposed the ITS test for RAP classification. Another possible classification may be based on the optimal preheating temperature, which has usually been determined through the extensive laboratory testing of RAMs with different RAP contents. In one study (Silva et al., 2012b) RAP was considered as a componental material whose optimal preheating temperature was determined by considering the compactability of Marshall specimens preheated at different temperatures, from 110 to 160ºC. A temperature of 145ºC was identified as the minimum temperature at which RAP should be heated to ensure appropriate workability, whereas the addition of recycling agents (RA) decreased the optimal temperature by approximately 20-25ºC. Taziani et al. (2017) performed a similar study by preparing specimens compacted in a gyratory compactor using a range of temperatures between 100 and 160ºC, measuring compactability, ITS, and stiffness. Although the optimal preheating temperature of RAP was not determined, it was concluded that the material preheated at the temperature of 160ºC had the highest strength and stiffness, showing the highest rutting resistance.

The increased use of RAP results in several identifiable benefits. It reduces production costs, emissions, and fuel usage due to the decreased demand for non-renewable resources, such as new aggregates and especially bitumen (Baghaee Moghaddam & Baaj, 2016; M Zaumanis et al., 2014). However, the use of high RAP content in RAM requires a specific focus on its preheating because its effect on performance and energy consumption is substantial. For example, the asphalt plant shows an increase in energy consumption of 14 to 17% for drying and heating when a second parallel drum is used for RAP (Anthonissen et al., 2014). This issue may be mitigated if the RAP preheating temperature is decreased through the potential benefits deriving from the addition of RAs (rejuvenators or lubricants) because they can decrease production temperature up to 40°C without compromising RAM properties, as reported by Pouranian and Shishenbour (2019) and Silva et al. (2012). Considering these facts, it can

be concluded that the identification of the optimal preheating temperature for RAP has an essential role, both on RAM performance and the environmental and economic aspects of the recycling process.
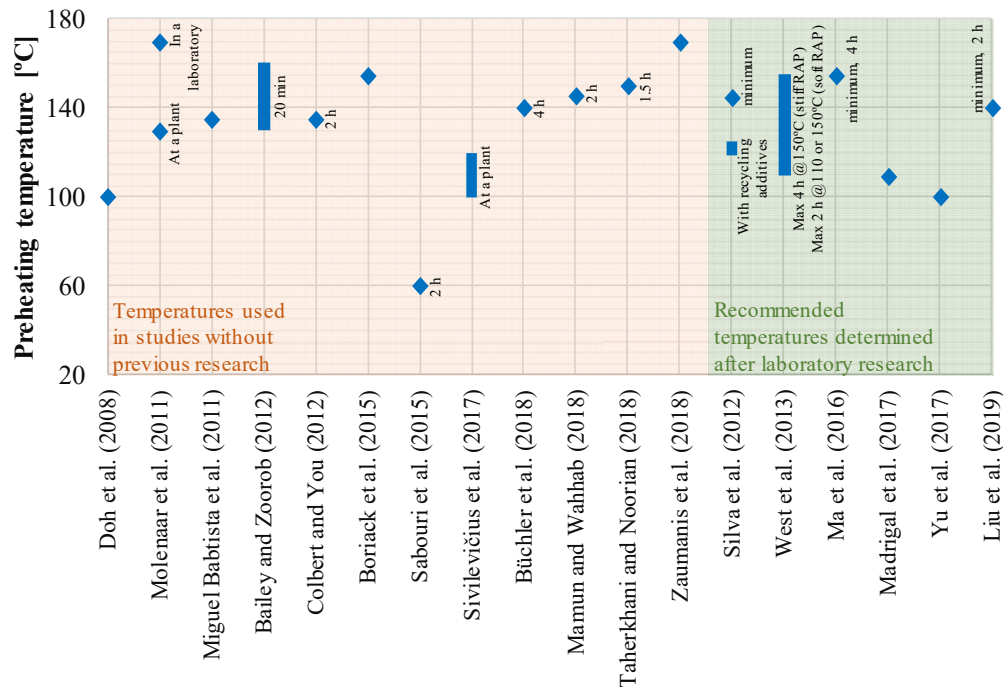
Figure 5.1 *Preheating temperatures used without a clear explanation of the selected temperature (red) and optimal preheating temperatures determined after laboratory research (green)*

This section proposes a methodology for the determination of the optimal preheating temperature of RAP developed by performing routine laboratory tests (volumetric properties, ITS, stiffness) on the same set of laboratory specimens prepared with different compaction methods (Marshall and gyratory compactors). A multi-objective optimization step was further used to calculate the optimal preheating temperature of RAP, integrating the uncertainties in determining the different properties through a Monte Carlo (MC) simulation.

5.1.1 Materials and Testing Methods

Two componental materials were used in this part of the study to produce RAM with 100% RAP (RAP100): RAP (Section 4.1.4) and product R0 (Section 4.1.5).

RAP fractions have been combined, respecting a specific proportion: 92% of 11/22 mm and 8% of 0/11 mm, to obtain a grading curve compatible with the AC 22 BASE mixture. White curves were considered to be, as much as possible, overlapped to the midpoint of the envelope following the target grading curve. The red line on Figure 4.13 displays the most satisfactory grading curve attainable with those fractions; only the passing through the sieve of 16 mm was slightly above the standard requirements.

Figure 5.2 displays the plan of each specimen's preparation and the tests performed. Each specimen's preparation is followed by the recommendations proposed by RILEM TC264-RAP – TG5 for interlaboratory tests as follows: the RAP material was first dried in the oven at 40°C for 48 hours, and both RAP fractions were mixed by hand, with and without a recycling agent, and left in the oven for four hours before mixing at temperatures of 70°C, 100°C, 140°C and 170°C and at an additional temperature of 190°C when only-RAP is used. The preheating temperature of 190°C was not applied for the RAM with RAP+RA because of the blue smoke appearance. Just before compaction, materials were mixed for an additional 60 seconds and placed in preheated moulds. Four specimens of 100 mm in diameter were compacted per each preheating temperature using a Marshall compactor (50 blows per each side of the specimen) and gyratory compactor (30 rotations). The initial objective was to use only a gyratory

compactor and apply as many rotations as necessary to achieve air void content within the allowed range for AC 22 BASE (4-9%) at each preheating temperature; so, 30 rotations were used. After a while, it was decided to expand the experiment to validate the methodology; so, additional sets of specimens were prepared using a Marshall compactor.
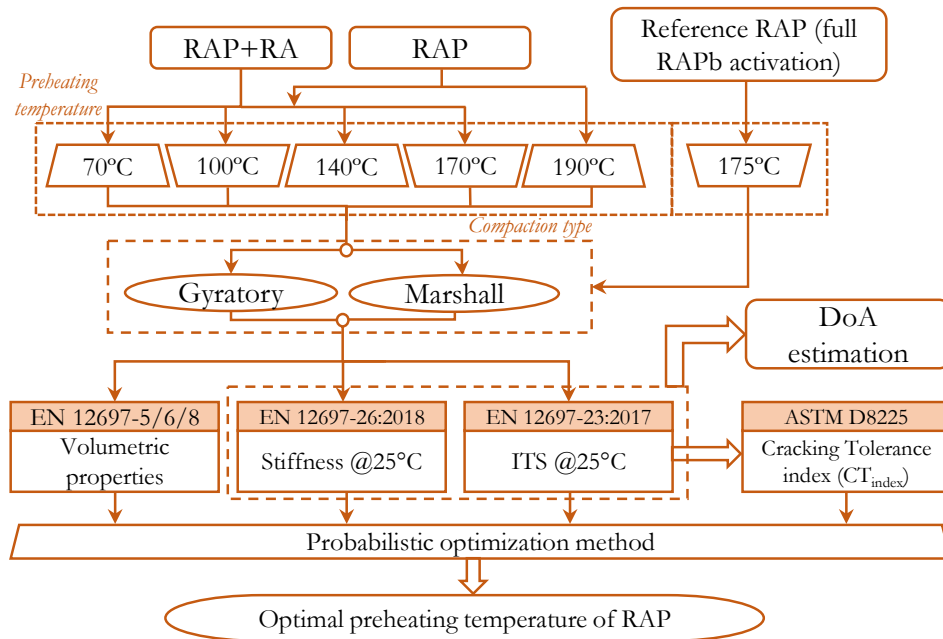
Figure 5.2 *The experimental plan for the determination of optimal preheating temperature*

Volumetric properties were determined according to Section 4.3.1 after which the stiffness was measured at a loading frequency of 125 ms and a temperature of 25°C, as stated in Section 4.3.4. The ITS value of each testing specimen was determined according to EN 12697-23:2018. Finally, the CT_{index} of each specimen was calculated (as explained in Section 4.3.5).

5.1.2 Optimization of the Preheating Temperature

Engineering problems are typically characterised by the need to achieve different objectives by simultaneously optimising different functions. One of the most common methods is to form a composite objective function as the weighted sum of the different objectives. The weights that can be assigned to each objective are proportional to the importance or preference attributed to this property. Therefore, when the composite objective function, or so-called *fitness function*, obtained from converting the multi-objective performance to a single objective, is optimised, it is possible to obtain one particular trade-off solution. This is called *preference-based* multi-objective optimisation. Furthermore, based on a potentially higher level of information, a preference vector of weights, *w,* can be selected. Different weighting approaches have been applied in previous studies for the asphalt mixtures properties (Cheng et al., 2019; Slebi-Acevedo et al., 2019).

The definition of the preference vector containing the weights of the objective functions requires experience-driven information and different evaluations. This method permits system flexibility and the possibility to change the preferences according to the needs of the user; alternatively, it is subjective to the particular user (Deb, 2011) and may be sensitive to the set of parameters considered (Slebi-Acevedo et al., 2019). In other words, if the number of parameters changes, the weights also change. Based on these considerations, and due to the lack of a higher level of information, a conservative approach has been adopted, and equal unitary weighting has been assigned to each parameter: air void content, stiffness, ITS, and CT_{index}. Therefore, each element of the objective's performance has been considered equal (set to 1) to avoid subjectivity in the process that would occur with the inclusion of surveys or human judgement-driven information.

Within the framework of this study, the fitness performance allows the measurement of the appropriateness of a solution for the problem, optimising the preheating temperature of RAP to obtain the highest possible performance. The fitness function has been defined as the sum of the normalized performance values for each preheating temperature, resulting in a *Fj* (fitness performance) value, as specified in Equation 3.1:

$$F_j = \sum_{i=1}^{4} w_i \cdot y_{ij}$$

Equation 3.1

where: y_{ij} is the value of the i-parameter at each preheating temperature j, and w_i is the weight assigned to each parameter, in this case, equal to 1.

An additional step consisted in considering the process of selecting the highest fitness, defined as a sum of performance, as a probabilistic process instead of considering the overall process as deterministic. An additional step consists of considering the process of selecting the highest fitness, defined as the sum of performance, as a probabilistic process instead of considering the overall process as deterministic. Indeed, the bitumen and asphalt mixture performance are affected by uncertainties and variability, especially when RAP is involved (Kim & Lee, 2002; Maji & Das, 2008; Bressi, Carter, et al., 2016). The uncertainties of the input parameters are one of the crucial aspects for a reliable preheating temperature selection; therefore, stochastic simulations were adopted through the use of a Monte Carlo (MC) analysis to incorporate the uncertainties in the process for the determination of the optimal preheating temperature. An MC analysis was based on the idea of associating to each input of the model adopted, not a deterministic value, but a suitable probability distribution function (pdf), and it is, thus, possible to determine all the uncertainty and variability related to the considered parameter (Kroese et al., 2011). The output of the model was then calculated assuming n-times, as input, a random extrapolation from the probability distribution representing the results obtained, assumed to be a normal distribution (Maji & Das, 2008; Bressi, Carter, et al., 2016).

After a complete set of simulations, the results in terms of fitness value allowed the determination of the pdf of the output itself (Saltelli, 2002) (Equations 3.2 and 3.3):

$$\hat{E}(F) = \frac{1}{n_s} \sum_{k=1}^{n_s} F_k$$

Equation 3.2

$$\hat{\sigma}(F) = \sqrt{\frac{1}{n_s - 1} \sum_{k=1}^{n_s} [F_k - \hat{E}(F)]^2}$$

Equation 3.3

where: F_k is equal to the results of simulations, n_s is the number of simulations, $\hat{E}(F)$ is the estimated value of output variable y, and $\hat{\sigma}(F)$ is the estimated standard deviation of output variable F.

Considering the expected value and standard deviation for a sequence of different numbers of simulations, it was possible to evaluate the stability of the output. Indeed, different numbers of simulations (100, 200, and 500) have been performed to achieve the stability of the solutions, i.e. the stable value of the fitness performance at each preheating temperature. Simulations have been performed with a random selection from the input distributions for each variable. The limiting values of each variable have been selected as the minimum and maximum values measured in laboratory tests regarding compaction type and RA presence (Appendix IV).

The fitness function has been estimated at different preheating temperatures of RAP considering the different parameters (y_{ij} in Equation 3.1): air void content, indirect tensile strength, stiffness, and CT$_{index}$. These parameters have been selected due to their importance in the mix design procedure, widely available equipment in laboratories, and the simplicity of the testing procedure.

To optimise the RAP preheating temperature, it was essential to determine the most favourable combination of different parameter values, establishing a target for each parameter, maximum or minimum:

- Minimization of air voids. Lower air void content is preferable (without exceeding the lower limit of the optimal range, depending on the mixture type), which means that the higher quantity of RAPb becomes fluid during preheating and mixing procedures, ensuring adequate compaction. This will lead to improved moisture resistance (Kassem et al., 2011), higher resistance to the effect of low temperature (Basueny et al., 2014), increased fatigue life (Harvey & Tsai, 1996), and indirect tensile strength (W. Zhao, 2011).

- Maximisation of ITS. ITS is an indicator of the cohesion between bitumen and aggregates, strongly correlated to the cracking properties of the bituminous mixture (W. Zhao, 2011). At low temperatures, ITS will be low because RAPb will not be fluid enough to recoat the aggregate particles (D. Lo Presti et al., 2019), causing an adhesive failure (break appears through the asphalt-aggregate interface). With the increase of the preheating temperature, RAPb becomes fluid, ITS increases, and the failure type becomes cohesive (through the binder film) or combined (cohesive/adhesive), as explained by (Canestrari et al., 2010). Since higher ITS values correspond to a stronger cracking resistance (Islam et al., 2015), it is crucial to achieve as high ITS as possible.

- Minimization of stiffness. The presence of RAP in a new RAM unequivocally increases the stiffness of the mixture (Colbert & You, 2012; Swamy et al., 2011). Aged bitumen coming from RAP is significantly harder, more aged, and prone to cracking when compared to virgin bitumen. Consequently, further hardening/ageing under the impact of high temperature should be avoided because bitumen overheating significantly decreases pavement durability (Sarnowski et al., 2019).

- The importance of ITS and stiffness, as well as their balance, have been previously investigated in detail by Pellinen (Pellinen, 2004), who concluded that the increase of both parameters leads to improved rutting and cracking resistance. Additionally, Pellinen and Xiao (Pellinen, T. and Xiao, 2006) found that low stiffness and high strength cause an increase in rutting potential problems, whereas high stiffness and low strength lead to a potential increase in low-temperature and top-down cracking. Overall, it can be concluded that a certain balance between these parameters should be preferable.

- Maximization of CT_{index}. The CT_{index} is a parameter that may be used for comparison among different asphalt mixtures compacted to approximately the same level of air voids (e.g. 7±0.5 %). It has a very good correlation with reflective and fatigue cracking, where a higher CT_{index} value means better cracking resistance and less aged RAPb (Zhou et al., 2017).

To turn the problem into a maximization problem, the air voids and stiffness values were adjusted as follows, and in the same way for ITS and CT_{index}:

$$Air\ voids = \frac{Air\ voids_{max}}{Air\ voids'}$$

Equation 3.4

$$Stiffness = \frac{Stiffness_{max}}{Stiffness'}$$

Equation 3.5

where: *Air voids$_{max}$* is the maximum value of air void content for the different preheating temperatures, *Stiffness$_{max}$* is the maximum value of stiffness for the different preheating temperatures, *Air voids'* is the value of air voids randomly sampled from the probability distribution representing the trend of the air voids values, and *Stiffness'* is the value of stiffness randomly sampled from the probability distribution, representing the trend of the stiffness values.

To summarize, the following steps were performed:

- Assuming the volumetric and mechanical properties being normally distributed (Bressi, Carter, et al., 2016), the parameters characterising the distributions (mean and standard deviation) of each set of results (air voids, ITS, stiffness and CT_{index}) were calculated based on the results of test repetitions for the different materials and compaction process (four specimens of RAP and RAP+RA mixtures at each preheating temperature).

- An n-times random extrapolation from the probability distribution of each parameter (air voids, ITS, stiffness, and CT_{index}) has been performed to obtain the data string.

- All the values of the different properties have been normalized to bring all the values on the same scale and avoid the issue related to different measurement units.

- The fitness values have been generated as the sum of the normalised, randomly extrapolated values. Equal weighting has been adopted (all weights equal to 1).

- A fitness function has been generated, interpolating the fitness values obtained for different preheating temperatures, and a trade-off solution (optimal preheating temperature) has been identified through the maximization of the fitness function.

A schematic representation of the method is shown in Figure 5.3.
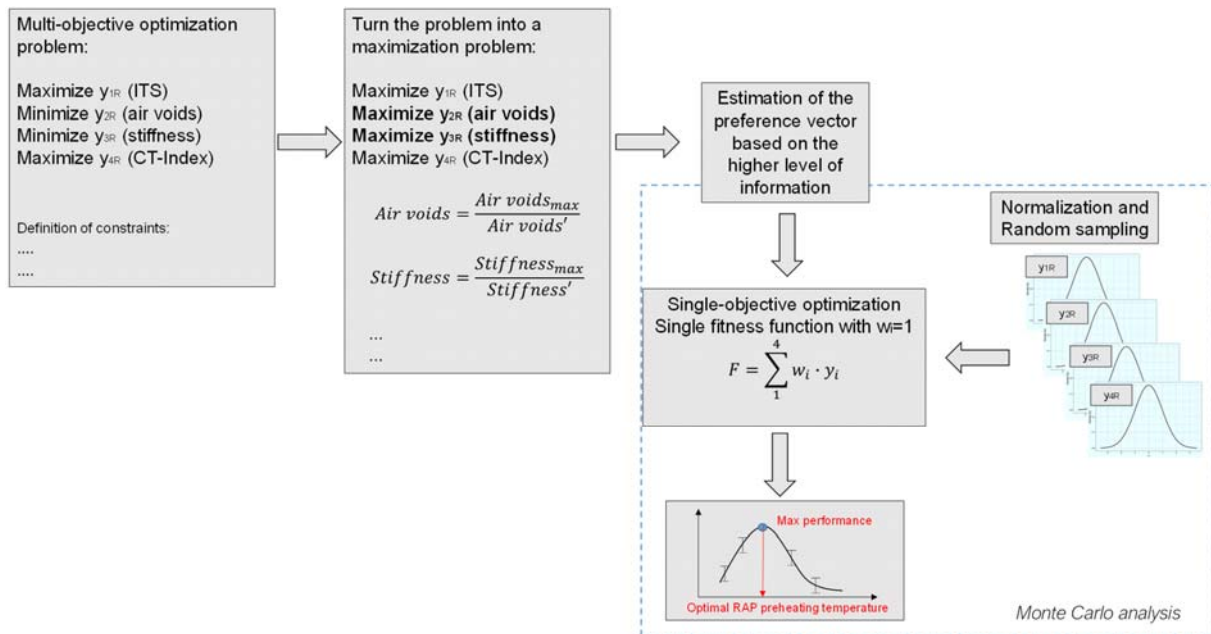
Figure 5.3 *Schematic representation of the probabilistic optimization methodology*

5.1.3 Testing Results

All the RAP mixtures had the same grading curve and bitumen content, therefore the effect of the different preheating temperatures on the performance was isolated and measured, which may lead also to certain conclusions regarding the bitumen stiffness and the degree of binder activation. First all the test results are shown and afterwards the results of the probabilistic optimization procedure for determining the optimal preheating temperature are reported.

5.1.3.1 Volumetric Properties

The air void content at different RAP preheating temperatures (average values and standard deviations) of the RAP and RAP+RA specimens, compacted with gyratory and Marshall compactors, is provided in Figure 5.4.
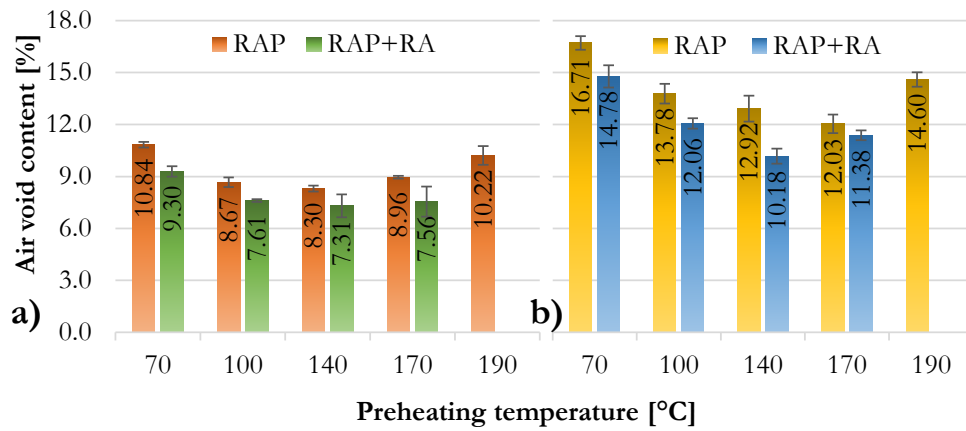
Figure 5.4 *Air void content of RAP and RAP+RA specimens preheated at different temperatures and compacted in (a) gyratory and (b) Marshall compactor*

The results show that, regardless of the compaction method used and the presence of a recycling agent, the air void content decreases with the increase of the preheating temperature up to 140°C, and afterwards, above this temperature, it is possible to observe a gradual increase of the air voids. The only exception was in the case of the only-RAP mixture compacted with a Marshall compactor, where the air void content gradually decreased to 170°C and then increased. Similar conclusions were drawn by Ma et al. (2016), who reported the similar performance of the RAM with 50% RAP, but after using a slightly higher preheating temperature (150°C). The trend emerging from Figure 5.4 can be explained considering the variation of the RAPb state: with the increasing of the temperature to a certain level, RAPb becomes fluid and recoats aggregate particles, facilitating the aggregate's packing and the compaction. The higher flow allows the void content to be reduced. However, a too-high temperature burns the already aged RAPb, making it too stiff ("black rock"). Considering the impact of RA on air void content, it can be seen that its addition decreases the air void content of the specimens compacted with the gyratory compactor from approximately 14-19%, regardless of the preheating temperature. Marshall specimens preheated at lower temperatures (70°C and 100°C) have a similar decrease of air void content (around 13-14%) as gyratory compacted specimens. However, the highest reduction occurred at 140°C (27%) and the lowest, at 170°C (6%), showing the highest potential benefits of RA use at temperatures below 140°C.

5.1.3.2 Stiffness

The average values and standard deviations of RAP and RAP+RA specimens prepared with a gyratory compactor and Marshall compactor are displayed in Figure 5.5a and Figure 5.5b, respectively.
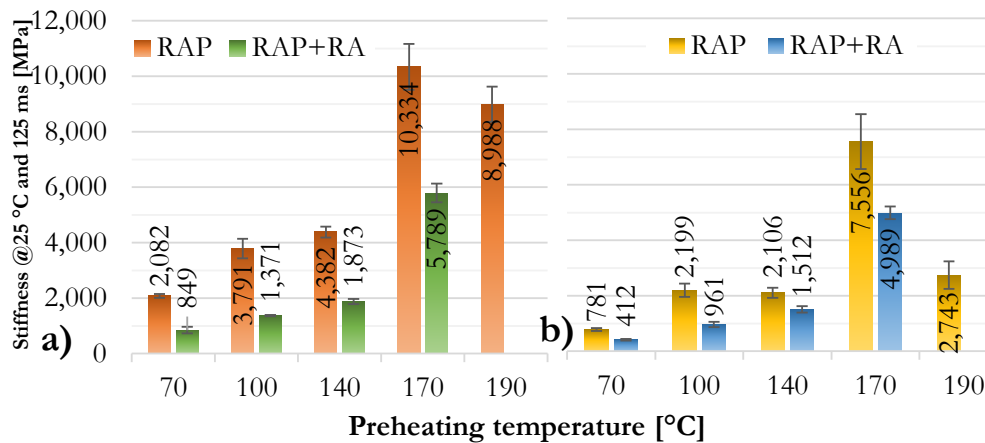
Figure 5.5. *Stiffness of RAP and RAP+RA specimens preheated at different temperatures and compacted in (a) gyratory and (b) Marshall compactor*

Focusing on the stiffness, it is possible to notice that the variation of stiffness with the preheating temperature is similar in both cases — the lowest value of the stiffness was measured at a preheating temperature of 70ºC because the RAPb was not sufficiently reactivated to create a new bitumen bridge between the particles; in a temperature range between 100ºC and 140ºC, RAMs had relatively similar stiffness, and afterwards, it rapidly increases up to a maximum value at 170ºC; after achieving a maximum value, stiffness started decreasing because the RAPb lost its binding properties under the impact of high temperature. As it can be observed from Figure 5.5a and Figure 5.5b, despite the similar trend of stiffness varying the preheating temperature, the values of stiffness are significantly higher for specimens prepared with a gyratory compactor. This is a consequence of the different compaction energy and type that caused lower air voids content.

The addition of RA, as might be expected, decreased the stiffness between 1.8 and 2.8 times in the case of the specimens compacted in the gyratory compactor and between 0.5 to 2.3 times in the case of the Marshall specimens. Additionally, RA helped in the reactivation of RAPb more than increasing the preheating temperature, especially in the range of temperatures between 100°C and 140°C. The stiffness of the gyratory and Marshall specimens of RAP mixture were 16% higher and 4% lower at 140°C than at 100°C, respectively. When considering the RAP+RA mixtures, specimens compacted at 140°C had 37% and 57% higher stiffness than the specimens compacted at 100°C (gyratory and Marshall, respectively).

5.1.3.3 Indirect Tensile Strength

The ITS test results are reported in Figure 5.6.

The trend of ITS versus the preheating temperature resembles the trend of the stiffness for the same mixtures: it increases with the increase of the preheating temperature up to the maximum value measured at 170°C, and then it decreases. This leads to the conclusions that higher temperature helps to release the RAPb and improve the degree of binder activation, whereas, at low temperature, it is impossible to release RAPb and make it available for blending (D. Lo Presti et al., 2019).

From Figure 5.6, it can be seen that the ITS, regardless of the compaction method used, shows similar values at 100°C, 140°C and 190°C, whereas the highest and the lowest values are obtained at 170°C and 70°C, respectively. It can also be concluded that ITS decreases when RA is used because it softens RAPb.
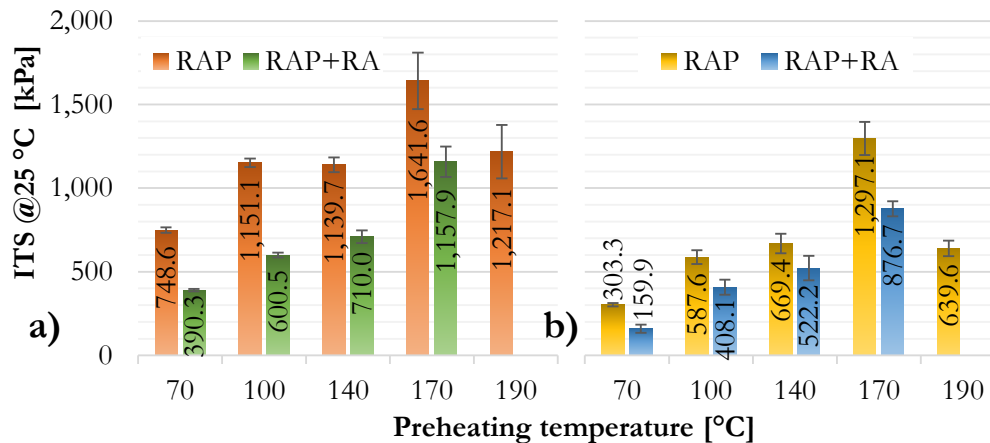
Figure 5.6 *ITS of RAP and RAP+RA specimens preheated at different temperatures and compacted in (a) gyratory and (b) Marshall compactor*

5.1.3.3.1.Correlation Between Stiffness and ITS

Figure 5.7 shows a clear increase in both properties (ITS and stiffness) with the increase of the preheating temperature, regardless of the presence of RA, up to a temperature of 170°C. This temperature, within the framework of this study, can be defined as the *critical temperature,* i.e. the temperature that, if exceeded, leads to a rapid decrease in the values of the properties, especially in the case of Marshall compacted

specimens, confirming the results obtained by Ma et al. (2016). Since there exists a significant correlation between stiffness and ITS values, an additional analysis was performed.
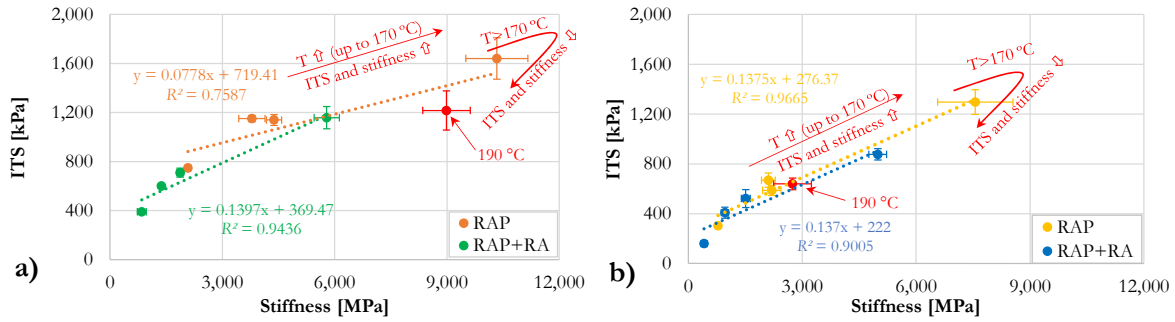
Figure 5.7 *Correlation between stiffness and ITS of RAP and RAP+RA specimens compacted in (a) gyratory and (b) Marshall compactor*

The correlation between ITS and stiffness has been assessed with the Pearson correlation coefficient (r), a widely used correlation statistic that calculates the relationship between the variables. When the coefficient is close to +1 or -1, it indicates a positive or negative linear correlation, respectively, while if the coefficient is closer to zero, it indicates a poor correlation or no correlation between the parameters (Schober & Schwarte, 2018).

Table 5.1 presents the Pearson correlation coefficients for the ITS and stiffness for the different combinations of RAMs (RAP or RAP+RA) and compaction methods (gyratory or Marshall compactor). It is possible to observe that ITS and stiffness have a strong positive linear correlation in all cases except the case of RAP specimens compacted using a gyratory compactor, where the r coefficient was slightly lower but still close to 1. The lower coefficient's value, in that case, is a consequence of including the testing results of the gyratory compacted RAP specimens preheated at a high temperature (190°C) in the analysis, once more highlighting the importance of defining and using the maximum allowable preheating temperature.

Table 5.1 *Correlation coefficients between ITS and stiffness considering the different composition of the RAM and compaction method*

Mixture	Compaction	Pearson r correlation
RAP	Gyratory compactor	0.87
RAP + RA	Gyratory compactor	0.97
RAP	Marshall	0.98
RAP + RA	Marshall	0.95

5.1.3.4 CT$_{index}$

After performing the ITS test, data were further used to calculate CT$_{index}$ of each mixture. The obtained results are displayed in Figure 5.8.

The results show that the preheating temperature had a significant impact on the CT$_{index}$, regardless of the compaction method. In the case of RAP specimens, it decreased with the increase of the preheating temperature up to the *critical temperature* of 170°C and then slightly increased. Similar trends were noticed when RA was added, but with significantly higher CT$_{index}$ values when compared to only-RAP mixtures.

Focusing on the values calculated for the Marshall specimens displayed in Figure 5.8b, it can be seen that the CT$_{index}$ values are much higher when compared to the results calculated for the gyratory specimens displayed in Figure 5.8a. This is a consequence of higher air void content, as reported also in the study conducted by Arámbula-Mercado et al. (2019), where the authors concluded that an increase of 4% in the air void content increased the CT$_{index}$ up to 1.6 times. Since the CT$_{index}$ is very sensitive to air void content, it is difficult to distinguish the impact of preheating temperature on the CT$_{index}$ based on air void content. To isolate only the effect of the preheating temperature, specimens with similar air void

content, as recommended by (Zhou et al., 2017), were compared (gyratory compacted specimens with and without RA prepared at 100°C, 140°C, and 170°C). From Figure 5.8, it can be seen that the increase of preheating temperature causes the decrease of the CT_{index}, confirming the conclusions from Zhou et al. (2017) that more aged mixtures have a lower CT_{index} than unaged mixtures. Specimens prepared in the Marshall compactor could not be compared due to a huge difference in air void content, but the effect of the variation of the preheating temperature on the variation of the CT_{index} was the same as in the case of gyratory compacted specimens. Overall, it can be concluded that the increase of the preheating temperature has a high impact on cracking resistance.
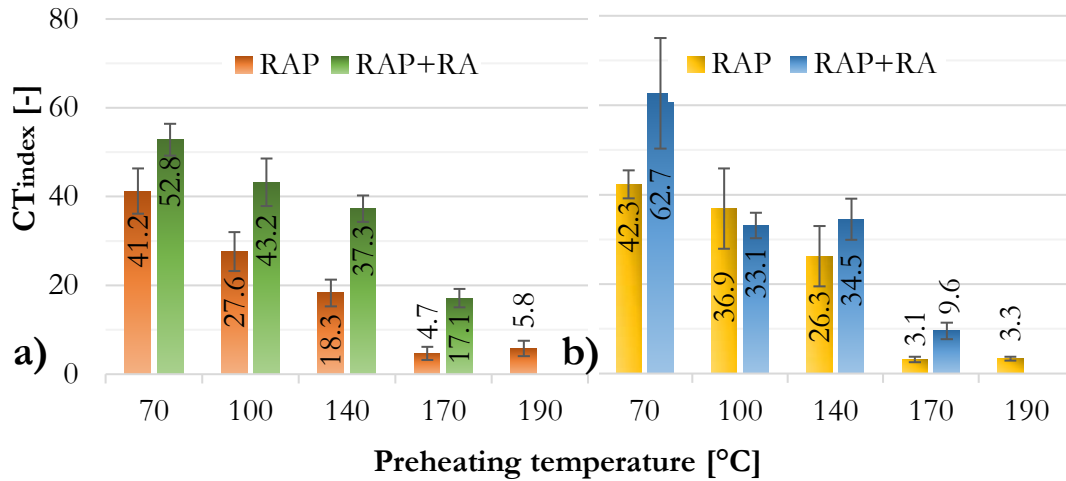
Figure 5.8 *CT_{index} of RAP and RAP+RA specimens preheated at different temperatures and compacted in (a) gyratory and (b) Marshall compactor*

5.1.4 Results of the Optimization Process

Once having measured the properties of each mixture (RAP and RAP+RA), depending on the compaction method (Marshall or gyratory compactor), the methodology for the optimisation of the preheating temperature is applied. Figure 5.9 shows that a steady state with high fitness value, i.e. the maximisation of all objectives, was achieved after approximately 300 simulations.
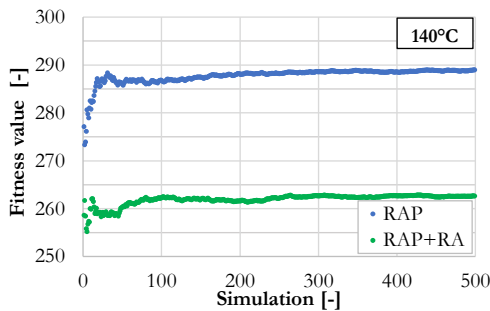
Figure 5.9 *Change of the fitness value in the first 500 simulations (example of the gyratory compacted RAM preheated at 140°C)*
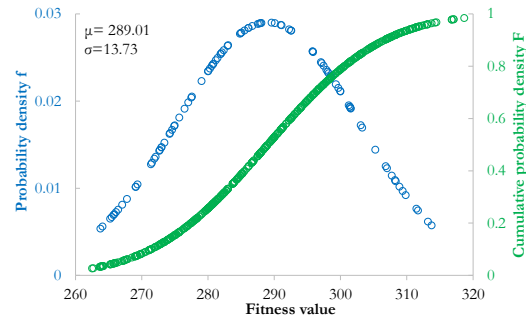
Figure 5.10 *The probability density function and cumulative distribution of the fitness values obtained for the RAP compacted with a gyratory compactor after preheating at 140°C*

Based on this, 500 simulations have been conservatively adopted as the number of simulations appropriate for this application.

Figure 5.10 displays an example of the probability density function and the cumulative distribution of the fitness values obtained for the RAP without a recycling agent preheated at 140°C and compacted with a gyratory compactor. Analogously, the same procedure was applied for all the other RAMs.

Figure 5.11 and Figure 5.12 display the fitness functions obtained for the mixtures composed of RAP and RAP+RA for the two compaction methods (gyratory and Marshall compactors).
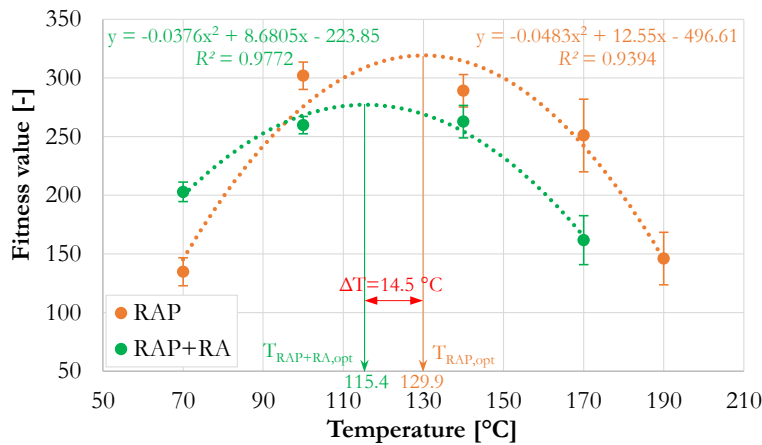
Figure 5.11 *Fitness functions obtained for the gyratory compacted RAP and RAP+RA specimens*
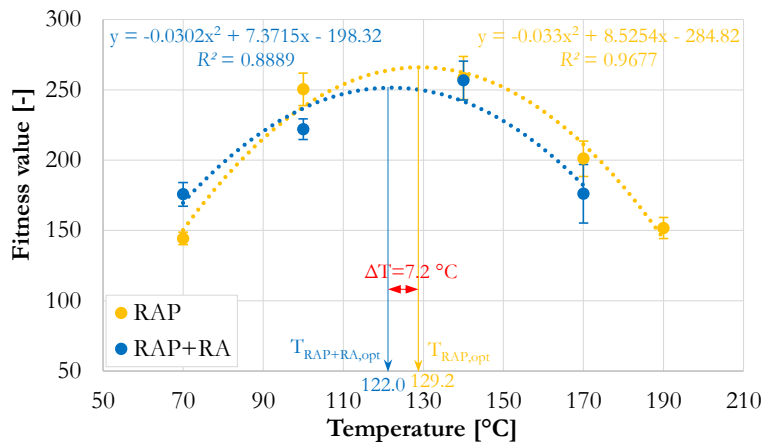
Figure 5.12 *Fitness functions obtained for the RAP and RAP+RA specimens compacted in Marhsall compactor*

From Figure 5.11 and Figure 5.12, it is possible to observe that the fitness value for the low preheating temperature is the lowest, indicating less reactivation of the aged binder trapped in the RAP and, consequently, a lower level of overall performance. Afterwards, the curve shows a rapid increase up to a maximum that corresponds to the optimal preheating temperature of the RAP or RAP + RA ($T_{RAP,opt}$ and $T_{RAP+RA,opt}$, respectively), and then it decreases because the too-high temperature of the RAP hardens the already aged bitumen.

Testing results show that the optimal preheating temperature of RAP is around 30°C, regardless of the compaction type, whereas the addition of RA decreases the preheating temperatures (ΔT) for 14.5°C and 7.2°C when the gyratory and Marshall compactor are used, respectively. This difference is caused by the different compaction type, compaction energy applied, and the effect of RA addition.

Further confirmation of the importance of the preheating temperature is presented in Figure 5.13, which highlights the different visual aspects of the specimens fabricated from RAP preheated at different temperatures. At the lowest temperature of 70°C, the material is not homogenous, and many aggregate particles without bitumen are visible, showing that low temperature cannot reactivate the RAPb, which remains stuck to a few aggregate particles. This caused an adhesive failure (separation of the RAPb from the aggregate). At 100°C, the picture shows another condition: the specimen appears more homogenous with a higher amount of coated particles. Similar cross-sections, considering a homogeneity and occurrence of a cohesive/adhesive failure type appeared at specimens compacted at 140°C and 170°C, but with a much paler colour of RAPb. This is probably a consequence of oil lost due to the exceeding of the optimal preheating temperature. To confirm these hypotheses, additional chemical tests should be performed on RAPb recovered from compacted specimens after preheating at different temperatures.
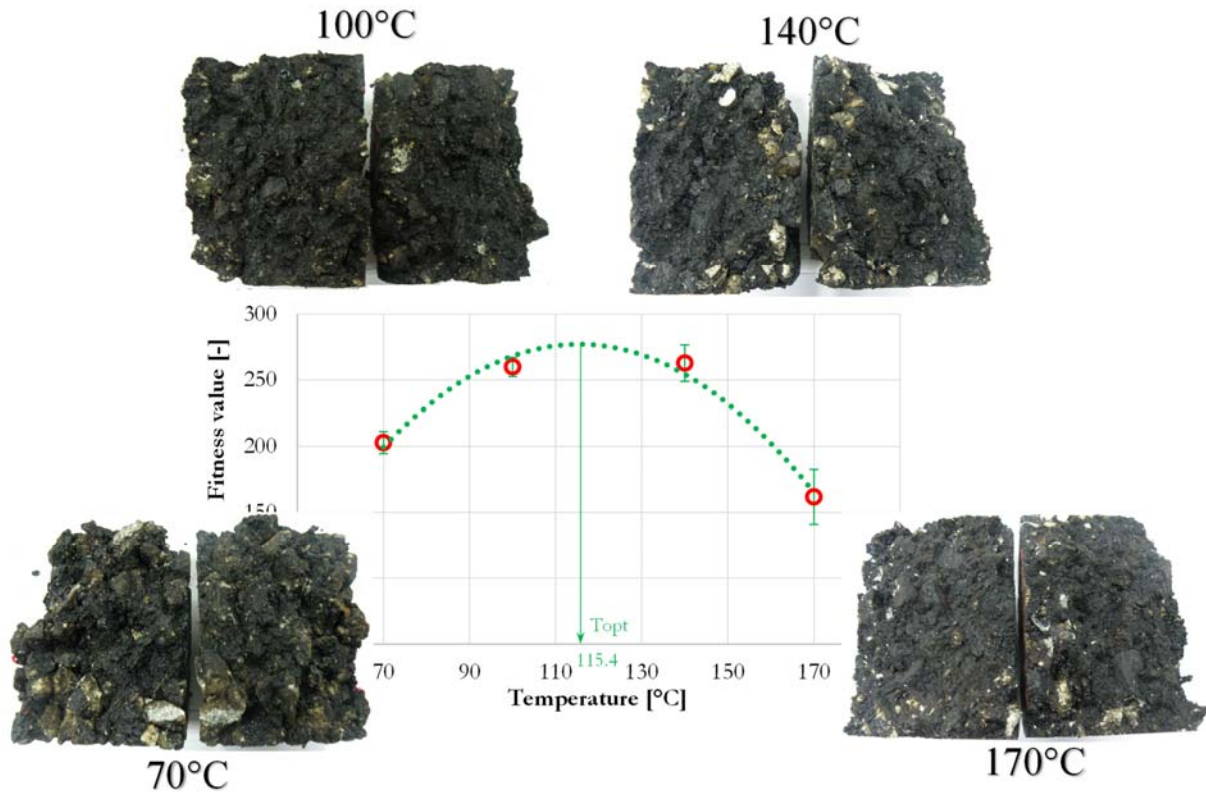
Figure 5.13 *Cross sections of specimens preheated at different temperatures after ITS test*

5.1.5 DoA Estimation

As mentioned in Section 2.2, a reliable testing method for the assessment of RAP's DoA is not yet developed. However, after a comprehensive literature review, the asphalt mixture testing method is used in this study to estimate DoA.

The estimate of DoA was done similarly as it was carried out by Menegusso Pires et al. (2019), who proposed the following equation for DoA estimation:

$$DoA = 100 \times \frac{ITS_{RAP}(X\ °C)}{maxITS_{RAP}} \quad [\%] \hspace{4cm} Equation\ 3.6$$

where ITS_{RAP} *(°C)* is the ITS test result of the only-RAP preheated at a specific temperature "X", and $maxITS_{RAP}$ is the maximum ITS test result of the same RAP material (in that study after preheating at 170 °C).

In this study, DoA is estimated considering two properties, ITS and stiffness, according to the following equation:

$$DoA = 100 \times \frac{Y_{RAP}\ (X°C)}{Y_{reference}} \hspace{4cm} Equation\ 3.7$$

where Y_{RAP} *(°C)* is the property of the only-RAP specimens (stiffness and ITS) preheated at a specific temperature "X", and $Y_{reference}$ is the same property of the reference RAP specimens (with artificially made full activation).

Considering the importance of the above-mentioned *critical temperature*, which may vary depending on RAP source, three specimens with artificially achieved full binder activation were produced using both a gyratory and Marshall compactor. These specimens were prepared as explained below:

- The RAPb was extracted from both RAP fractions (0/11 mm and 11/22 mm).

- An extraction procedure was applied to the blend of solvent and the RAPb to extract the RAPb.

- The rotational viscosity of extracted RAPb was measured at 135 and 165°C, as described in Section 4.1.3. The mixing and compaction temperatures of the reference RAP mixture were determined following the recommendations proposed by Yildirim et al. (2006) (157-162 °C and 172-176°C, respectively, as displayed in Figure 5.14).
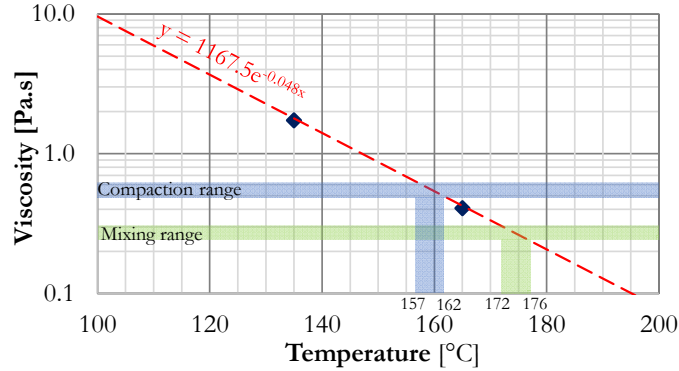
Figure 5.14 *Determination of the mixing and compaction temperatures of the RAP100 mixture*

- The stiffness and ITS of each specimen were measured in the same way as it was performed in Section 5.1.1.

After determining the ITS and stiffness of each specimen, their average values were calculated and compared with the same properties of the RAP mixtures previously preheated at different temperatures (Figure 5.5 and Figure 5.6) using Equation 3.7. DoA values, depending on the preheating temperature and compaction method, as well as the ITS and stiffness of reference specimens, are given in the table below.

In the case of the reference mixture, with artificially made full binder activation, compaction type does not seem to have a significant impact on the stiffness modulus (around 10% less stiffness when using the Marshall compactor). When considering ITS, Marshall specimens have around 20% less stiffness compared to gyratory compacted specimens. However, when discussing DoA at optimal preheating temperature, it is only around 22% when considering the stiffness modulus, and around 35% when considering the ITS value in the case of Marshall compacted specimens. In the case of gyratory compacted specimens, these values are much higher: around 40% and 54%, depending on the selected parameter (stiffness or ITS, respectively).

Table 5.2 *DoA depending on the preheating temperature, compaction type, and a certain property*

	Property	Compaction type	Preheating temperature [°C]					
			70	100	Optimal	140	170	190
Various temperatures	Stiffness [MPa]	Gyratory	2,082	3,790		4,831	10,333	8,987
		Marshall	780	2,198		2,106	7,555	2,743
	ITS [kPa]	Gyratory	748.6	1,151.1		1,139.7	1,641.6	1,217.1
		Marshall	303.3	587.6		669.4	1,297.1	639.6
Full activation	Stiffness [MPa]	Gyratory			10,691			
		Marshall			9,642			
	ITS [kPa]	Gyratory			2,132.2			
		Marshall			1,792.2			
DoA [%]	Stiffness [MPa]	Gyratory	19.5	35.5	~40	45.2	96.7	84.1
		Marshall	8.1	22.8	~22	21.8	78.4	28.4
	ITS [kPa]	Gyratory	35.1	54.0	~54	53.5	77.0	57.1
		Marshall	16.9	32.8	~35	37.4	72.4	35.7

Overall, it can be concluded that the estimation of DoA strongly depends not only on preheating temperature, but also on selected RAP property and compaction type, especially if binder activation is poor. However, it is not possible to accurately assert which parameter is an appropriate indicator of DoA.

5.2 Determination of Optimal Virgin Bitumen and Recycling Agent Contents

This section presents the development of a model for predicting the performance of the RAM, starting from the different dosage of the components, particularly virgin bitumen and the recycling agent, during the mix design procedure. This allows the definition of the optimal contents of the two components, VB and RA, which ensures the achievement of the optimal performance of bituminous mixtures with high RAP content.

5.2.1 Research Methodology, Materials and Methods

5.2.1.1 Research Methodology

To predict the performance and define the optimal VBC and RAC in a high RAP mixture, a multiple variable model was developed using the Response Surface Methodology (RSM). As more than one variable at a time was treated, these variables were expressed in different units, and, thus, the variables were standardized, making the coefficients independent of the unit of measurement (Ayyub & McCuen, 2016).

5.2.1.1.1.Response Surface Methodology
To model systems with multiple variables varying in a defined domain of experiments, it was possible to apply a Response Surface Methodology (RSM) using a limited set of combinations of tests (Bressi, Pittet, et al., 2016). RSM is based on using mathematical laws and statistics to develop an appropriate functional relationship between an independent variable y (output) and a certain number of dependent variables (input) (Khuri & Mukhopadhyay, 2010). These functional relationships allow obtaining predictive models for drawing certain conclusions about the performance of materials and possibly defining the optimum of certain parameters. In this section, RSM was employed to develop an empirical multivariable model to predict the air void content, stiffness, ITS, and CT_{index} of the RAP50 mixture considering the different VBC and RAC. Moreover, in the validity domain, the optimum content of both components has been defined to optimise the performance of the mixture. To do that, it is necessary to proceed with the following steps:

- To establish an adequate experimental design to optimise a response variable using the minimum experimental effort.
- To apply RSM to define the most appropriate predictive performance models by estimating its coefficients from experimental data.
- To test the statistical hypotheses on the goodness (or lack) of fit of the obtained models.
- To validate the obtained models on an independent set of laboratory tests.

5.2.1.1.2. Experimental Design

To develop a predictive response for each parameter (air void content, ITS, stiffness, and CTindex, which are dependent variables) by varying two independent variables (VBC and RAC), it was necessary to set an experimental design that can envisage the possibility of building a second-order polynomial relationship that might be more appropriate in describing the real response surface problems (Khodaii et al., 2016). The most popular experimental designs for fitting a second-order polynomial model for RSM application are the Central Composite Designs (CCD), introduced by Box and Wilson in 1951 (G. E. P. Box & Wilson, 1951), and the Box and Behnken design (G. E.P. Box & Behnken, 1960), introduced in 1960. Later, in the '70s, Doehlert, (Doehlert, 1970) introduced the uniform shell design, which differs from the other designs, for the position of the experiments in the experimental domain. The first advantage of the Doehlert design is that it requires less experimental combinations compared to the central composite or Box-Behnken

Figure 5.15 *Doehlert network for two factors*

designs. Therefore, the arrangement of the measurement points can be optimised to minimise the variance of the fitted model over the experimental space, with a uniform distribution of the points across the experimental space with a rhomboidal net pattern (two factors give a hexagonal shape). This allows obtaining the same variance of the predicted response, i.e. the equal precision of estimation in all directions (rotatable design) (Bressi, Pittet, et al., 2016). Moreover, another advantage of the Doehlert design, compared to the CCD, is the possibility to extend the domain by adding other factors at a second point in time without changing the coordinates of the previously conducted experiments (Bressi, Pittet, et al., 2016).

For two variables (VBC and RAC), the design matrix envisaged seven experiments, where six of them are equidistant from the central experiment, as shown in Figure 5.15. Hence, according to the coordinates of the Doehlert's network, the combinations in Table 5.3 were tested for each parameter (air void content, stiffness, ITS, and CT_{index}). The interval of VBC was selected in the way that final binder content (VB+RAPb) in RAP50 mixture is around ±0.5 %, respecting the binder content of the control mixture (3.6%), whereas the interval of RAC was selected to ensure that the final binder blend has an estimated penetration value as close as possible to the VB.

Table 5.3 *Summary of the experimental points considered in the Dohelert design*

No. of experiment	The interval of RAC [%]	The interval of VBC [%]	Doehlert network coordinates	x_1: RAC [%]	x_2: VBC [%]
1			0; 0	0.230	1.350
2			-1; 0	0.110	1.350
3			1; 0	0.350	1.350
4	0.11-0.35	0.9-1.8	-0.5; -0.866	0.170	0.960
5			0.5; 0.866	0.290	1.740
6			-0.5; 0.866	0.170	1.740
7			0.5; -0.866	0.290	0.960

5.2.1.2 Materials and Methods

Materials of the same origin were used in this part of the research and in the rest of the study (Section 3.4). For mix design methodology, seven mixtures with 50% RAP and different VBCs and RACs were prepared according to the Doehlert's experiment design (Table 5.3), respecting the sample preparation procedure from Section 4.2.

The proportion of RAP fractions was always the same: 4% 0/11 mm and 46% 11/22 mm, whereas the amounts of the other virgin aggregate fractions were modified to achieve the same grading curve for each RAM, as close as possible to the CM (green line in Figure 4.13). The compositions of each mixture are given in Table 5.4.

Table 5.4 *Componential materials of RAP50 mixtures*

Constituent [%]		Mix 1	Mix 2	Mix 3	Mix 4	Mix 5	Mix 6	Mix 7
Virgin aggregate	Filler	0.5	0.5	0.5	0.5	0.5	0.5	0.5
	0/4 mm	16.7	16.7	16.6	16.8	16.5	16.5	16.8
	4/8 mm	13.9	13.9	13.8	14.0	13.8	13.8	14.0
	8/16 mm	1.4	1.4	1.4	1.4	1.4	1.4	1.4
	16/22 mm	16.0	16.1	16.0	16.2	15.9	15.9	16.2
Bitumen	RAPb*				2.34			
	Virgin	1.35	1.35	1.35	0.96	1.74	1.74	0.96
Recycling agent		0.23	0.11	0.35	0.17	0.29	0.17	0.29
RAP	0/11 mm				4			
	11/22 mm				46			
	Total				50			

* Bitumen coming from RAP

As each asphalt mixture contained different VBC and RAC, causing the different stiffness/viscosity of the final binder blend, it was first necessary to determine the optimal mixing and preheating temperatures of each blend. Blends with different VBC, RAC, and RAPb contents, in the same proportion as in an appropriate RAM, were prepared, and their rotational viscosities were measured at 135 and 165°C. Mixing and compaction temperatures were determined according to the procedure explained in Figure 5.14, and results are given in Table 5.5. Additionally, the equations of the trend lines are given in the same table.

Table 5.5 *Mixing and compaction temperatures of RAM with 50% and different VBC and RAC*

Binder blend	Viscosity [mPa.s]		Equation	Mixing range [ºC]	Compaction range [ºC]
	135 ºC	*165 ºC*			
Blend 1	0.753	0.250	$y=108.47e^{-0.037x}$	159-165	140-146
Blend 2	0.950	0.280	$y=230.64e^{-0.041x}$	162-167	145-150
Blend 3	0.555	0.214	$y=40.02e^{-0.032x}$	152-159	131-138
Blend 4	0.940	0.281	$y=218.87e^{-0.04x}$	164-170	147-152
Blend 5	0.600	0.241	$y=36.487e^{-0.03x}$	159-167	136-144
Blend 6	0.726	0.245	$y=96.119e^{-0.036x}$	160-166	141-147
Blend 7	0.531	0.206	$y=37.494e^{-0.032x}$	150-157	129-136

After the preparation of the testing specimens, the volumetric properties were measured using the standardized procedures mentioned in Section 4.3.1 The stiffness and ITS were determined respecting the conditions given in Section 5.1.1, whereas the CT_{index} of each specimen was calculated following the methodology proposed in Section 4.3.5. The experimental plan of this section is displayed in Figure 5.16.
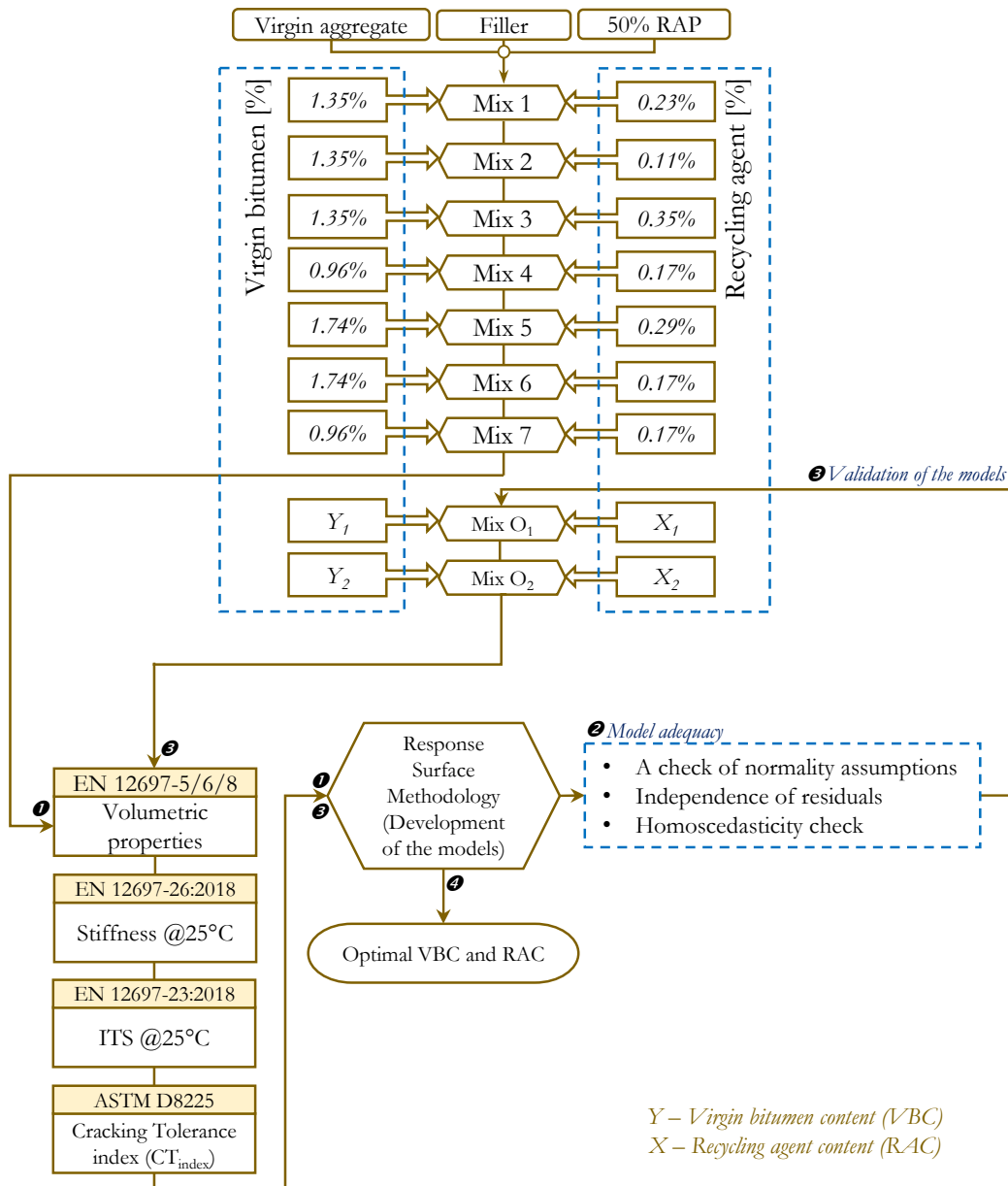
Figure 5.16 *Experimental plan of the mix design methodology development*

5.2.2 Testing Results and Determination of Optimum Conditions

5.2.2.1 Testing Results

Four replicates for each combination reported in Table 5.3 were conducted. The average values and standard deviations of each property investigated were displayed in Figure 5.17. As these testing results were used as input data for calculation of regression coefficients of different models, they are not discussed in detail.
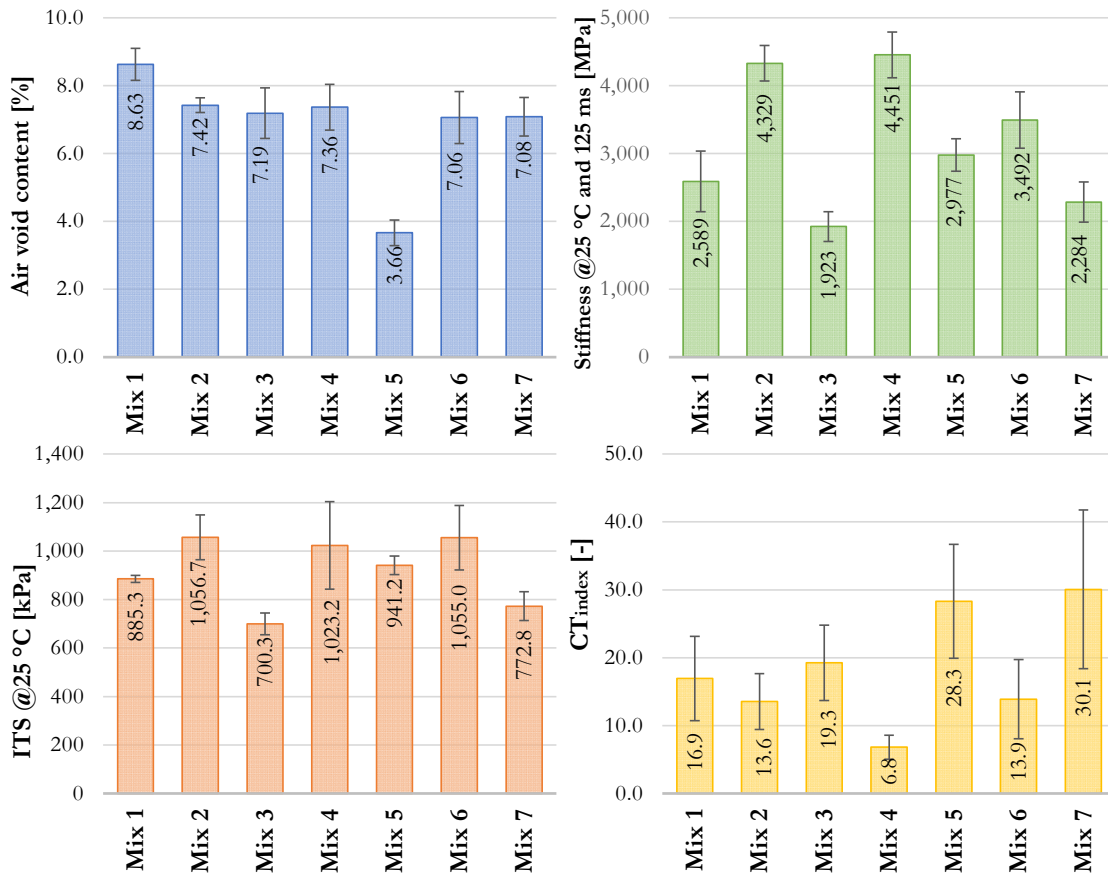
Figure 5.17 *Testing results of RAP50 mixtures required for development of appropriate models*

5.2.2.2 Development of Models

Empirical response models are based on the experimental data to adequately represent the responses, both in the domain where experiments were performed and outside the domain. It is necessary to find a suitable approximation for the true correlation between independent variables and appropriate response surfaces. The three objectives of considering these models are (Khuri & Mukhopadhyay, 2010):

1. To predict the response values for a given set of input data by identifying an appropriate relationship between the results and the VBC and RAC.

2. To measure the importance of the input factors VBC and RAC for those models.

3. To determine the values of the input factors VBC and RAC to optimise the response value over the validity domain.

Depending on the complexity of the model, different sets of coefficients can be selected. To understand and select which type of model is more appropriate to fit the data, and, therefore, which set of coefficients is useful for predicting the response variable, several regression-related analyses were performed, including the computation of the coefficient of determination R^2, goodness of fit, and Lack of Fit (LoF). Initially, a first-order response surface model was applied to each set of experimental data since this is the simplest linear model following the parsimony principle If the curvature of the response was strong enough that the first-order model is inadequate to appropriately describe the experimental data, a second-order or a third-order model were then applied, and the analyses were repeated, or the interactions between the variables were added (Myers & Myers, 2007). The relationship between the input variables and the response variables (air void content, stiffness, ITS and CT_{index}) was expressed according to the equation:

$$y = \beta_0 + \beta_1 x_1 + \beta_2 x_2 + \beta_{12} x_1 x_2 + \beta_{11} x_1^2 + \beta_{22} x_2^2 + \beta_{111} x_1^3 + \varepsilon \qquad \text{*Equation 3.8*}$$

where x_1 is the RAC [%], x_2 is the VBC [%], β_0 is the coefficient of the constant factor term, β_1 and β_2 are the coefficients of the main effects (RAC and VBC, respectively), β_{12} is the coefficient of the interaction terms (recycling agent/virgin bitumen), β_{11} and β_{22} are the coefficients of the second-degree terms (related to the RAC and VBC, respectively), and β_{111} is the coefficient of the third-degree term (related to the RAC).

It should be mentioned that a polynomial with degree greater than two is usually not used in RSM (Sarabia et al., 2020), but in the case of the CT_{index} response model, this was necessary due to its complexity. Finally, the selected models for certain responses are given in the table below.

Table 5.6 *Appropriate models selected for the description of investigated properties*

Response	Degree of the polynomial
Air void content	Second
Stiffness	Second
ITS	First
CT_{index}	Third

5.2.2.3 Estimation of Regression Coefficients

The estimation of the regression coefficients was performed using an iterative least-square procedure, whereas their significance was checked using the *t-test*. A student's *t-test* was used to test the significance of individual regression coefficients on every proposed model (Equation 3.8). The p-value for each term tests the null hypothesis that a coefficient is equal to zero, i.e. it is not statistically significant. A p-value lower than the significance level (0.05) indicates that the null hypothesis can be rejected. Alternatively, if the p-value is greater than the significance level, there is insufficient evidence in the sample to conclude that a non-zero correlation exists, i.e. coefficients are not statistically significant (red values). In Table 5.7, the values of the individual regression coefficients of each response are given together with the statistical parameters required to test the null hypotheses.

Table 5.8 presents a summary of the selected models and the individual regression coefficients of each model.

Table 5.7 *Student's t-test on significance of individual regression coefficients*

Model	Notation	Coefficients	Standard error	Stat t	p-value	Significance at 5% confidence level
Air void content	β_0	-20.56	5.85	-3.52	0.001	Yes
	β_1	55.90	18.35	3.05	0.005	Yes
	β_2	37.44	7.12	5.26	2.81E-05	Yes
	β_{12}	-24.92	9.13	-2.73	0.012	Yes
	β_{11}	-64.38	34.69	-1.86	0.076	No
	β_{22}	-12.71	2.57	-4.94	6.09E-05	Yes
Stiffness	β_0	12,227.45	1,811.42	6.75	1.78E-08	Yes
	β_1	-27,625.27	5,381.91	-5.13	5.12E-06	Yes
	β_2	-8,462.32	2,172.13	-3.90	3.02E-04	Yes
	β_{12}	7,760.82	2,678.54	2.90	0.005	Yes
	β_{11}	19,480.99	10,299.19	1.89	0.064	No
	β_{22}	2,604.87	754.99	3.45	0.001	Yes
ITS	β_0	926.08	91.88	10.08	2.66E-11	Yes
	β_1	-1,179.67	228.86	-5.15	1.38E-05	Yes
	β_2	182.33	64.48	2.83	0.008	Yes
CT_{index}	β_0	192.14	63.36	3.03	0.005	Yes
	β_1	-2,012.53	552.64	-3.64	0.001	Yes
	β_2	-72.42	62.55	-1.16	0.257	No
	β_{12}	-12.43	76.82	-0.16	0.872	No
	β_{11}	9,432.51	2,493.94	3.78	7.85E-04	Yes
	β_{22}	28.05	23.37	1.20	0.240	No
	β_{111}	-13,330.40	3,608.36	-3.69	9.87E-04	Yes

Considering the table above, it can be seen that there are several coefficients with insignificant p-values, suggesting that changes in the predictors are not associated with changes in the responses. This means that they can theoretically be neglected, but it is decided to keep them to have a more precise model, because it has been proven that, for example, VBC has a crucial impact on the CT_{index}; so, it should not be neglected (Zhou et al., 2019).

Table 5.8 *Summary on the selected models and related regression coefficients*

Parameter	Model	Regression coefficients						
		β_0	β_1	β_2	β_{11}	β_{12}	β_{22}	β_{111}
Air void content	2nd order	-20.56	55.90	37.44	-64.38	-24.92	-12.71	-
Stiffness	2nd order	12,227.45	-27,625.27	-8462.32	19,480.99	7,760.82	2,604.87	-
ITS	Linear	926.08	-1,179.67	182.33	-	-	-	-
CT_{index}	3rd order	192.14	-2,012.54	-72.42	9,432.51	-12.43	28.05	-13,330.4

5.2.2.4 Response Surface Plots

The 3D response surface models of the air void content, stiffness, ITS, and CT_{index} are plotted using developed models and displayed in Figures 5.18-5.21. In each surface plot, the two input variables (VBC and RAC), are plotted on the *x* and *y*-axis, and the response surfaces (air void content, stiffness, ITS and CT_{index}) are represented in the *z* direction.
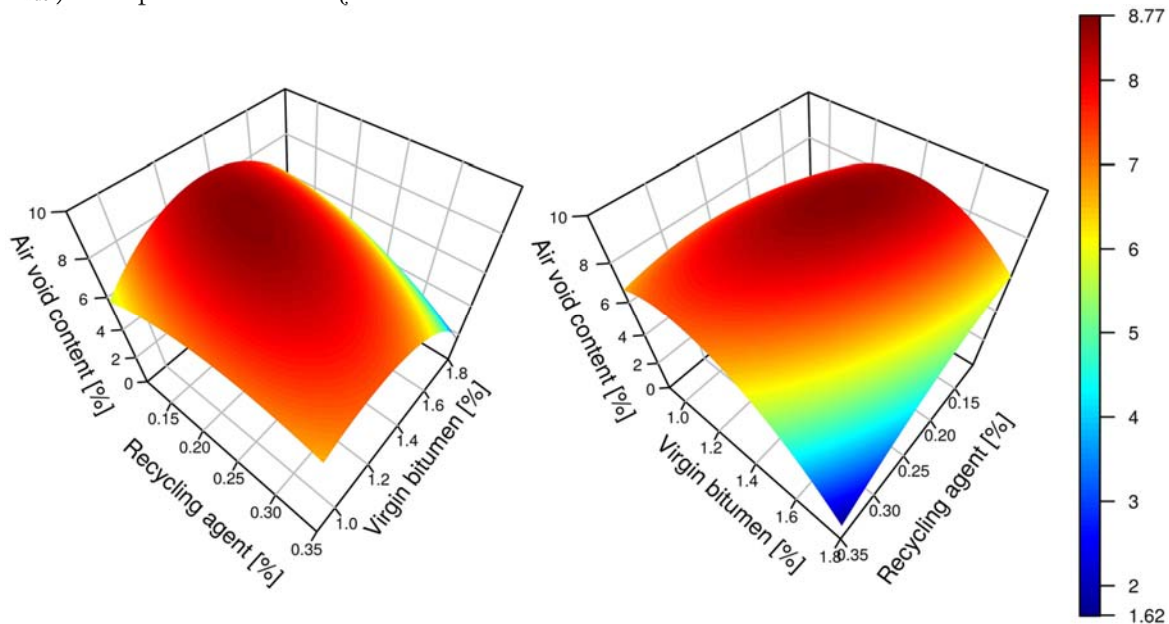
Figure 5.18 *3D response surface model of air void content*
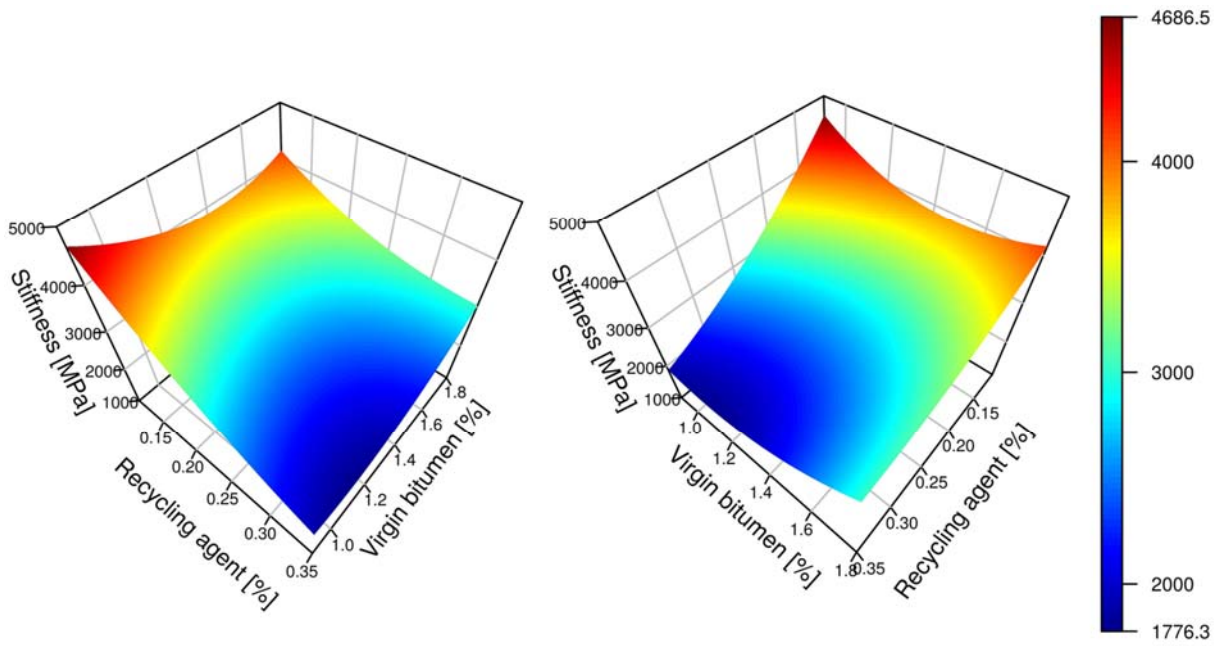
Figure 5.19 *3D response surface model of stiffness*
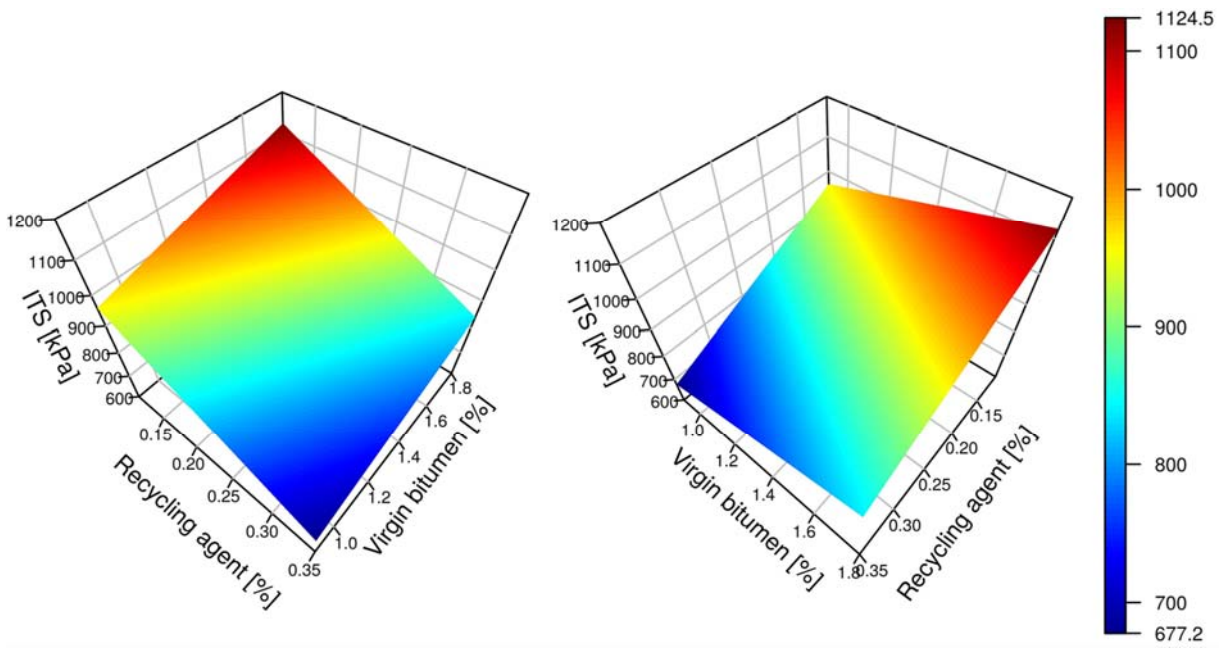
Figure 5.20 *3D response surface model of ITS*
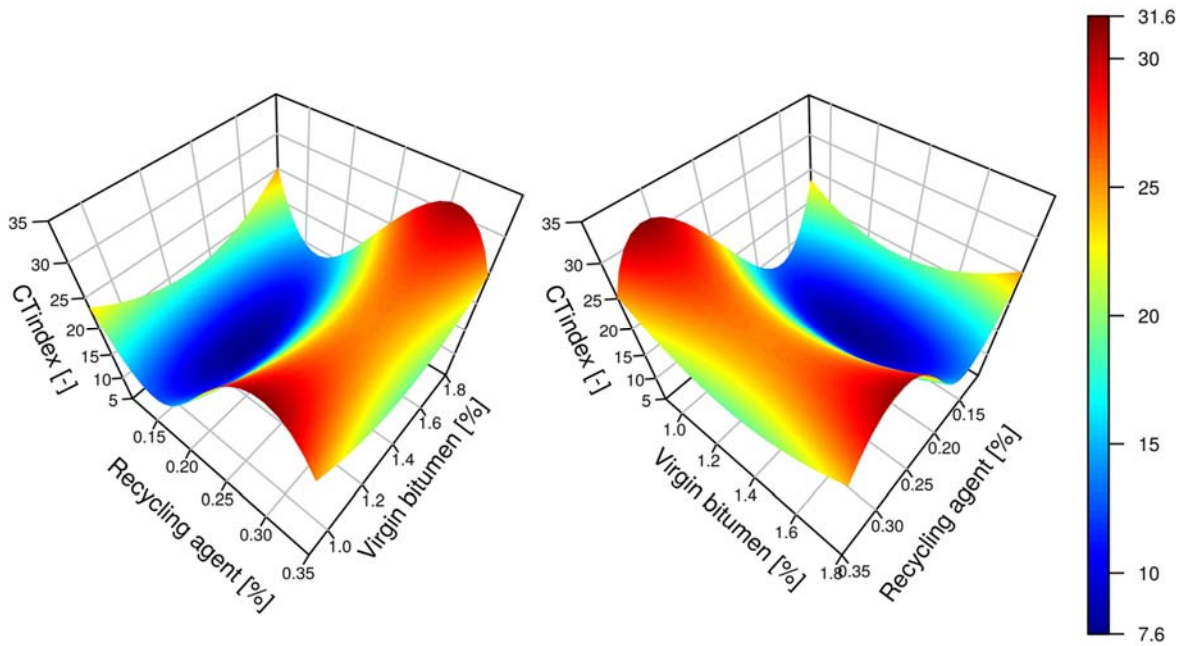
Figure 5.21 *3D response surface model of the CT_{index}*

As expected, with the increase of VBC and RAC, air void content decreases. Stiffness is mostly influenced by RAC: if a fixed RAC is considered, it can be observed that stiffness does not show significant variations when the VBC changes. In the case of ITS, it depends on both variables: when VBC decreases and RAC increases, ITS decreases. Finally, the CT_{index} is also mainly influenced by RAC, and it is typically very poor for low RAC (below 0.25%), regardless of the VB content.

5.2.3 Model Adequacy

The **AN**alysis **O**f **VA**riance (ANOVA) represents a collection of statistical models used to analyse the differences between two or more means. It allows the evaluation of the probability p to test the null hypothesis and, consequently, the reliability of the model. In the ANOVA, the variation in the response measurements is partitioned into components that correspond to different sources of variation. ANOVA is also used when assessing the Lack of Fit (LoF) of a model. An LoF test is based on the components of a partition of the sum of the squares in ANOVA, and it is used when replicate runs are available (i.e. more than one observation of y at the same design point x).

When this procedure is used, it is expected that the mean square is significantly greater than the mean square of the residual errors. Table 5.9 summarizes the decomposition of the sum of squares with the corresponding degrees of freedom.

Table 5.9 *ANOVA for significance and lack of fit, adapted from (Sarabia et al., 2020)*

Source of variation	Degrees of freedom	Sum of squares	Mean square	F^*
Regression	p-1	SS_R	MS_R	MS_R/MS_E
Error or residual	N-p	SS_E	MS_E	
Lack of fit	n-p	SS_{LOF}	MS_{LoF}	MS_{LoF}/MS_{PE}
Pure error	N-n	SS_{PE}	MS_{PE}	
Total	N-1	SS_T		

5.2.3.1 ANOVA Hypotheses

Hypotheses underlying the use of the ANOVA are as follows (George E.P. Box et al., 2005):

- Data are normally distributed.

- The data set consists of independent values;

- The homoscedasticity (i.e. the variance of the groups) is the same as for the population).

5.2.3.1.1.A Check of Normality Assumptions

A statistical analysis of the measured (empirical) values and regression residuals of each parameter investigated were performed graphically and mathematically to check if it is reasonable to assume that they are normally distributed. In Figure 5.22a and Figure 5.22c, examples of the histograms of measured stiffness and appropriate regression residuals are given, respectively, suggesting that the variables are normally distributed. To evaluate their normality of the distribution (whether and to what extent the distribution of the variable follows the normal distribution), normal probability plots (the deviations from the mean) were also prepared. Examples of normal probability plots of measured stiffness and regression residuals are displayed in Figure 5.22b and Figure 5.22d, from which it can be assumed that the data are normally distributed. Finally, the Kolmogorov-Smirnov statistical test (Kottegoda & Rosso, 2008) was applied to control if the random variable has a normal distribution, as specified earlier. The test was performed under the following conditions:

- H_0: the random variable (representing the measured values of air void content, stiffness, ITS, and CT_{index} and their appropriate regression residuals) has a normal distribution.

- H_A: the random variable has a different distribution.

- Level of significance: $\alpha=0.05$

- Critical region: The $D_{n,0.05}$ of each parameter is determined considering the number of variables investigated, and these values are given in Table 5.10.

The observed values of the maximum absolute difference between the theoretical and step functions, D_n, are given in Table 5.10.

Table 5.10 *A check of normality using Kolmogorov-Smirnov test*

Variable		D_n	$D_{n,0.05}$	Decision
Air void content	Measured values	0.194	0.25	$D_n< D_{n,0.05}$
	Regression residuals	0.089	0.227	$D_n< D_{n,0.05}$
Stiffness	Measured values	0.097	0.264	$D_n< D_{n,0.05}$
	Regression residuals	0.111	0.185	$D_n< D_{n,0.05}$
ITS	Measured values	0.117	0.25	$D_n< D_{n,0.05}$
	Regression residuals	0.149	0.227	$D_n< D_{n,0.05}$
CT_{index}	Measured values	0.051	0.25	$D_n< D_{n,0.05}$
	Regression residuals	0.036	0.227	$D_n< D_{n,0.05}$

The D_n values of each parameter are less than the critical values; so, the null hypothesis is not rejected, i.e. random variables have a normal distribution.
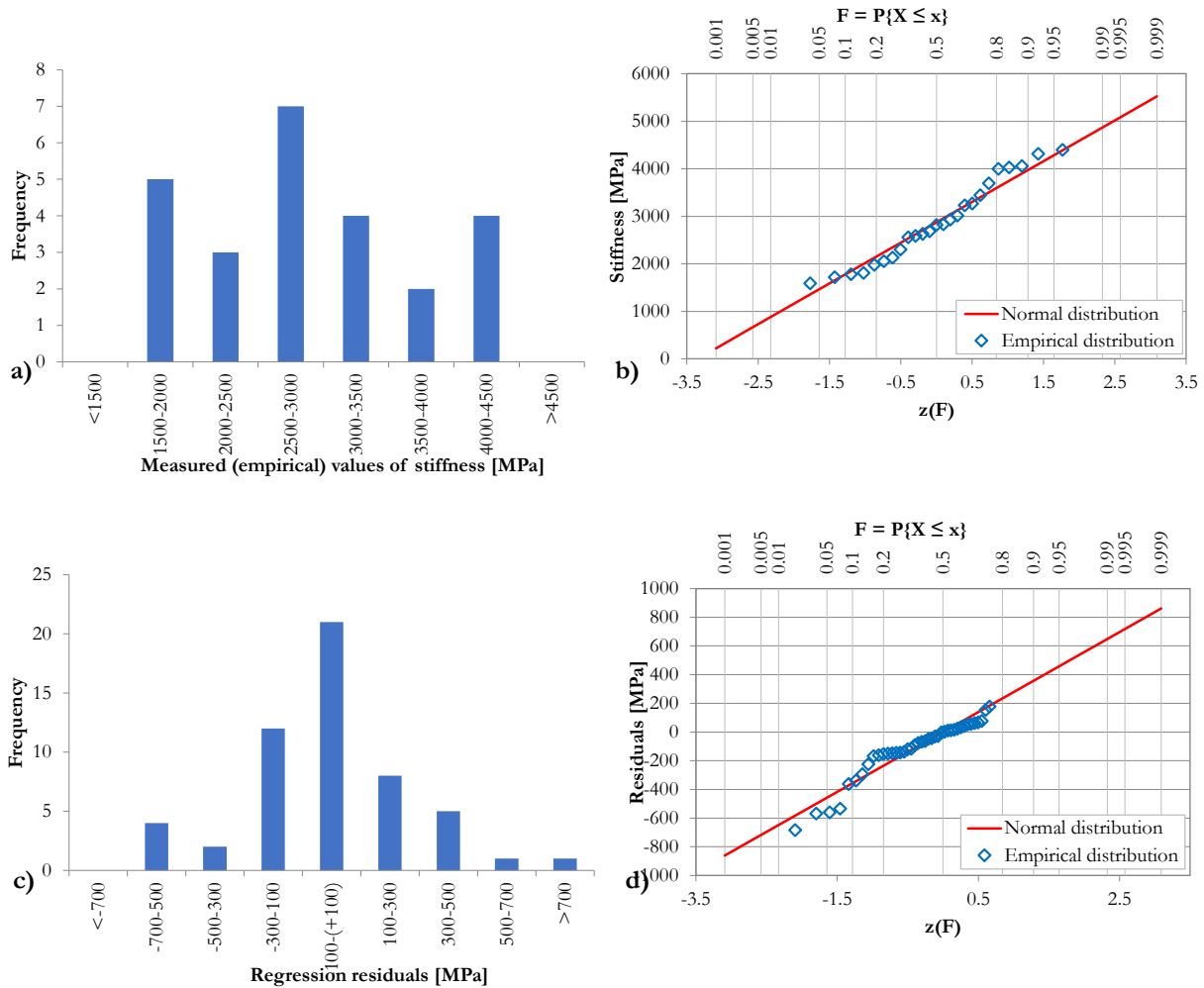
Figure 5.22 *(a) Histogram and (b) normal probability plot for the measured values of stiffness and (c) histogram and (d) normal probability plot for the residuals of stiffness*

5.2.3.1.2. Independence of Residuals

In addition to the assumption that residuals and variables are normally distributed, it is also necessary to prove that residuals are independent of the corresponding predicted (fitted) values. The check may also be performed graphically and mathematically.

The most frequently used graph for analysing residuals is a *residual vs. fitted value* plot. If the assumption about the independence is met, the residuals will be randomly scattered around the centreline of zero, without an obvious pattern.
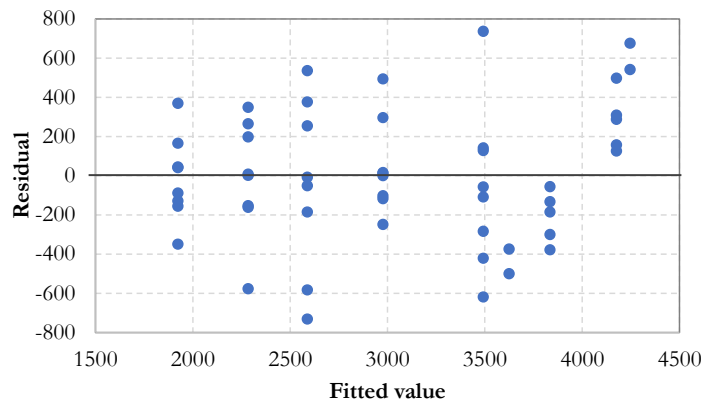
Figure 5.23 *The residuals vs. fitted plot of the stiffness*

Figure 5.23 displays a plot of residuals versus the corresponding stiffness values predicted with the developed model. Visually, the residuals are scattered randomly; so, it can be said that residuals are independent of one another. However, it was necessary to mathematically confirm the absence of dependence between the variables.

The correlation between two continuous variables was evaluated using the Pearson coefficient of correlation, r. The coefficient values were calculated for each response considered (air void content,

stiffness, ITS and CT_{index}), giving a value equal to zero in all cases, confirming that there is no correlation between residuals and corresponding predicted values.

5.2.3.1.3. Heteroscedasticity Test

To determine if the heteroscedasticity is present in a regression analysis, the Breusch-Pagan test was used (Breusch & Pagan, 1979). The appropriate hypotheses were:

- H_0: the error variances are equal (homoscedasticity – Figure 5.24a).
- H_A: the error variances are a multiplicative function of one or more variables (heteroscedasticity – Figure 5.24b).
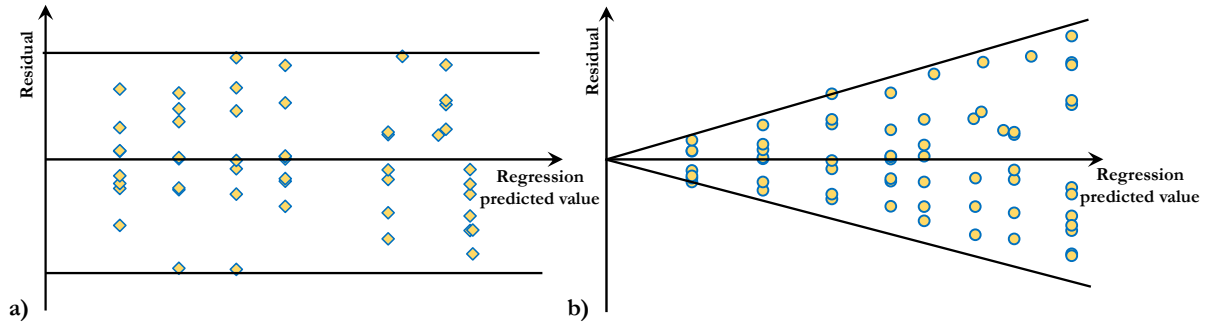
Figure 5.24 *(a) Homoscedasticity and (b) heteroscedasticity residual plots*

It was first necessary to calculate the Chi-Square test statistic, using Equation 3.9, and then to compare it with the p-value associated with this test statistic.

$$X^2 = n \cdot R^2_{new}$$
<div align="right">*Equation 3.9*</div>

where n is the number of observations, and R^2_{new} is the R square of the "new" regression, in which the squared residuals are used as response variables.

The p-value of each data set was calculated and it is displayed in Figure 5.25. It can be concluded that all p-values are greater than 0.05; so, the null hypothesis cannot be rejected. There is insufficient evidence to conclude that heteroscedasticity is present in the proposed regression model.
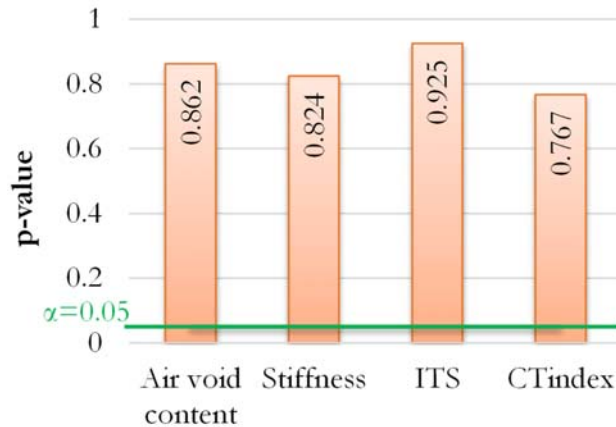
Figure 5.25 *The p-values of the investigated parameters*

5.2.3.2 Goodness of Fit

The reliability of the developed models was assessed by determining the coefficient of determination and application of ANOVA to calculate the statistical parameters, F, and p-values. The results are shown in Table 5.11.

The coefficient of determination (R^2) is defined as:

$$R^2 = \frac{SS_R}{SS_T} = 1 - \frac{SS_E}{SS_T}$$
<div align="right">*Equation 3.10*</div>

where SS_R is the sum of squares due to regression, and SS_T is the sum of squares due to the errors.

It represents the measure of to what extent the models explain experimental data. The coefficient of determination normally ranges between 0 and 1, where higher values indicate that regression predictions fit the data well. However, a large value of R^2 does not necessarily imply that the regression model is satisfactory, meaning that there can be models with large R^2 that yield poor predictions of new observations or poor estimates of the mean response (Sarabia et al., 2020).

To confirm the existence of a correlation between the response and the variables X_j, at least one of the regression coefficients β_j must be non-null. The appropriate hypotheses were:

- H_0: $\beta_1 = \beta_2 = \beta_3 = \ldots = \beta_{p-1} = 0$

- H_A: $\beta_j \neq 0$ for at least one j

The test procedure was based on the partitioning of the adjusted total sum of squares (SS_T) in a sum of squares due to residual (SS_E) and a sum of squares due to the model (regression) (SS_R):

$$SS_T = SS_E + SS_R = \sum_{i=1}^{N}(y_i - \hat{y}_i)^2 + \sum_{i=1}^{N}(\hat{y}_i - \bar{y})^2$$
<div align="right">*Equation 3.11*</div>

where y_i are the observations, $\hat{y}_i$ are the regression estimates, and $\bar{y}$ is the sample mean.

If the null hypothesis was true, then SS_R/σ^2 is distributed as X_{p-1}^2, X^2 with p-1 degrees of freedom. Also, it is known that SS_E/σ^2 is distributed as X_{N-p}^2, and SS_R and SS_E are independent; so, the statistic

$$F^* = \frac{\frac{SS_R}{p-1}}{\frac{SS_E}{N-p}} = \frac{MS_R}{MS_E}$$
<div align="right">*Equation 3.12*</div>

is distributed as $F_{p-1,N-p}$, and the null hypothesis would be rejected at the significance level α if F_{calc} exceeds the critical value at level α, $F_{\alpha,p-1,N-p}$. In other words, the relationship is statistically significant at level α (Sarabia et al., 2020).

Hypotheses were further checked by computing the probability P{Fp−1, N−p > Fcal}, called the p-value, so that the null hypothesis can be rejected (the model is significant) at a significance level α if the p-value is less than α (Sarabia et al., 2020).

Table 5.11 *ANOVA and Lack of Fit tables related to the models for air voids, ITS, CTindex and stiffness.*

ANOVA (air voids)	df*	SS*	MS*	F*	F_{crit}	p-value	R^2
Regression (2rd degree)	5	41.4	8.28	11.59	2.661	1.43E-05	0.72
Residual	22	15.7	0.71				
Lack of Fit	9	8.2	0.91	1.58		0.219	
Pure error	13	7.5	0.58				
Total	27	57.1					
ANOVA (stiffness)	**df***	**SS***	**MS***	**F***	**F_{crit}**	**p-value**	**R^2**
Regression (2rd degree)	5	29,185,106	5,837,021	47.4	2.409	1.96E-17	0.83
Residual	48	5,907,461	123,072				
Lack of Fit	9	1,790,311	198,923	1.88		0.084	
Pure error	39	4,117,150	105,568				
Total	53	35,092,567					

ANOVA (ITS)	df*	SS*	MS*	F*	F_{crit}	p-value	R^2
Regression (linear)	2	358,296	179,148	15.35	3.305	2.32E-05	0.50
Residual	31	361,811	11,671				
Lack of Fit	9	127,836	14,204	1.52		0.196	
Pure error	25	233,975	9,359				
Total	33	720,107					
ANOVA (CT$_{index}$)	**df***	**SS***	**MS***	**F***	**F_{crit}**	**p-value**	**R^2**
Regression (3rd degree)	6	1,419	236.6	3.59	2.495	0.0096	0.44
Residual	27	1,781	66.0				
Lack of Fit	9	356	39.5	0.50		0.856	
Pure error	18	1,425	79.2				
Total	33	3,200					

* df=degree of freedom, SS=Sum of the Squares, MS=Mean Squares, F=SS/MS

The F* values of each model developed (Table 5.11) are much greater than the critical values at a level of 0.05; so, the null hypothesis can be rejected.

When considering the p-values of the selected regression models from Table 5.11, it can be seen that models are significant at the customary 0.05 level; thus, the selected models (2nd degree for air voids and stiffness, 3rd degree of CT$_{index}$, and linear for ITS) explain the variance of the response well. Null hypotheses can be rejected since there is no experimental evidence to reject the proposed models.

In two cases (air voids and stiffness), the coefficients of determination R^2 revealed a very good fit of the selected models to the distribution of the real data. In the other two cases (ITS and CT$_{index}$), which have the R^2 as a bit less than 0.5, it was even more important to go a step further in the statistical analysis and compute the LoF to verify the appropriateness of the models.

5.2.3.3 Lack of Fit

A step further for evaluating the goodness of fit of the models was represented by the application of a *Lack of Fit* (LoF) test. The *LoF* was computed to achieve a more precise evaluation of which part of the total error is due to the regression and which was due to random error (Table 5.11). As repetitions for each combination were available, LoF allowed the decomposition of the error into the pure error (random) and error due to lack of fit:

$$SS_E = SS_{PE} + SS_{LoF} = \sum_{i=1}^{c} \sum_{j=1}^{n_i} (y_{ij} - \bar{y}_i)^2 + \sum_{i=1}^{c} \sum_{j=1}^{n_i} (\bar{y}_i - \hat{y}_{i,j})^2 \qquad \text{Equation 3.13}$$

where y_{ij} is the observed response, $\hat{y}_{i,j}$ is the predicted response, and $\bar{y}_i$ is the average observed response.

If ε is N(0,σ²) and β_2=0, it can be shown that (Sarabia et al., 2020):

$$F^* = \frac{\frac{SS_{LOF}}{n-p}}{\frac{SS_{PE}}{N-n}} = \frac{MS_{LoF}}{MS_{PE}} \qquad \text{Equation 3.14}$$

After a while, standardized hypothesis test procedures in the lack of fit F-test were followed by specifying the null and alternative hypothesis:

- H_0: The relationship assumed in the model is reasonable, i.e. there is no lack of fit in the model.

- H_A: The relationship assumed in the model is not reasonable, i.e. there is a lack of fit in the model.

The p-value was then calculated, which helps in determining the LoF as follows:

- If the p-value is smaller than the significance level α (0.05), the null-hypothesis is rejected, i.e. there is sufficient evidence at the α level to conclude that there is lack of fit in the model.

- If the p-value is greater than the significance level α (0.05), the null-hypothesis is not rejected, i.e. there is not enough evidence at the α level to conclude that there is lack of fit in the model.

As it can be observed from Table 5.11, all the p-values of LoF for all the models are greater than α=0.05, meaning that the models assumed to predict the results are reasonable, and there is not enough evidence at the α level to conclude that there is lack of fit in the model (a model fits well).

5.2.4 Validation of the Models

To validate the developed models and test their reliability, two additional mixtures were prepared (Mix O_1 and Mix O_2, Table 5.12). The VBC and RAC in these mixtures have been selected using the developed models so that the final mixtures have properties as close to the CM's as possible. The following criteria, which RAP50 should satisfy, were established:

1) Air void content: between 5% and 7%
2) Stiffness at 25 °C: greater than 3,500 MPa
3) ITS at 25 °C: greater than 1,000 kPa
4) CT_{index}: greater than 20

Two amounts of VB and RA have satisfied all these criteria (Mix O_1: 1.62% VB and 0.11% RA, and Mix O_2: 1.8% VB and 0.12% RA), and they are shown as points in Figure 5.26. The composition of the mixtures, as well as the mixing and compaction temperatures, are given in Table 5.12. Four specimens of each mixture were prepared according to Section 4.2 and their properties were evaluated. The obtained results were further compared with values predicted from the developed models (Table 5.13).

Table 5.12 *Componential materials of optimized RAP50 mixtures*

Constituent [%]		Mix O1	Mix O2
Virgin aggregate	Filler	0.5	0.5
	0/4 mm	16.6	16.5
	4/8 mm	13.8	13.8
	8/16 mm	1.4	1.4
	16/22 mm	16.0	15.9
Bitumen	RAPb*	2.34	
	Virgin	1.62	1.80
Recycling agent		0.11	0.12
RAP	0/11 mm	4	
	11/22 mm	46	
	Total	50	
Viscosity	135 °C	0.793	0.773
[Pas]	163 °C	0.259	0.248
Mixing temp.		162-168	159-165
Compaction temp.		143-149	141-147
Equation		$y = 120.96e^{-0.037x}$	$y = 128.81e^{-0.038x}$

* Bitumen coming from RAP
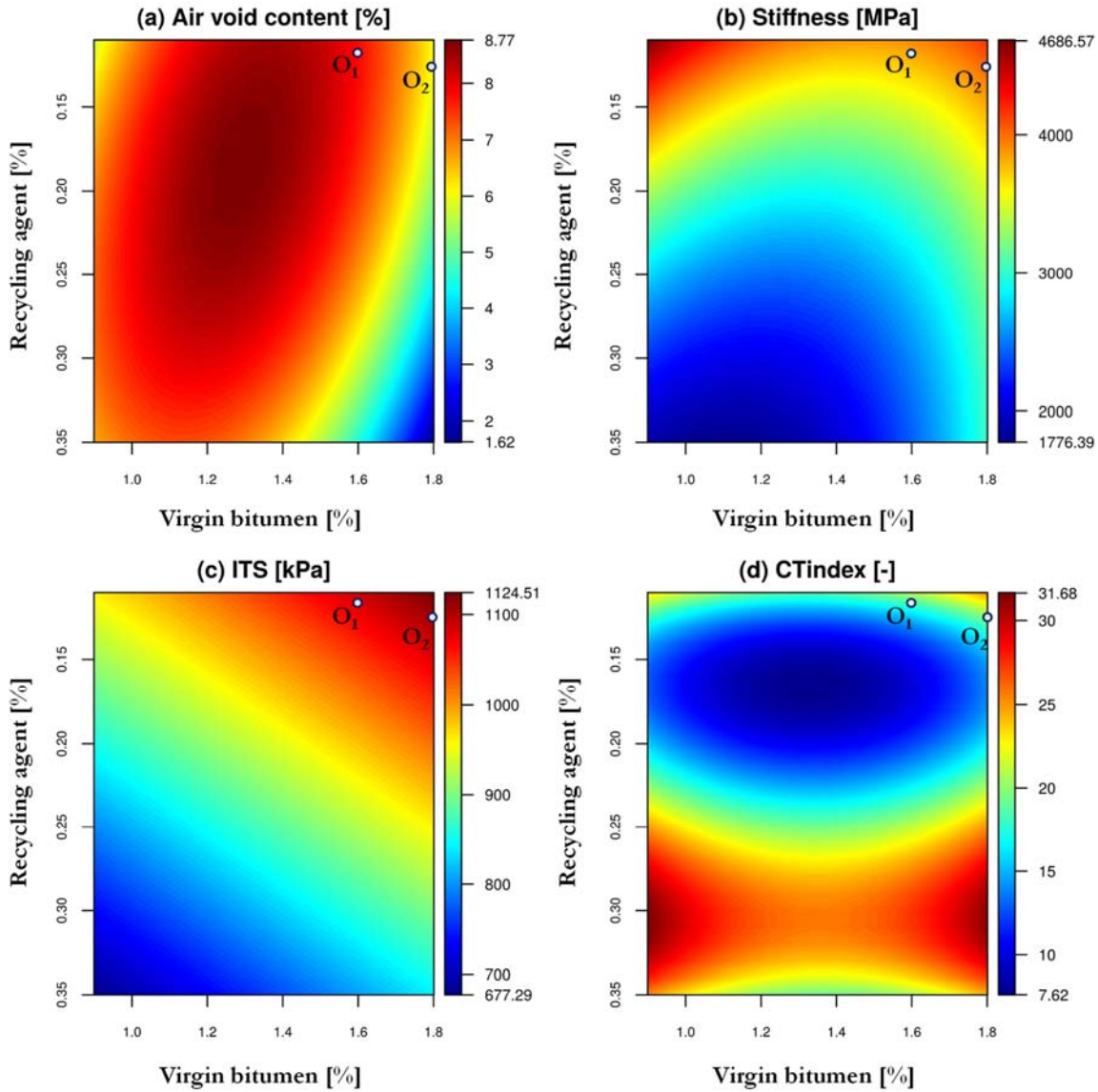
Figure 5.26 *2D response surface models for (a) air void content, (b) stiffness, (c) ITS, and (d) CT$_{index}$*

Table 5.13 *Validation of the developed models by comparing predicted and measured properties of asphalt mixtures*

Mixture	Air voids [%]		ITS [kPa]		CTIndex [-]		Stiffness [MPa]	
	Predicted	Measured	Predicted	Measured	Predicted	Measured	Predicted	Measured
Mix O1	7.7	6.2	1,092	1,028	21.3	22.7	3,935	3,971
Mix O2	6.0	6.4	1,113	1,000	21.3	23.8	4,077	3,630
Average difference between predicted and measured [%]	12.3		8.0		9.3		6.0	

The average difference between the values predicted using the models and the measured values does not differ more than 13%; so, it is considered satisfactory for the application of the models.

Finally, it was necessary to determine the optimal VBC and RAC in the final RAP50 mixture. As both mixtures used for model verification have shown comparable properties with the CM, the mixture with less bitumen (Mix O$_1$) was selected as a reference RAP50 mixture, and its structure is displayed in Figure 5.27. This amount of bitumen has been selected considering two aspects: on one side, the lower quantity

allows the conservation of economic resources, and on the other side, a high content could enhance the mixture properties. Testing the worst-case scenario ensures staying on the safe side.
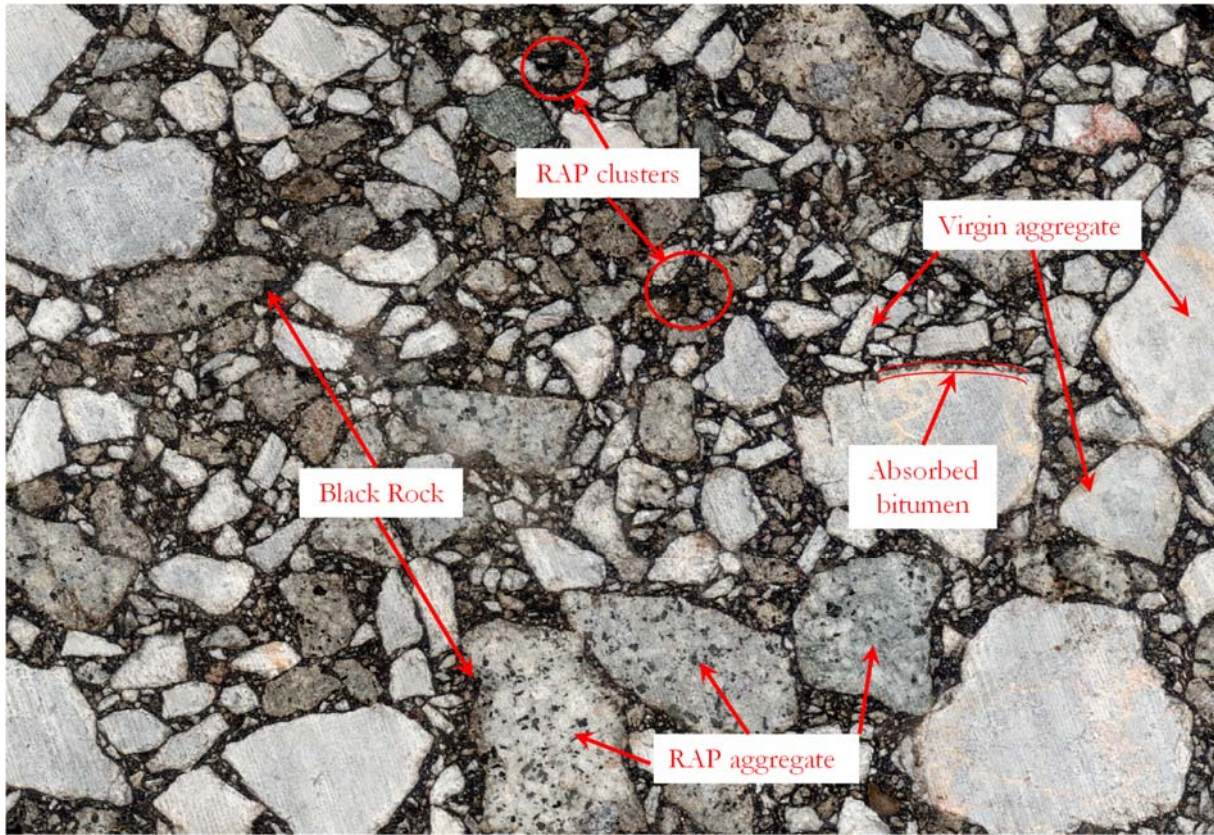
Figure 5.27 *Structure of the designed RAP50 mixture*

Chapter 6. Experimental Results and Discussion

After the development of the mix design procedure of the hot asphalt mixture with 50% RAP (denoted as RAP50), testing specimens were prepared, and their properties were compared with the properties of the control mixture (CM) and the HMA with 15% RAP (RAP15) according to the experimental plan displayed in Figure 6.1.

The following properties of each mixture were determined:

1) Stiffness

2) Cracking resistance — Cracking Tolerance Index — CT_{index} (IDEAL-CT)

3) Water sensitivity

4) Freeze-thaw resistance (repeated Lottman test)

5) Fatigue resistance

6) Resistance to permanent deformation
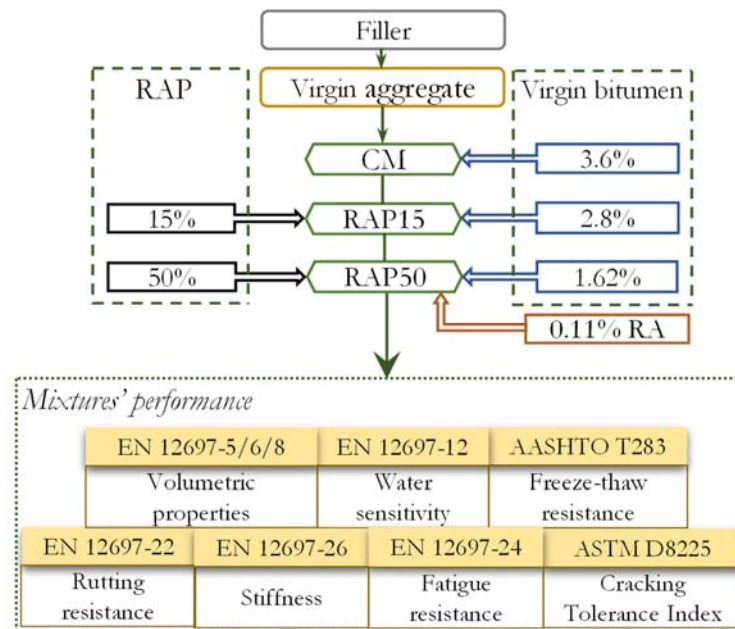
Figure 6.1 *Experimental plan of the mixtures' characteristics*

6.1 Stiffness

The testing procedure, described in Section 4.3.4, was applied to each of the four testing specimens of every mixture. Testing results (average values and standard deviations) are displayed in Figure 6.2, from which it can be seen that at each testing frequency at 5°C and 10°C, the RAP15 mixture has the highest stiffness, the CM, slightly lower, and the RAP50, the lowest. At 20°C, the RAP15 still has the highest stiffness modulus, whereas the CM and RAP50 mixtures have changed places; so, the CM has the lowest

stiffness. At testing temperatures of 30°C and 40°C, the order is different than at previous temperatures: the RAP50 mixture has the highest stiffness, the RAP15 has slightly lower, and the CM has the lowest. Various stiffness of the RAP50 mixture depending on the testing temperature is a consequence of the high RAPb content (that is probably modified, as discussed in Section 4.1.4), which has a dominant impact on binder viscosity, especially in the domain of high temperatures.
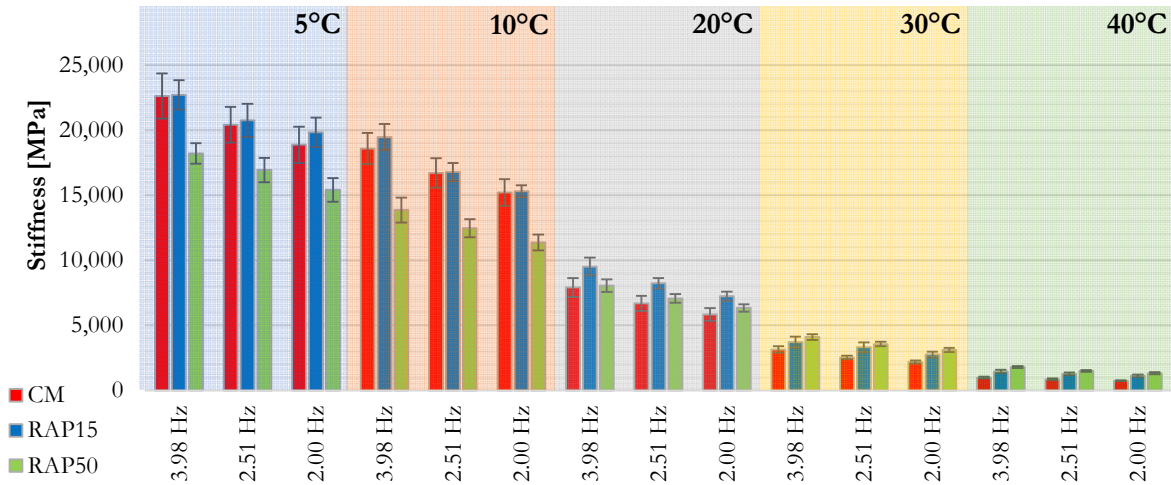
Figure 6.2 *Stiffness modulus from IT-CY test at T=5°C, 10°C, 20°C, 30°C and 40°C and f=3.98, 2.51, and 2.00 Hz*

The obtained testing results were further used for the construction of master curves to predict the linear viscoelastic behaviour of the asphalt mixtures outside the testing range. Master curves were constructed using a modified version of the master curve equation (Witczak & Bari, 2004):

$$log|E| = log(Min) + \frac{Log(Max) - \log(Min)}{1 + e^{\beta + \gamma \log \omega_r}}$$ *Equation 4.1*

where: $|E|$ is the stiffness modulus [MPa], ω_r is the reduced frequency [Hz], *Max* is the limiting maximum modulus [MPa], *Min* is the limiting minimum modulus [MPa], and β and γ are the fitting parameters [-].

The reduced frequency was computed using the Arrhenius equation:

$$log\omega_r = log\omega + \frac{\Delta EA}{19.14714}\left(\frac{1}{T} - \frac{1}{T_r}\right)$$ *Equation 4.2*

where: ω_r is reduced frequency at the reference temperature [Hz], ω is the loading frequency at the test temperature [Hz], T_r is the reference temperature [°K], T is the test temperature [°K], and ΔEA is the activation energy (treated as a fitting parameter) [kJ/mol].

Figure 6.3 displays the principle of master curve construction (CM) for a reference temperature of 20°C, whereas Figure 6.4 and Figure 6.5 display the resulting master curves of the RAP15 and RAP50 mixtures.
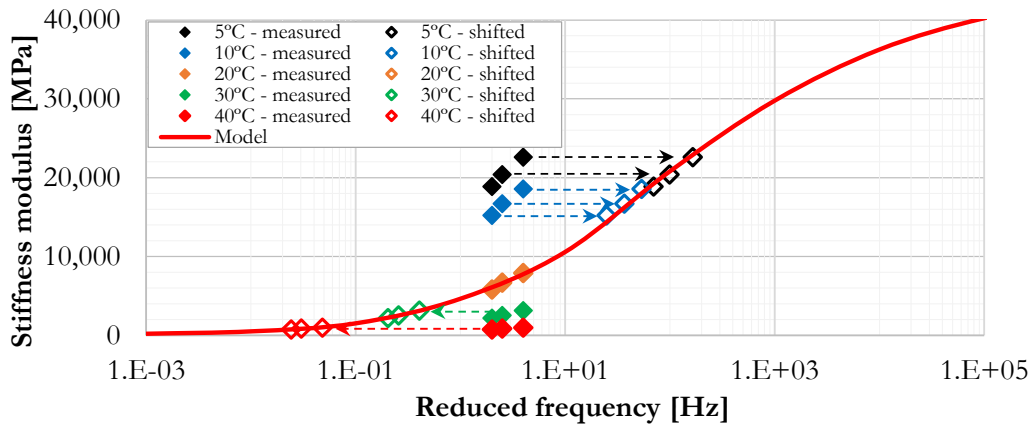
Figure 6.3 *The principle of master curve construction and resulting master curve of the CM*
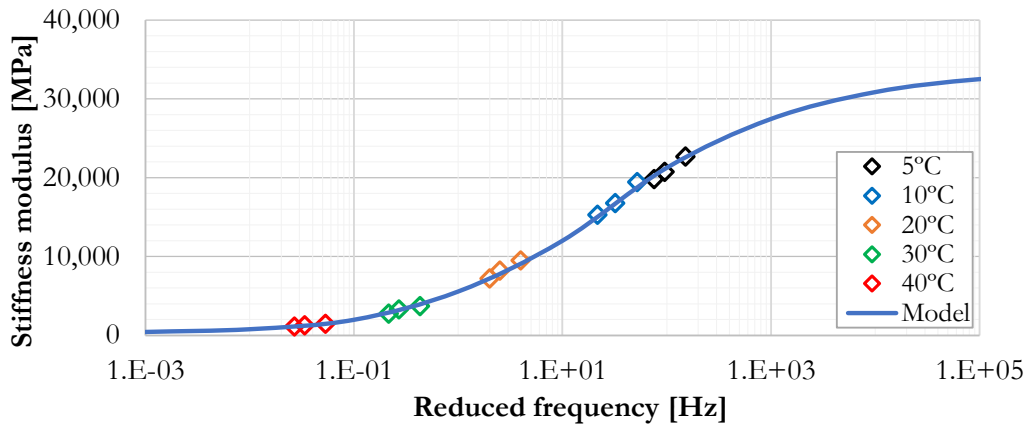
Figure 6.4 *Master curve of the RAP15 mixture*
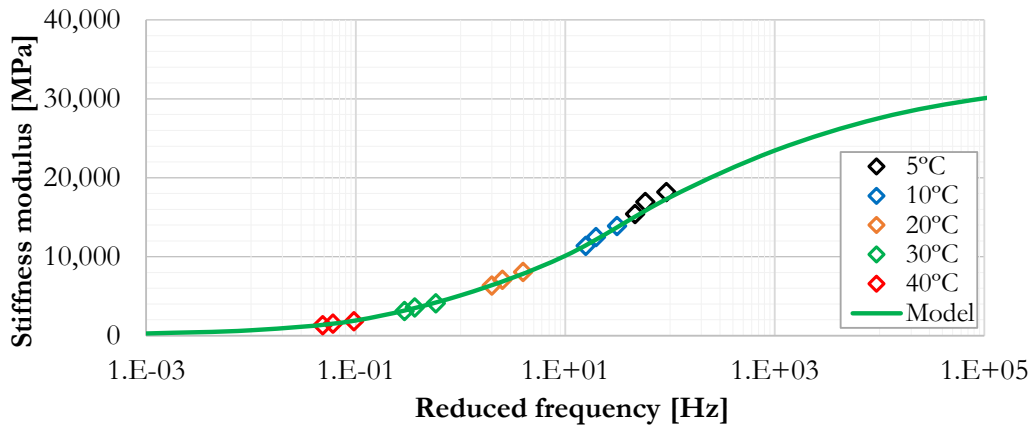
Figure 6.5 *Master curve of the RAP50 mixture*

The impact of both RAP and RA on the stiffness of the asphalt mixture can be seen from Figure 6.6 and Table 6.1. In the domain of low testing frequencies (i.e. testing temperatures above 20°C), the CM and RAP50 mixtures have approximately the same limiting stiffness value (E_{min}), whereas the RAP15 mixture is slightly stiffer. The effect of high RAPb content on the stiffness of the RAP50 mixture is compensated with the addition of RA and VB, which significantly decrease the final stiffness and may have a positive impact on low-temperature cracking resistance (Marasteanu et al., 2004). When considering the domain of high frequencies (i.e. testing temperatures below 20°C), the RAP15 mixture unexpectedly has much a lower stiffness than the CM.
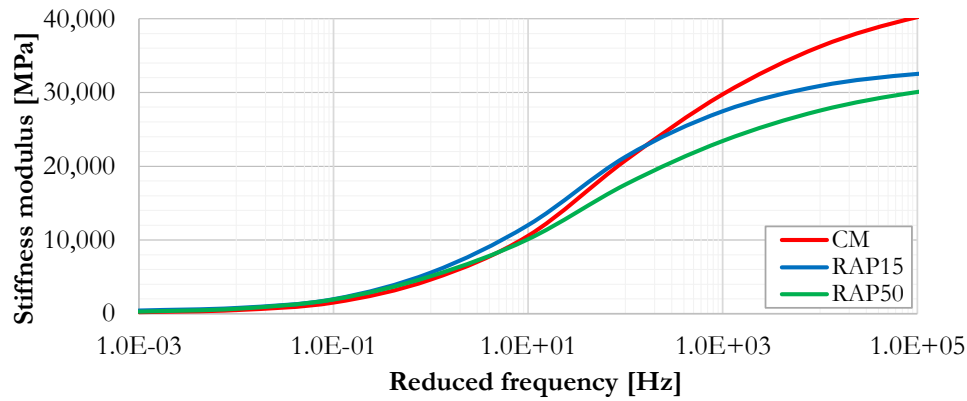
Figure 6.6 *The master curves of the tested asphalt mixtures*

Table 6.1 *Fitting parameters of the master curves*

Parameter	Unit	Mixture		
		CM	RAP15	RAP50
$\log(E_{max})$	MPa	4.652	4.529	4.520
$\log(E_{min})$	MPa	1.705	2.388	1.678
β	-	-0.687	-0.551	-0.911
γ	-	-0.685	-0.858	-0.657
ΔEA	kJ/mol	168,565	164,513	143,063

6.2 Cracking Resistance (IDEAL-CT)

To have specimens with comparable air void content, Marshall specimens with air void content of 7±0.5%, whose ITS had been previously measured (at a testing temperature of 25°C and loading rate of 50 mm/min), were selected for the calculation of the CT_{index}. Some of the testing specimens, compacted with various compaction energy, belonged to dry subsets used for the determination of water sensitivity or freeze-thaw resistance or to specimens prepared for stiffness measurement.

Figure 6.7 presents average load vs. displacement curves of the investigated mixtures.
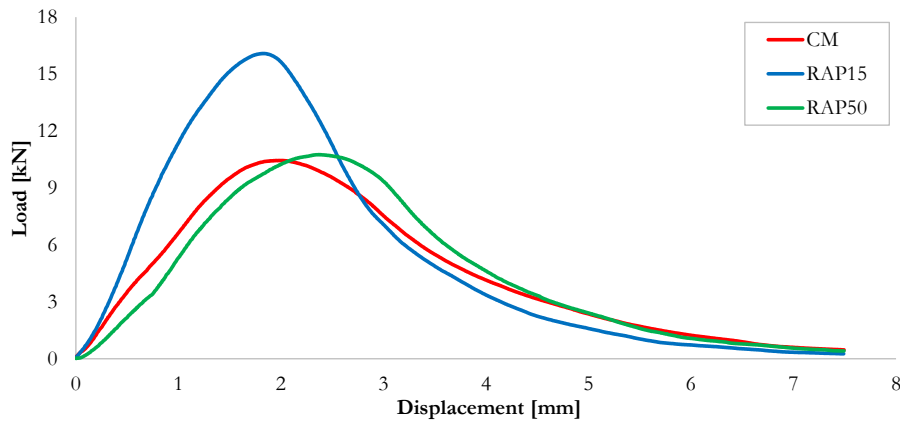
Figure 6.7 *Load vs. displacement curves of the investigated mixtures*

It can be seen that the RAP15 mixture achieves the highest strength due to the presence of RAP without the presence of RA; the slope of the curve after the peak load was much steeper compared to the other two mixtures, leading to the lowest CT_{index} value (Table 6.2), showing that the RAP15 mixture is the most brittle. The other two mixtures, CM and RAP50, have similar peak loads, fracture energy, and

curve slopes, resulting in nearly the same CT_{index} values, approximately three times higher than the RAP15 mixture. Despite the presence of high RAP content in the RAP50 mixture, its performance is comparable with CM due to the presence of RA. The opposite conclusion can be drawn for the RAP15 mixture, where spent fracture energy is higher when compared with other mixtures due to the absence of RA. Since that higher CT_{index} value leads to the higher cracking resistance of the asphalt mixture, it can be concluded that the newly designed RAP50 mixture has nearly the same cracking resistance as the CM and much better than that of the RAP15 mixture.

Table 6.2 *CT_{index} values of the investigated mixtures*

Mixture	Fracture energy [J/m²]	Slope	CT_{index} Average [-]	Standard deviation [%]	COV [%]
CM	5,264	5.1	31.9	9.0	28.2
RAP15	6,235	14.4	10.9	2.2	20.1
RAP50	5,231	6.2	29.2	9.3	31.7

6.3 Water Sensitivity

After testing both sets of specimens following the explanations given in Section 4.3.2, the ITS of each specimen was calculated according to EN 12697-23:2017 using Equation 2.1.

The water sensitivity of the asphalt mixtures is expressed through the indirect tensile strength ratio (ITSR) of the ITS of each of the wet and dry sets of specimens, according to the equation:

$$ITSR = \frac{ITS_w}{ITS_d} \cdot 100$$

Equation 4.3

where: ITSR is the indirect tensile strength ratio [%], ITS_w is the average indirect tensile strength of the wet group [kPa], and ITS_{dry} is the average indirect tensile strength of the dry group [kPa].

The average ITS values of the dry and wet subsets of each mixture, their standard deviations, and their coefficients of variation are given in Table 6.3 and graphically displayed in Figure 6.8.

Table 6.3 *Average values and standard deviations of measured ITS values and their ITSR*

Mixture	Condition	ITS_{DRY} [kPa]	ITS_{WET} [kPa]	ITSR [%]
	Average	905.0	936.2	
CM	Standard deviation	48.5	71.4	103.4
	COV [%]	5.4	7.6	
	Average	983.2	1,059.9	
RAP15	Standard deviation	83.8	15.6	107.8
	COV [%]	8.5	1.5	
	Average	1,117.5	946.5	
RAP50	Standard deviation	105.8	101.4	84.7
	COV [%]	9.5	10.7	

The average ITS values of dry sets increase as the RAP content increases, regardless of the presence of RA. The ITS_{DRY} values of the RAP15 and RAP50 mixtures increased by 8.6% and 23.5%, respectively when compared with the CM. Additionally, the 15% RAP mixture increased its ITS_{WET} value by 13.2% compared to the CM, and the addition of 50% RAP slightly increased it (by roughly 1%).

Considering the ITSR values, it can be seen that the addition of 15% RAP has no impact on the water sensitivity of the asphalt mixture. The water even increased the ITS of the specimens, causing ITSRs higher than 100%. This increase is a

Figure 6.8 *Testing results of the water sensitivity test*

consequence of the pore pressure that appears when water is trapped between asphalt particles. Alternatively, the addition of 50% RAP decreased the ITSR by roughly 20% when compared to CM and RAP15 mixtures. This decrease may be due to highly aged RAPb that lost its cohesive properties over time and, additionally, due to the impact of water. However, all mixtures satisfy the minimum criteria proposed in EN 13108-1:2016 (60%) and the requirements from the General Specification for Road Construction of Public Enterprise Roads of Serbia (70%).

6.4 Freeze-Thaw Resistance

The freeze-thaw resistance of asphalt mixtures due to damage caused by the stripping of the bitumen in laboratory conditions was determined by applying the ITS test to specimens prepared according to ASTM D4867-2014, as described in Section 4.3.3. After the calculation of the ITS of each testing specimen from all subsets, the average values of these subsets were determined, and the tensile strength ratio was calculated according to the following equation:

$$TSR_n = \frac{S_{tm,n}}{S_{td}} \cdot 100$$

Equation 4.4

where TSR_n is the Tensile Strength Ratio [%] after *n* cycles (three or six), S_{tm} is the average indirect tensile strength of the freeze-thaw conditioned subset [MPa] after *n* cycles (three or six), and S_{td} is the average indirect tensile strength of the unconditioned (dry) subset [MPa].

Table 6.4 *Testing results of the freeze-thaw resistance test*

Mixture	Condition	S_{td}	$S_{tm,3}$	$S_{tm,6}$	TSR_3	TSR_6
		[kPa]	[kPa]	[kPa]	[%]	[%]
CM	Average	1,186.8	690.0	528.7		
	Standard deviation	79.20	54.0	85.0	58.1	44.5
	COV [%]	6.7	7.8	16.1		
RAP15	Average	1,531.4	1,198.9	896.4		
	Standard deviation	64.3	116.8	51.3	78.3	58.5
	COV [%]	4.2	9.7	5.7		
RAP50	Average	971.7	798.7	607.7		
	Standard deviation	36.1	56.7	51.2	82.2	62.5
	COV [%]	3.7	7.1	8.4		

The average ITS values of the unconditioned set of each mixture and after three and six conditioning cycles, as well as the TSRs, standard deviations, and coefficients of variations, are displayed in Figure 6.9 and Table 6.4.
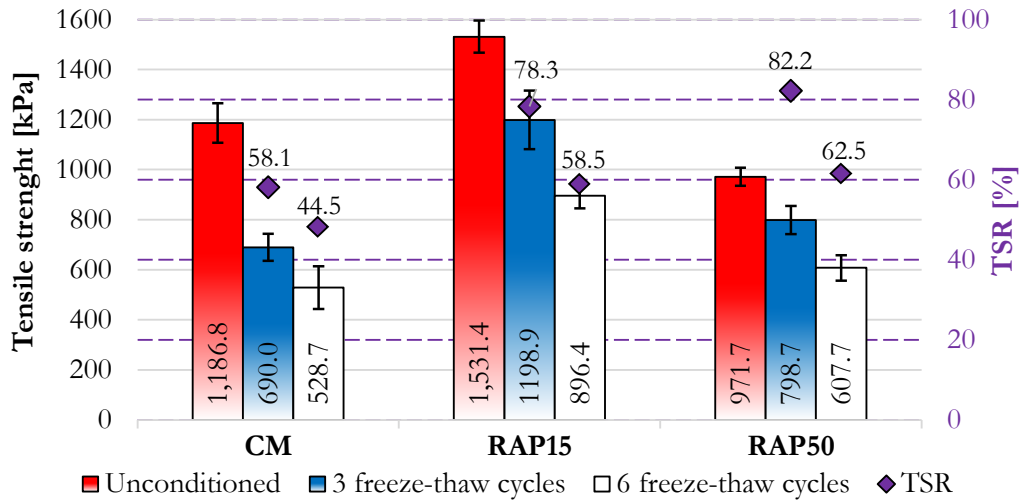
Figure 6.9 *Testing results of the freeze-thaw resistance test*

Figure 6.9 illustrates that the RAP15 mixture has the highest tensile strength in each condition due to the presence of only RAPb. Alternatively, the RAP50 mixture has the lowest tensile strength because of the impact of RA and due to a slightly higher air void content than the other two mixtures (by approximately 0.5% — see Appendixes IV and VI). When comparing mixtures in different conditions, the unconditioned subset of the RAP15 mixture has a higher tensile strength than the CM and RAP50 mixtures by 30% and 58%, respectively. After the application of three freeze-thaw cycles, that difference becomes significantly higher — 74% and 50%, respectively, whereas after three more cycles (six in total) the differences remained similar (around 70% and 48%).

Considering the TSR values, the negative impact of freeze and thaw is most conspicuous in the case of the CM, which has approximately 20-24% lower values after three freeze-thaw cycles than both RAMs and 24-28% lower values after six freeze-thaw cycles. When comparing the RAMs, it can be concluded that the TSR values are approximately the same, regardless of their RAP content; however, RAP may improve freeze-thaw resistance. Since the acceptable TSR value after only one freeze-thaw cycle is 70% (Wang et al., 2018), it can be concluded that both RAMs with RAP satisfy this criterion.

6.5 Resistance to Permanent Deformation

The testing of resistance to permanent deformation (rutting resistance) was performed following the procedure described in Section 4.3.7. Rut depth has been measured during the test, and obtained results are further used to calculate the wheel-tracking slope (Equation 4.7) and mean proportional rut depth, which represents the ratio of the measured rut depth to the thickness of the tested specimen. The evaluation of the proportional rut during the test is displayed in Figure 6.10, and the summarized testing results are given in Table 6.5.

$$WTS_{AIR} = \frac{(d_{10,000} - d_{5,000})}{5} \qquad\qquad Equation\ 4.5$$

where WTS_{AIR} is the wheel-tracking slope [mm/10^3 loading cycles] and $d_{5,000}$ and $d_{10,000}$ are the rut depths after 5,000 and 10,000 loading cycles [mm].

Table 6.5 *Results of the wheel-tracking test*

Mixture	RD$_{AIR}$	PRD$_{AIR}$	WTS$_{AIR}$
	[mm]	[%]	[mm/10^3 load cycles]
CM	3.92	5.5	0.10
RAP15	3.09	4.2	0.08
RAP50	3.2	4.5	0.10
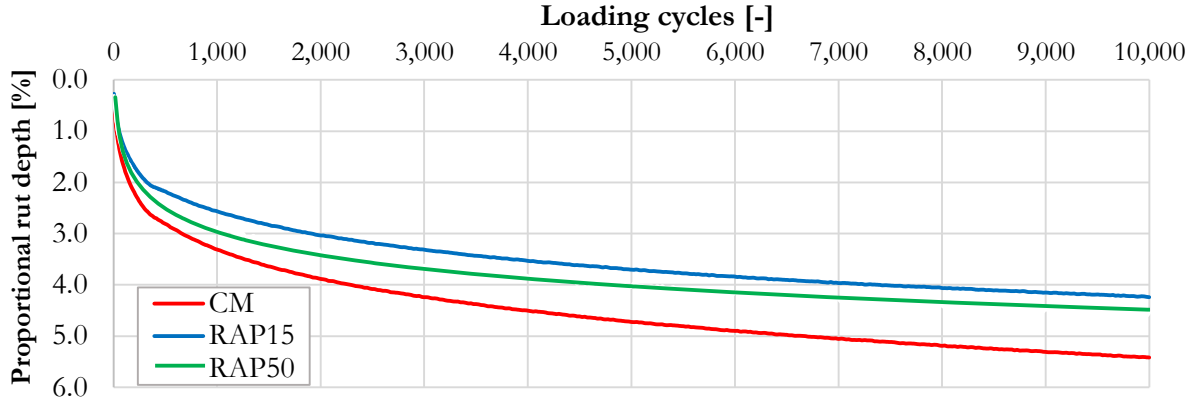
Figure 6.10 *Proportional rut depth of the asphalt mixtures*

The testing results show that the addition of only RAP improves resistance to permanent deformation. The amount of 15% RAP decreased PRD$_{AIR}$ by 21.8%, whereas the addition of 50% RAP and RA decreased it by 16.2%, compared with the CM. Wheel-tracking slopes are similar for all mixtures tested, around 0.10 [mm/10^3 load cycles]. Since the use of too much RA can reduce mixture stiffness and possibly cause a problem with rutting resistance, it is essential to select an optimum content to achieve a certain criterion. The mix design methodology developed in this study shows that the selected RA and VB contents are appropriate when considering resistance to permanent deformation.

6.6 Fatigue Resistance

The fatigue resistance of each mixture was determined according to the testing procedure described in Section 4.3.6. The energy ratio (ER) approach, introduced by (Hopman et al., 1989), is used to estimate the fatigue life of every testing specimen. Within the ER approach, the failure in a strain-controlled mode is defined as the number of loading cycles (N$_{f,w}$) at which cracks are considered to initiate. The energy ratio is defined as:

$$R_E = \frac{nW_o}{W_n} = \frac{n[\pi\sigma_0\epsilon_0 sin\varphi_0]}{\pi\sigma_n\epsilon_n sin\varphi_n}$$

Equation 4.6

where *n* is the number of loading cycles, *W$_0$* and *W$_n$* are the amounts of dissipated energy in the first and nth cycles, *σ$_0$* and *σ$_n$* are the stress levels in the first and nth cycles, *ε$_0$* and *ε$_n$* are the strain levels in the first and nth cycles, and *φ$_0$* and *φ$_n$* are the phase angles in the first and nth cycles.

The simplified version of the Equation 4.6 for calculating the energy ratio (R$_\varepsilon$) was developed by Rowe (1993), who considered strain as a constant during the strain-controlled test and replaced stress with the product of the strain and modulus:

$$R_\epsilon \cong \frac{n}{E_n^*}$$

Equation 4.7

where n is the number of loading cycles, and *E$^*_n$* is the complex modulus in the nth cycle [MPa].

Similarly, Equation 4.6 was simplified for calculating the energy ratio (R$_\sigma$) in a stress-controlled test, where the load amplitude remains constant, and after crack initiation, the stress at the crack tip increases

rapidly. In this case, the number of cycles leading to failure, $N_{f,w}$, can be visually determined from the peak value of the R_σ curve (Figure 6.11) or using the following equation:

$$R_\sigma \cong nE_n^*$$

Equation 4.8

where n is the number of loading cycles, and E_n^* is the complex modulus in the nth cycle [MPa].

The results from the individual test were further fitted and presented in the form of a power (fatigue) function:

$$\lg(N_{i,j,k}) = A_0 + A_1 \cdot \lg(\epsilon_i)$$

Equation 4.9

where i is the specimen number, j is the chosen failure criteria (ER), k is the set of test conditions (20°C and 2 Hz), i is the initial strain amplitude measured at the 100th load cycle (μm/m), A1 is the slope of the fatigue line, and A0 is the fitting parameter.

Figure 6.11 displays an example of the R_σ evaluation for the testing specimen 3-1 of the control mixture and the resulting fatigue line for CM. The fatigue lines of the two remaining mixtures, RAP15 and RAP50, were determined in the same way, and their fatigue lines are presented in Figure 6.12 and Figure 6.13. The ranking of the asphalt mixtures regarding the fatigue resistance is based on the strain amplitude value ϵ_6, whereby a fatigue life of 10^6 cycles is obtained. The resulting regression coefficients of fatigue lines, coefficients of correlation, and calculated values are given in Table 6.6.

Table 6.6 *Regression coefficients of the fatigue lines*

Mixture	A_0	A_1	R^2	ϵ_6
	[-]	[-]	[-]	[μm/m]
CM	15.46	-5.29	0.942	61.6
RAP15	15.01	-5.04	0.956	61.2
RAP50	14.97	-4.90	0.957	67.8
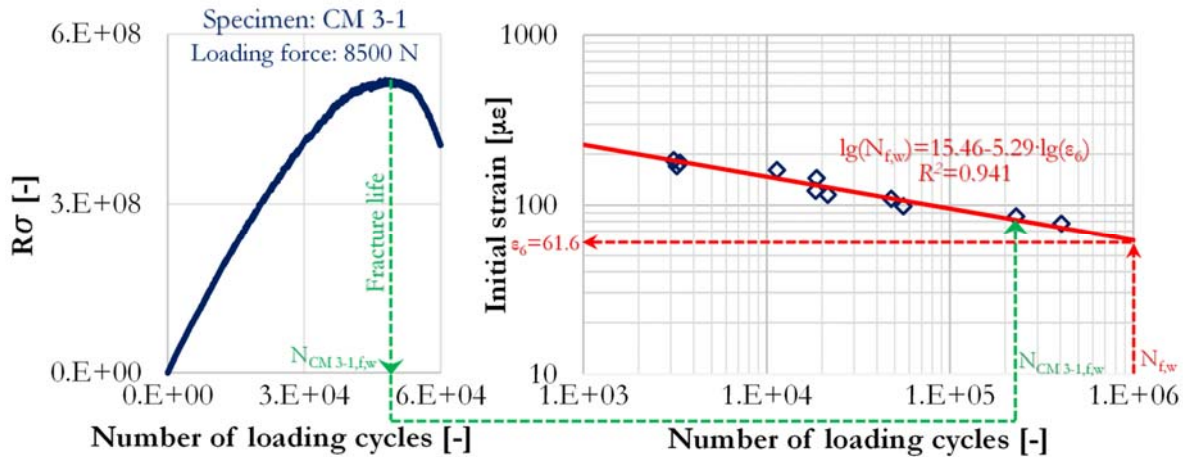
Figure 6.11 R_σ *evaluation in the fatigue test of the testing specimen CM 3-1 and the fatigue line of the CM*
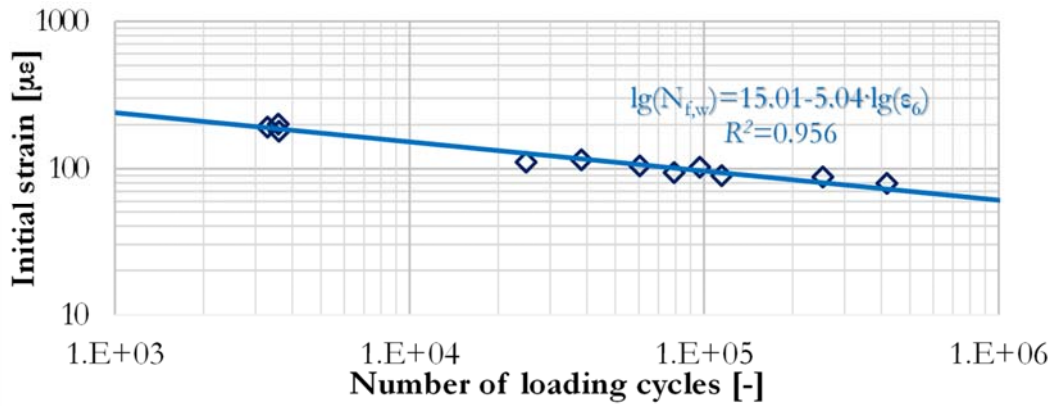
Figure 6.12 *Fatigue line of the RAP15 mixture*
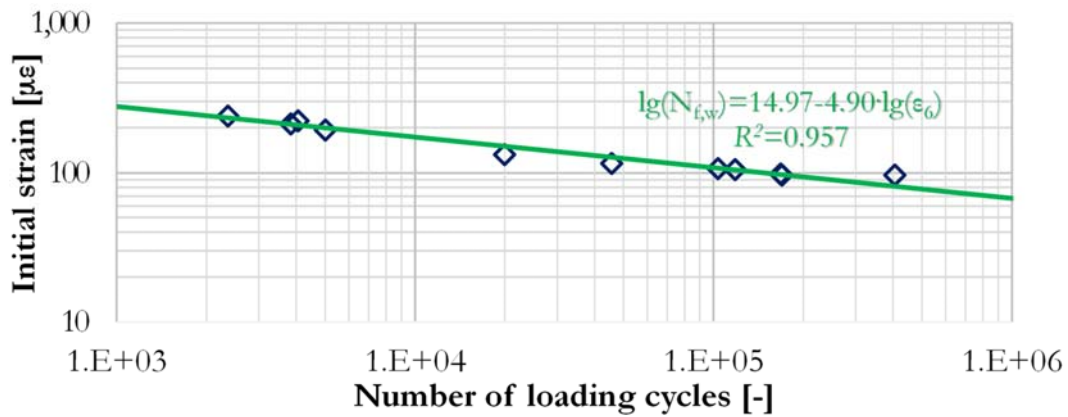
Figure 6.13 *Fatigue line of the RAP50 mixture*

Figure 6.14 shows all the fatigue lines in the same plot. As this graph shows, the fatigue line of the RAP15 mixture almost completely overlapped with the fatigue line of the CM, resulting in the same ε_6 value. The RAP50 mixture shows the best performance, with the fatigue line of a similar slope as the other two mixtures, but with a 10% higher ε_6 value. Based on this, it is concluded that RAP50 mixture is properly designed and that it meets the desired fatigue resistance performance.
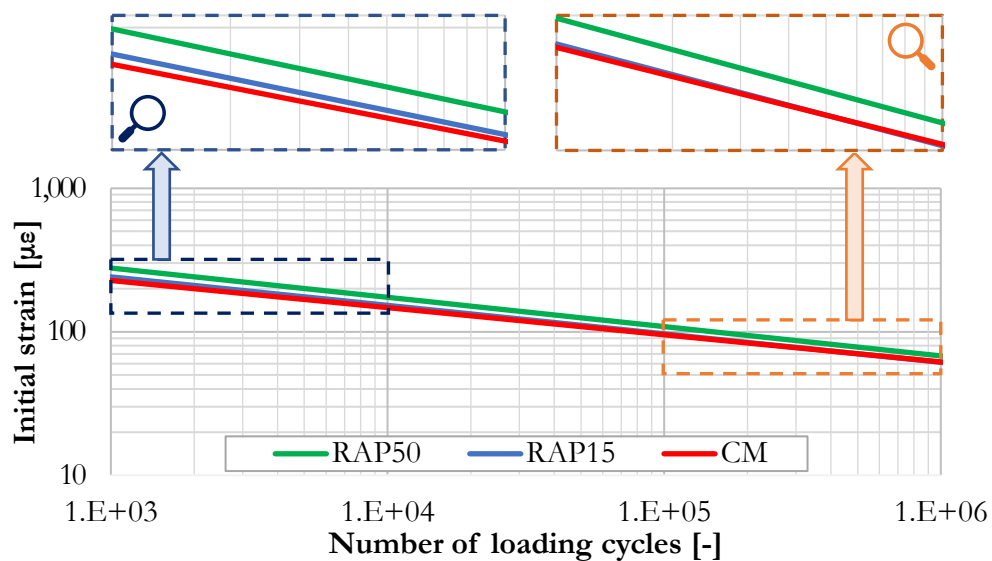
Figure 6.14 *The fatigue lines of the tested mixtures*

Chapter 7. Conclusions and Recommendations for Further Research

7.1 Summary

The use of reclaimed asphalt pavement in new asphalt mixtures is becoming a routine practice around the world, especially in developed countries. For example, only 1% RAP is sent to landfills in the USA, whereas in Japan, they have just started to use a second cycle of recycling (the reuse of already recycled asphalt mixtures). In Germany, Austria, Spain, France, and the Netherlands, more than 70% of the available RAP is used for hot and warm mix asphalt production, where it is used, up to 100%, in new RAM (for instance, in Germany). Together with the positive impact on RAM properties (e.g. improvement of rutting resistance, water sensitivity) and CO_2 emission reduction, under certain conditions, RAP has a great potential to completely replace new materials in asphalt mixtures. However, there are still many limitations against the use of 100% RAP in RAM, some of which are related to the activation of aged binder from the RAP and its blending with a recycling agent (RA). These limitations have been extensively investigated in previous studies.

Although blending phenomena, occurring when RAP is used, have been the research topic of many studies, their clear explanations and definitions have not been established. Likewise, testing methods for their determination have not been uniquely accepted. In the first, theoretical part of the study, the definitions and formulations of two newly introduced terms were included: Degree of Binder Activity and Degree of Binder Activity. The formulation of the Degree of Blending is not provided due to its complexity, but this study provides its formulation, as well as the correlation with the other two parameters. Testing methods, which have been used in previous studies for determining these parameters, were investigated in detail, and recommendations for their usage are proposed.

It is known that RAP, by itself, is a very heterogeneous material with diverse properties that vary from source to source, mostly depending on the RAPb type and content and aggregate characteristics. It may also influence the optimal preheating temperature of the RAP — if the RAPb is too stiff, the preheating temperature will be high and opposite — RAP with soft bitumen will need lower preheating temperature. As a procedure for the determination of optimal preheating temperature is not yet established, in the second part of the study, a new and easy-to-perform procedure was developed, which may also assess the impact of RA addition on the preheating temperature using samples compacted in a gyratory or Marshall compactor. It was developed by evaluating certain fundamental properties of the mixtures (air void content, stiffness, indirect tensile strength, and CT_{index}). Tests have been performed on 100% RAP specimens prepared in a Marshall compactor with 50 blows per side and in a gyratory compactor with 30 gyrations, after preheating the RAP at different temperatures. The obtained results have been analysed and used to apply a probabilistic optimisation method to determine the optimal preheating temperature of RAP with and without RA. In the same part of the study, the DoA of RAP was estimated depending on the test method and preheating temperature.

Traditional mix design methods (Marshall, Superpave, etc.) may not be appropriate when high RAP content is used, because they are mostly based on volumetric and basic mixture properties (flow, stability); so, the impact of different RA and RAP content on mixture performance cannot be easily isolated. Due to these facts, a previously determined optimal preheating temperature was used as an input in the development of the mix design procedure of HMA with high RAP content. The optimal contents of RA and VB in RAM with 50% RAP were determined considering the following properties: air void content, stiffness, indirect tensile strength, and CT_{index}.

Finally, to assess if the RAM with 50% RAP was properly designed, its properties (water sensitivity, freeze-thaw resistance, stiffness, fatigue resistance, and resistance to permanent deformation) were evaluated and compared with the properties of the control mixture, composed of all virgin materials, and a mixture with 15% RAP. Testing results showed that the developed mix design method ensures an RAM with properties comparable to both mixtures.

7.2 Conclusions

The main objective of this research study was to develop a mix design methodology of hot mix asphalt with a high content of reclaimed asphalt pavement (50%), i.e. to determine the optimal content of VB and RA in new RAM.

After the characterisation of componential materials, a procedure for determining the optimal preheating temperature of RAP and investigating the potential benefits of the RA addition in decreasing the RAP preheating temperature is shown in the study. The results showed that the preheating temperature of reclaimed asphalt pavement has an important role during the manufacturing process of RAM. On one hand, a too-low temperature does not allow the reactivation of the aged bitumen coming from RAP, whereas, on the other hand, a too-high temperature causes the over-ageing of the RAPb; so, it is important to preheat the RAP as much as necessary to obtain the best possible properties of RAPb. Moreover, based on the obtained results, the following conclusions can be drawn:

- The optimal preheating temperature for the RAP used in the study, resulting from the optimisation method, was approximately 130°C, regardless of the method of compaction.

- The addition of RA decreased the preheating temperature by 7.2°C and 14.5°C when considering Marshall and gyratory compacted specimens, respectively.

- Additional benefits can be achieved when RAs (i.e. lubricants or rejuvenators) are used because the optimal preheating temperature decreases; consequently, potential benefits arise, such as reduced energy consumption and CO_2 emission.

After the determination of the optimal preheating temperature of RAP, the mix design methodology of RAM, in this case base course mix, with 50% RAP was developed. In the first stage, seven asphalt mixtures with different RA and VB contents (0.10-0.35% and 0.9-1.8% of the final binder content, respectively) were prepared according to Doehlert experimental design. The properties of each mixture (air void content, stiffness, indirect tensile strength, and CT_{index}) have been determined, and the obtained results were used to develop predictive models of each parameter tested. The relative effect of the factors (linear, second and third degree, and interaction terms) and the statistical significance of the developed models have been evaluated by calculating the coefficient of R^2 and applying the ANalysis Of VAriance (ANOVA) and Lack of Fit (LoF). The student's t-test was used to test the significance of individual regression coefficients on each proposed model, and finally, a correlation between investigated properties and the amounts of RA and VB was explored using Response Surface Methodology (RSM). In the second stage, the developed models were validated by preparing two additional mixtures that had properties as close to the control mixture as possible. These mixtures contained 1.62% VB and 0.11% RA and 1.80% VB and 0.12% RA, respectively. The first mixture was selected for a final RAP50 mixture. Considering the testing results, the following conclusions are drawn:

- A linear model was found to be appropriate for the description of the indirect tensile strength. The third-degree model was found to be appropriate for the description of the CT_{index}, whereas the second-degree model best described the air void content and stiffness of the RAM mixture with 50% RAP, depending on the RA and VB content.

- The developed models were validated with two additional mixtures. The average difference between the values predicted using the models and the measured values of the additional mixtures did not differ more than 13%; so, it is considered satisfactory for the application of the models.

- The designed RAP50 mixture had around 50% less virgin aggregate and 2% less virgin bitumen than the CM (which contained 3.6% VB); that, with the addition of only 0.11% RA, may lead to benefits in terms of economy and environmental protection.
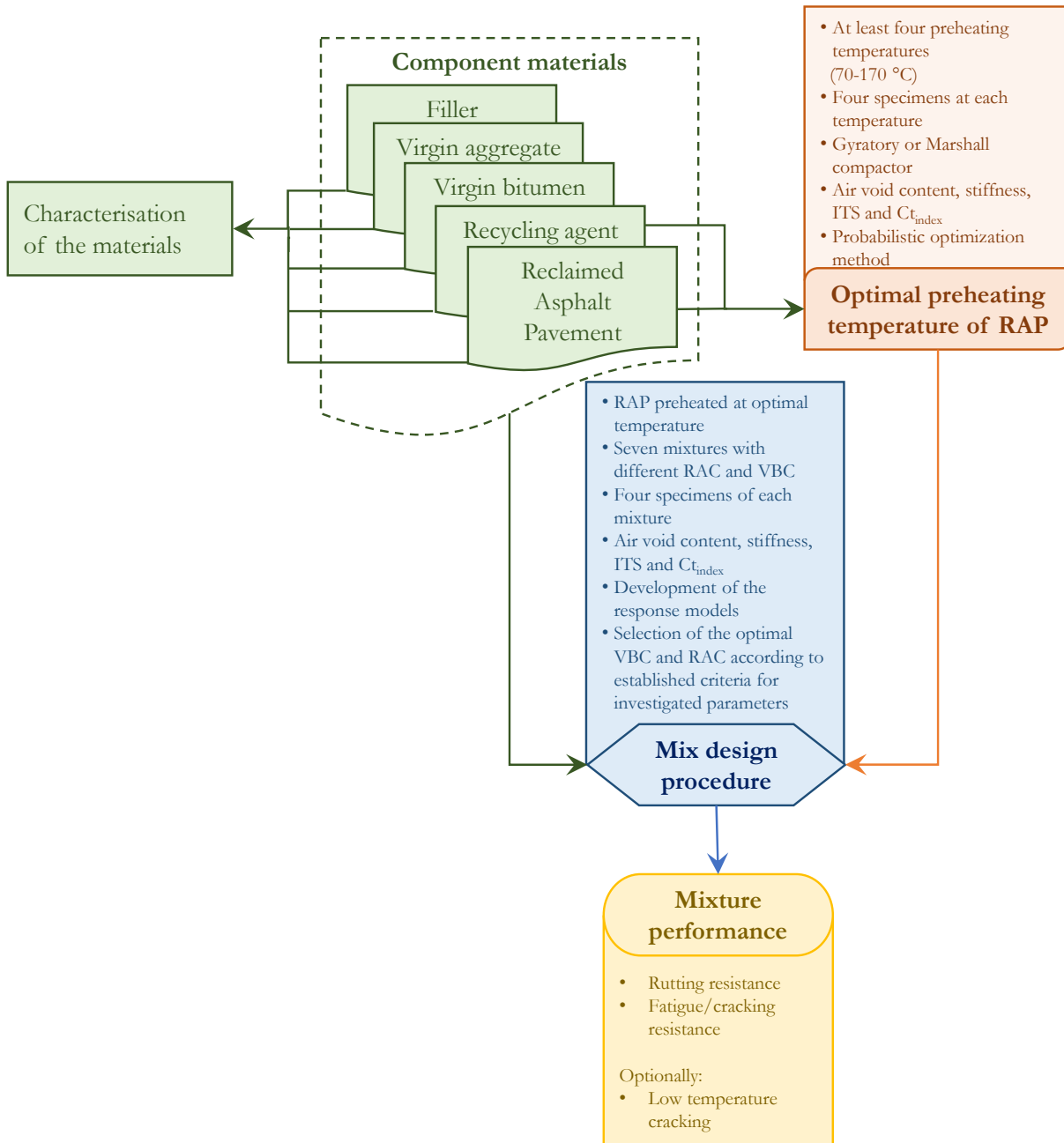
Figure 7.1 *Schematic plan of the mix design methodology of hot mix asphalt with a high content of reclaimed asphalt pavement*

Finally, it was necessary to evaluate the properties of the designed mixture to determine the properties that were not included in the mix design procedure. The obtained properties were then compared with the same properties of the CM and the RAP15 mixture, which was selected as the most commonly used RAM. Testing results are given in Table 7.1, from where it can be seen whether RAMs behave better, similarly, or worse than the control mixture.

Testing results from this study show that the RAM with 50% RAP has better freeze-thaw, fatigue, and rutting resistance than the control mixture, whereas its cracking resistance is almost the same. When considering water sensitivity and stiffness, the RAP50 mixture has inferior or diverse properties,

respectively, compared to the control mixture. Overall, it can be concluded that the mix design methodology developed in this study, with the schematic plan displayed in Figure 7.1, ensures the production of high-RAP mixtures with comparable properties to the control mixture, although the DoA was not considered.

Table 7.1 *Comparison of RAMs' properties with the properties of the CM*

Properties	Mixture	
	RAP15	RAP50
Stiffness	⬆	⬆⬇
Water sensitivity	⚌	⬇
Freeze-thaw resistance	⬆	⬆
Cracking resistance (IDEAL-CT)	⬇	⚌
Fatigue resistance	⚌	⬆
Resistance to permanent deformation	⬆	⬆

⬆ Indicates an improvement of a certain property when compared to the CM
⬇ Indicates a worsening of a certain property when compared to the CM
⬆⬇ Mixed results when compared to the CM
⚌ Similar properties to the CM

7.3 Recommendations for Further Studies

The research work performed in this study can be divided into three parts: 1) methodology for determining the optimal preheating temperature of RAP, 2) mix design methodology of HMA with high RAP content, and 3) properties of asphalt mixtures.

Further studies should include the following recommendations to verify the effectiveness of the developed methodologies:

1) Methodology for determining the optimal preheating temperature:

- Since RAP is very heterogeneous material, different RAP sources should be used.

- Many products have been used as RAs (waste oils, industrial rejuvenators, Styrene-butadiene rubber, soft bitumen, bitumen emulsions, etc.); so, the proposed methodology should be applied to RAP with different amounts of various RAs to assess the method's sensitivity.

- Different levels of compaction energy should be applied (i.e. number of gyrations).

- Proposed testing methods can be performed at additional temperatures, or additional testing methods can be included, while still keeping the developed methodology simple to perform.

2) Mix design method of HMA with high RAP content:

- RAP, aggregate, and bitumen coming from different sources should be used.

- Different RAP contents should be applied in HMAs.

- The trigger values of the proposed testing methods should be established (e.g. minimum ITS value, minimum/maximum stiffness).

- Additional testing methods can be included (e.g. chemical test of a binder blend, tests in the low-temperature domain).

- The software for determining the optimal RA and VB contents can be developed based on the findings from this study.

3) Properties of asphalt mixtures:

- Previous studies have shown that asphalt mixtures with high RAP content are more sensitive to low-temperature cracking; so, additional tests should be carried out in the domain of low temperatures.

- The interaction between the VB and RAPb, together with the diffusion process, has an important impact on mixture performance; so, the performance of RAMs with high RAP content should be investigated after long-term ageing.

- The life-cycle cost analysis of RAMs with different RAP, RA, and VB contents, considering different levels of DoA, DoAv, and DOB, should be performed to assess the impact of these mixtures on the environment.

References

AASHTO Guide for Design of Pavement. (1993). American Association of State Highway and Transportation Officials.

AASTHO M323-12: Standard Specification for Superpave Volumetric Mix Design. (2012).

Abd, D., Al-Khalid, H., & Akhtar, R. (2018). Novel Methodology to Investigate and Obtain a Complete Blend between RAP and Virgin Materials. *Journal of Materials in Civil Engineering, 30*(5), 1–12. https://doi.org/10.1061/(ASCE)MT.1943-5533.0002230.

Abed, A., Thom, N., & Lo Presti, D. (2018). Design considerations of high RAP-content asphalt produced at reduced temperatures. *Materials and Structures/Materiaux et Constructions, 51*(4), 1–16. https://doi.org/10.1617/s11527-018-1220-1

Al-Qadi, I., Carpenter, S., Roberts, G., Ozer, H., Aurangzeb, Q., Elseifi, M., & Trepanier, J. (2009). *Determination of Usable Residual Asphalt Binder in RAP.* http://hdl.handle.net/2142/13714

Al-Qadi, I., Elseifi, M., & Carpenter, S. (2007). Reclaimed Asphalt Pavement - A Literature Review. In *FHWA-ICT-07-001.*

AllBack2Pave. (2014). http://allback2pave.fehrl.org/

Anderson, E. D., & Daniel, J. S. (2013). *Long-Term Performance of Pavement with High Recycled Asphalt Content Case Studies. 2371*, 1–12. https://doi.org/10.3141/2371-01

Anthonissen, J., Van den bergh, W., & Braet, J. (2014). Cradle-to-Gate Life Cycle Assessment of Recycling and Impact of Reduced Production Temperature for the Asphalt sector in Belgium. *International Symposium on Pavement LCA 2014.*

Arámbula-Mercado, E., Caro, S., Torres, C. A. R., Karki, P., Sánchez-Silva, M., & Par, E. S. (2019). *Evaluation of Fc-5 With Pg 76-22 Hp To Reduce Raveling BE287: Final Report* (Issue May).

Ashtiani, M. Z., Mogawer, W. S., & Austerman, A. J. (2018). A Mechanical Approach to Quantify Blending of Aged Binder from Recycled Materials in New Hot Mix Asphalt Mixtures. *Transportation Research Record: Journal of the Transportation Research Board, 2672*(28), 107–118. https://doi.org/10.1177/0361198118787634

Ayyub, B. M., & McCuen, R. H. (2016). *Probability, Statistics, and Realibility for Engineers and Scientists* (Third). CRC PRess. https://doi.org/https://doi.org/10.1201/b12161

Baghaee Moghaddam, T., & Baaj, H. (2016). The use of rejuvenating agents in production of recycled hot mix asphalt: A systematic review. *Construction and Building Materials, 114*, 805–816. https://doi.org/10.1016/j.conbuildmat.2016.04.015

Bailey, H. K., & Zoorob, S. E. (2012). The Use of Vegetable Oil in Asphalt Mixtures, in the Laboratory and Field. *5th Eurasphalt & Eurobitume Congress, October 2009*, 13–15.

Basueny, A., Perraton, D., & Carter, A. (2014). Laboratory study of the effect of RAP conditioning on the mechanical properties of hot mix asphalt containing RAP. *Materials and Structures/Materiaux et Constructions, 47*(9), 1425–1450. https://doi.org/10.1617/s11527-013-0127-0

Bonaquist, R. (2005). *Laboratory Evaluation of Hot Mix Asphalt (HMA) Mixtures Containing Recycled or Waste Product Materials Using Performance Testing. FHWA-PA-2005-006+98-32(19).*

Booshehrian, A., Mogawer, W. S., & Bonaquist, R. (2013). How to Construct an Asphalt Binder Master Curve and Assess the Degree of Blending between RAP and Virgin Binders. *Journal of Materials in Civil Engineering, 25*(12), 1813–1821. https://doi.org/10.1061/(ASCE)MT.1943-5533.0000726

Boriack, P. C., Katicha, S. W., Flintsch, G. W., & Tomlinson, C. R. (2014). *Laboratory Evaluation of Asphalt Concrete Mixtures Containing High Contents of Reclaimed Asphalt Pavement (RAP) and Binder.* http://www.virginiadot.org/vtrc/main/online_reports/pdf/15-r8.pdf

Bowers, B. F., Huang, B., Shu, X., & Miller, B. C. (2014). Investigation of Reclaimed Asphalt Pavement blending efficiency through GPC and FTIR. *Construction and Building Materials, 50*(JANUARY), 517–523. https://doi.org/10.1016/j.conbuildmat.2013.10.003

Bowers, B. F., Moore, J., Huang, B., & Shu, X. (2014). Blending efficiency of reclaimed asphalt pavement: An approach utilizing rheological properties and molecular weight distributions. *Fuel, 135*, 63–68. https://doi.org/10.1016/j.fuel.2014.05.059

Box, G. E. P., & Wilson, K. B. (1951). On the Experimental Attainment of Optimum Conditions. *Journal of the Royal Statistical Society: Series B (Methodological).* https://doi.org/10.1111/j.2517-6161.1951.tb00067.x

Box, G. E.P., & Behnken, D. W. (1960). Some New Three Level Designs for the Study of Quantitative Variables. *Technometrics.* https://doi.org/10.1080/00401706.1960.10489912

Box, George E.P., Hunter, J. S., & Hunter, W. G. (2005). Statistics of Experimenters 2nd Edition. *John Wiley & Sons.* https://doi.org/10.1080/00401706.1979.10489788

Bressi, S., Carter, A., Bueche, N., & Dumont, A. G. (2016). Impact of different ageing levels on binder rheology. *International Journal of Pavement Engineering.* https://doi.org/10.1080/10298436.2014.993197

Bressi, S., Cavalli, M. C., Partl, M. N., Tebaldi, G., Dumont, A. G., & Poulikakos, L. D. (2015). Particle clustering phenomena in hot asphalt mixtures with high content of reclaimed asphalt pavements. *Construction and Building Materials, 100*, 207–217. https://doi.org/10.1016/j.conbuildmat.2015.09.052

Bressi, S., Dumont, A. G., & Partl, M. N. (2016). A new laboratory methodology for optimization of mixture design of asphalt concrete containing reclaimed asphalt pavement material. *Materials and Structures, 49*(12), 4975–4990. https://doi.org/10.1617/s11527-016-0837-1

Bressi, S., Pittet, M., Dumont, A. G., & Partl, M. N. (2016). A framework for characterizing RAP clustering in asphalt concrete mixtures. *Construction and Building Materials.* https://doi.org/10.1016/j.conbuildmat.2015.12.132

Bressi, S., Santos, J., Orešković, M., & Losa, M. (2019). A comparative environmental impact analysis of asphalt mixtures containing crumb rubber and reclaimed asphalt pavement using life cycle assessment. *International Journal of Pavement Engineering.* https://doi.org/10.1080/10298436.2019.1623404

Breusch, T. S., & Pagan, A. R. (1979). A Simple Test for Heteroscedasticity and Random Coefficient Variation. *Econometrica, 47*(5), 1287–1294. https://doi.org/https://doi.org/10.2307/1911963

Büchler, S., Falchetto, A. C., Walther, A., Riccardi, C., Wang, D., & Wistuba, M. P. (2018). Wearing course mixtures prepared with high reclaimed asphalt pavement content modified by rejuvenators. *Transportation Research Record, 2672*(28), 96–106. https://doi.org/10.1177/0361198118773193

Campher, L. (2012). *HERWONNE ASFALT : Hoe effektief is verouderde bitumen in Bitumen Stabiliserende Asfalt .* Universiteit van Stellenbosch Departement.

Canestrari, F., Cardone, F., Graziani, A., Santagata, F. A., & Bahia, H. U. (2010). Adhesive and cohesive properties of asphalt-aggregate systems subjected to moisture damage. *Road Materials and Pavement Design, 11*(January), 11–32. https://doi.org/10.1080/14680629.2010.9690325

Castorena, C., Pape, S., & Mooney, C. (2016). Blending Measurements in Mixtures with Reclaimed

Asphalt. *Transportation Research Record: Journal of the Transportation Research Board*, *2574*, 57–63. https://doi.org/10.3141/2574-06

Cavalli, M. C., Griffa, M., Bressi, S., Partl, M. N., Tebaldi, G., & Poulikakos, L. D. (2016). Multiscale imaging and characterization of the effect of mixing temperature on asphalt concrete containing recycled components. *Journal of Microscopy*, *264*(1), 22–33. https://doi.org/10.1111/jmi.12412

Cavalli, M. C., Partl, M. N., & Poulikakos, L. D. (2017). Measuring the binder film residues on black rock in mixtures with high amounts of reclaimed asphalt. *Journal of Cleaner Production*, *149*, 665–672. https://doi.org/10.1016/j.jclepro.2017.02.055

Cheng, Y., Li, L., Zhou, P., Zhang, Y., & Liu, H. (2019). Multi-objective optimization design and test of compound diatomite and basalt fiber asphalt mixture. *Materials*. https://doi.org/10.3390/ma12091461

Coffey, S., Dubois, E., Mehta, Y., Nolan, A., & Purdy, C. (2013). Determining the impact of degree of blending and quality of reclaimed asphalt pavement on predicted pavement performance using pavement ME design. *Construction and Building Materials*, *48*(November 2015), 473–478. https://doi.org/10.1016/j.conbuildmat.2013.06.012

Coffey, S., Dubois, E., Mehta, Y., & Purdy, C. (2013). Determine the Impact of Degree of Blending between Virgin and Reclaimed Asphalt Binder on Predicted Pavement Performance using Mechanistic-Empirical Design Guide (MEPDG). *Transportation Research Board (TRB) 92nd Annual Meeting*.

Colbert, B., & You, Z. (2012). The determination of mechanical performance of laboratory produced hot mix asphalt mixtures using controlled RAP and virgin aggregate size fractions. *Construction and Building Materials*, *26*(1), 655–662. https://doi.org/10.1016/j.conbuildmat.2011.06.068

Copeland, A. (2011). Reclaimed Asphalt Pavement in Asphalt Mixtures: State of the Practice. In *Report No. FHWA-HRT-11-021* (Issue FHWA). https://doi.org/10.1016/j.proeng.2016.06.119

COREPASOL. (2014). http://silnice.fsv.cvut.cz/corepasol/

Daniel, J. S., & Lachance, A. (2005). Mechanistic and volumetric properties of asphalt mixtures with recycled asphalt pavement. *Transportation Research Record*, *1929*, 28–36. https://doi.org/10.3141/1929-04

Delfosse, F., Drouadaine, I., Largeaud, S., & Dumont, S. F. (2016). Performance control of bituminous mixtures with a high RAP content. In K. Suchý, J. Valentin, M. Southern, C. Karcher, H. Odelius, J. P. Michaut, & F. Cointe (Eds.), *6th Eurasphalt & Eurobitume Congress*. Czech Technical University in Prague. https://doi.org/dx.doi.org/10.14311/EE.2016.050

Di Mino, G., Di Liberto, C. M., Noto, S., Wellner, F., Blasl, A., Airey, G., & Lo Presti, D. (2015). *AllBack2Pave AllBack2Pave End-User Manual* (Issue November). http://www.cedr.eu/download/other_public_files/research_programme/call_2012/recycling/all back2pave/AllBack2Pave_End-User-Manual.pdf

Ding, Y., Huang, B., & Shu, X. (2016). Characterizing blending efficiency of plant produced asphalt paving mixtures containing high RAP. *Construction and Building Materials*, *126*, 172–178. https://doi.org/10.1016/j.conbuildmat.2016.09.025

Ding, Y., Huang, B., & Shu, X. (2018). Blending efficiency evaluation of plant asphalt mixtures using fluorescence microscopy. *Construction and Building Materials*, *161*, 461–467. https://doi.org/10.1016/j.conbuildmat.2017.11.138

Ding, Y., Huang, B., Shu, X., Zhang, Y., & Woods, M. E. (2016). Use of molecular dynamics to investigate diffusion between virgin and aged asphalt binders. *Fuel*, *174*(March), 267–273. https://doi.org/10.1016/j.fuel.2016.02.022

DIRECT-MAT. (2011). http://direct-mat.fehrl.org/

Doehlert, D. H. (1970). Uniform Shell Designs. *Applied Statistics*. https://doi.org/10.2307/2346327

Doh, Y. S., Amirkhanian, S. N., & Kim, K. W. (2008). Analysis of unbalanced binder oxidation level in recycled asphalt mixture using GPC. *Construction and Building Materials*, *22*(6), 1253–1260. https://doi.org/10.1016/j.conbuildmat.2007.01.026

Don Brock, J., & Richmond, J. L. (2006). Technical Paper T-127: Milling and Recycling. In *Technical Paper*.

EARN. (2014). https://trl.co.uk/projects/effects-availability-road-network-earn

Gaitan, L., Mehta, Y., Nolan, A., Dubois, E., Coffey, S., McCarthy, L., & Welker, A. (2013). Evaluation of the Degree of Blending and Polymer Degradation of Reclaimed Asphalt Pavement (RAP) for Warm Mix Asphalt. *The Journal of Solid Waste Technology and Management*, *39*(2), 101–113. https://doi.org/10.5276/JSWTM.2013.101

Gottumukkala, B., Ph, D., Kusam, S. R., Tandon, V., & Asce, A. M. (2018). *Estimation of Blending of Rap Binder in a Recycled Asphalt Pavement Mix. 30*(2), 1–8. https://doi.org/10.1061/(ASCE)MT.1943-5533.0002403.

Gundla, A., & Underwood, S. (2015). Evaluation of in situ RAP binder interaction in asphalt mastics using micromechanical models. *International Journal of Pavement Engineering*, *18*(9), 798–810. https://doi.org/10.1080/10298436.2015.1066003

Hajj, E., Salazar, L., & Sebaaly, P. (2012). Methodologies for Estimating Effective Performance Grade of Asphalt Binders in Mixtures with High Recycled Asphalt Pavement Content. *Transportation Research Record: Journal of the Transportation Research Board*, *2294*, 53–63. https://doi.org/10.3141/2294-06

Harvey, J. T., & Tsai, B. W. (1996). Effects of asphalt content and air void content on mix fatigue and stiffness. *Transportation Research Record*, *1543*, 38–45. https://doi.org/10.3141/1543-05

He, Y., Alavi, Z., Harvey, J., & Jones, D. (2016). Evaluating Diffusion and Aging Mechanisms in Blending of New and Age-Hardened Binders during Mixing and Paving. *Transportation Research Record: Journal of the Transportation Research Board*, *16*, 64–73. https://doi.org/10.3141/2574-07

Hofko, B., Eberhardsteiner, L., Füssl, J., Grothe, H., Handle, F., Hospodka, M., Grossegger, D., Nahar, S. N., Schmets, A. J. M., & Scarpas, A. (2016). Impact of maltene and asphaltene fraction on mechanical behavior and microstructure of bitumen. *Materials and Structures*, *49*(3), 829–841. https://doi.org/10.1617/s11527-015-0541-6

Hopman, P. C., Kunst, P. A. J. C., & Pronk, A. C. (1989). Renewed Interpretation Method for Fatigue Measurement, Verifica-tion of Miner's Rule. *Proceedings of 4th Eurobitumen Symposium*, 557–561.

Hossain, M., Musty, H. Y., & Sabahfer, N. (2012). *Use of High-Volume Reclaimed Asphalt Pavement (RAP) for Asphalt Pavement Rehabilitation Due to Increased Highway Truck Traffic from Freight Transportation*. https://digitalcommons.unl.edu/matcreports/74/

Howard, I. L., Cooley, L. A., & Doyle, J. (2009). *Laboratory Testing and Economic Analysis of High RAP Warm Mixed Asphalt*. https://rosap.ntl.bts.gov/view/dot/20311

Huang, B., Li, G., Vukosavljevic, D., Shu, X., & Egan, B. (2005a). Laboratory Investigation of Mixing Hot-Mix Asphalt with Reclaimed Asphalt Pavement. *Transportation Research Record: Journal of the Transportation Research Board*, *1929*(Figure 1), 37–45. https://doi.org/10.3141/1929-05

Huang, B., Li, G., Vukosavljevic, D., Shu, X., & Egan, B. K. (2005b). Laboratory Investigation of Mixing Hot-Mix Asphalt with Reclaimed Asphalt Pavement. *Transportation Research Record: Journal of the Transportation Research Board*, *1929*, 37–45. https://doi.org/http://dx.doi.org/10.1080/14680629.2014.926625

Huang, S.-C., Pauli, A. T., Grimes, R. W., & Turner, F. (2014). Ageing characteristics of RAP binder blends – what types of RAP binders are suitable for multiple recycling? *Road Materials and Pavement Design*, *15*(sup1), 113–145. https://doi.org/10.1080/14680629.2014.926625

Im, S., Karki, P., & Zhou, F. (2016). Development of new mix design method for asphalt mixtures containing RAP and rejuvenators. *Construction and Building Materials*, *115*, 727–734. https://doi.org/10.1016/j.conbuildmat.2016.04.081

Islam, M. R., Hossain, M. I., & Tarefder, R. A. (2015). A study of asphalt aging using Indirect Tensile Strength test. *Construction and Building Materials*, *95*, 218–223. https://doi.org/10.1016/j.conbuildmat.2015.07.159

Jiang, Y., Gu, X., Zhou, Z., Ni, F., & Dong, Q. (2018). Laboratory Observation and Evaluation of Asphalt Blends of Reclaimed Asphalt Pavement Binder with Virgin Binder using SEM/EDS. *Transportation Research Record*, 1–10. https://doi.org/10.1177/0361198118782023

Jiménez del Barco Carrión, A., Lo Presti, D., & Airey, G. D. (2015). Binder design of high RAP content hot and warm asphalt mixture wearing courses. *Road Materials and Pavement Design*, *16*(sup1), 460–474. https://doi.org/10.1080/14680629.2015.1029707

Kaseer, F., Arámbula-Mercado, E., Cucalon, L. G., & Martin, A. E. (2020). Performance of asphalt mixtures with high recycled materials content and recycling agents. *International Journal of Pavement Engineering*, *21*(7), 863–877. https://doi.org/10.1080/10298436.2018.1511990

Kaseer, F., Arámbula-Mercado, E., & Martin, A. E. (2019). A Method to Quantify Reclaimed Asphalt Pavement Binder Availability (Effective RAP Binder) in Recycled Asphalt Mixes. *Transportation Research Record: Journal of the Transportation Research Board*, 036119811882136. https://doi.org/10.1177/0361198118821366

Kaseer, F., Garcia Cucalon, L., Arambula-Mercado, E., Epps Martin, A., & Epps, J. (2018). Practical Tools for Optimizing Recycled Materials Content and Recycling Agent Dosage for Improved Short- and Long-Term Performance of Rejuvenated Asphalt Mixtures. *Association of Asphalt Paving Technologists*.

Kassem, E., Masad, E., Lytton, R., & Chowdhury, A. (2011). Influence of air voids on mechanical properties of asphalt mixtures. *Road Materials and Pavement Design*, *12*(3), 493–524. https://doi.org/10.3166/rmpd.12.492-524

Khodaii, A., Mousavi, E. S., Khedmati, M., & Iranitalab, A. (2016). Identification of dominant parameters for stripping potential in warm mix asphalt using response surface methodology. *Materials and Structures/Materiaux et Constructions*. https://doi.org/10.1617/s11527-015-0658-7

Khuri, A. I., & Mukhopadhyay, S. (2010). Response surface methodology. In *Wiley Interdisciplinary Reviews: Computational Statistics*. https://doi.org/10.1002/wics.73

Kim, H. B., & Lee, S. H. (2002). Reliability-based design model applied to mechanistic empirical pavement design. *KSCE Journal of Civil Engineering*. https://doi.org/10.1007/bf02829149

Kottegoda, N., & Rosso, R. (2008). *Applied Statistics for Civil and Enviromental Engineers* (Second Edi). Blackwell Publishing Ltd.

Kriz, P., Grant, D. L., Veloza, B. a., Gale, M. J., Blahey, A. G., Brownie, J. H., Shirts, R. D., & Maccarrone, S. (2014). Blending and diffusion of reclaimed asphalt pavement and virgin asphalt binders. *Road Materials and Pavement Design*, *15*(sup1), 78–112. https://doi.org/10.1080/14680629.2014.927411

Kroese, D. P., Taimre, T., & Botev, Z. I. (2011). Handbook of Monte Carlo Methods. In *Handbook of Monte Carlo Methods*. https://doi.org/10.1002/9781118014967

Liphardt, A., Radziszewski, P., & Król, J. (2015). Binder blending estimation method in hot mix asphalt with reclaimed asphalt. *Procedia Engineering*, *111*(TFoCE), 502–509. https://doi.org/10.1016/j.proeng.2015.07.123

Liu, Y., Wang, H., Tighe, S. L., Zhao, G., & You, Z. (2019). Effects of preheating conditions on performance and workability of hot in-place recycled asphalt mixtures. *Construction and Building Materials*, *226*, 288–298. https://doi.org/10.1016/j.conbuildmat.2019.07.277

Lo Presti, D., Tebaldi, G., Kuna, K., Apeagyei, A., Grenfell, J., Airey, G., Dave, E., Perraton, D., Muraya, P., Grilli, A., Graziani, A., Hugener, M., Pasetto, M., Hajj, E., Campher, L., & Jenkins, K. (2015). *Evaluation of the Indirect Tensile Strength test to characterize Reclaimed Asphalt.*

Lo Presti, D., Vasconcelos, K., Orešković, M., Pires, G. M., & Bressi, S. (2019). On the degree of binder activity of reclaimed asphalt and degree of blending with recycling agents. *Road Materials and Pavement Design.* https://doi.org/10.1080/14680629.2019.1607537

Lo Presti, Davide, Jimenez del Barco Carrion, A., Airey, G., & Hajj, E. (2016). Towards 100% recycling of reclaimed asphalt in road surface courses: Binder design methodology and case studies. *Journal of Cleaner Production*, *131*(May), 43–51. https://doi.org/10.1016/j.jclepro.2016.05.093

Lo Presti, Davide, Vasconcelos, K., Menegusso Pires, G., Jimenez Del Barco Carrion, A., Zaumanis, M., Orešković, M., Dave, E., & Tebaldi, G. (2017). *RILEM TC 264-RAP - Task Group 5 - Degree of Asphalt binder Activation.* https://www.researchgate.net/project/RILEM-TC-RAP-Task-Group-5-Degree-of-asphalt-binder-activation

Ma, T., Huang, X., Zhao, Y., Zhang, Y., & Wang, H. (2016). Influences of Preheating Temperature of RAP on Properties of Hot-Mix Recycled Asphalt Mixture. *Journal of Testing and Evaluation*, *44*(2), 20150157. https://doi.org/10.1520/jte20150157

Madrigal, D. P., Iannone, A., Martìnez, A. H., & Giustozzi, F. (2017). Effect of mixing time and temperature on cracking resistance of bituminous mixtures containing reclaimed asphalt pavement material. *Journal of Materials in Civil Engineering*, *29*(8), 1–8. https://doi.org/10.1061/(ASCE)MT.1943-5533.0001831

Maji, A., & Das, A. (2008). Reliability considerations of bituminous pavement design by mechanistic-empirical approach. *International Journal of Pavement Engineering.* https://doi.org/10.1080/10298430600997240

Mamun, A. A., & Al-Abdul Wahhab, H. I. (2018). Comparative laboratory evaluation of waste cooking oil rejuvenated asphalt concrete mixtures for high contents of reclaimed asphalt pavement. *International Journal of Pavement Engineering*, *0*(0), 1–12. https://doi.org/10.1080/10298436.2018.1539486

Marasteanu, M. O., Li, X., Clyne, T. R., Voller, V. R., Timm, D. H., & Newcomb, D. E. (2004). *Low Temperature Cracking of Asphalt Concrete Pavements.*

McDaniel, R. S., Soleymani, H., Anderson, R. M., Turner, P., & Peterson, R. (2000). Recommended Use of Reclaimed Asphalt Pavement in the Superpave Mix Design Method. NCHRP Web Document 30 (Project D9-12). In *Transportation Reserach Board 0f National Academics, Washington D.C.* (Vol. 30, Issue October). http://onlinepubs.trb.org/onlinepubs/nchrp/nchrp_w30-a.pdf

Menegusso Pires, G., Lo Presti, D., & Airey, G. D. (2019). A practical approach to estimate the degree of binder activity of reclaimed asphalt materials. *Road Materials and Pavement Design*, 1–24. https://doi.org/10.1080/14680629.2019.1663244

Miguel Baptista, A., Picado-Santos, L. G., & Capitão, S. D. (2013). Design of hot-mix recycled asphalt concrete produced in plant without preheating the reclaimed material. *International Journal of Pavement Engineering*, *14*(1–2), 95–102. https://doi.org/10.1080/10298436.2011.587009

Mogawer, W., Bennert, T., Daniel, J. S., Bonaquist, R., Austerman, A., & Booshehrian, A. (2012). Performance characteristics of plant produced high RAP mixtures. *Road Materials and Pavement Design*, *13*(March 2015), 183–208. https://doi.org/10.1080/14680629.2012.657070

Mogawer, W., Booshehrian, A., Vahidi, S., & Austerman, A. J. (2013). Evaluating the effect of rejuvenators on the degree of blending and performance of high RAP, RAS, and RAP/RAS mixtures. *Road Materials and Pavement Design*, *14*(sup2), 193–213. https://doi.org/10.1080/14680629.2013.812836

Mohajeri, M., Molenaar, A. A. A., & Van de Ven, M. F. C. (2014). Experimental study into the

fundamental understanding of blending between reclaimed asphalt binder and virgin bitumen using nanoindentation and nano-computed tomography. *Road Materials and Pavement Design*, *15*(2), 372–384. https://doi.org/10.1080/14680629.2014.883322

Molenaar, A. A. A., Mohajeri, M., & van de Ven, M. F. C. (2011). Design of Recycled Asphalt Mixtures. *14 Th AAPA International Flexible Pavements Conference*.

Mollenhauer, K., De Bock, L., Olesen, E., Brosseaud, Y., Gaspar, L., McNally, C., Gibney, A., Mirski, K., Antunes, M. L., Batista, F., Smiljanic, M., Ipavec, A., Pavsic, P., Sinis, F., Rubio, B., Karlsson, R., & Wik, O. (2010). *Deliverable D5: Synthesis of national and international documents on existing knowledge regarding the recycling of reclaimed road materials in asphalt*.

Myers, R. H., & Myers, S. L. (2007). Probability & Statistics - Engineers & Scientists. In *Education*. https://doi.org/10.2307/2288012

Nahar, S., Mohajeri, M., Schmets, A., Scarpas, A., van de Ven, M., & Schitter, G. (2013). First Observation of Blending-Zone Morphology at Interface of Reclaimed Asphalt Binder and Virgin Bitumen. *Transportation Research Record: Journal of the Transportation Research Board*, *2370*, 1–9. https://doi.org/10.3141/2370-01

Navaro, J., Bruneau, D., Drouadaine, I., Colin, J., Dony, A., & Cournet, J. (2012). Observation and evaluation of the degree of blending of reclaimed asphalt concretes using microscopy image analysis. *Construction and Building Materials*, *37*, 135–143. https://doi.org/10.1016/j.conbuildmat.2012.07.048

Newcomb, D. E., Ray Brown, E., & Epps, J. A. (2007). *Designing HMA mixtures with High RAP content: A practical guide*. 41. www.asphaltpavement.org

Norton, A., Reger, D., DuBois, E., Kehr, D., Nolan, A., & Mehta, Y. a. (2014). A Study to Evaluate Low Temperature Performance of Reclaimed Asphalt Pavement in Hot Mix Asphalt at Different Degrees of Blending. *The Journal of Solid Waste Technology and Management*, *39*(4), 234–243. https://doi.org/10.5276/JSWTM.2013.234

Oliver, J. W. H. (2001). The Influence of the Binder in RAP on Recycled Asphalt Properties. *Road Materials and Pavement Design*, *2*(3), 311–325. https://doi.org/10.1080/14680629.2001.9689906

Orešković, M., Bressi, S., Di Mino, G., & Lo Presti, D. (2017). Influence of bio-based additives on RAP clustering and asphalt binder rheology. In A. Loizos, I. Al-Qadi, & T. Scarpas (Eds.), *Proceedings of Tenth International Conference on the Bearing Capacity of Roads, Railways and Airfields* (pp. 1301–1306). CRC-Taylor & Francis Group.

Orešković, M., Menegusso Pires, G., Bressi, S., Vasconcelos, K., & Lo Presti, D. (2020). Quantitative assessment of the parameters linked to the blending between reclaimed asphalt binder and recycling agent: A literature review. *Construction and Building Materials*, *234*. https://doi.org/10.1016/j.conbuildmat.2019.117323

Partl, M. N., Bahia, H. U., Canestrari, F., Roche, C. de la, Benedetto, H. Di, Piber, H., & Sybilski, D. (Eds.). (2013). *Advances in Interlaboratory Testing and Evaluation of Bituminous Materials*. Springer Netherlands. https://doi.org/10.1007/978-94-007-5104-0

Pellinen, T. and Xiao, S. (2006). *Stiffness of Hot Mix Asphalt.Final report FHWA/IN/JTRP-2005/20*.

Pellinen, T. K. (2004). Conceptual performance criteria for asphalt mixtures. *Asphalt Paving Technology: Association of Asphalt Paving Technologists-Proceedings of the Technical Sessions*.

Porot, L. (2019). Rheology and Bituminous binder, a review of different analyses. In L. D. Poulikakos, A. C. Falchetto, M. P. Wistuba, B. Hofko, L. Porot, & H. Di Benedetto (Eds.), *RILEM 252-CMB-Symposium: Rheology and Bituminous Binder, A Review of Different Analyses* (Vol. 20, Issue October 2018, pp. 50–55). https://doi.org/10.1007/978-3-030-00476-7

Pouranian, M. R., & Shishehbor, M. (2019). Sustainability assessment of green asphalt mixtures: A review. *Environments - MDPI*, *6*(73). https://doi.org/10.3390/environments6060073

Rad, F., Sefidmazgi, N., & Bahia, H. (2014). Application of Diffusion Mechanism. Degree of Blending Between Fresh and Recycled Asphalt Pavement Binder in Dynamic Shear Rheometer. *Transportation Research Record: Journal of the Transportation Research Board*, *2444*(1), 71–77. https://doi.org/10.3141/2444-08

Re-Road. (2012). http://re-road.fehrl.org/

Rinaldini, E., Schuetz, P., Partl, M. N., Tebaldi, G., & Poulikakos, L. D. (2014). Investigating the blending of reclaimed asphalt with virgin materials using rheology, electron microscopy and computer tomography. *Composites Part B: Engineering*, *67*(March 2016), 579–587. https://doi.org/10.1016/j.compositesb.2014.07.025

Rowe, G. M. (1993). Performance of Asphalt Mixtures in the Trapezoidal Fatigue Test. *Proceedings of the Association of Asphalt Paving Technologist, Volume 62*, 344–384.

Sabouri, M, Bennert, T., Daniel, J. S., & Kim, Y. R. (2015). A comprehensive evaluation of the fatigue behaviour of plant-produced RAP mixtures. *Road Materials and Pavement Design*, *16*(May), 29–54. https://doi.org/10.1080/14680629.2015.1076997

Sabouri, Mohammedreza, Bennert, T., Daniel, J. S., & Kim, Y. R. (2015). Fatigue and rutting evaluation of laboratory-produced asphalt mixtures containing reclaimed asphalt pavement. *Transportation Research Record*, *2506*, 32–44. https://doi.org/10.3141/2506-04

Saltelli, A. (2002). Sensitivity analysis for importance assessment. *Risk Analysis.* https://doi.org/10.1111/0272-4332.00040

Sarabia, L. A., Ortiz, M. C., & Sánchez, M. S. (2020). Response Surface Methodology. In *Comprehensive Chemometrics (Second Edition)* (2nd ed., Issue November, pp. 287–326). Elsevier Inc. https://doi.org/10.1016/b978-0-12-409547-2.14756-0

Sarnowski, M., Kowalski, K. J., Król, J. B., & Radziszewski, P. (2019). Influence of overheating phenomenon on bitumen and asphalt mixture properties. *Materials*, *12*(4). https://doi.org/10.3390/ma12040610

Schober, P., & Schwarte, L. A. (2018). Correlation coefficients: Appropriate use and interpretation. *Anesthesia and Analgesia*, *126*(5), 1763–1768. https://doi.org/10.1213/ANE.0000000000002864

Sharma, S. K. (Ed.). (2012). *X-Ray Spectroscopy.* InTech. http://www.issp.ac.ru/ebooks/books/open/X-Ray_Spectroscopy.pdf

Shirodkar, P., Mehta, Y., Nolan, A., Dubois, E., Reger, D., & McCarthy, L. (2013). Development of blending chart for different degrees of blending of RAP binder and virgin binder. *Resources, Conservation and Recycling*, *73*, 156–161. https://doi.org/10.1016/j.resconrec.2013.01.018

Shirodkar, P., Mehta, Y., Nolan, A., Sonpal, K., Norton, A., Tomlinson, C., Dubois, E., Sullivan, P., & Sauber, R. (2011). A study to determine the degree of partial blending of reclaimed asphalt pavement (RAP) binder for high RAP hot mix asphalt. *Construction and Building Materials*, *25*(1), 150–155. https://doi.org/10.1016/j.conbuildmat.2010.06.045

Shu, X., Huang, B., & Vukosavljevic, D. (2008). *Laboratory evaluation of fatigue characteristics of recycled asphalt mixture. 22*, 1323–1330. https://doi.org/10.1016/j.conbuildmat.2007.04.019

Silva, H. M. R. D., Oliveira, J. R. M., & Jesus, C. M. G. (2012a). Are totally recycled hot mix asphalts a sustainable alternative for road paving? *Resources, Conservation and Recycling*, *60*, 38–48. https://doi.org/10.1016/j.resconrec.2011.11.013

Silva, H. M. R. D., Oliveira, J. R. M., & Jesus, C. M. G. (2012b). Are totally recycled hot mix asphalts a sustainable alternative for road paving? *Resources, Conservation and Recycling*, *60*, 38–48. https://doi.org/10.1016/j.resconrec.2011.11.013

Sivilevičius, H., Bražiunas, J., & Prentkovskis, O. (2017). Technologies and principles of hot recycling and investigation of preheated reclaimed asphalt pavement batching process in an asphalt mixing

plant. *Applied Sciences (Switzerland)*, *7*(11). https://doi.org/10.3390/app7111104

Slebi-Acevedo, C. J., Pascual-Muñoz, P., Lastra-González, P., & Castro-Fresno, D. (2019). A multi-criteria decision-making analysis for the selection of fibres aimed at reinforcing asphalt concrete mixtures. *International Journal of Pavement Engineering.* https://doi.org/10.1080/10298436.2019.1645848

Soleymani, H., Bahia, H., & Bergan, A. (1999). Blending Charts Based on Performance-Graded Asphalt Binder Specification. *Transportation Research Record*, *1661*(1), 7–14. https://doi.org/10.3141/1661-02

Sreeram, A., Leng, Z., Zhang, Y., & Padhan, R. K. (2018). Evaluation of RAP binder mobilisation and blending efficiency in bituminous mixtures : An approach using ATR-FTIR and artificial aggregate. *Construction and Building Materials*, *179*, 245–253. https://doi.org/10.1016/j.conbuildmat.2018.05.154

Stephens, J., Mahoney, J., & Dippold, C. (2001). *Determination of the PG binder grade to use in a RAP mix.* https://rosap.ntl.bts.gov/view/dot/14366

Stimilli, A., Virgili, A., & Canestrari, F. (2015). New method to estimate the "re-activated" binder amount in recycled hot-mix asphalt. *Road Materials and Pavement Design*, *16*(sup1), 442–459. https://doi.org/10.1080/14680629.2015.1029678

SUP&R ITN. (2017). http://superitn.eu

Swamy, A. K., Mitchell, L., Hall, S., & Daniel, J. S. (2011). Impact of RAP on the Volumetric, Stiffness, Strength, and Low-Temperature Performance of HMA. *Journal of Materials in Civil Engineering*, *23*(11), 1490–1497. https://doi.org/10.1061/(ASCE)MT.1943-5533.0000245

Taherkhani, H., & Noorian, F. (2018). Comparing the effects of waste engine and cooking oil on the properties of asphalt concrete containing reclaimed asphalt pavement (RAP). *Road Materials and Pavement Design*, *0*(0), 1–20. https://doi.org/10.1080/14680629.2018.1546220

Taziani, E. A., Toraldo, E., Mariani, E., & Crispino, M. (2017). Investigation on the compaction temperature effect on reactivating aged bitumen of 100% RAP mixtures. *Pavement and Asset Management - Proceedings of the World Conference on Pavement and Asset Management, WCPAM 2017*, *June*, 663–670. https://doi.org/10.1201/9780429264702-79

Tebaldi, G., Dave, E. V., Cannone Falchetto, A., Hugener, M., Perraton, D., Grilli, A., Lo Presti, D., Pasetto, M., Loizos, A., Jenkins, K., Apeagyei, A., Grenfell, J., & Bocci, M. (2018). Recommendation of RILEM TC237-SIB: protocol for characterization of recycled asphalt (RA) materials for pavement applications. *Materials and Structures/Materiaux et Constructions*, *51*(6). https://doi.org/10.1617/s11527-018-1253-5

Tiwari, A. (2012). Nanomechanical Analysis of Hybrid Silicones and Hybrid Epoxy Coatings—A Brief Review. *Advances in Chemical Engineering and Science*, *2*(01), 34–44. https://doi.org/10.4236/aces.2012.21005

Valdés, G., Pérez-jiménez, F., Miró, R., Martínez, A., & Botella, R. (2011). *Experimental study of recycled asphalt mixtures with high percentages of reclaimed asphalt pavement (RAP).* *25*, 1289–1297. https://doi.org/10.1016/j.conbuildmat.2010.09.016

Van den bergh, W., Kara, P., Anthonissen, J., Margaritis, A., Jacobs, G., & Couscheir, K. (2017). Recommendations and strategies for using reclaimed asphalt pavement in the Flemish Region based on a first life cycle assessment research. *IOP Conference Series: Materials Science and Engineering*, *236*(1). https://doi.org/10.1088/1757-899X/236/1/012088

Vassaux, S., Gaudefroy, V., Boulangé, L., Pevere, A., Michelet, A., Barragan-Montero, V., & Mouillet, V. (2019). Assessment of the binder blending in bituminous mixtures based on the development of an innovative sustainable infrared imaging methodology. *Journal of Cleaner Production*, *215*, 821–828. https://doi.org/https://doi.org/10.1016/j.jclepro.2019.01.105

Vassaux, S., Gaudefroy, V., Boulangé, L., Soro, L. J., Pévère, A., Michelet, A., Barragan-Montero, V., & Mouillet, V. (2018). Study of remobilization phenomena at reclaimed asphalt binder/virgin binder

interphases for recycled asphalt mixtures using novel microscopic methodologies. *Construction and Building Materials*, *165*, 846–858. https://doi.org/10.1016/j.conbuildmat.2018.01.055

Vukosavljevic, D. (2006). *Fatigue Characteristics of Field HMA Surface Mixtures Containing Recycled Asphalt Pavement (RAP)* [University of Tennessee - Knoxville]. http://trace.tennessee.edu/utk_gradthes/1829

Wang, J., Guo, M., & Tan, Y. (2018). Study on application of cement substituting mineral fillers in asphalt mixture. *International Journal of Transportation Science and Technology*, *7*(3), 189–198. https://doi.org/10.1016/j.ijtst.2018.06.002

West, R. C. (2015). Best Practices for RAP and RAS Management - NAPA, Quality Imprvement Series 129. In *National Asphalt Pavement Association (NAPA)*. https://www.asphaltpavement.org/PDFs/EngineeringPubs/QIP129_RAP_-_RAS_Best_Practices_lr.pdf

West, R., Willis, J. R., & Marasteanu, M. (2013). Improved Mix Design, Evaluation, and Materials Management Practices for Hot Mix Asphalt with High Reclaimed Asphalt Pavement Content. In *Improved Mix Design, Evaluation, and Materials Management Practices for Hot Mix Asphalt with High Reclaimed Asphalt Pavement Content*. https://doi.org/10.17226/22554

Witczak, M. W., & Bari, J. (2004). *Development of a master curve (E*) database for lime modified asphaltic mixtures*.

Xu, J., Hao, P., Zhang, D., & Yuan, G. (2018). Investigation of reclaimed asphalt pavement blending efficiency based on micro-mechanical properties of layered asphalt binders. *Construction and Building Materials*, *163*, 390–401. https://doi.org/10.1016/j.conbuildmat.2017.12.030

Yildirim, Y., Ideker, J., & Hazlett, D. (2006). Evaluation of viscosity values for mixing and compaction temperatures. *Journal of Materials in Civil Engineering*, *18*(4), 545–553. https://doi.org/10.1061/(ASCE)0899-1561(2006)18:4(545)

Yu, B., Gu, X., Wu, M., & Ni, F. (2017). Application of a high percentage of reclaimed asphalt pavement in an asphalt mixture: blending process and performance investigation. *Road Materials and Pavement Design*, *18*(3), 753–765. https://doi.org/10.1080/14680629.2016.1182941

Yu, S., Shen, S., Zhang, C., Zhang, W., & Jia, X. (2017). Evaluation of the blending effectiveness of reclaimed asphalt pavement binder. *Journal of Materials in Civil Engineering*, *29*(12), 1–8. https://doi.org/10.1061/(ASCE)MT.1943-5533.0002095.

Yu, Shuai, Shen, S., Zhou, X., & Li, X. (2018). Effect of Partial Blending on High Content Reclaimed Asphalt Pavement (RAP) Mix Design and Mixture Properties. *Transportation Research Record: Journal of the Transportation Research Board*, *2672*(28), 79–87. https://doi.org/10.1177/0361198118780703

Zaumanis, M, Mallick, R., & Frank, R. (2014). *100 % Recycled Hot-Mix Asphalt*. 2014.

Zaumanis, Martins, Cavalli, M. C., & Poulikakos, L. D. (2018). Design of 100 % RAP Hot-Mix Asphalt to Balance Rutting and Cracking Performance. *International Society for Asphalt Pavements*, 1–7.

Zhang, K., Wen, H., & Hobbs, A. (2015). Laboratory Tests and Numerical Simulations of Mixing Superheated Virgin Aggregate with Reclaimed Asphalt Pavement Materials. *Transportation Research Record: Journal of the Transportation Research Board*, *2506*, 62–71. https://doi.org/10.3141/2506-07

Zhao, S., Bowers, B., Huang, B., & Shu, X. (2014). Characterizing Rheological Properties of Binder and Blending Efficiency of Asphalt Paving Mixtures Containing RAS through GPC. *Journal of Materials in Civil Engineering*, *26*(September), 941–946. https://doi.org/10.1061/(ASCE)MT.1943-5533.0000896

Zhao, S., Huang, B., Shu, X., & Woods, M. E. (2015). Quantitative Characterization of Binder Blending: How Much Recycled Binder Is Mobilized During Mixing? *Transportation Research Record: Journal of the Transportation Research Board*, *2506*(2506), 72–80. https://doi.org/10.3141/2506-08

Zhao, S., Huang, B., Shu, X., & Woods, M. E. (2016). Quantitative evaluation of blending and diffusion

in high RAP and RAS mixtures. *Materials and Design*, *89*, 1161–1170. https://doi.org/10.1016/j.matdes.2015.10.086

Zhao, W. (2011). The effects of fundamental mixture parameters on hot-mix asphalt performance properties [Clemson University]. In *ProQuest Dissertations and Theses* (Issue August 2011). https://tigerprints.clemson.edu/all_dissertations/801

Zhou, F., Hu, S., Das, G., & Scullion, T. (2011). *High RAP mixes design methodology with balanced performance* (Vol. 7, Issue 2). http://tti.tamu.edu/documents/0-6092-2.pdf

Zhou, F., Im, S., & Hu, S. (2019). Development and Validation of the IDEAL Cracking Test. *Relationship Between Laboratory Cracking Tests and Field Performance of Asphalt Mixtures*. www.trb.org

Zhou, F., Im, S., Sun, L., & Scullion, T. (2017). Development of an IDEAL cracking test for asphalt mix design and QC/QA. *Asphalt Paving Technology: Association of Asphalt Paving Technologists-Proceedings of the Technical Sessions*, *86*(0), 549–577. https://doi.org/10.1080/14680629.2017.1389082

Standards

AASHTO M323-17 — Standard Specification for Superpave Volume Mix design

AASHTO R92-18 — Standard Practice for Evaluating the Elastic Behavior of Asphalt Binders Using the Multiple Stress Creep Recovery (MSCR) Test

AASHTO T283-14 — Standard Method of Test for Resistance of Compacted Asphalt Mixtures to Moisture-Induced Damage

ASTM D2172/D2172M – 17e1 — Standard Test Methods for Quantitative Extraction of Asphalt Binder from Asphalt Mixtures

ASTM D4867/D4867M – 09(2014) — Standard Test Method for Effect of Moisture on Asphalt Concrete Paving Mixtures

ASTM D7405-15 — Standard Test Method for Multiple Stress Creep and Recovery (MSCR) of Asphalt Binder Using a Dynamic Shear Rheometer

ASTM D8225-19 — Standard Test Method for Determination of Cracking Tolerance Index of Asphalt Mixture Using the Indirect Tensile Cracking Test at Intermediate Temperature

EN 1097-2:2020 — Tests for mechanical and physical properties of aggregates. Methods for the determination of resistance to fragmentation

EN 1097-4:2008 — Tests for mechanical and physical properties of aggregates. Determination of the voids of dry compacted filler

EN 1097-6:2013 — Tests for mechanical and physical properties of aggregates. Determination of particle density and water absorption

EN 12591:2009 — Bitumen and bituminous binders. Specifications for paving grade bitumens.

EN 12593:2015 — Bitumen and bituminous binders. Determination of the Fraass breaking point

EN 12697-1:2012 — Bituminous mixtures. Test methods for hot mix asphalt. Soluble binder content

EN 12697-4:2015 — Bituminous mixtures. Test methods. Bitumen recovery: Fractionating column

EN 12697-5:2018 — Bituminous mixtures. Test methods. Determination of the maximum density

EN 12697-6:2020 — Bituminous mixtures. Test methods. Determination of bulk density of bituminous specimens

EN 12697-8:2018 — Bituminous mixtures. Test methods. Determination of void characteristics of bituminous specimens

EN 12697-12:2018 — Bituminous mixtures. Test methods. Determination of the water sensitivity of bituminous specimens

EN 12697-22:2003 — Bituminous mixtures. Test methods for hot mix asphalt. Wheel tracking

EN 12697-23:2017 — Bituminous mixtures. Test methods. Determination of the indirect tensile strength of bituminous specimens

EN 12697-24:2018 — Bituminous mixtures. Test methods. Resistance to fatigue

EN 12697-26:2018 — Bituminous mixtures. Test methods. Stiffness

EN 12697-30:2018 — Bituminous mixtures. Test methods. Specimen preparation by impact compactor

EN 12697-31:2019 — Bituminous mixtures. Test methods. Specimen preparation by gyratory compactor

EN 12697-33:2019 — Bituminous mixtures. Test method. Specimen prepared by roller compactor

EN 13302:2018 — Bitumen and bituminous binders. Determination of dynamic viscosity of bituminous binder using a rotating spindle apparatus

EN 1426:2015 — Bitumen and bituminous binders. Determination of needle penetration.

EN 1427:2015 — Bitumen and bituminous binders. Determination of the softening point. Ring and Ball method.

EN 14770:2012 — Bitumen and bituminous binders. Determination of complex shear modulus and phase angle. Dynamic Shear Rheometer (DSR)

EN 15326:2007+A1:2009 — Bitumen and bituminous binders. Measurement of density and specific gravity. Capillary-stoppered pyknometer method

EN 933-1:2012 — Tests for geometrical properties of aggregates. Determination of particle size distribution. Sieving method

EN 933-8:2012+A1:2015 — Tests for geometrical properties of aggregates. Assessment of fines. Sand equivalent test

EN 933-9:2009+A1:2013 — Tests for geometrical properties of aggregates. Assessment of fines. Methylene blue test

Appendix I — Particle Size Distribution and Binder Content of RAP Fractions

Properties		Unit	Standard	Fraction [mm]			
				0/11 black curve	0/11 white curve	11/22 black curve	11/22 white curve
Particle size distribution				Average passing percentage (standard deviation)			
Sieve size [mm]	0.063	mm		0.1 (0.0)	13.0 (0.5)	0.0 (0.0)	8.3 (0.4)
	0.09	mm		0.3 (0.1)	14.7 (0.6)	0.0 (0.0)	9.3 (0.4)
	0.25	mm		1.8 (0.2)	23.7 (0.6)	0.3 (0.0)	14.7 (0.6)
	0.71	mm		8.0 (0.6)	36.4 (0.8)	0.6 (0.0)	22.7 (0.9)
	2.0	mm		23.8 (2.6)	53.3 (1.1)	0.8 (0.0)	32.0 (1.4)
	4.0	mm	EN 933-1:2012	45.8 (2.4)	69.5 (1.2)	1.0 (0.1)	39.8 (1.6)
	8.0	mm		86.2 (1.2)	94.3 (0.6)	2.8 (0.4)	52.1 (1.4)
	11.2	mm		100.0 (0.0)	100.0 (0.0)	25.2 (3.5)	73.3 (2.8)
	16.0	mm		100.0 (0.0)	100.0 (0.0)	80.9 (2.8)	95.5 (1.6)
	22.4	mm		100.0 (0.0)	100.0 (0.0)	100.0 (0.0)	100.0 (0.0)
	31.5	mm		100.0 (0.0)	100.0 (0.0)	100.0 (0.0)	100.0 (0.0)
Average bitumen content (standard deviation)		%	EN 12697-1:2012	5.75 (0.12)		4.59 (0.20)	

Appendix II — Mix Design and Resistance to Permanent Deformation of the Control Mixture

Marshall mix design procedure of the control mixture

No.	Bitumen content	Bulk density	Maximum density	Air void content	Voids filled with bitumen	Voids in the mineral aggregate	Stability	Flow	Stiffness (S/F)
	[%]	[Mg/m^3]	[Mg/m^3]	[%]	[%]	[%]	[kN]	[mm]	[kN/mm]
1	3.0	2.393	2.590	7.6	48.5	14.8	11.5	2.2	5.2
2	3.4	2.408	2.573	6.4	56.0	14.6	11.4	2.3	5.0
3	3.8	2.421	2.556	5.3	63.5	14.5	10.6	2.4	4.4
4	4.2	2.430	2.540	4.3	70.1	14.5	9.6	2.6	3.8
5	4.6	2.429	2.524	3.8	74.7	14.9	8.2	2.7	3.0

Resistance to permanent deformation of the control mixture

Specimen	RD_{air} [mm]	PRD_{air} [%]	WTS_{air} [mm/10^3 load cycles]	Air void content [%]
1-1	4.32	6.1	0.11	4.1
1-2	6.41	9.0	0.22	4.1
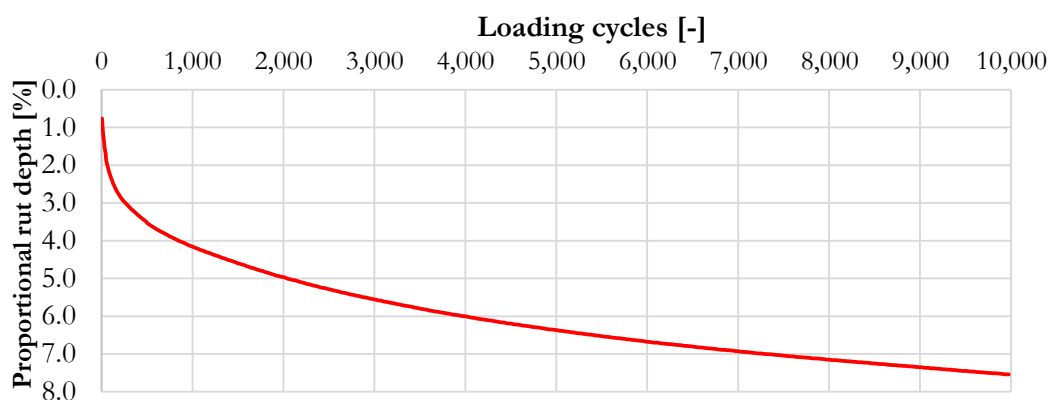
Appendix III — Fourier Transformation

The full-length measured signal of 300 ms is shown in Figure A-1. Since the evaluation is carried out in the frequency domain and the signal is periodic, only one period of the signal is considered (Figure A-1). Given that the sampling frequency of the signal is $F_S \approx 714$ Hz, the number of data points N within one period, $T = 3$s, is 2412.
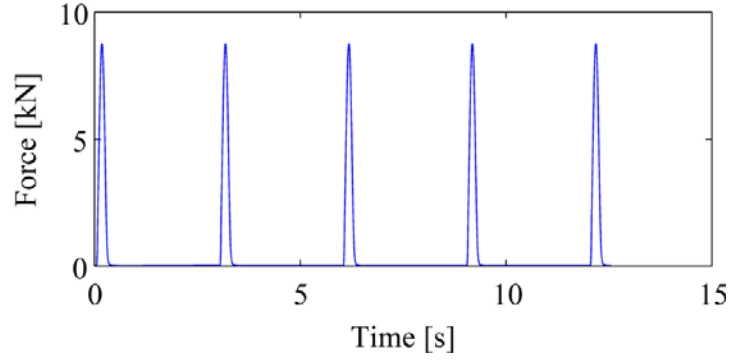
Figure A-1 *Measured signal — full length*
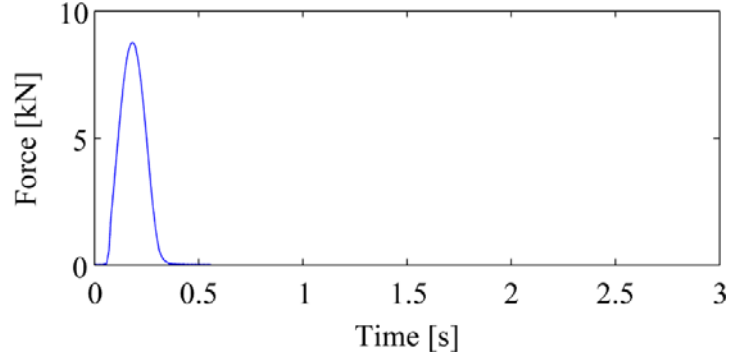
Figure A-2 *Measured signal — one period*

The representative frequency is obtained by using an energy approach. First, the Power Spectral Density (*PSD*) of the signal *s(t)*, displayed in Figure A-3, is calculated as:

$$PSD = \frac{1}{F_S N}|S(f)|^2 \qquad\qquad Equation\ A.1$$

where *S(f)* is a Fourier Transformation of the signal *s(t)*. Since *s(t)* is not a continuous function but a discrete one, *S(f)* is obtained by using a Discrete Fourier Transformation:

$$S\left(\frac{n}{NT_S}\right) = \sum_{k=0}^{N-1} s(kT_S)e^{-i2\pi nk/N}, \quad n = 0,1,\ldots,N-1 \qquad\qquad Equation\ A.2$$

where $T_S = 1/F_S$ is the sampling period.
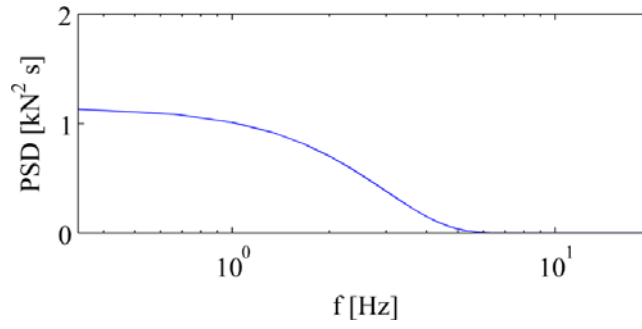
Figure A-3 *Power Spectral Density (PSD) of the signal*

To simplify the evaluation, 1/3 octave band analysis is introduced. The energy level of the signal in decibels, *L*, is given as the ratio of the average value of *PSD* over 1/3 octave bands, Δ*f*, and the sensitivity of the device, $a_{ref} = 10^{-6}$ kN:

$$L = 10 \cdot \log \frac{PSD \cdot \Delta f}{a_{ref}}$$

Equation A.3

The bandwidth of the ith band, Δf_i is defined as:

$$\Delta f_i = f_i^u - f_i^l$$

Equation A.4

where the lower, f_i^l, and the upper, f_i^u, limits of the ith band are given as:

$$f_i^l = \frac{1}{2^{1/6}} f_i^c, \quad f_i^u = 2^{1/6} f_i^c$$

Equation A.5

and the centre frequency of the ith band, f_i^c, is given in terms of the centre frequency of the $(i-1)^{th}$ band:

$$f_i^c = 2^{1/3} f_{i-1}^c.$$

Equation A.6

The 1/3 octave bands are obtained for the frequency bandwidth [F_S/N, F_S], assuming that 1000 Hz is a centre frequency. The energy level, *L*, is displayed in Figure A-4.

The representative loading frequency, f_R, is calculated as the centre frequency of the *-3dB band* of the energy level *L*. The *-3dB band* represents the bandwidth of *L* that contains frequencies higher than 50% of the highest frequency of *PSD*. Since f_R is the centre frequency of the band, according to Equation A.5 it could be calculated as

$$f_R = \sqrt{f^l \cdot f^h}$$

Equation A.7

Therefore, f_R, is equal to 2 Hz.

Comparably, for the signal length of 125 ms, f_R equals to 3.98 Hz, and for the signal of 200 ms, 2.51 Hz.
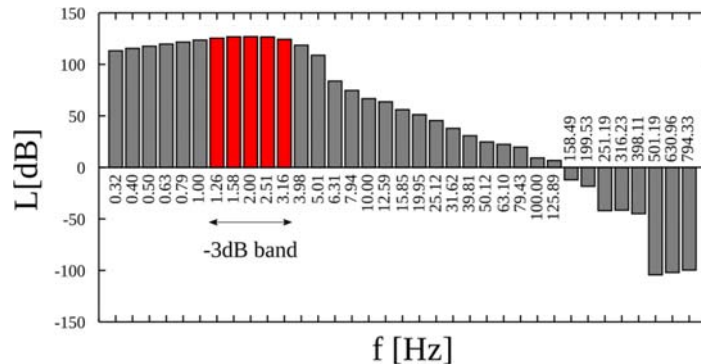
Figure A-4 *Energy Level and the -3dB band*

121

Appendix IV — Ranges of Input Variables for Monte Carlo Simulations

Mixture	Compaction type	Air void content [%]		Stiffness [MPa]		ITS [kPa]		CT_{index} [-]	
		min	max	min	max	min	max	min	max
RAP	Gyratory	8.0	11.1	1,986	10,911	720.6	1,854.9	3.2	45.2
	Marshall	11.3	17.3	725	8,728	292.8	1,378.8	2.6	50.5
RAP+RA	Gyratory	6.8	9.7	730	6,287	381.1	1,230.3	15.1	57.8
	Marshall	9.8	15.7	383	5,255	135.3	922.0	7.8	75.0

Appendix V — Testing Results of the Control Mixture

	T [°C]	Average stiffness [MPa]			Air void content [%]
		2.00 Hz	2.51 Hz	3.98 Hz	
Stiffness	5	18,877	20,417	22,619	1-1 – 5.8
	10	15,216	16,712	18,593	1-2 – 5.2
	20	5,833	6,701	7,909	1-3 – 5.4
	30	2,195	2,543	3,145	1-4 – 5.0
	40	742	861	991	

	Set	Specimen	ITS [kPa]	Air void content [%]
Water sensitivity	Dry	1-5	917.0	6.2
		1-6	851.7	7.0
		1-8	946.4	6.8
	Wet	1-7	867.7	6.7
		1-9	930.8	7.0
		1-10	1,010.1	6.6

	Set	Specimen	ITS [kPa]	Air void content [%]
Freeze-thaw resistance	Unconditioned	1-3	1,121.0	7.3
		1-5	1,164.7	7.9
		1-8	1,274.8	6.3
	3 cycles	1-2	629.0	7.8
		1-4	731.7	6.6
		1-9	709.3	7.4
	6 cycles	1-1	430.8	7.4
		1-6	584.2	7.5
		1-7	571.1	6.8

	Specimen	RD_{air} [mm]	PRD_{air} [%]	WTS_{air} [mm/10³ load cycles]	Air void content [%]
Resistance to permanent deformation	1-1	3.51	4.8	0.08	5.7
	1-2	4.34	6.1	0.12	5.1

	Specimen	Initial stress [N]	Initial strain [µε]	Initial stiffness [MPa]	Loading cycles leading to failure [-]	Air void content [%]
Fatigue resistance	1-1	6,750	85.9	13,897	229,601	5.0
	1-2	12,000	167.8	12,697	3,241	5.6
	1-3	7,000	98.4	12,656	55,622	4.9
	1-4	7,000	77.5	16,114	405,121	4.4
	2-2	13,500	178.1	13,504	3,361	4.7
	2-3	7,500	115.3	11,409	21,581	5.0
	2-4	10,000	144.6	12,273	18,761	5.1
	3-1	8,500	109.0	13,882	47,801	5.1
	3-2	10,000	161.2	11,059	11,381	5.9
	3-3	12,000	184.4	11,653	3,111	5.5
	3-4	9,000	121.7	10,332	18,501	5.7

Appendix VI — Testing Results of the RAP15 Mixture

	T [°C]	Average stiffness [MPa]			Air void content [%]
		2.00 Hz	2.51 Hz	3.98 Hz	
Stiffness	5	19,831	20,755	22,712	2-1 – 6.6
	10	15,305	16,790	19,474	2-2 – 6.0
	20	7,242	8,232	9,515	2-3 – 6.2
	30	2,758	3,314	3,715	2-4 – 5.8
	40	1,118	1,275	1,459	

	Set	Specimen	ITS [kPa]	Air void content [%]
Water sensitivity	Dry	2-6	970.0	8.3
		2-7	1,072.8	8.3
		2-10	906.8	8.9
	Wet	2-5	1,060.2	8.3
		2-8	1,044.0	8.4
		2-9	1,075.3	8.6

	Set	Specimen	ITS [kPa]	Air void content [%]
Freeze-thaw resistance	Unconditioned	2-1	1,478.3	7.8
		2-2	1,513.1	7.2
		2-6	1,602.9	6.6
	3 cycles	2-5	1,227.5	7.6
		2-7	1,070.5	7.3
		2-8	1,298.8	7.1
	6 cycles	2-3	879.5	7.5
		2-4	855.8	7.4
		2-9	954.0	7.2

	Specimen	RD_{air} [mm]	PRD_{air} [%]	WTS_{air} [mm/10³ load cycles]	Air void content [%]
Resistance to permanent deformation	2-1	2.57	3.5	0.06	6.5
	2-2	3.61	5.0	0.10	5.9

	Specimen	Initial stress [N]	Initial strain [µε]	Initial stiffness [MPa]	Loading cycles leading to failure [-]	Air void content [%]
Fatigue resistance	1-1	6,500	87.8	13,014	252,452	8.8
	1-2	13,500	201.4	11,992	3,581	5.3
	1-3	7,000	102.8	12,263	96,561	6.3
	1-4	6,500	79.6	14,409	416,712	5.0
	2-1	13,500	180.4	13,266	3,601	5.4
	2-2	8,000	90.1	15,677	114,561	5.3
	2-3	7,000	94.3	13,192	79,121	5.9
	2-4	13,500	192.6	12,390	3,291	5.5
	3-1	8,500	104.8	14,400	60,321	5.5
	3-2	8,500	115.4	13,062	38,241	5.7
	3-4	10,000	111.2	16,147	24,841	4.7

Appendix VII — Testing Results of the RAP50 Mixture

	T [°C]	Average stiffness [MPa]			Air void content [%]
		2.00 Hz	2.51 Hz	3.98 Hz	
Stiffness	5	15,411	16,942	18,209	I-1 – 6.0
	10	11,370	12,462	13,871	I-2 – 6.0
	20	6,338	7,068	8,053	I-3 – 6.8
	30	3,110	3,559	4,104	I-4 – 6.4
	40	1,322	1,502	1,796	

	Set	Specimen	ITS [kPa]	Air void content [%]
Water sensitivity	Dry	1-3	995.4	7.3
		1-4	1,176.8	6.9
		1-5	1,180.3	6.7
	Wet	1-1	928.1	7.1
		1-2	855.6	6.9
		1-6	1,055.8	6.4

	Set	Specimen	ITS [kPa]	Air void content [%]
Freeze-thaw resistance	Unconditioned	I	993.3	8.3
		III	930.0	7.1
		VII	991.9	7.7
	3 cycles	II	848.8	7.3
		VIII	737.2	8.2
		IX	810.1	7.5
	6 cycles	IV	607.5	7.8
		V	556.6	7.8
		X	658.9	7.3

	Specimen	RD_{air} [mm]	PRD_{air} [%]	WTS_{air} [mm/10^3 load cycles]	Air void content [%]
Resistance to permanent deformation	2-1	2.57	3.5	0.06	6.5
	2-2	3.61	5.0	0.10	5.9

	Specimen	Initial stress [N]	Initial strain [με]	Initial stiffness [MPa]	Loading cycles leading to failure [-]	Air void content [%]
Fatigue resistance	1-2	5,500	107.1	10,097	103,601	6.2
	1-3	5,750	98.4	11,357	167,943	4.8
	1-4	10,000	222.6	8,555	4,061	4.7
	2-1	10,000	212.1	9,033	3,841	4.6
	2-2	6,250	96.6	12,453	169,921	4.5
	2-3	6,500	105.0	11,877	118,321	4.4
	2-4	5,750	96.6	11,470	406,422	4.1
	3-1	11,000	239.4	8,738	2,361	4.3
	3-2	10,000	193.2	9,920	5,011	5.4
	3-3	7,000	132.3	10,037	19,981	4.4
	3-4	6,500	115.5	10,622	45,641	4.9

Biografija autora

Marko Orešković je rođen 19.03.1988. godine u Pančevu. Osnovnu školu „Žarko Zrenjanin" je završio u Kačarevu, a gimnaziju „Mihajlo Pupin" u Kovačici.

Osnovne studije na Građevinskom fakultetu Univerziteta u Beogradu je upisao 2007. godine, gde je diplomirao 2011. godine na odseku za Puteve, železnice i aerodrome, sa prosečnom ocenom 8.11 i ocenom 10 na diplomskom radu. 2012. godine je završio master akademske studije na istom fakultetu sa prosečnom ocenom 9.29 i ocenom 10 na završnom radu. Doktorske studije, studijski program Građevinarstvo, na istom fakultetu je upisao 2012. godine i položio sve ispite sa prosečnom ocenom 9.63.

Tokom studija je učestvovao kao student demonstrator u izvođenju vežbi na predmetima Kolovozne konstrukcije, Održavanje puteva i Upravljanje održavanjem saobraćajnica. Od 01.01.2013. godine je zaposlen na Građevinskom fakultetu u zvanju asistenta-studenta doktorstkih studija za užu naučnu oblast Građenje i održavanje puteva i aerodroma na Katedri za puteve, železnice i aerodrome. Od 13.12.2018. godine se nalazi u zvanju istraživača saradnika.

Kao autor i koautor je do sada objavio 28 istraživačkih radova, od čega 5 u časopisima indeksiranim na SCI listi. Izlagao je radove na više domaćih i međunarodnih konferencija i stručnih skupova. Angažovan je u okviru projekta TR36017 koji finansira Ministarstvo za obrazovanje, nauku i tehnološki razvoj Srbije. Učestvovao je u dva bilateralna projekta (EASPHALT i HARAC). Član je nekoliko RILEM-ovih komiteta (264-RAP, 279-WMR, FBB), a bio je i član naučnih komiteta nekoliko međunarodnih konferencija.

Od početka zaposlenja na fakultetu obavlja poslove inženjera u Laboratoriji za kolovozne konstrukcije Insituta za saobraćajnice i geotehniku. Aktivno je učestvovao u ispitivanjima za potrebe izrade studentskih radova, kao i u okviru saradnje sa privredom. Učestvovao je u izradi nekoliko idejnih projekata, projekata za građevinsku dozvolu, kao i projekata za izvođenje. Kandidat aktivno govori engleski jezik i služi se nemačkim jezikom.

Изјава о ауторству

Име и презиме аутора: Марко Д. Орешковић

Број индекса: 910/12

Изјављујем

да је докторска дисертација под насловом

MIX DESIGN METHODOLOGY OF HOT MIX ASPHALT WITH HIGH CONTENT OF RECLAIMED ASPHALT PAVEMENT

(МЕТОДОЛОГИЈА ПРОЈЕКТОВАЊА ВРУЋИХ АСФАЛТНИХ МЕШАВИНА СА ВИСОКИМ САДРЖАЈЕМ СТРУГАНОГ АСФАЛТА)

- резултат сопственог истраживачког рада;
- да дисертација у целини ни у деловима није била предложена за стицање друге дипломе према студијским програмима других високошколских установа;
- да су резултати коректно наведени и
- да нисам кршио ауторска права и користио интелектуалну својину других лица.

Потпис аутора

У Београду, 09.11.2020. године

_____

Изјава о истоветности штампане и електронске верзије докторског рада

Име и презиме аутора: Марко Д. Орешковић

Број индекса: 910/12

Студијски програм: Грађевинарство

Наслов рада: MIX DESIGN METHODOLOGY OF HOT MIX ASPHALT WITH HIGH CONTENT OF RECLAIMED ASPHALT PAVEMENT

(МЕТОДОЛОГИЈА ПРОЈЕКТОВАЊА ВРУЋИХ АСФАЛТНИХ МЕШАВИНА СА ВИСОКИМ САДРЖАЈЕМ СТРУГАНОГ АСФАЛТА)

Ментор: в. проф. др Горан Младеновић, дипл.инж.грађ.

Изјављујем да је штампана верзија мог докторског рада истоветна електронској верзији коју сам предао ради похрањења у **Дигиталном репозиторијуму Универзитета у Београду.**

Дозвољавам да се објаве моји лични подаци везани за добијање академског назива доктора наука, као што су име и презиме, година и место рођења и датум одбране рада.

Ови лични подаци могу се објавити на мрежним страницама дигиталне библиотеке, у електронском каталогу и у публикацијама Универзитета у Београду.

Потпис аутора

У Београду, 09.11.2020. године

_____

Изјава о коришћењу

Овлашћујем Универзитетску библиотеку „Светозар Марковић" да у Дигитални репозиторијум Универзитета у Београду унесе моју докторску дисертацију под насловом:

MIX DESIGN METHODOLOGY OF HOT MIX ASPHALT WITH HIGH CONTENT OF RECLAIMED ASPHALT PAVEMENT

(МЕТОДОЛОГИЈА ПРОЈЕКТОВАЊА ВРУЋИХ АСФАЛТНИХ МЕШАВИНА СА ВИСОКИМ САДРЖАЈЕМ СТРУГАНОГ АСФАЛТА)

као моје ауторско дело.

Дисертацију са свим прилозима предао сам у електронском формату погодном за трајно архивирање.

Моју докторску дисертацију похрањену у Дигиталном репозиторијуму Универзитета у Београду и доступну у отвореном приступу могу да користе сви који поштују одредбе садржане у одабраном типу лиценце Креативне заједнице (Creative Commons) за коју сам се одлучио.

1. Ауторство (CC BY)

2. Ауторство – некомерцијално (CC BY-NC)

3. Ауторство – некомерцијално – без прерада (CC BY-NC-ND)

4. Ауторство – некомерцијално – делити под истим условима (CC BY-NC-SA)

5. Ауторство – без прерада (CC BY-ND)

6. Ауторство – делити под истим условима (CC BY-SA)

(Молимо да заокружите само једну од шест понуђених лиценци.

Кратак опис лиценци је саставни део ове изјаве).

Потпис аутора

У Београду, 09.11.2020. године

_____

1. **Ауторство**. Дозвољавате умножавање, дистрибуцију и јавно саопштавање дела, и прераде, ако се наведе име аутора на начин одређен од стране аутора или даваоца лиценце, чак и у комерцијалне сврхе. Ово је најслободнија од свих лиценци.

2. **Ауторство – некомерцијално**. Дозвољавате умножавање, дистрибуцију и јавно саопштавање дела, и прераде, ако се наведе име аутора на начин одређен од стране аутора или даваоца лиценце. Ова лиценца не дозвољава комерцијалну употребу дела.

3. **Ауторство – некомерцијално – без прерада**. Дозвољавате умножавање, дистрибуцију и јавно саопштавање дела, без промена, преобликовања или употребе дела у свом делу, ако се наведе име аутора на начин одређен од стране аутора или даваоца лиценце. Ова лиценца не дозвољава комерцијалну употребу дела. У односу на све остале лиценце, овом лиценцом се ограничава највећи обим права коришћења дела.

4. **Ауторство – некомерцијално – делити под истим условима**. Дозвољавате умножавање, дистрибуцију и јавно саопштавање дела, и прераде, ако се наведе име аутора на начин одређен од стране аутора или даваоца лиценце и ако се прерада дистрибуира под истом или сличном лиценцом. Ова лиценца не дозвољава комерцијалну употребу дела и прерада.

5. **Ауторство – без прерада**. Дозвољавате умножавање, дистрибуцију и јавно саопштавање дела, без промена, преобликовања или употребе дела у свом делу, ако се наведе име аутора на начин одређен од стране аутора или даваоца лиценце. Ова лиценца дозвољава комерцијалну употребу дела.

6. **Ауторство – делити под истим условима**. Дозвољавате умножавање, дистрибуцију и јавно саопштавање дела, и прераде, ако се наведе име аутора на начин одређен од стране аутора или даваоца лиценце и ако се прерада дистрибуира под истом или сличном лиценцом. Ова лиценца дозвољава комерцијалну употребу дела и прерада. Слична је софтверским лиценцама, односно лиценцама отвореног кода.